ISSN 1007-9327 (print)
ISSN 2219-2840 (online)

World Journal of *Gastroenterology*

World J Gastroenterol 2018 November 28; 24(44): 4959-5056

Published by Baishideng Publishing Group Inc

World Journal of Gastroenterology

Contents

Weekly Volume 24 Number 44 November 28, 2018

ABOUT COVER

Editorial board member of *World Journal of Gastroenterology*, Wan-Long Chuang, MD, PhD, Doctor, Professor, Hepatobiliary Division, Department of Internal Medicine, Kaohsiung Medical University Hospital, Kaohsiung Medical University, Kaohsiung 807, Taiwan

AIMS AND SCOPE

World Journal of Gastroenterology (*World J Gastroenterol*, *WJG*, print ISSN 1007-9327, online ISSN 2219-2840, DOI: 10.3748) is a peer-reviewed open access journal. *WJG* was established on October 1, 1995. It is published weekly on the 7th, 14th, 21st, and 28th each month. The *WJG* Editorial Board consists of 642 experts in gastroenterology and hepatology from 59 countries.

The primary task of *WJG* is to rapidly publish high-quality original articles, reviews, and commentaries in the fields of gastroenterology, hepatology, gastrointestinal endoscopy, gastrointestinal surgery, hepatobiliary surgery, gastrointestinal oncology, gastrointestinal radiation oncology, gastrointestinal imaging, gastrointestinal interventional therapy, gastrointestinal infectious diseases, gastrointestinal pharmacology, gastrointestinal pathophysiology, gastrointestinal pathology, evidence-based medicine in gastroenterology, pancreatology, gastrointestinal laboratory medicine, gastrointestinal molecular biology, gastrointestinal immunology, gastrointestinal microbiology, gastrointestinal genetics, gastrointestinal translational medicine, gastrointestinal diagnostics, and gastrointestinal therapeutics. *WJG* is dedicated to become an influential and prestigious journal in gastroenterology and hepatology, to promote the development of above disciplines, and to improve the diagnostic and therapeutic skill and expertise of clinicians.

INDEXING/ABSTRACTING

World Journal of Gastroenterology (*WJG*) is now indexed in Current Contents®/Clinical Medicine, Science Citation Index Expanded (also known as SciSearch®), Journal Citation Reports®, Index Medicus, MEDLINE, PubMed, PubMed Central and Directory of Open Access Journals. The 2018 edition of Journal Citation Reports® cites the 2017 impact factor for *WJG* as 3.300 (5-year impact factor: 3.387), ranking *WJG* as 35th among 80 journals in gastroenterology and hepatology (quartile in category Q2).

NAME OF JOURNAL
World Journal of Gastroenterology

ISSN
ISSN 1007-9327 (print)
ISSN 2219-2840 (online)

LAUNCH DATE
October 1, 1995

FREQUENCY
Weekly

EDITORIAL OFFICE
Ze-Mao Gong, Director
World Journal of Gastroenterology
Baishideng Publishing Group Inc
7901 Stoneridge Drive, Suite 501,
Pleasanton, CA 94588, USA
Telephone: +1-925-2238242
Fax: +1-925-2238243
E-mail: editorialoffice@wjgnet.com
Help Desk: http://www.f6publishing.com/helpdesk
http://www.wjgnet.com

PUBLISHER
Baishideng Publishing Group Inc
7901 Stoneridge Drive, Suite 501,
Pleasanton, CA 94588, USA
Telephone: +1-925-2238242
Fax: +1-925-2238243
E-mail: bpgoffice@wjgnet.com
Help Desk: http://www.f6publishing.com/helpdesk
http://www.wjgnet.com

PUBLICATION DATE
November 28, 2018

World Journal of Gastroenterology

Submit a Manuscript: http://www.f6publishing.com

World J Gastroenterol 2018 November 28; 24(44): 4959-4961

DOI: 10.3748/wjg.v24.i44.4959

ISSN 1007-9327 (print) ISSN 2219-2840 (online)

EDITORIAL

Hepatitis elimination by 2030: Progress and challenges

Yasir Waheed, Masood Siddiq, Zubia Jamil, Muzammil Hasan Najmi

Yasir Waheed, Multidisciplinary Laboratory, Foundation University Medical College, Foundation University Islamabad, Islamabad 44000, Pakistan

Masood Siddiq, Department of Medicine, Jinnah Memorial Hospital, 2-Civil Lines, Rawalpindi 46000, Pakistan

Zubia Jamil, Department of Medicine, Fauji Foundation Hospital, Foundation University Medical College, Foundation University Islamabad, Islamabad 44000, Pakistan

Muzammil Hasan Najmi, Department of Pharmacology and Therapeutics, Foundation University Medical College, Foundation University Islamabad, Islamabad 44000, Pakistan

ORCID number: Yasir Waheed (0000-0002-5789-4215); Masood Siddiq (0000-0003-4072-7282); Zubia Jamil (0000-0003-3144-837X); Muzammil Hasan Najmi (0000-0002-6114-5540).

Author contributions: Waheed Y designed study and wrote manuscript; Waheed Y, Siddiq M, Jamil Z, Najmi MH did literature search, data analysis and gave the final approval of the study.

Conflict-of-interest statement: The authors have no conflict of interest to declare.

Manuscript source: Invited manuscript

Corresponding author to: Yasir Waheed, PhD, Assistant Professor, Multidisciplinary Laboratory, Foundation University Medical College, Foundation University Islamabad, Defense Avenue, DHA 1, Islamabad 44000, Pakistan. yasir.waheed@fui.edu.pk
Telephone: +92-300-5338171

Received: August 30, 2018
Peer-review started: August 30, 2018
First decision: October 9, 2018
Revised: October 23, 2018
Accepted: November 2, 2018
Article in press: November 2, 2018
Published online: November 28, 2018

Abstract

Globally, over 300 million people are living with viral hepatitis with approximately 1.3 million deaths per year. In 2016, World Health Assembly adopted the Global Health Sector Strategy on viral hepatitis to eliminate hepatitis by 2030. Different World Health Organization member countries are working on hepatitis control strategies to achieve hepatitis elimination. So far, only 12 countries are on track to achieve hepatitis elimination targets. The aim of the study was to give an update about the progress and challenges to achieving hepatitis elimination by 2030. According to the latest data, 87% of infants had received the three doses of hepatitis B virus (HBV) vaccination in the first year of their life and 46% of infants had received a timely birth dose of HBV vaccination. There is a strong need to improve blood and injection safety. Rates of hepatitis B and C diagnosis are very low and only 11% of hepatitis B and C cases are diagnosed. There is a dire need to speed up hepatitis diagnosis and find the missing millions of people living with viral hepatitis. Up to 2016, only 3 million hepatitis C cases have been treated. Pricing of hepatitis C virus drugs is also reduced in many countries. The major hurdle to achieve hepatitis elimination is lack of finances to support hepatitis programs. None of the major global donors are committed to invest in the fight against hepatitis. It will be very difficult for the low and middle-income countries to fund their hepatitis control program. Hepatitis elimination needs strong financial and political commitment, support from civil societies, and support from pharmaceutical and medical companies around the globe.

Key words: Hepatitis; Global Health Sector Strategy; Hepatitis B virus vaccination; Injection safety; Find

missing millions; Harm reduction

Core tip: Viral hepatitis is one of the leading causes of deaths worldwide. World Health Organization has produced a strategy to eliminate hepatitis by 2030. The major hurdle to achieve hepatitis elimination is lack of financial resources. If the targets in Global Health Sector Strategy are achieved, then the millions of lives will be saved from liver related premature deaths.

Waheed Y, Siddiq M, Jamil Z, Najmi MH. Hepatitis elimination by 2030: Progress and challenges. *World J Gastroenterol* 2018; 24(44): 4959-4961 Available from: URL: http://www.wjgnet.com/1007-9327/full/v24/i44/4959.htm DOI: http://dx.doi.org/10.3748/wjg.v24.i44.4959

INTRODUCTION

Hepatitis B and C are major causes of liver-related deaths[1]. Globally, 257 million and 71 million people are living with hepatitis B virus (HBV) and hepatitis C virus (HCV), respectively[2]. In the last 15 years, massive progress has been achieved in the fights against human immunodeficiency virus, malaria and tuberculosis, mainly by heavy commitments by the global donor agencies while viral hepatitis remains neglected[3]. In 2015, United Nations included hepatitis in its Sustainable Development Goals.

In 2016, World Health Assembly has adopted the Global Health Sector Strategy (GHSS) on viral hepatitis to eliminate hepatitis by 2030. The goal of the World Health Organization (WHO) GHSS is to reduce hepatitis incidence from 6-10 million cases to 0.9 million cases, and to reduce annual hepatitis deaths from 1.4 million to 0.5 million, by 2030[4].

The WHO is helping different countries to develop hepatitis control programs[5]. By November 2017, 84 countries had developed hepatitis control programs[6]. Due to lack of international investment in viral hepatitis programs, only a few countries included hepatitis treatment and prevention strategies for all patients in their national hepatitis programs[1]. According to Polaris data, only 12 countries, namely Australia, Iceland, Switzerland, Italy, Mongolia, Spain, Egypt, France, Georgia, Japan, Netherlands, and United Kingdom are on track to achieve the WHO hepatitis elimination targets[7].

GLOBAL HEALTH SECTOR STRATEGY ON VIRAL HEPATITIS: TARGETS AND PROGRESS

World Health Organization's GHSS document showed the five areas, in which efforts are required to eliminate hepatitis by 2030. These five core intervention areas are (1) HBV vaccination; (2) prevention of mother to child transmission of HBV; (3) injection and blood safety; (4) harm reduction; and (5) test and treatment of HBV and HCV[4].

In 2015, the global coverage of 3rd dose infant HBV vaccination was 82%, which is close to the target of 90% HBV vaccine coverage by 2030[4]. According to the latest data, 87% of infants had received the three doses of HBV vaccination in the first year of their life[8]. There are many countries in the European Union who have not included the HBV vaccination into their routine immunization schedule[9]. There is a dire need to speed up HBV vaccination and reach every child for vaccination, to save the future generations from HBV.

Mother to child transmission of HBV is prevented by the timely administration of HBV birth dose vaccine (within 24 h of birth)[9]. In 2015, only 38% of children were administered the birth dose of HBV vaccine in a timely manner and the target is to administer the timely HBV vaccine to 90% of children[4]. According to the latest data, 46% of infants were administered the birth dose of HBV vaccine in a timely manner[8].

Blood and injection safety is very important to achieve the global hepatitis elimination target. In 2015, 39 countries were not routinely screening all blood donations for transfusion transmitted infections and 89% of donations underwent a quality control check[4]. There is a strong need to improve injection safety and also reduce the use of unnecessary injections, especially in the low and middle-income countries (LMICs).

The prevalence of HBV and HCV are very high in People who inject drugs (PWID)[4]. In 2015, only 20 sterile syringes were provided to per PWID per year and the target is to provide 300 syringes per PWID per year[4]. A lot of financial effort is needed to reach the 2030 target of harm reduction.

Only 11% of HBV and HCV cases are diagnosed. The target in GHSS is to diagnose 90% of HBV and HCV positive cases by 2030[4]. Observing the miserable condition of hepatitis diagnosis, World Hepatitis Alliance has started an initiative named "Find the Missing Millions", to find the millions of undiagnosed people living with viral hepatitis[10].

Current hepatitis B and C treatment rates are very low. According to Global Hepatitis Report 2017, 1.7 million HBV and 1.1 million HCV patients were on treatment in the year 2015[2]. In 2016, 1.76 million additional HCV patients received treatment and the cumulative 2015-2016 HCV treatment number reached 3 million[6]. To eliminate hepatitis, the goal is to treat 80% of HBV and HCV patients by 2030[4]. Highly effective HCV drugs are available in the market. The price of HCV drugs has been reduced in over 100 countries, but drug pricing is still a problem in many developed countries. There is a strong need to find a highly effective treatment for hepatitis B virus.

CONCLUSION

There is a dire need to strengthen the health care sys-

tems in different LMICs. There are many low-income countries in which a large proportion of births are not taking place in health care settings. The major obstacle to eliminate hepatitis by 2030 is lack of financial resources. None of the major global donors gave a financial commitment to eliminate viral hepatitis. There is also a strong need to provide funds to The Global Alliance for Vaccines and Immunisation to support the HBV birth dose vaccination scheme. Donors are also needed to develop and support the national hepatitis plans in LMICs[1]. Hepatitis elimination needs strong financial and political commitment, support from civil societies, and support from pharmaceutical and medical companies around the globe[11].

REFERENCES

1 **Gore C**, Hicks J, Deelder W. Funding the elimination of viral hepatitis: donors needed. *Lancet Gastroenterol Hepatol* 2017; **2**: 843-845 [PMID: 29100843 DOI: 10.1016/S2468-1253(17)30333-3]

2 **World Health Organization**. Global Hepatitis Report 2017. Available from: URL: http://apps.who.int/iris/bitstream/handle/10665/255016/9789241565455-eng.pdf;jsessionid=A1E5CF10018D99C7C1291A9BCA6F05A9?sequence=1

3 **Waheed Y**. Transition from millennium development goals to sustainable development goals and hepatitis. *Pathog Glob Health* 2015; **109**: 353 [PMID: 26924344 DOI: 10.1080/20477724.2015.1126035]

4 **World Health Organization**. Global Health Sector Strategies on Viral Hepatitis 2016-2021. Available from: URL: http://apps.who.int/gb/ebwha/pdf_files/WHA69/A69_32-en.pdf?ua=1

5 **Waheed Y**, Siddiq M. Elimination of hepatitis from Pakistan by 2030: Is it possible? *Hepatoma Res* 2018; **4**: 45 [DOI: 10.20517/2394-5079.2018.58]

6 **World Health Organization**. Progress report on access to Hepatitis C treatment, focus on overcoming barriers in low and middle income countries. Available from: URL: http://apps.who.int/iris/bitstream/10665/260445/1/WHO-CDS-HIV-18.4-eng.pdf?ua=1

7 **Polaris Observatory**. Center for Disease Analysis. Available from: URL: http://cdafound.org/polaris/

8 **Polaris Observatory Collaborators**. Global prevalence, treatment, and prevention of hepatitis B virus infection in 2016: a modelling study. *Lancet Gastroenterol Hepatol* 2018; **3**: 383-403 [PMID: 29599078 DOI: 10.1016/S2468-1253(18)30056-6]

9 **Hutin YJ**, Bulterys M, Hirnschall GO. How far are we from viral hepatitis elimination service coverage targets? *J Int AIDS Soc* 2018; **21** Suppl 2: e25050 [PMID: 29633520 DOI: 10.1002/jia2.25050]

10 **World Hepatitis Alliance**. Find the Missing Millions. Available from: URL: http://www.worldhepatitisalliance.org/find-missing-millions

11 **Waheed Y**. Hepatitis C eradication: A long way to go. *World J Gastroenterol* 2015; **21**: 12510-12512 [PMID: 26604658 DOI: 10.3748/wjg.v21.i43.12510]

P- Reviewer: Mihaila RG, Said ZN, Zhao HT **S- Editor**: Wang XJ
L- Editor: A **E- Editor**: Yin SY

World Journal of Gastroenterology

Submit a Manuscript: http://www.f6publishing.com

World J Gastroenterol 2018 November 28; 24(44): 4962-4973

DOI: 10.3748/wjg.v24.i44.4962

ISSN 1007-9327 (print) ISSN 2219-2840 (online)

REVIEW

Mononuclear phagocyte system in hepatitis C virus infection

Yu Yang, Zheng-Kun Tu, Xing-Kai Liu, Ping Zhang

Yu Yang, Xing-Kai Liu, Ping Zhang, Department of Hepatobiliary and Pancreatic Surgery, The First Hospital of Jilin University, Changchun 130021, Jilin Province, China

Zheng-Kun Tu, Institute of Translational Medicine, The First Hospital of Jilin University, Changchun 130061, Jilin Province, China

ORCID number: Yu Yang (0000-0002-1513-4883); Zheng-Kun Tu (0000-0001-6803-2015); Xing-Kai Liu (0000-0001-7856-3899); Ping Zhang (0000-0003-4944-2937).

Author contributions: Liu XK collected the information; Yang Y wrote the paper; Tu ZK and Zhang P revised the paper.

Conflict-of-interest statement: No potential conflicts of interest and no financial support.

Manuscript source: Unsolicited manuscript

Corresponding author to: Ping Zhang, MD, Chief Doctor, Professor, Surgeon, Department of Hepatobiliary and Pancreatic Surgery, The First Hospital of Jilin University, No. 71, Xinmin Street, Changchun 130021, Jilin Province, China. z_ping@jlu.edu.cn
Telephone: +86-431-81875168
Fax: +86-431-81875168

Received: September 8, 2018
Peer-review started: September 10, 2018
First decision: October 24, 2018
Revised: October 30, 2018
Accepted: November 7, 2018
Article in press: November 8, 2018
Published online: November 28, 2018

Abstract

The mononuclear phagocyte system (MPS), which consists of monocytes, dendritic cells (DCs), and macrophages, plays a vital role in the innate immune defense against pathogens. Hepatitis C virus (HCV) is efficient in evading the host immunity, thereby facilitating its development into chronic infection. Chronic HCV infection is the leading cause of end-stage liver diseases, liver cirrhosis, and hepatocellular carcinoma. Acquired immune response was regarded as the key factor to eradicate HCV. However, innate immunity can regulate the acquired immune response. Innate immunity-derived cytokines shape the adaptive immunity by regulating T-cell differentiation, which determines the outcome of acute HCV infection. Inhibition of HCV-specific T-cell responses is one of the most important strategies for immune system evasion. It is meaningful to illustrate the role of innate immune response in HCV infection. With the MPS being the important factor in innate immunity, therefore, understanding the role of the MPS in HCV infection will shed light on the pathophysiology of chronic HCV infection. In this review, we outline the impact of HCV infection on the MPS and cytokine production. We discuss how HCV is detected by the MPS and describe the function and impairment of MPS components in HCV infection.

Key words: Mononuclear phagocyte system; Hepatitis C virus; Monocyte; Dendritic cell; Macrophage

Core tip: Hepatitis C virus (HCV) infection is efficient to develop into chronic infection. Innate immune system can shape the acquired immune response, which can eradicate HCV directly. As the main component of innate immunity, the mononuclear phagocyte system (MPS) plays a vital role in HCV infection. In this review, we discuss the interaction between the HCV and MPS. MPS can detect HCV to promote virus eradication, and HCV can

shape the MPS to facilitate HCV persistence. We hope that this review will enable us to better understand HCV infection.

Yang Y, Tu ZK, Liu XK, Zhang P. Mononuclear phagocyte system in hepatitis C virus infection. *World J Gastroenterol* 2018; 24(44): 4962-4973 Available from: URL: http://www.wjgnet.com/1007-9327/full/v24/i44/4962.htm DOI: http://dx.doi.org/10.3748/wjg.v24.i44.4962

INTRODUCTION

Hepatitis C virus and hepatitis C virus infection

Hepatitis C virus (HCV) is a positive sense single-stranded RNA virus that belongs to the family *Flaviviridae*[1]. HCV infection affects more than 170 million people worldwide and is regarded as a leading cause of chronic liver disease[2]. The viral genome is approximately 9.6 kb, encoding a single 3011-amino acid-long polyprotein. The polyprotein is cleaved into three structural proteins (core, E1, and E2) and seven non-structural proteins (p7, NS2, NS3, NS4A, NS4B, NS5A, and NS5B)[3]. HCV is classified into seven genotypes as well as 67 subtypes, and it shows significant genetic diversity among different nations[4]. Even within the same patient, HCV usually exists in blood as a group of related quasispecies[5]. Acute HCV infections are anicteric and asymptomatic[6]. Nevertheless, 15%-20% of HCV-infected patients can recover from an acute infection, whereas the remaining 80%-85% of patients will progress to chronic infection[6-8]. Chronic HCV infection is a leading cause of end-stage liver diseases, liver failure, and hepatocellular carcinoma, resulting in approximately 350000 deaths per year[9,10]. HCV infection is usually diagnosed *via* the detection of both HCV antibody and HCV RNA. In the absence of viral RNA, the detection of HCV antibody indicates a spontaneously resolved or cured infection[10]. The combination of subcutaneous pegylated interferon (peginterferon) alpha and oral ribavirin was once the standard treatment for chronic HCV infection. However, this combination results in a sustained virological response (SVR) in only approximately 50% of patients[11]. In 2011, the United States Food and Drug Administration approved a novel HCV therapy including direct-acting antiviral drugs and protease inhibitor drugs. These drugs significantly increased the response rate, thereby revealing a new era of HCV treatment[12,13].

Mononuclear phagocyte system

The term mononuclear phagocyte system (MPS) was developed in the late 1960s and early 1970s by van Furth[14]. The MPS encompasses monocytes, dendritic cells (DCs), and macrophages, and altogether they play vital roles in tissue development, maintenance of homeostasis, inflammation, and the innate immune defense against pathogens.

Monocytes constitute 5%-10% of the peripheral blood leukocytes in humans and are generated in the bone marrow and spleen[14]. During inflammation, monocytes can differentiate into macrophages and DCs[15-19], and they play important roles in both innate and adaptive immunity[20-24]. Circulating monocytes can traffic through the sinusoids, and thus, it has been proposed that liver-resident monocytes and circulating monocytes should be distinguished[25]. However, blood monocytes pass through the liver numerous times, and therefore, we will consider circulating monocytes with liver-resident monocytes as one entity in this review.

Human blood DCs are major histocompatibility complex (MHC) class Ⅱ [human leukocyte antigen D-related (HLA-DR)] positive and can be divided into myeloid DCs (mDCs) and plasmacytoid DCs (pDCs)[26]. pDCs are CD11c negative and are distinguished from mDCs using positive markers such as CD123, CD303, and CD304[26]. Alternatively, mDCs can be subdivided according to CD1c and CD141 expression[26]. Accordingly, DCs exist in $CD303^+$ pDCs, $CD11c^+$ $CD1c^+$ mDCs, and $CD11c^+$ $CD141^+$ mDCs populations. It is worth mentioning that all these subsets are present in the liver[25], and the $CD1c^+$ mDC population is the most prevalent liver DC subset[27]. Compared to blood DCs, hepatic DCs present an immature phenotype and have a lower capacity to stimulate T cells[27-29]. Furthermore, hepatic DCs produce more interleukin (IL)-10 and less IL-12p70[30,31], highlighting the tolerogenic peculiarity of hepatic DCs.

Macrophages are large phagocytic cells with multifunctional roles in development, homeostasis, and diseases[32]. Kupffer cells (KCs) are tissue-resident macrophages of the liver that have important functions in both the innate and acquired immune responses[32-34]. However, owing to their stationary state, they are not as potent as DCs in stimulating T cells[35]. Additionally, KCs can also regulate the functions of other hepatic cells[36,37]. As early as the 1990s, the interaction between KCs with natural killer (NK) cells and liver stellate cells was identified by electron microscopy, implying that the functions of NK cells and stellate cells may be shaped by KCs[38]. In our lab, we previously identified Toll-like receptor (TLR)-dependent crosstalk between human KCs and NK cells[39].

HCV infection is notorious for its propensity to become chronic due to the lack of robust acquired immune responses. The immune response against HCV infection is primarily controlled by the adaptive immune system; however, a robust acquired immune response is determined by the innate immune response[40]. In other words, proper innate immunity is essential for the initiation of the acquired immune response. Mounting evidence confirms that the MPS is crucial for innate immunity and plays an important role in multiple infections, including parasitic infections[41], tuberculosis[42], human immunodeficiency virus (HIV) infection[43,44], and respiratory syncytial virus infection[45]. Therefore, it is necessary to clarify the interaction between HCV and the MPS. The immunophenotype of the MPS in normal liver has been previously reviewed[25]. However, the impact

of HCV infection on the MPS has not been reviewed yet. Therefore, in this review, we summarize recent findings regarding the role of the MPS in HCV infection, and we focus on the function and impairment of MPS components following HCV infection.

DETECTION OF HCV BY THE MPS

Pathogen-associated molecular patterns (PAMPs) on HCV can be detected by three classes of pattern recognition receptors (PRRs): RIG I-like receptors (RLRs), TLRs, and NOD-like receptors (NLRs)[46]. These PRRs function early after infection, thereby restricting HCV replication[46].

RIG-I, representative of RLRs, can sense HCV RNA as non-self through the 5′-triphosphate (5′-ppp) found on the viral RNA in addition to the 3′ poly-U/UC tract[47,48]. Blocking of the signaling pathway of melanoma differentiation-associated gene 5 (MDA5), another member of the RLRs, led to enhanced HCV replication[49]. Both RIG-I and MDA5 utilize the adaptor protein mitochondrial antiviral signaling (MAVS) to initiate immune signaling, and they recognize different PAMPs, indicating that they may function complementarily[50-52]. In West Nile virus infection, RIG-I was found to play an important role in the early immune response after infection, whereas MDA5 was more important in the later period of infection[53].

Endosomal TLRs are the main sensors that detect HCV. Among them, TLR3 can sense double-stranded (ds)RNA[54,55], whereas the GU-rich sequences in HCV RNA can be recognized by TLR7 and TLR8[56,57]. Additionally, TLR2 is specialized in HCV protein detection[58]. Wang *et al*[54] previously demonstrated that interferon (IFN)-stimulated genes (ISGs) are upregulated in primary human hepatocytes after polyinosinic: polycytidylic acid (polyI:C) stimulation, owing to the expression of TLR3. However, the authors observed that HCV infection weakened the ability of hepatocytes to induce ISG expression compared to the polyI:C stimulation[54], indicating that TLR3 signaling may be impaired by HCV. Consistently, it was previously established that TIR-domain-containing adapter-inducing interferon-β (TRIF), an adaptor protein of TLR3 signaling, can also be cleaved by the NS3/4A protease[59,60].

It is worth mentioning that the results described above were derived from primary human hepatocytes or hepatocyte cell lines infected by HCV. *In vivo,* uninfected hepatocytes were able to sense the adjacent infected cells by TLR3[55]. Extracellular dsRNA was detected by the uninfected hepatocytes in a macrophage scavenger receptor 1 (MSR1)-dependent manner[55]. MSR1 can bind to the viral dsRNA and transport it to the endosome, within which TLR3 is engaged[55]. This mechanism may be employed by the MPS to trigger an antiviral state in a TLR3-dependent manner. Furthermore, HCV-infected cells can induce the production of type Ⅰ IFN from pDCs[61]. Additionally, HCV RNA activates the MPS populations like mDCs and pDCs to produce proinflammatory cytokines and chemokines, including IL-1β, tumor necrosis factor (TNF)-α, IL-6, IL-12, IL-10, CXCL9, and CXCL10[57]. Particularly, the GU-rich sequences induce type I IFN from monocytes and pDCs[57]. In contrast, the polyU/UC sequences of HCV RNA activate IL-1β production from the nucleotide-binding oligomerization domain-like receptor family pyrin domain containing 3 (NLRP3) inflammasome of macrophages, resulting in persistent liver inflammation[62,63].

In addition, HCV proteins can also activate the MPS. It was identified that HCV core protein (HCVc) and NS3 activate monocytes[64] and macrophages[58], thereby triggering inflammatory pathways in a TLR2-dependent manner[58]. Additionally, HCVc and NS3 inhibit DC differentiation[64]. Furthermore, TLR1 and TLR6, co-receptors of TLR2, are also involved in HCVc and NS3-induced macrophage activation[65].

Compared to the HCV RNA, HCV viral particles are less efficient in stimulating the MPS[57]. Nevertheless, they can activate macrophages, leading to production of proinflammatory cytokines like IL-6, IL-1β, and TNF-α rather than the antiviral cytokines including IL-12 and type Ⅰ IFN[57].

IMPACT OF HCV ON THE MPS

HCV and monocytes

Effect of HCV on TLR signaling: TLR signaling is associated with the outcome of acute HCV infection as well as the therapeutic outcome[66]. Accumulating evidence suggests that HCV infection can influence the expression of TLRs[67-69]. Particularly, the expression levels of TLR2 and TLR4 are elevated after HCV infection in monocytes[67-69]. The expression of TLR2 is significantly correlated with serum TNF-α and alanine transaminase (ALT) levels[67], indicating that the inflammation associated with HCV infection is partially attributed to production of proinflammatory cytokines in a TLR2-dependent manner. Similarly, HCVc can activate the MPS in a TLR2-dependent manner[58]. In contrast, TLR3 and TLR4 in monocytes are compromised after HCV infection[70]. In healthy individuals, the repeated stimulation of monocytes *via* the TLR ligands leads to tolerance, thereby providing a protective mechanism to limit inflammation. However, this tolerance is disrupted in HCV-infected patients[71]. Therefore, monocytes from HCV-infected patients are hyper-responsive, and their expression of TNF-α is upregulated. The loss of TLR tolerance can be attributed to IFN-γ[71]. Alternatively, other reports demonstrated that HCVc can induce down-regulation of IL-6 production after stimulation with TLR2 and TLR4 ligands[72,73]. We hypothesize that HCVc induces hyporesponsiveness, leading to the evasion of immunity in the early period of infection, whereas IFN-γ-induced loss of tolerance may contribute to inflammation and subsequent liver damage in chronic infection.

Impact of HCV on cytokine production from monocytes: IL-10, an anti-inflammatory cytokine, can be produced by monocytes[74]. IL-10 has several immunoregulatory functions after HCV infection. It is involved

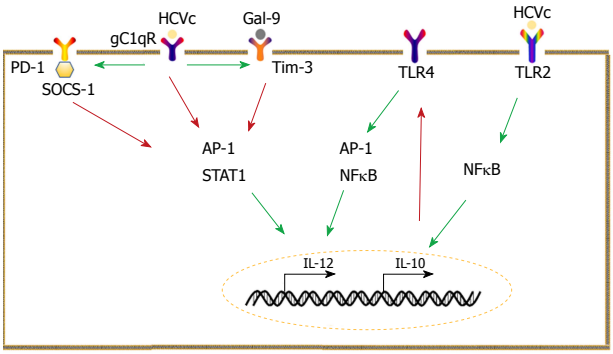

Figure 1 Mechanisms underlying aberrant interleukin-10 and interleukin -12 expression. Monocytes are a main producer of interleukin-10 (IL-10) in hepatitis C virus (HCV) infection. HCV core protein (HCVc) can stimulate monocytes to produce IL-10, which selectively inhibits Toll-like receptor 4 signaling, leading to impairment of interleukin -12 (IL-12). Programmed cell death 1 (PD-1)/ ligand of PD-1 (PD-L1) signaling and the galectin-9 (Gal-9)/ T cell immunoglobulin and mucin domain 3 (Tim-3) pathways suppress IL-12 production by inhibiting activator protein 1 and signal transducer and activator of transcription 1 activation. The interaction between HCVc and receptor for the globular heads of C1q also inhibits IL-12 production but promotes PD-1/PD-L1 and Gal-9/Tim-3 pathways. The red arrow represents inhibition, whereas the green arrow indicates promotion. HCVc: HCV core protein; IL: Interleukin; TLR: Toll-like receptor; PD-1: Programmed cell death 1; PD-L1: Ligand of PD-1; Gal-9: Galectin-9; TIM-3: T cell immunoglobulin and mucin domain 3; AP-1: Activator protein 1; STAT: Signal transducer and activator of transcription; gC1qR: Receptor for the globular heads of C1q; SOCS: Suppressor of cytokine signaling; NFκB: Nuclear factor-κB.

in HCV-specific $CD8^+$ T cell regulation; specifically, IL-10 can reduce the frequency of $CD8^+$ T cells and impair their differentiation[75]. Furthermore, IL-10 preferentially targets TLR4 signaling[76]. The inhibitory role of IL-10 against the production of proinflammatory cytokines was preferentially mediated by TLR4 signaling, *i.e.*, the stimulation of chronic hepatitis C (CHC) patient-derived monocytes by lipopolysaccharide (LPS) (a TLR4 ligand) rather than R848 (a TLR8 agonist) led to lower TNF-α and IL-12 production[76].

Analysis of serum samples collected from CHC patients often shows higher IL-10 levels either produced spontaneously or after stimulation with HCV antigens[77,78]. Particularly, CHC patients have high IL-10 levels and relatively low levels of IFN-γ and IL-2[79], whereas patients with the self-limiting HCV produce lower IL-10 levels in response to both viral antigens and unspecific stimulation[80].

HCV NS4 can stimulate peripheral blood mononuclear cells (PBMCs) to produce IL-10 and transforming growth factor (TGF)-β[81]. TGF-β cooperates with IL-10 to inhibit the host-protective immune responses[82]. Additionally, supernatants of NS4-stimulated monocytes can inhibit DC maturation and DC stimulatory function[81].

In our lab, we studied the network of cytokines that regulate IL-10 production and the cytokines regulated by IL-10 upon HCV infection[74]. The stimulation of monocytes with HCVc and polyI:C induces the secretion of TNF-α, IL-1β, IL-10, and type Ⅰ IFN. Interestingly, TNF-α, IL-1β, and IFN promote the IL-10 production, whereas high IL-10 levels inhibit TNF-α, IL-1β, and IFN production[74]. Furthermore, receptors for IL-10 on monocytes are also elevated during HCV infection and the type Ⅰ as well as type Ⅲ IFNs upregulate the IL-10 monocyte receptors, leading to higher sensitivity of monocytes to IL-10[83].

Programmed cell death-1 (PD-1) is primarily expressed on activated lymphocytes, whereas its ligand (PD-L) is widely expressed by many cells[84]. PD-1/ PD-L interactions can affect responses against self and foreign antigens[84]. Consistently, PD-1/PD-L1 signaling in monocytes has critical roles in HCV infection. Monocytes from CHC patients are endowed with high levels of PD-L1, which enables the suppression of T cell proliferation, reduces the frequency of HCV-specific effector T cells, and downregulates the production of type 1 help T cell (Th1) cytokines as well[85]. PD-L1 signaling downregulates IL-12 expression, leading to low Th1 cytokine production[86]. HCVc interacts with the receptor for the globular heads of C1q (gC1qR) to increase PD-1 expression by monocytes[87]. PD-1 is associated with suppressor of cytokine signaling 1 (SOCS-1), and they work together to inhibit the activation of signal transducer and activator of transcription (STAT)-1 and the subsequent IL-12 production[87].

The galectin-9 (Gal-9) and T cell immunoglobulin and mucin domain 3 (Tim-3) pathway in monocytes is also vital for HCV infection. Monocytes express Gal-9 upon exposure to HCV-infected cells or the subgenomic replicon cells and exosomes from infected cells[88]. Consistently, Tim-3, receptor of Gal-9, is constitutively expressed on resting monocytes and can be up-regulated in CHC patients[89]. HCVc upregulates Tim-3 in a c-Jun N-terminal kinase (JNK) and T-bet-dependent manner[90]. The Gal-9/Tim-3 pathway is involved in the dysfunction of IL-12, IL-23, and IL-17[89,91]. Crosstalk between PD-1 and SOCS-1, Gal-9, and Tim-3 inhibits IL-12 production by limiting STAT-1 phosphorylation[89].

In conclusion, imbalance between IL-10 and IL-12 is a key feature of HCV infection. High levels of IL-10 combined with low IL-12 levels lead to a poor antiviral microenvironment. To make matters worse, HCV-infected patients and healthy controls show different responses to IL-10 and IL-12, *i.e.*, IL-10 can suppress IFN-γ production in both HCV-infected patients and healthy controls, whereas the stimulatory effect of IL-12 on IFN-γ is compromised in HCV-infected patients[92] (Figure 1).

Regulatory function of monocytes following HCV infection: Following HCV infection, monocytes modulate the functions of other immune cells, such as NK cells and T cells. Additionally, NS5A can upregulate IL-10 and TGF-β expression in monocytes, and in turn, these cytokines suppress NK cell function by downregulating the expression of NKG2D, an activating receptor expressed on the surface of NK cells[93]. Furthermore, monocytes secrete the IL-18 and IL-36 inhibitory proteins, which can reduce NK cell activation, TNF-related apoptosis-inducing ligand (TRAIL) expression, and the ability to kill target cells[94]. Monocyte-derived Gal-9 upregulates the cytotoxicity of NK cells, leading to HCV-specific T cell apoptosis and liver injury[95]. Co-culture of

monocytes with T cells leads to elevated mortality rate of T cells[96]. In addition to these detrimental functions, monocytes were found to be beneficial in the following situation: elevated OX40L expression, which is involved in the $CD4^+$ T cell response. Blocking OX40L expression from monocytes leads to HCV-specific $CD4^+$ T cell impairment[97]. Upon co-culture with JFH-1/HuH7.5 cells, NK cells from PBMCs produce high levels of IFN-γ. pDC-derived IFN-α is indispensable for IFN-γ production, whereas the monocyte-derived IL-15 can augment IFN-γ production to the maximum[98].

HCV and DCs

Impaired functions of DCs following HCV infection: *In vivo* study showed that gene expression in DCs from acute HCV resolving patients and from patients who become chronically infected is different[99]. The same result is also confirmed in healthy controls and CHC patients[99]. All these indicate that DCs play an important role in HCV infection.

DCs derived from peripheral blood progenitors *in vitro* enabled the extensive study of DC populations. Compared to healthy control DCs, HCV-DCs (derived from CHC patients) exhibit a normal phenotype and morphology but stimulate allogeneic T cells poorly[100,101]. Owing to the low expression of IL-12 in HCV-DCs, they induce lower amounts of IFN-γ from T cells compared with control DCs in co-cultures of allogeneic DCs and T cells[102]. Additionally, HCV-DCs are refractory to maturation stimuli and maintain an immature phenotype[103]. Interestingly, the observed defects in HCV-DCs are improved after viral clearance[100,103]. In agreement, transfection of DCs from a healthy donor with adenovirus encoding HCV E1 and HCVc resulted in poor ability to stimulate the allogeneic and autologous T cells[104].

To confirm the results obtained from *in vitro* generated DCs, researchers evaluated the functions and phenotypes of blood DCs *ex vivo* directly during chronic HCV infection[105-109]. Compared to those among healthy controls, the frequencies of mDCs, pDCs, and DC progenitors are significantly lower in HCV-infected patients[106,108-110]. DCs from HCV-infected patients have a reduced ability to stimulate allogeneic $CD4^+$ T cells[105,107,110]. Additionally, they show abnormalities in the production of cytokines, such as reduced IFN-α and IL-12 levels[107,110] and increased IL-10 production[107,108]. Interestingly, these defects are resolved after viral elimination, indicating that HCV can indeed infect DCs and alter their function[106,108,109]. Additionally, the tryptophan-catabolizing enzyme indolamine 2,3-dioxygenase (IDO), an inducer of immune tolerance, was found to be significantly increased in mDCs of CHC patients[111]. Moreover, HCV-infected patient monocyte-derived DCs and infected control monocyte-derived DCs (infected *ex vivo* with HCV) show an inability to mature, and this impairment can be reversed by IDO inhibitors[111].

The anti-HCV immune response mainly occurs in the liver; therefore, it is reasonable to speculate that the behavior of circulating DCs can be different from that of liver-resident DCs. Therefore, studies were designed to isolate and characterize human liver DCs[112]. In contrast to the circulating DCs, mDCs from livers of HCV-infected patients did not show noticeable defects in stimulating T cells and produced lower levels of IL-10 than mDCs from healthy individuals[112]. However, the livers of HCV-infected patients harbored decreased numbers of pDCs compared to the livers of healthy individuals[112], and thus, the amount of IFN-α was lower in the HCV-infected patients[112]. In summary, lower amount of IFN-α and lower levels of IL-10 can contribute to persistent viral infection and inflammation in HCV infection, respectively[112].

Additionally, DCs from HCV-infected patients showed lower production of IFN-λ[113], abolished cytotoxic activity[114], upregulated levels of Fas ligand as well as PD-L2[115], and imbalanced expression between the co-stimulatory and co-inhibitory markers[116,117].

HCV-derived mechanisms underlying DC impairment: The mechanisms underlying DC impairment as well as the HCV proteins modulating DC functions have been previously investigated[118]. HCVc and NS3 proteins are involved in the impairment of DC maturation, lower levels of T cell stimulation as well as higher levels of IL-10 production from DCs in HCV-infected patients[64] (Table 1). Additionally, HCVc protein can engage gC1qR to inhibit IL-12 production and further restrain Th1 responses[119]. HCV E2 protein interacts with CD81 of DCs to alter DC migratory behavior, thereby incapacitating the recirculation of DCs to the lymphoid tissue, which can cause impairment of T cell priming[120] (Table 1). In our lab, we isolated liver-derived pDCs from normal liver tissues collected from benign tumor dissections and liver transplant donors. We observed that the interaction of E2 with CD81 inhibits pDC maturation, activation, and IFN-α production[121]. HCV NS4 protein can change the DC phenotype and is involved in the reduction of Th1 cytokine production and impairment of T cell stimulation[122]. NS3 and E2 proteins can hinder IFN-λ production from DCs[113]. NS5A increases IL-8 production from DCs and influences the phosphorylation of STAT1 and STAT2[123] (Table 1).

On the other hand, a number of studies failed to find defects in DCs during HCV infection[124-128]. It was reported that both HCV patients and chimpanzees infected with HCV harbor phenotypic and functional intact mDCs and pDCs[124,125]. DCs (both pDCs and monocyte-derived DCs) from healthy donors and HCV patients show comparable functions[127]. These discrepancies can be attributed to the inhomogeneous disease state of the patient cohorts, technicalities in methods used for DC purification, stimuli used to induce maturation, and the evaluation of discrepant effector functions.

HCV and macrophages

Fundamental functions of macrophages after HCV infection: The number of proinflammatory macrophages is increased significantly in HCV-infected livers, highlighting the importance of macrophages in HCV infection[129-131]. This increase is dependent

Table 1 Hepatitis C virus-derived mechanisms underlying dendritic cell impairment

HCV protein	Target cells	Functional change	Mechanism	Ref.
HCV core and NS3	mDCs	Impaired maturation Impaired T-cell stimulation	Increased IL-10 and decreased IL-12 production	[64]
E2	mDCs	Alter DC migratory behavior	Interacts with CD81	[120]
	pDCs	Inhibited maturation Impaired activation Decreased IFN-α production		[121]
E2 andNS3	mDCs	Impaired IFN-λ production	Not shown	[113]
NS4	mDCs	Th1 cytokine reduction T-cell stimulatory impairment	Not shown	[122]
NS5A	mDCs	Increased IL-8 production Impaired interferon signaling	Not shown Influence the phosphorylation of STAT1 and STAT2	[123]

HCV: Hepatitis C virus; NS: Nonstructural protein; mDC: Myeloid dendritic cell; pDC: Plasmacytoid dendritic cell; IL: Interleukin; Th1: Type 1 help T cell; IFN: Interferon; STAT: Signal transducer and activator of transcription.

on the proliferation of resident KCs and recruitment of monocytes[129]. Macrophages express TRAIL, Fas-ligand, granzyme B, perforin, and reactive oxygen species, which cause direct cytotoxicity to the infected hepatocytes[132,133]. Furthermore, macrophage-derived IL-6 and IL-1β can inhibit HCV replication[134,135]. Moreover, TLR3 and TLR4 ligands can activate KCs to secrete IFN-β, therefore restricting HCV replication[136]. This observation is in agreement with the results obtained by our group. We isolated KCs from living donor allografts and stimulated them with TLR ligands and/or HCVc. Indeed, we observed that TLR3 induced KCs to secrete type Ⅰ IFNs, and this effect was blocked by HCVc[133]. Additionally, KCs were reported to produce TGF-β, IL-10, Gal-9, PD-L1, and PD-L2 during CHC, which suppresses the antiviral functions of T cells[133,137-139].

HCV infection can influence the macrophage phenotype: Burgio *et al*[140] observed that the immunophenotypes of KCs can change during HCV infection. The expression of CD80, CD40, and MHC-Ⅱ was aberrantly regulated during HCV infection. Those KCs form clusters with T cells (mostly $CD4^+$) in the livers from HCV-infected patients. In contrast, in healthy livers, the KC-T cell clusters are scarce and the T cells are mostly $CD8^+$. Taken together, these results indicate that HCV infection can change the phenotype of KCs from efficient antigen endocytic cells to professional antigen-presenting cells[140]. Additionally, the HCV E2 protein can polarize monocyte-derived macrophages to the M2 phenotype by enhancing STAT3 and inhibiting STAT1 activation[141]. In our group, we observed that HCVc can also affect the differentiation states of cells from monocytes to macrophages. Both M1 and M2 polarization are inhibited in a TLR2-dependent manner[142].

Role of macrophages in mediating HCV-associated inflammation: HCV proteins and RNA can activate macrophages, leading to the production of proinflammatory cytokines such as IL-1β, IL-6, IL-18, and TNF-α[62,63,133,143]. It is noteworthy that upon macrophage activation with HCV viral particles, the response is proinflammatory rather than antiviral[57]. This could be attributed to the polyU/UC sequences of HCV RNA, which activate the NLRP3 inflammasome of macrophages. Additionally, macrophage-derived TNF-α was reported to promote HCV entry into polarized hepatoma cells[144]. In HCV-infected patients, LPS can induce significantly high levels of TNF-α, because macrophages of HCV-infected patients are deprived of TLR-tolerance[71,130]. The combination of increased TNF-α production along with the enhanced HCV entry may represent an important mechanism by which macrophages enhance HCV infection and infection-associated inflammation (Figure 2).

Macrophages play an important role in HCV-associated liver fibrosis and/or cirrhosis: Progressive fibrosis and/or cirrhosis is a characteristic of CHC, and macrophages play an important role in this process[145]. In CHC, the role of macrophages in fibrosis is mediated by the pro-inflammatory cytokines IL-1β and TNF-α, which have a well-established pro-fibrotic function[146-149]. Additionally, conditioned medium from HCV-exposed macrophages can modulate the primary human hepatic stellate cells (HSC) and LX2 cell line. CCL5 derived from macrophages activates HSCs, leading to the increased expression of inflammatory and pro-fibrogenic markers such as NLRP3, IL-1β, IL-6, CCL5, TGFβ1, COL4A1, matrix metalloproteinase 2 (MMP2), and α-smooth muscle actin (SMA)[150].

HCV-infected patients have elevated serum levels of macrophage colony-stimulating factor (M-CSF) and IL-34[151], and these proteins are intensely expressed around the liver lesions. *In vitro*, hepatocytes produce IL-34, M-CSF, and inflammatory cytokines in response to HCV infection[151]. IL-34 and M-CSF promote the differentiation of monocytes into macrophages and endow the macrophages with profibrotic properties[151]. These profibrotic macrophages recruit monocytes to the liver and activate HSCs *via* platelet-derived growth factor, TGF-β, and galectin-3[151].

CONCLUSION

Components of the MPS have redundant but non-identical roles in HCV infection. Monocytes act as progenitors for DCs as well as macrophages, and they play an important role in blunting the immune system by

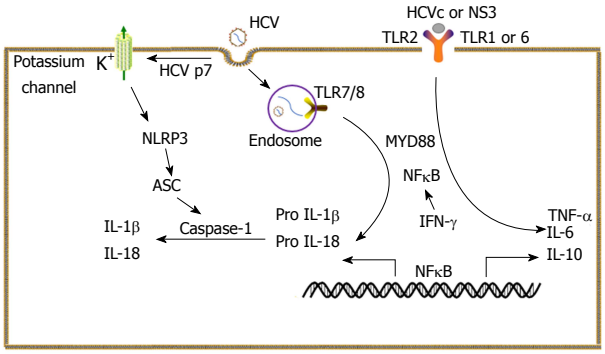

Figure 2 Role of macrophages in hepatitis C virus infection-associated inflammation. During hepatitis C virus (HCV) infection, macrophages are the main source of the proinflammatory cytokines [interleukin (IL)-1β, IL-18, tumor necrosis factor (TNF)-α, and IL-6] and the anti-inflammatory IL-10. The production of IL-1β and IL-18 requires two signals, which are initiated by the uptake of intact HCV particles. Signal 1: Following dendritic cell-specific intercellular adhesion molecule-3-grabbing non-integrin-mediated endocytosis, the HCV genome is released into cytoplasm and the uridine-rich HCV RNA is recognized by endosomal Toll-like receptor 7 (TLR7). This recognition leads to pro-IL-1β and IL-18 production in a myeloid differentiation primary response gene 88 and nuclear factor-κB (NFκB)-dependent manner. Signal 2: Pro IL-1β and IL-18 become activated in this pathway. HCV p7, an ion channel protein, promotes potassium efflux that activates the nucleotide-binding oligomerization domain-like receptor family pyrin domain containing 3 (NLRP3) inflammasome. Utilizing apoptosis-associated speck-like protein containing a CARD as an adaptor protein, NLRP3 activates caspase-1, which induces the maturation of pro-IL-1β and pro-IL-18 into their active forms. HCV core and NS3 proteins interact with TLR1 or TLR6 and TLR2 to activate NFκB, which results in the production of TNF-α, IL-6, and IL-10. Additionally, HCV particles can also be recognized by TLR7/8, inducing TNF-α production. TLR tolerance is a protection mechanism against uncontrolled inflammation. In HCV infection, it can be abrogated by interferon-γ through NF-κB signaling, leading to the production of high levels of proinflammatory cytokines. HCV: Hepatitis C virus; HCVc: HCV core protein; IL: Interleukin; TLR: Toll-like receptor; TNF-α: Tumor necrosis factor α; DC-SIGN: Dendritic cell-specific intercellular adhesion molecule-3-grabbing non-integrin; TLR: Toll-like receptor; MYD88: Myeloid differentiation primary response gene 88; NF-κB: Nuclear factor-κB; NLRP3: Nucleotide-binding oligomerization domain-like receptor family pyrin domain containing 3; ASC: Apoptosis-associated speck-like protein containing a CARD; NS3: Nonstructural protein 3; IFN-γ: Interferon-γ.

secreting large amounts of IL-10 and decreasing IL-12 production. Altered TLR signaling is the most probable cause for abnormal cytokine production in HCV infection. Results from studies examining the impairment of DCs during HCV infection are still controversial. In this review, we adopt the argument that mDCs show a reduced ability to stimulate T cells, whereas pDCs produce decreased amounts of IFN-α in HCV infection. However, a definitive conclusion requires further investigation. Macrophages are a double-edged sword in HCV infection, with both beneficial and detrimental effects. Macrophage-derived proinflammatory cytokines can control the viral spread in acute infection. However, if HCV infection is not controlled, these proinflammatory cytokines contribute to persistent inflammation and complications, including fibrosis and cirrhosis. Persistent inflammation is a characteristic of HCV infection, and thus, the differentiation of monocytes into DCs and macrophages should happen frequently. Will the impairments of the precursor monocytes be inherited by DCs and macrophages? Or will those impairments be reversed during differentiation? These questions remain to be investigated.

The majority of previous studies focused on only one component of the MPS, and thus, data on the interplay and cooperation between MPS components are scarce[98,152,153]. For instance, the recruitment of DCs to the liver requires KCs and the majority of the recruited DCs bind to KCs. This DC-KC binding is indispensable, because KC depletion leads to the inhibition of DC migration to the liver[152]. Furthermore, monocytes produce IL-10 and TNF-α, leading to the apoptosis of pDCs and consequently inhibiting the production of IFN-α by pDCs[153]. Additionally, pDC-derived IFN-α and monocyte-derived IL-15 work together to maximize the IFN-γ induction by NK cells and NKT cells during HCV infection[98]. Other forms of interplay and cooperation involving the MPS remain to be analyzed.

In this review, we describe the impact of HCV infection on each population of the MPS. As a precursor of DCs and macrophages, monocytes are the major contributors to the regulation of the immune system following HCV infection. Monocytes produce high levels of IL-10 and low levels of IL-12, which leads to a blunted microenvironment. On the other hand, DCs demonstrate an impaired ability to stimulate T cells that inhibit efficient anti-HCV T-cell function. As tissue-resident cells, macrophages are tightly associated with HCV-induced inflammation and cirrhosis.

REFERENCES

1 **Douam F**, Lavillette D, Cosset FL. The mechanism of HCV entry into host cells. *Prog Mol Biol Transl Sci* 2015; **129**: 63-107 [PMID: 25595801 DOI: 10.1016/bs.pmbts.2014.10.003]

2 **Szabó E**, Lotz G, Páska C, Kiss A, Schaff Z. Viral hepatitis: new data on hepatitis C infection. *Pathol Oncol Res* 2003; **9**: 215-221 [PMID: 14688826]

3 **Halliday J**, Klenerman P, Barnes E. Vaccination for hepatitis C virus: closing in on an evasive target. *Expert Rev Vaccines* 2011; **10**: 659-672 [PMID: 21604986 DOI: 10.1586/erv.11.55]

4 **Pybus OG**, Barnes E, Taggart R, Lemey P, Markov PV, Rasachak B, Syhavong B, Phetsouvanah R, Sheridan I, Humphreys IS, Lu L, Newton PN, Klenerman P. Genetic history of hepatitis C virus in East Asia. *J Virol* 2009; **83**: 1071-1082 [PMID: 18971279 DOI: 10.1128/JVI.01501-08]

5 **Gray RR**, Salemi M, Klenerman P, Pybus OG. A new evolutionary model for hepatitis C virus chronic infection. *PLoS Pathog* 2012; **8**: e1002656 [PMID: 22570609 DOI: 10.1371/journal.ppat.1002656]

6 **Thomson EC**, Smith JA, Klenerman P. The natural history of early hepatitis C virus evolution; lessons from a global outbreak in human immunodeficiency virus-1-infected individuals. *J Gen Virol* 2011; **92**: 2227-2236 [PMID: 21775583 DOI: 10.1099/vir.0.033910-0]

7 **Loomba R**, Rivera MM, McBurney R, Park Y, Haynes-Williams V, Rehermann B, Alter HJ, Herrine SK, Liang TJ, Hoofnagle JH, Heller T. The natural history of acute hepatitis C: clinical presentation, laboratory findings and treatment outcomes. *Aliment Pharmacol Ther* 2011; **33**: 559-565 [PMID: 21198704 DOI: 10.1111/j.1365-2036.2010.04549.x]

8 **Thomson EC**, Fleming VM, Main J, Klenerman P, Weber J, Eliahoo J, Smith J, McClure MO, Karayiannis P. Predicting spontaneous clearance of acute hepatitis C virus in a large cohort of HIV-1-infected men. *Gut* 2011; **60**: 837-845 [PMID: 21139063 DOI: 10.1136/gut.2010.217166]

9 **Zaltron S**, Spinetti A, Biasi L, Baiguera C, Castelli F. Chronic HCV infection: epidemiological and clinical relevance. *BMC Infect Dis* 2012; **12** Suppl 2: S2 [PMID: 23173556 DOI: 10.1186/1471-2334-12-S2-S2]

10 **Webster DP**, Klenerman P, Dusheiko GM. Hepatitis C. *Lancet* 2015; **385**: 1124-1135 [PMID: 25687730 DOI: 10.1016/S0140-6736(14)62401-6]

11 **Fried MW**, Shiffman ML, Reddy KR, Smith C, Marinos G, Gonçales FL Jr, Häussinger D, Diago M, Carosi G, Dhumeaux D, Craxi A, Lin A, Hoffman J, Yu J. Peginterferon alfa-2a plus ribavirin for chronic hepatitis C virus infection. *N Engl J Med* 2002; **347**: 975-982 [PMID: 12324553 DOI: 10.1056/NEJMoa020047]

12 **Poordad F**, McCone J Jr, Bacon BR, Bruno S, Manns MP, Sulkowski MS, Jacobson IM, Reddy KR, Goodman ZD, Boparai N, DiNubile MJ, Sniukiene V, Brass CA, Albrecht JK, Bronowicki JP; SPRINT-2 Investigators. Boceprevir for untreated chronic HCV genotype 1 infection. *N Engl J Med* 2011; **364**: 1195-1206 [PMID: 21449783 DOI: 10.1056/NEJMoa1010494]

13 **Jacobson IM**, McHutchison JG, Dusheiko G, Di Bisceglie AM, Reddy KR, Bzowej NH, Marcellin P, Muir AJ, Ferenci P, Flisiak R, George J, Rizzetto M, Shouval D, Sola R, Terg RA, Yoshida EM, Adda N, Bengtsson L, Sankoh AJ, Kieffer TL, George S, Kauffman RS, Zeuzem S; ADVANCE Study Team. Telaprevir for previously untreated chronic hepatitis C virus infection. *N Engl J Med* 2011; **364**: 2405-2416 [PMID: 21696307 DOI: 10.1056/NEJMoa1012912]

14 **Jenkins SJ**, Hume DA. Homeostasis in the mononuclear phagocyte system. *Trends Immunol* 2014; **35**: 358-367 [PMID: 25047416 DOI: 10.1016/j.it.2014.06.006]

15 **Yona S**, Kim KW, Wolf Y, Mildner A, Varol D, Breker M, Strauss-Ayali D, Viukov S, Guilliams M, Misharin A, Hume DA, Perlman H, Malissen B, Zelzer E, Jung S. Fate mapping reveals origins and dynamics of monocytes and tissue macrophages under homeostasis. *Immunity* 2013; **38**: 79-91 [PMID: 23273845 DOI: 10.1016/j.immuni.2012.12.001]

16 **Hettinger J**, Richards DM, Hansson J, Barra MM, Joschko AC, Krijgsveld J, Feuerer M. Origin of monocytes and macrophages in a committed progenitor. *Nat Immunol* 2013; **14**: 821-830 [PMID: 23812096 DOI: 10.1038/ni.2638]

17 **Epelman S**, Lavine KJ, Beaudin AE, Sojka DK, Carrero JA, Calderon B, Brija T, Gautier EL, Ivanov S, Satpathy AT, Schilling JD, Schwendener R, Sergin I, Razani B, Forsberg EC, Yokoyama WM, Unanue ER, Colonna M, Randolph GJ, Mann DL. Embryonic and adult-derived resident cardiac macrophages are maintained through distinct mechanisms at steady state and during inflammation. *Immunity* 2014; **40**: 91-104 [PMID: 24439267 DOI: 10.1016/j.immuni.2013.11.019]

18 **Varol C**, Vallon-Eberhard A, Elinav E, Aychek T, Shapira Y, Luche H, Fehling HJ, Hardt WD, Shakhar G, Jung S. Intestinal lamina propria dendritic cell subsets have different origin and functions. *Immunity* 2009; **31**: 502-512 [PMID: 19733097 DOI: 10.1016/j.immuni.2009.06.025]

19 **Bogunovic M**, Ginhoux F, Helft J, Shang L, Hashimoto D, Greter M, Liu K, Jakubzick C, Ingersoll MA, Leboeuf M, Stanley ER, Nussenzweig M, Lira SA, Randolph GJ, Merad M. Origin of the lamina propria dendritic cell network. *Immunity* 2009; **31**: 513-525 [PMID: 19733489 DOI: 10.1016/j.immuni.2009.08.010]

20 **Serbina NV**, Pamer EG. Monocyte emigration from bone marrow during bacterial infection requires signals mediated by chemokine receptor CCR2. *Nat Immunol* 2006; **7**: 311-317 [PMID: 16462739 DOI: 10.1038/ni1309]

21 **Geissmann F**. The origin of dendritic cells. *Nat Immunol* 2007; **8**: 558-560 [PMID: 17514208 DOI: 10.1038/ni0607-558]

22 **Varol C**, Landsman L, Fogg DK, Greenshtein L, Gildor B, Margalit R, Kalchenko V, Geissmann F, Jung S. Monocytes give rise to mucosal, but not splenic, conventional dendritic cells. *J Exp Med* 2007; **204**: 171-180 [PMID: 17190836 DOI: 10.1084/jem.20061011]

23 **Serbina NV**, Jia T, Hohl TM, Pamer EG. Monocyte-mediated defense against microbial pathogens. *Annu Rev Immunol* 2008; **26**: 421-452 [PMID: 18303997 DOI: 10.1146/annurev.immunol.26.021607.090326]

24 **Auffray C**, Sieweke MH, Geissmann F. Blood monocytes: development, heterogeneity, and relationship with dendritic cells. *Annu Rev Immunol* 2009; **27**: 669-692 [PMID: 19132917 DOI: 10.1146/annurev.immunol.021908.132557]

25 **Strauss O**, Dunbar PR, Bartlett A, Phillips A. The immunophenotype of antigen presenting cells of the mononuclear phagocyte system in normal human liver--a systematic review. *J Hepatol* 2015; **62**: 458-468 [PMID: 25315649 DOI: 10.1016/j.jhep.2014.10.006]

26 **Collin M**, McGovern N, Haniffa M. Human dendritic cell subsets. *Immunology* 2013; **140**: 22-30 [PMID: 23621371 DOI: 10.1111/imm.12117]

27 **Bamboat ZM**, Stableford JA, Plitas G, Burt BM, Nguyen HM, Welles AP, Gonen M, Young JW, DeMatteo RP. Human liver dendritic cells promote T cell hyporesponsiveness. *J Immunol* 2009; **182**: 1901-1911 [PMID: 19201843 DOI: 10.4049/jimmunol.0803404]

28 **Goddard S**, Youster J, Morgan E, Adams DH. Interleukin-10 secretion differentiates dendritic cells from human liver and skin. *Am J Pathol* 2004; **164**: 511-519 [PMID: 14742257 DOI: 10.1016/s0002-9440(10)63141-0]

29 **Zhu J**, Yamane H, Paul WE. Differentiation of effector CD4 T cell populations (*). *Annu Rev Immunol* 2010; **28**: 445-489 [PMID: 20192806 DOI: 10.1146/annurev-immunol-030409-101212]

30 **Cabillic F**, Rougier N, Basset C, Lecouillard I, Quelvennec E, Toujas L, Guguen-Guillouzo C, Corlu A. Hepatic environment elicits monocyte differentiation into a dendritic cell subset directing Th2 response. *J Hepatol* 2006; **44**: 552-559 [PMID: 16310277 DOI: 10.1016/j.jhep.2005.08.010]

31 **Tomiyama C**, Watanabe H, Izutsu Y, Watanabe M, Abo T. Suppressive role of hepatic dendritic cells in concanavalin A-induced hepatitis. *Clin Exp Immunol* 2011; **166**: 258-268 [PMID: 21985372 DOI: 10.1111/j.1365-2249.2011.04458.x]

32 **Wynn TA**, Chawla A, Pollard JW. Macrophage biology in development, homeostasis and disease. *Nature* 2013; **496**: 445-455 [PMID: 23619691 DOI: 10.1038/nature12034]

33 **Kwekkeboom J**, Kuijpers MA, Bruyneel B, Mancham S, De Baar-Heesakkers E, Ijzermans JN, Bouma GJ, Zondervan PE, Tilanus HW, Metselaar HJ. Expression of CD80 on Kupffer cells is enhanced in cadaveric liver transplants. *Clin Exp Immunol* 2003; **132**: 345-351 [PMID: 12699427 DOI: 10.1046/j.1365-2249.2003.02129.x]

34 **Guo S**, Yang C, Mei F, Wu S, Luo N, Fei L, Chen Y, Wu Y. Down-regulation of Z39Ig on macrophages by IFN-gamma in patients with chronic HBV infection. *Clin Immunol* 2010; **136**: 282-291 [PMID: 20399148 DOI: 10.1016/j.clim.2010.03.007]

35 **Davies LC**, Jenkins SJ, Allen JE, Taylor PR. Tissue-resident macrophages. *Nat Immunol* 2013; **14**: 986-995 [PMID: 24048120 DOI: 10.1038/ni.2705]

36 **Wahid B**, Ali A, Rafique S, Saleem K, Waqar M, Wasim M, Idrees M. Role of altered immune cells in liver diseases: a review. *Gastroenterol Hepatol* 2018; **41**: 377-388 [PMID: 29605453 DOI: 10.1016/j.gastrohep.2018.01.014]

37 **Krenkel O**, Tacke F. Liver macrophages in tissue homeostasis and disease. *Nat Rev Immunol* 2017; **17**: 306-321 [PMID: 28317925 DOI: 10.1038/nri.2017.11]

38 **Le Bail B**, Bioulac-Sage P, Senuita R, Quinton A, Saric J, Balabaud C. Fine structure of hepatic sinusoids and sinusoidal cells in disease. *J Electron Microsc Tech* 1990; **14**: 257-282 [PMID: 2338589 DOI: 10.1002/jemt.1060140307]

39 **Tu Z**, Bozorgzadeh A, Pierce RH, Kurtis J, Crispe IN, Orloff MS. TLR-dependent cross talk between human Kupffer cells and NK cells. *J Exp Med* 2008; **205**: 233-244 [PMID: 18195076 DOI: 10.1084/jem.20072195]

40 **Fearon DT**, Locksley RM. The instructive role of innate immunity in the acquired immune response. *Science* 1996; **272**: 50-53 [PMID: 8600536 DOI: 10.1126/science.272.5258.50]

41 **Stijlemans B**, De Baetselier P, Magez S, Van Ginderachter JA, De Trez C. African Trypanosomiasis-Associated Anemia: The Contribution of the Interplay between Parasites and the Mononuclear Phagocyte System. *Front Immunol*2018; **9**: 218 [PMID: 29497418 DOI: 10.3389/fimmu.2018.00218]

42 **Pahari S**, Kaur G, Negi S, Aqdas M, Das DK, Bashir H, Singh S,

Nagare M, Khan J, Agrewala JN. Reinforcing the Functionality of Mononuclear Phagocyte System to Control Tuberculosis. *Front Immunol* 2018; **9**: 193 [PMID: 29479353 DOI: 10.3389/fimmu.2018.00193]

43 **Perry VH**, Lawson LJ, Reid DM. Biology of the mononuclear phagocyte system of the central nervous system and HIV infection. *J Leukoc Biol* 1994; **56**: 399-406 [PMID: 8083615 DOI: 10.1002/jlb.56.3.399]

44 **Roy S**, Wainberg MA. Role of the mononuclear phagocyte system in the development of acquired immunodeficiency syndrome (AIDS). *J Leukoc Biol* 1988; **43**: 91-97 [PMID: 3275735 DOI: 10.1002/jlb.43.1.91]

45 **Bohmwald K**, Espinoza JA, Pulgar RA, Jara EL, Kalergis AM. Functional Impairment of Mononuclear Phagocyte System by the Human Respiratory Syncytial Virus. *Front Immunol* 2017; **8**: 1643 [PMID: 29230219 DOI: 10.3389/fimmu.2017.01643]

46 **Sumpter R Jr**, Loo YM, Foy E, Li K, Yoneyama M, Fujita T, Lemon SM, Gale M Jr. Regulating intracellular antiviral defense and permissiveness to hepatitis C virus RNA replication through a cellular RNA helicase, RIG-I. *J Virol* 2005; **79**: 2689-2699 [PMID: 15708988 DOI: 10.1128/jvi.79.5.2689-2699.2005]

47 **Saito T**, Owen DM, Jiang F, Marcotrigiano J, Gale M Jr. Innate immunity induced by composition-dependent RIG-I recognition of hepatitis C virus RNA. *Nature* 2008; **454**: 523-527 [PMID: 18548002 DOI: 10.1038/nature07106]

48 **Uzri D**, Gehrke L. Nucleotide sequences and modifications that determine RIG-I/RNA binding and signaling activities. *J Virol* 2009; **83**: 4174-4184 [PMID: 19224987 DOI: 10.1128/JVI.02449-08]

49 **Andrus L**, Marukian S, Jones CT, Catanese MT, Sheahan TP, Schoggins JW, Barry WT, Dustin LB, Trehan K, Ploss A, Bhatia SN, Rice CM. Expression of paramyxovirus V proteins promotes replication and spread of hepatitis C virus in cultures of primary human fetal liver cells. *Hepatology* 2011; **54**: 1901-1912 [PMID: 22144107 DOI: 10.1002/hep.24557]

50 **Loo YM**, Fornek J, Crochet N, Bajwa G, Perwitasari O, Martinez-Sobrido L, Akira S, Gill MA, García-Sastre A, Katze MG, Gale M Jr. Distinct RIG-I and MDA5 signaling by RNA viruses in innate immunity. *J Virol* 2008; **82**: 335-345 [PMID: 17942531 DOI: 10.1128/jvi.01080-07]

51 **Kato H**, Takeuchi O, Mikamo-Satoh E, Hirai R, Kawai T, Matsushita K, Hiiragi A, Dermody TS, Fujita T, Akira S. Length-dependent recognition of double-stranded ribonucleic acids by retinoic acid-inducible gene-I and melanoma differentiation-associated gene 5. *J Exp Med* 2008; **205**: 1601-1610 [PMID: 18591409 DOI: 10.1084/jem.20080091]

52 **Pichlmair A**, Schulz O, Tan CP, Rehwinkel J, Kato H, Takeuchi O, Akira S, Way M, Schiavo G, Reis e Sousa C. Activation of MDA5 requires higher-order RNA structures generated during virus infection. *J Virol* 2009; **83**: 10761-10769 [PMID: 19656871 DOI: 10.1128/JVI.00770-09]

53 **Fredericksen BL**, Keller BC, Fornek J, Katze MG, Gale M Jr. Establishment and maintenance of the innate antiviral response to West Nile Virus involves both RIG-I and MDA5 signaling through IPS-1. *J Virol* 2008; **82**: 609-616 [PMID: 17977974 DOI: 10.1128/jvi.01305-07]

54 **Wang N**, Liang Y, Devaraj S, Wang J, Lemon SM, Li K. Toll-like receptor 3 mediates establishment of an antiviral state against hepatitis C virus in hepatoma cells. *J Virol* 2009; **83**: 9824-9834 [PMID: 19625408 DOI: 10.1128/JVI.01125-09]

55 **Dansako H**, Yamane D, Welsch C, McGivern DR, Hu F, Kato N, Lemon SM. Class A scavenger receptor 1 (MSR1) restricts hepatitis C virus replication by mediating toll-like receptor 3 recognition of viral RNAs produced in neighboring cells. *PLoS Pathog* 2013; **9**: e1003345 [PMID: 23717201 DOI: 10.1371/journal.ppat.1003345]

56 **Zhang YL**, Guo YJ, Bin Li, Sun SH. Hepatitis C virus single-stranded RNA induces innate immunity via Toll-like receptor 7. *J Hepatol* 2009; **51**: 29-38 [PMID: 19443072 DOI: 10.1016/j.jhep.2009.03.012]

57 **Zhang Y**, El-Far M, Dupuy FP, Abdel-Hakeem MS, He Z, Procopio FA, Shi Y, Haddad EK, Ancuta P, Sekaly RP, Said EA. HCV RNA Activates APCs via TLR7/TLR8 While Virus Selectively Stimulates Macrophages Without Inducing Antiviral Responses. *Sci Rep* 2016; **6**: 29447 [PMID: 27385120 DOI: 10.1038/srep29447]

58 **Dolganiuc A**, Oak S, Kodys K, Golenbock DT, Finberg RW, Kurt-Jones E, Szabo G. Hepatitis C core and nonstructural 3 proteins trigger toll-like receptor 2-mediated pathways and inflammatory activation. *Gastroenterology* 2004; **127**: 1513-1524 [PMID: 15521019 DOI: 10.1053/j.gastro.2004.08.067]

59 **Ferreon JC**, Ferreon AC, Li K, Lemon SM. Molecular determinants of TRIF proteolysis mediated by the hepatitis C virus NS3/4A protease. *J Biol Chem* 2005; **280**: 20483-20492 [PMID: 15767257 DOI: 10.1074/jbc.M500422200]

60 **Katakura K**, Lee J, Rachmilewitz D, Li G, Eckmann L, Raz E. Toll-like receptor 9-induced type I IFN protects mice from experimental colitis. *J Clin Invest* 2005; **115**: 695-702 [PMID: 15765149 DOI: 10.1172/jci22996]

61 **Takahashi K**, Asabe S, Wieland S, Garaigorta U, Gastaminza P, Isogawa M, Chisari FV. Plasmacytoid dendritic cells sense hepatitis C virus-infected cells, produce interferon, and inhibit infection. *Proc Natl Acad Sci USA* 2010; **107**: 7431-7436 [PMID: 20231459 DOI: 10.1073/pnas.1002301107]

62 **Negash AA**, Ramos HJ, Crochet N, Lau DT, Doehle B, Papic N, Delker DA, Jo J, Bertoletti A, Hagedorn CH, Gale M Jr. IL-1β production through the NLRP3 inflammasome by hepatic macrophages links hepatitis C virus infection with liver inflammation and disease. *PLoS Pathog* 2013; **9**: e1003330 [PMID: 23633957 DOI: 10.1371/journal.ppat.1003330]

63 **Shrivastava S**, Mukherjee A, Ray R, Ray RB. Hepatitis C virus induces interleukin-1β (IL-1β)/IL-18 in circulatory and resident liver macrophages. *J Virol* 2013; **87**: 12284-12290 [PMID: 24006444 DOI: 10.1128/JVI.01962-13]

64 **Dolganiuc A**, Kodys K, Kopasz A, Marshall C, Do T, Romics L Jr, Mandrekar P, Zapp M, Szabo G. Hepatitis C virus core and nonstructural protein 3 proteins induce pro- and anti-inflammatory cytokines and inhibit dendritic cell differentiation. *J Immunol* 2003; **170**: 5615-5624 [PMID: 12759441 DOI: 10.4049/jimmunol.170.11.5615]

65 **Chang S**, Dolganiuc A, Szabo G. Toll-like receptors 1 and 6 are involved in TLR2-mediated macrophage activation by hepatitis C virus core and NS3 proteins. *J Leukoc Biol* 2007; **82**: 479-487 [PMID: 17595379 DOI: 10.1189/jlb.0207128]

66 **Lee CM**, Hu TH, Lu SN, Wang JH, Hung CH, Chen CH, Yen YH. Peripheral blood toll-like receptor 4 correlates with rapid virological response to pegylated-interferon and ribavirin therapy in hepatitis C genotype 1 patients. *BMC Gastroenterol* 2016; **16**: 73 [PMID: 27457659 DOI: 10.1186/s12876-016-0492-6]

67 **Riordan SM**, Skinner NA, Kurtovic J, Locarnini S, McIver CJ, Williams R, Visvanathan K. Toll-like receptor expression in chronic hepatitis C: correlation with pro-inflammatory cytokine levels and liver injury. *Inflamm Res* 2006; **55**: 279-285 [PMID: 16955390 DOI: 10.1007/s00011-006-0082-0]

68 **Wang JP**, Zhang Y, Wei X, Li J, Nan XP, Yu HT, Li Y, Wang PZ, Bai XF. Circulating Toll-like receptor (TLR) 2, TLR4, and regulatory T cells in patients with chronic hepatitis C. *APMIS* 2010; **118**: 261-270 [PMID: 20402671 DOI: 10.1111/j.1600-0463.2010.02586.x]

69 **Sato K**, Ishikawa T, Okumura A, Yamauchi T, Sato S, Ayada M, Matsumoto E, Hotta N, Oohashi T, Fukuzawa Y, Kakumu S. Expression of Toll-like receptors in chronic hepatitis C virus infection. *J Gastroenterol Hepatol* 2007; **22**: 1627-1632 [PMID: 17845690 DOI: 10.1111/j.1440-1746.2006.04783.x]

70 **Villacres MC**, Literat O, DeGiacomo M, Du W, Frederick T, Kovacs A. Defective response to Toll-like receptor 3 and 4 ligands by activated monocytes in chronic hepatitis C virus infection. *J Viral Hepat* 2008; **15**: 137-144 [PMID: 18184197 DOI: 10.1111/j.1365-2893.2007.00904.x]

71 **Dolganiuc A**, Norkina O, Kodys K, Catalano D, Bakis G, Marshall C, Mandrekar P, Szabo G. Viral and host factors induce macrophage activation and loss of toll-like receptor tolerance in chronic HCV infection. *Gastroenterology* 2007; **133**: 1627-1636 [PMID: 17916356 DOI: 10.1053/j.gastro.2007.08.003]

72 **Chung H**, Watanabe T, Kudo M, Chiba T. Hepatitis C virus core protein induces homotolerance and cross-tolerance to Toll-like

receptor ligands by activation of Toll-like receptor 2. *J Infect Dis* 2010; **202**: 853-861 [PMID: 20677943 DOI: 10.1086/655812]
73 **Chung H**, Watanabe T, Kudo M, Chiba T. Correlation between hyporesponsiveness to Toll-like receptor ligands and liver dysfunction in patients with chronic hepatitis C virus infection. *J Viral Hepat* 2011; **18**: e561-e567 [PMID: 21914077 DOI: 10.1111/j.1365-2893.2011.01478.x]
74 **Pang X**, Wang Z, Zhai N, Zhang Q, Song H, Zhang Y, Li T, Li H, Su L, Niu J, Tu Z. IL-10 plays a central regulatory role in the cytokines induced by hepatitis C virus core protein and polyinosinic acid: polycytodylic acid. *Int Immunopharmacol* 2016; **38**: 284-290 [PMID: 27337528 DOI: 10.1016/j.intimp.2016.06.013]
75 **Niesen E**, Schmidt J, Flecken T, Thimme R. Suppressive effect of interleukin 10 on priming of naive hepatitis C virus-specific CD8+ T cells. *J Infect Dis* 2015; **211**: 821-826 [PMID: 25355941 DOI: 10.1093/infdis/jiu541]
76 **Liu BS**, Groothuismink ZM, Janssen HL, Boonstra A. Role for IL-10 in inducing functional impairment of monocytes upon TLR4 ligation in patients with chronic HCV infections. *J Leukoc Biol* 2011; **89**: 981-988 [PMID: 21385948 DOI: 10.1189/jlb.1210680]
77 **Amaraa R**, Mareckova H, Urbanek P, Fucikova T. Production of interleukins 10 and 12 by activated peripheral blood monocytes/macrophages in patients suffering from chronic hepatitis C virus infection with respect to the response to interferon and ribavirin treatment. *Immunol Lett* 2002; **83**: 209-214 [PMID: 12095711 DOI: 10.1016/s0165-2478(02)00102-5]
78 **Woitas RP**, Petersen U, Moshage D, Brackmann HH, Matz B, Sauerbruch T, Spengler U. HCV-specific cytokine induction in monocytes of patients with different outcomes of hepatitis C. *World J Gastroenterol* 2002; **8**: 562-566 [PMID: 12046093 DOI: 10.3748/wjg.v8.i3.562]
79 **Flynn JK**, Dore GJ, Hellard M, Yeung B, Rawlinson WD, White PA, Kaldor JM, Lloyd AR, Ffrench RA; ATAHC Study Group. Early IL-10 predominant responses are associated with progression to chronic hepatitis C virus infection in injecting drug users. *J Viral Hepat* 2011; **18**: 549-561 [PMID: 20626625 DOI: 10.1111/j.1365-2893.2010.01335.x]
80 **Martin-Blondel G**, Gales A, Bernad J, Cuzin L, Delobel P, Barange K, Izopet J, Pipy B, Alric L. Low interleukin-10 production by monocytes of patients with a self-limiting hepatitis C virus infection. *J Viral Hepat* 2009; **16**: 485-491 [PMID: 19302337 DOI: 10.1111/j.1365-2893.2009.01094.x]
81 **Brady MT**, MacDonald AJ, Rowan AG, Mills KH. Hepatitis C virus non-structural protein 4 suppresses Th1 responses by stimulating IL-10 production from monocytes. *Eur J Immunol* 2003; **33**: 3448-3457 [PMID: 14635055 DOI: 10.1002/eji.200324251]
82 **Rowan AG**, Fletcher JM, Ryan EJ, Moran B, Hegarty JE, O'Farrelly C, Mills KH. Hepatitis C virus-specific Th17 cells are suppressed by virus-induced TGF-beta. *J Immunol* 2008; **181**: 4485-4494 [PMID: 18802051 DOI: 10.4049/jimmunol.181.7.4485]
83 **Liu BS**, Janssen HL, Boonstra A. Type I and III interferons enhance IL-10R expression on human monocytes and macrophages, resulting in IL-10-mediated suppression of TLR-induced IL-12. *Eur J Immunol* 2012; **42**: 2431-2440 [PMID: 22685028 DOI: 10.1002/eji.201142360]
84 **Chamoto K**, Al-Habsi M, Honjo T. Role of PD-1 in Immunity and Diseases. *Curr Top Microbiol Immunol* 2017; **410**: 75-97 [PMID: 28929192 DOI: 10.1007/82_2017_67]
85 **Jeong HY**, Lee YJ, Seo SK, Lee SW, Park SJ, Lee JN, Sohn HS, Yao S, Chen L, Choi I. Blocking of monocyte-associated B7-H1 (CD274) enhances HCV-specific T cell immunity in chronic hepatitis C infection. *J Leukoc Biol* 2008; **83**: 755-764 [PMID: 18086898 DOI: 10.1189/jlb.0307168]
86 **Ma CJ**, Ni L, Zhang Y, Zhang CL, Wu XY, Atia AN, Thayer P, Moorman JP, Yao ZQ. PD-1 negatively regulates interleukin-12 expression by limiting STAT-1 phosphorylation in monocytes/macrophages during chronic hepatitis C virus infection. *Immunology* 2011; **132**: 421-431 [PMID: 21091911 DOI: 10.1111/j.1365-2567.2010.03382.x]
87 **Zhang Y**, Ma CJ, Ni L, Zhang CL, Wu XY, Kumaraguru U, Li CF, Moorman JP, Yao ZQ. Cross-talk between programmed death-1 and suppressor of cytokine signaling-1 in inhibition of IL-12 production by monocytes/macrophages in hepatitis C virus infection. *J Immunol* 2011; **186**: 3093-3103 [PMID: 21263070 DOI: 10.4049/jimmunol.1002006]
88 **Harwood NM**, Golden-Mason L, Cheng L, Rosen HR, Mengshol JA. HCV-infected cells and differentiation increase monocyte immunoregulatory galectin-9 production. *J Leukoc Biol* 2016; **99**: 495-503 [PMID: 26475932 DOI: 10.1189/jlb.5A1214-582R]
89 **Zhang Y**, Ma CJ, Wang JM, Ji XJ, Wu XY, Jia ZS, Moorman JP, Yao ZQ. Tim-3 negatively regulates IL-12 expression by monocytes in HCV infection. *PLoS One* 2011; **6**: e19664 [PMID: 21637332 DOI: 10.1371/journal.pone.0019664]
90 **Yi W**, Zhang P, Liang Y, Zhou Y, Shen H, Fan C, Moorman JP, Yao ZQ, Jia Z, Zhang Y. T-bet-mediated Tim-3 expression dampens monocyte function during chronic hepatitis C virus infection. *Immunology* 2017; **150**: 301-311 [PMID: 27809352 DOI: 10.1111/imm.12686]
91 **Wang JM**, Shi L, Ma CJ, Ji XJ, Ying RS, Wu XY, Wang KS, Li G, Moorman JP, Yao ZQ. Differential regulation of interleukin-12 (IL-12)/IL-23 by Tim-3 drives T(H)17 cell development during hepatitis C virus infection. *J Virol* 2013; **87**: 4372-4383 [PMID: 23388728 DOI: 10.1128/JVI.03376-12]
92 **Kakumu S**, Okumura A, Ishikawa T, Iwata K, Yano M, Yoshioka K. Production of interleukins 10 and 12 by peripheral blood mononuclear cells (PBMC) in chronic hepatitis C virus (HCV) infection. *Clin Exp Immunol* 1997; **108**: 138-143 [PMID: 9097922 DOI: 10.1046/j.1365-2249.1997.d01-987.x]
93 **Sène D**, Levasseur F, Abel M, Lambert M, Camous X, Hernandez C, Pène V, Rosenberg AR, Jouvin-Marche E, Marche PN, Cacoub P, Caillat-Zucman S. Hepatitis C virus (HCV) evades NKG2D-dependent NK cell responses through NS5A-mediated imbalance of inflammatory cytokines. *PLoS Pathog* 2010; **6**: e1001184 [PMID: 21085608 DOI: 10.1371/journal.ppat.1001184]
94 **Mele D**, Mantovani S, Oliviero B, Grossi G, Lombardi A, Mondelli MU, Varchetta S. Monocytes inhibit hepatitis C virus-induced TRAIL expression on $CD56^{bright}$ NK cells. *J Hepatol* 2017; **67**: 1148-1156 [PMID: 28803951 DOI: 10.1016/j.jhep.2017.07.028]
95 **Nishio A**, Tatsumi T, Nawa T, Suda T, Yoshioka T, Onishi Y, Aono S, Shigekawa M, Hikita H, Sakamori R, Okuzaki D, Fukuhara T, Matsuura Y, Hiramatsu N, Takehara T. $CD14^{+}$ monocyte-derived galectin-9 induces natural killer cell cytotoxicity in chronic hepatitis C. *Hepatology* 2017; **65**: 18-31 [PMID: 27640362 DOI: 10.1002/hep.28847]
96 **Nakamoto Y**, Kaneko S, Kobayashi K. Monocyte-dependent cell death of T lymphocyte subsets in chronic hepatitis C. *Immunol Lett* 2001; **78**: 169-174 [PMID: 11578691 DOI: 10.1016/s0165-2478(01)00257-7]
97 **Zhang JY**, Wu XL, Yang B, Wang Y, Feng GH, Jiang TJ, Zeng QL, Xu XS, Li YY, Jin L, Lv S, Zhang Z, Fu J, Wang FS. Upregulation of OX40 ligand on monocytes contributes to early virological control in patients with chronic hepatitis C. *Eur J Immunol* 2013; **43**: 1953-1962 [PMID: 23589118 DOI: 10.1002/eji.201243097]
98 **Zhang S**, Saha B, Kodys K, Szabo G. IFN-γ production by human natural killer cells in response to HCV-infected hepatoma cells is dependent on accessory cells. *J Hepatol* 2013; **59**: 442-449 [PMID: 23665181 DOI: 10.1016/j.jhep.2013.04.022]
99 **Zabaleta A**, Riezu-Boj JI, Larrea E, Villanueva L, Lasarte JJ, Guruceaga E, Fisicaro P, Ezzikouri S, Missale G, Ferrari C, Benjelloun S, Prieto J, Sarobe P. Gene expression analysis during acute hepatitis C virus infection associates dendritic cell activation with viral clearance. *J Med Virol* 2016; **88**: 843-851 [PMID: 26447929 DOI: 10.1002/jmv.24399]
100 **Bain C**, Fatmi A, Zoulim F, Zarski JP, Trépo C, Inchauspé G. Impaired allostimulatory function of dendritic cells in chronic hepatitis C infection. *Gastroenterology* 2001; **120**: 512-524 [PMID: 11159892 DOI: 10.1053/gast.2001.21212]
101 **Ryan EJ**, Stevenson NJ, Hegarty JE, O'Farrelly C. Chronic hepatitis C infection blocks the ability of dendritic cells to secrete IFN-α and stimulate T-cell proliferation. *J Viral Hepat* 2011; **18**: 840-851 [PMID: 22093032 DOI: 10.1111/j.1365-2893.2010.01384.x]

102 **Kanto T**, Hayashi N, Takehara T, Tatsumi T, Kuzushita N, Ito A, Sasaki Y, Kasahara A, Hori M. Impaired allostimulatory capacity of peripheral blood dendritic cells recovered from hepatitis C virus-infected individuals. *J Immunol* 1999; **162**: 5584-5591 [PMID: 10228041]

103 **Auffermann-Gretzinger S**, Keeffe EB, Levy S. Impaired dendritic cell maturation in patients with chronic, but not resolved, hepatitis C virus infection. *Blood* 2001; **97**: 3171-3176 [PMID: 11342445 DOI: 10.1182/blood.v97.10.3171]

104 **Sarobe P**, Lasarte JJ, Casares N, López-Díaz de Cerio A, Baixeras E, Labarga P, García N, Borrás-Cuesta F, Prieto J. Abnormal priming of CD4(+) T cells by dendritic cells expressing hepatitis C virus core and E1 proteins. *J Virol* 2002; **76**: 5062-5070 [PMID: 11967322 DOI: 10.1128/jvi.76.10.5062-5070.2002]

105 **Tsubouchi E**, Akbar SM, Horiike N, Onji M. Infection and dysfunction of circulating blood dendritic cells and their subsets in chronic hepatitis C virus infection. *J Gastroenterol* 2004; **39**: 754-762 [PMID: 15338369 DOI: 10.1007/s00535-003-1385-3]

106 **Wertheimer AM**, Bakke A, Rosen HR. Direct enumeration and functional assessment of circulating dendritic cells in patients with liver disease. *Hepatology* 2004; **40**: 335-345 [PMID: 15368438 DOI: 10.1002/hep.20306]

107 **Averill L**, Lee WM, Karandikar NJ. Differential dysfunction in dendritic cell subsets during chronic HCV infection. *Clin Immunol* 2007; **123**: 40-49 [PMID: 17239662 DOI: 10.1016/j.clim.2006.12.001]

108 **Della Bella S**, Crosignani A, Riva A, Presicce P, Benetti A, Longhi R, Podda M, Villa ML. Decrease and dysfunction of dendritic cells correlate with impaired hepatitis C virus-specific CD4+ T-cell proliferation in patients with hepatitis C virus infection. *Immunology* 2007; **121**: 283-292 [PMID: 17462079 DOI: 10.1111/j.1365-2567.2007.02577.x]

109 **Mengshol JA**, Golden-Mason L, Castelblanco N, Im KA, Dillon SM, Wilson CC, Rosen HR; Virahep-C Study Group. Impaired plasmacytoid dendritic cell maturation and differential chemotaxis in chronic hepatitis C virus: associations with antiviral treatment outcomes. *Gut* 2009; **58**: 964-973 [PMID: 19193669 DOI: 10.1136/gut.2008.168948]

110 **Kanto T**, Inoue M, Miyatake H, Sato A, Sakakibara M, Yakushijin T, Oki C, Itose I, Hiramatsu N, Takehara T, Kasahara A, Hayashi N. Reduced numbers and impaired ability of myeloid and plasmacytoid dendritic cells to polarize T helper cells in chronic hepatitis C virus infection. *J Infect Dis* 2004; **190**: 1919-1926 [PMID: 15529255 DOI: 10.1086/425425]

111 **Schulz S**, Landi A, Garg R, Wilson JA, van Drunen Littel-van den Hurk S. Indolamine 2,3-dioxygenase expression by monocytes and dendritic cell populations in hepatitis C patients. *Clin Exp Immunol* 2015; **180**: 484-498 [PMID: 25605587 DOI: 10.1111/cei.12586]

112 **Lai WK**, Curbishley SM, Goddard S, Alabraba E, Shaw J, Youster J, McKeating J, Adams DH. Hepatitis C is associated with perturbation of intrahepatic myeloid and plasmacytoid dendritic cell function. *J Hepatol* 2007; **47**: 338-347 [PMID: 17467113 DOI: 10.1016/j.jhep.2007.03.024]

113 **Langhans B**, Kupfer B, Braunschweiger I, Arndt S, Schulte W, Nischalke HD, Nattermann J, Oldenburg J, Sauerbruch T, Spengler U. Interferon-lambda serum levels in hepatitis C. *J Hepatol* 2011; **54**: 859-865 [PMID: 21145813 DOI: 10.1016/j.jhep.2010.08.020]

114 **Ciesek S**, Liermann H, Hadem J, Greten T, Tillmann HL, Cornberg M, Aslan N, Manns MP, Wedemeyer H. Impaired TRAIL-dependent cytotoxicity of CD1c-positive dendritic cells in chronic hepatitis C virus infection. *J Viral Hepat*2008; **15**: 200-211 [PMID: 18233993 DOI: 10.1111/j.1365-2893.2007.00930.x]

115 **Zhao L**, Tyrrell DL. Myeloid dendritic cells can kill T cells during chronic hepatitis C virus infection. *Viral Immunol* 2013; **26**: 25-39 [PMID: 23374153 DOI: 10.1089/vim.2012.0058]

116 **Fouad H**, Raziky MS, Aziz RA, Sabry D, Aziz GM, Ewais M, Sayed AR. Dendritic cell co-stimulatory and co-inhibitory markers in chronic HCV: an Egyptian study. *World J Gastroenterol* 2013; **19**: 7711-7718 [PMID: 24282359 DOI: 10.3748/wjg.v19.i43.7711]

117 **Shen T**, Chen X, Chen Y, Xu Q, Lu F, Liu S. Increased PD-L1 expression and PD-L1/CD86 ratio on dendritic cells were associated with impaired dendritic cells function in HCV infection. *J Med Virol* 2010; **82**: 1152-1159 [PMID: 20513078 DOI: 10.1002/jmv.21809]

118 **Krishnadas DK**, Ahn JS, Han J, Kumar R, Agrawal B. Immunomodulation by hepatitis C virus-derived proteins: targeting human dendritic cells by multiple mechanisms. *Int Immunol* 2010; **22**: 491-502 [PMID: 20410260 DOI: 10.1093/intimm/dxq033]

119 **Waggoner SN**, Hall CH, Hahn YS. HCV core protein interaction with gC1q receptor inhibits Th1 differentiation of CD4+ T cells via suppression of dendritic cell IL-12 production. *J Leukoc Biol* 2007; **82**: 1407-1419 [PMID: 17881511 DOI: 10.1189/jlb.0507268]

120 **Nattermann J**, Zimmermann H, Iwan A, von Lilienfeld-Toal M, Leifeld L, Nischalke HD, Langhans B, Sauerbruch T, Spengler U. Hepatitis C virus E2 and CD81 interaction may be associated with altered trafficking of dendritic cells in chronic hepatitis C. *Hepatology* 2006; **44**: 945-954 [PMID: 17006905 DOI: 10.1002/hep.21350]

121 **Tu Z**, Zhang P, Li H, Niu J, Jin X, Su L. Cross-linking of CD81 by HCV-E2 protein inhibits human intrahepatic plasmacytoid dendritic cells response to CpG-ODN. *Cell Immunol* 2013; **284**: 98-103 [PMID: 23954883 DOI: 10.1016/j.cellimm.2013.07.012]

122 **Takaki A**, Tatsukawa M, Iwasaki Y, Koike K, Noguchi Y, Shiraha H, Sakaguchi K, Nakayama E, Yamamoto K. Hepatitis C virus NS4 protein impairs the Th1 polarization of immature dendritic cells. *J Viral Hepat* 2010; **17**: 555-562 [PMID: 19804500 DOI: 10.1111/j.1365-2893.2009.01213.x]

123 **Wertheimer AM**, Polyak SJ, Leistikow R, Rosen HR. Engulfment of apoptotic cells expressing HCV proteins leads to differential chemokine expression and STAT signaling in human dendritic cells. *Hepatology* 2007; **45**: 1422-1432 [PMID: 17538964 DOI: 10.1002/hep.21637]

124 **Larsson M**, Babcock E, Grakoui A, Shoukry N, Lauer G, Rice C, Walker C, Bhardwaj N. Lack of phenotypic and functional impairment in dendritic cells from chimpanzees chronically infected with hepatitis C virus. *J Virol* 2004; **78**: 6151-6161 [PMID: 15163708 DOI: 10.1128/jvi.78.12.6151-6161.2004]

125 **Longman RS**, Talal AH, Jacobson IM, Albert ML, Rice CM. Presence of functional dendritic cells in patients chronically infected with hepatitis C virus. *Blood* 2004; **103**: 1026-1029 [PMID: 14525790 DOI: 10.1182/blood-2003-04-1339]

126 **Longman RS**, Talal AH, Jacobson IM, Rice CM, Albert ML. Normal functional capacity in circulating myeloid and plasmacytoid dendritic cells in patients with chronic hepatitis C. *J Infect Dis* 2005; **192**: 497-503 [PMID: 15995965 DOI: 10.1086/431523]

127 **Piccioli D**, Tavarini S, Nuti S, Colombatto P, Brunetto M, Bonino F, Ciccorossi P, Zorat F, Pozzato G, Comar C, Abrignani S, Wack A. Comparable functions of plasmacytoid and monocyte-derived dendritic cells in chronic hepatitis C patients and healthy donors. *J Hepatol* 2005; **42**: 61-67 [PMID: 15629508 DOI: 10.1016/j.jhep.2004.09.014]

128 **Barnes E**, Salio M, Cerundolo V, Francesco L, Pardoll D, Klenerman P, Cox A. Monocyte derived dendritic cells retain their functional capacity in patients following infection with hepatitis C virus. *J Viral Hepat* 2008; **15**: 219-228 [PMID: 18194173 DOI: 10.1111/j.1365-2893.2007.00934.x]

129 **Khakoo SI**, Soni PN, Savage K, Brown D, Dhillon AP, Poulter LW, Dusheiko GM. Lymphocyte and macrophage phenotypes in chronic hepatitis C infection. Correlation with disease activity. *Am J Pathol* 1997; **150**: 963-970 [PMID: 9060834]

130 **Tan-Garcia A**, Wai LE, Zheng D, Ceccarello E, Jo J, Banu N, Khakpoor A, Chia A, Tham CYL, Tan AT, Hong M, Keng CT, Rivino L, Tan KC, Lee KH, Lim SG, Newell EW, Pavelka N, Chen J, Ginhoux F, Chen Q, Bertoletti A, Dutertre CA. Intrahepatic CD206^{+} macrophages contribute to inflammation in advanced viral-related liver disease. *J Hepatol* 2017; **67**: 490-500 [PMID: 28483682 DOI: 10.1016/j.jhep.2017.04.023]

131 **McGuinness PH**, Painter D, Davies S, McCaughan GW. Increases in intrahepatic CD68 positive cells, MAC387 positive cells, and proinflammatory cytokines (particularly interleukin 18) in chronic hepatitis C infection. *Gut* 2000; **46**: 260-269 [PMID: 10644323 DOI: 10.1136/gut.46.2.260]

132 **Tordjmann T**, Soulie A, Guettier C, Schmidt M, Berthou C,

Beaugrand M, Sasportes M. Perforin and granzyme B lytic protein expression during chronic viral and autoimmune hepatitis. *Liver* 1998; **18**: 391-397 [PMID: 9869393 DOI: 10.1111/j.1600-0676.1998.tb00823.x]

133 **Tu Z**, Pierce RH, Kurtis J, Kuroki Y, Crispe IN, Orloff MS. Hepatitis C virus core protein subverts the antiviral activities of human Kupffer cells. *Gastroenterology* 2010; **138**: 305-314 [PMID: 19769973 DOI: 10.1053/j.gastro.2009.09.009]

134 **Zhu H**, Liu C. Interleukin-1 inhibits hepatitis C virus subgenomic RNA replication by activation of extracellular regulated kinase pathway. *J Virol* 2003; **77**: 5493-5498 [PMID: 12692250 DOI: 10.1128/jvi.77.9.5493-5498.2003]

135 **Zhu H**, Shang X, Terada N, Liu C. STAT3 induces anti-hepatitis C viral activity in liver cells. *Biochem Biophys Res Commun* 2004; **324**: 518-528 [PMID: 15474458 DOI: 10.1016/j.bbrc.2004.09.081]

136 **Broering R**, Wu J, Meng Z, Hilgard P, Lu M, Trippler M, Szczeponek A, Gerken G, Schlaak JF. Toll-like receptor-stimulated non-parenchymal liver cells can regulate hepatitis C virus replication. *J Hepatol* 2008; **48**: 914-922 [PMID: 18362039 DOI: 10.1016/j.jhep.2008.01.028]

137 **Ju C**, Tacke F. Hepatic macrophages in homeostasis and liver diseases: from pathogenesis to novel therapeutic strategies. *Cell Mol Immunol* 2016; **13**: 316-327 [PMID: 26908374 DOI: 10.1038/cmi.2015.104]

138 **Mengshol JA**, Golden-Mason L, Arikawa T, Smith M, Niki T, McWilliams R, Randall JA, McMahan R, Zimmerman MA, Rangachari M, Dobrinskikh E, Busson P, Polyak SJ, Hirashima M, Rosen HR. A crucial role for Kupffer cell-derived galectin-9 in regulation of T cell immunity in hepatitis C infection. *PLoS One* 2010; **5**: e9504 [PMID: 20209097 DOI: 10.1371/journal.pone.0009504]

139 **Sandler NG**, Koh C, Roque A, Eccleston JL, Siegel RB, Demino M, Kleiner DE, Deeks SG, Liang TJ, Heller T, Douek DC. Host response to translocated microbial products predicts outcomes of patients with HBV or HCV infection. *Gastroenterology* 2011; **141**: 1220-1230, 1230.e1-1230.e3 [PMID: 21726511 DOI: 10.1053/j.gastro.2011.06.063]

140 **Burgio VL**, Ballardini G, Artini M, Caratozzolo M, Bianchi FB, Levrero M. Expression of co-stimulatory molecules by Kupffer cells in chronic hepatitis of hepatitis C virus etiology. *Hepatology* 1998; **27**: 1600-1606 [PMID: 9620333 DOI: 10.1002/hep.510270620]

141 **Kwon YC**, Meyer K, Peng G, Chatterjee S, Hoft DF, Ray R. Hepatitis C virus E2 envelope glycoprotein induces an immunoregulatory phenotype in macrophages. *Hepatology* 2018; Epub ahead of print [PMID: 29443378 DOI: 10.1002/hep.29843]

142 **Zhang Q**, Wang Y, Zhai N, Song H, Li H, Yang Y, Li T, Guo X, Chi B, Niu J, Crispe IN, Su L, Tu Z. HCV core protein inhibits polarization and activity of both M1 and M2 macrophages through the TLR2 signaling pathway. *Sci Rep* 2016; **6**: 36160 [PMID: 27786268 DOI: 10.1038/srep36160]

143 **Hosomura N**, Kono H, Tsuchiya M, Ishii K, Ogiku M, Matsuda M, Fujii H. HCV-related proteins activate Kupffer cells isolated from human liver tissues. *Dig Dis Sci* 2011; **56**: 1057-1064 [PMID: 20848204 DOI: 10.1007/s10620-010-1395-y]

144 **Fletcher NF**, Sutaria R, Jo J, Barnes A, Blahova M, Meredith LW, Cosset FL, Curbishley SM, Adams DH, Bertoletti A, McKeating JA. Activated macrophages promote hepatitis C virus entry in a tumor necrosis factor-dependent manner. *Hepatology* 2014; **59**: 1320-1330 [PMID: 24259385 DOI: 10.1002/hep.26911]

145 **Wallace K**, Burt AD, Wright MC. Liver fibrosis. *Biochem J* 2008; **411**: 1-18 [PMID: 18333835 DOI: 10.1042/BJ20071570]

146 **Mancini R**, Benedetti A, Jezequel AM. An interleukin-1 receptor antagonist decreases fibrosis induced by dimethylnitrosamine in rat liver. *Virchows Arch* 1994; **424**: 25-31 [PMID: 7981900 DOI: 10.1007/bf00197389]

147 **Tiggelman AM**, Boers W, Linthorst C, Sala M, Chamuleau RA. Collagen synthesis by human liver (myo)fibroblasts in culture: evidence for a regulatory role of IL-1 beta, IL-4, TGF beta and IFN gamma. *J Hepatol* 1995; **23**: 307-317 [PMID: 8550995 DOI: 10.1016/0168-8278(95)80475-7]

148 **Han YP**, Zhou L, Wang J, Xiong S, Garner WL, French SW, Tsukamoto H. Essential role of matrix metalloproteinases in interleukin-1-induced myofibroblastic activation of hepatic stellate cell in collagen. *J Biol Chem* 2004; **279**: 4820-4828 [PMID: 14617627 DOI: 10.1074/jbc.M310999200]

149 **Simeonova PP**, Gallucci RM, Hulderman T, Wilson R, Kommineni C, Rao M, Luster MI. The role of tumor necrosis factor-alpha in liver toxicity, inflammation, and fibrosis induced by carbon tetrachloride. *Toxicol Appl Pharmacol* 2001; **177**: 112-120 [PMID: 11740910 DOI: 10.1006/taap.2001.9304]

150 **Sasaki R**, Devhare PB, Steele R, Ray R, Ray RB. Hepatitis C virus-induced CCL5 secretion from macrophages activates hepatic stellate cells. *Hepatology* 2017; **66**: 746-757 [PMID: 28318046 DOI: 10.1002/hep.29170]

151 **Preisser L**, Miot C, Le Guillou-Guillemette H, Beaumont E, Foucher ED, Garo E, Blanchard S, Frémaux I, Croué A, Fouchard I, Lunel-Fabiani F, Boursier J, Roingeard P, Calès P, Delneste Y, Jeannin P. IL-34 and macrophage colony-stimulating factor are overexpressed in hepatitis C virus fibrosis and induce profibrotic macrophages that promote collagen synthesis by hepatic stellate cells. *Hepatology* 2014; **60**: 1879-1890 [PMID: 25066464 DOI: 10.1002/hep.27328]

152 **Uwatoku R**, Suematsu M, Ezaki T, Saiki T, Tsuiji M, Irimura T, Kawada N, Suganuma T, Naito M, Ando M, Matsuno K. Kupffer cell-mediated recruitment of rat dendritic cells to the liver: roles of N-acetylgalactosamine-specific sugar receptors. *Gastroenterology* 2001; **121**: 1460-1472 [PMID: 11729125 DOI: 10.1053/gast.2001.29594]

153 **Dolganiuc A**, Chang S, Kodys K, Mandrekar P, Bakis G, Cormier M, Szabo G. Hepatitis C virus (HCV) core protein-induced, monocyte-mediated mechanisms of reduced IFN-alpha and plasmacytoid dendritic cell loss in chronic HCV infection. *J Immunol* 2006; **177**: 6758-6768 [PMID: 17082589 DOI: 10.4049/jimmunol.177.10.6758]

P- Reviewer: Boonstra A, Larrea **S- Editor**: Ma RY
L- Editor: Wang TQ **E- Editor**: Yin SY

World Journal of Gastroenterology

Submit a Manuscript: http://www.f6publishing.com

World J Gastroenterol 2018 November 28; 24(44): 4974-4978

DOI: 10.3748/wjg.v24.i44.4974

ISSN 1007-9327 (print) ISSN 2219-2840 (online)

MINIREVIEWS

Learning curves in minimally invasive esophagectomy

Frans van Workum, Laura Fransen, Misha DP Luyer, Camiel Rosman

Frans van Workum, Camiel Rosman, Department of Surgery, Radboud University Medical Center, Nijmegen 6500 HB, Netherlands

Laura Fransen, Misha DP Luyer, Department of Surgery, Catharina Hospital, Eindhoven 5602 ZA, Netherlands

ORCID number: Frans van Workum (0000-0003-0623-9066); Laura Fransen (0000-0002-8404-673X); Misha DP Luyer (0000-0002-9483-1520); Camiel Rosman (0000-0002-9152-3987).

Author contributions: van Workum F, Luyer MDP and Rosman C designed research; van Workum F and Fransen L performed research; van Workum F analyzed data; all authors wrote the paper.

Conflict-of-interest statement: The authors have no conflict of interest to declare. The work has not been previously published and has not been submitted for publication elsewhere.

Manuscript source: Invited manuscript

Corresponding author to: Frans van Workum, MD, Academic Research, Doctor, Department of Surgery, Radboud University Medical Center, Geert Grooteplein-Zuid 10, Nijmegen 6500 HB, Netherlands. frans.vanworkum@radboudumc.nl
Telephone: +31-24-3611111
Fax: +31-24-3540501

Received: August 25, 2018
Peer-review started: August 27, 2018
First decision: October 11, 2018
Revised: October 28, 2018
Accepted: November 2, 2018
Article in press: November 2, 2018
Published online: November 28, 2018

Abstract

Surgical innovation and pioneering are important for improving patient outcome, but can be associated with learning curves. Although learning curves in surgery are a recognized problem, the impact of surgical learning curves is increasing, due to increasing complexity of innovative surgical procedures, the rapid rate at which new interventions are implemented and a decrease in relative effectiveness of new interventions compared to old interventions. For minimally invasive esophagectomy (MIE), there is now robust evidence that implementation can lead to significant learning associated morbidity (morbidity during a learning curve, that could have been avoided if patients were operated by surgeons that have completed the learning curve). This article provides an overview of the evidence of the impact of learning curves after implementation of MIE. In addition, caveats for implementation and available evidence regarding factors that are important for safe implementation and safe pioneering of MIE are discussed.

Key words: Minimally invasive esophagectomy; Learning curve; Pioneering; Safe implementation; Proficiency gain curve

Core tip: Surgical innovation and pioneering are important for improving patient outcome, but can be associated with learning curves. The impact of surgical learning curves is increasing, due to increasing complexity of innovative surgical procedures and the rapid rate at which new interventions are implemented. Learning curves of minimally invasive esophagectomy can take years to complete and evidence based training and safe implementation programs are paramount to decrease implementation associated morbidity.

van Workum F, Fransen L, Luyer MDP, Rosman C. Learning curves in minimally invasive esophagectomy. *World J Gastroenterol*

2018; 24(44): 4974-4978 Available from: URL: http://www.wjgnet.com/1007-9327/full/v24/i44/4974.htm DOI: http://dx.doi.org/10.3748/wjg.v24.i44.4974

INTRODUCTION

A surgical learning curve is a phase after implementation of a new procedure, that is characterized by improving performance as experience with the new procedure increases[1,2]. Learning curves were first described in aviation and manufacturing science[3]. but it has become a widely used concept in medicine and surgery[1,4,5]. Although surgical innovation is necessary to improve care, it is important to take surgical learning curves into account since they have been associated with a negative impact on patient outcome[6-8].

An emerging problem of ongoing surgical innovation

Surgeons are aware of the existence of learning curves, the beneficial effects of "learning before doing" and the importance of safely implementing new surgical procedures. However, ongoing surgical innovation is presenting new challenges regarding surgical learning curves, since new interventions are associated with increasing surgical complexity and decreasing relative effectiveness compared to older procedures.

For example, when the tension-free mesh repair was introduced for inguinal hernias, this lead to a dramatically lower incidence of hernia recurrence compared to conventional non-mesh repairs[9,10]. The large difference in relative effectiveness and the limited complexity (associated with short learning curves) of tension-free mesh repair surgery contributed to making the learning curve insignificant for this procedure (Figure 1A). However, surgical procedures that are currently implemented are of a higher complexity[4,11], are associated with longer learning curves, and the new procedures have a much lower relative effectiveness benefit compared to the old procedures (Figure 1B). For example, trials comparing laparoscopic *vs* open gastrointestinal procedures have shown more modest improvements in outcome for patients[12-14] and the difference in relative effectiveness is even smaller in trials comparing robotic *vs* laparoscopic procedures[15].

These developments have contributed to the situation in which the clinical effectiveness of a new surgical procedure has become more dependent on the delivery of the treatment. In addition, new interventions are implemented at an increasing rate, driven by the patient's increasing expectation to be operated by the newest, most technically challenging, minimally invasive procedures[11]. Together, these factors have contributed to the situation in which learning curves have become more important in contemporary surgical practice. The impact of learning curves is likely to become even more significant for patient outcome in the near future, as surgical innovation progresses further. Although surgeons are always searching for the best way to treat their patients and innovation is needed to further improve surgical care, implementation of technically challenging procedures may come at a price.

LEARNING CURVES OF MINIMALLY INVASIVE ESOPHAGECTOMY

For esophagectomy, beneficial effects of minimally invasive surgery have been well documented[13,14,16]. However, extensive learning curve effects of minimally invasive esophagectomy(MIE) have also been described. Earlier MIE learning curve studies have focused on outcome parameters directly related to the procedure itself, such as blood loss and operative time[17-19]. More recently however, the effect of learning curves on clinically relevant outcome measures has been established for anastomotic leakage[8], mortality[6], and survival[7]. Learning associated morbidity (morbidity during a learning curve, that could have been avoided if patients were operated by surgeons that have completed the learning curve)[8] is now a recognized problem, since there is accumulating data that learning curves have significant impact on critical outcome parameters. Despite beneficial results of MIE compared to older techniques, this implicates that there is significant room for improvement regarding patient safety during surgical learning curves. However, it can take years to become proficient in MIE with low postoperative morbidity and possibly the impact of learning associated morbidity is greater than the direct benefit of MIE compared to open esophagectomy during the learning curve phase[6,8,13,14]. This puts the effectiveness of recent innovations into perspective and exposes the importance of ensuring safety during learning curves. In addition, the evidence of the impact of learning curves and learning associated morbidity comes with the opportunity and obligation to determine what factors contribute to safer implementation and to investigate how to shorten the learning curve and decrease learning associated morbidity. It might be hypothesized that this type of research is more beneficial to patients than research into new innovations in the current time.

Another important consideration is that it is plausible that various types of MIE with different levels of complexity (*i.e.,* transhiatal, transthoracic with cervical anastomosis and transthoracic with intrathoracic anastomosis), have different learning curves. Although these differences have not been exposed clearly in studies, it is likely that they result in differences in learning associated morbidity. This may also be true for hybrid MIE, in which either the thoracic or abdominal phase is performed by open surgery. For example, by performing an open intrathoracic anastomosis instead of a thoracoscopic anastomosis, a surgeon can omit performing the most important and complex part of the procedure in a technically more demanding, thoracoscopic fashion. This may shorten the learning curve and reduce

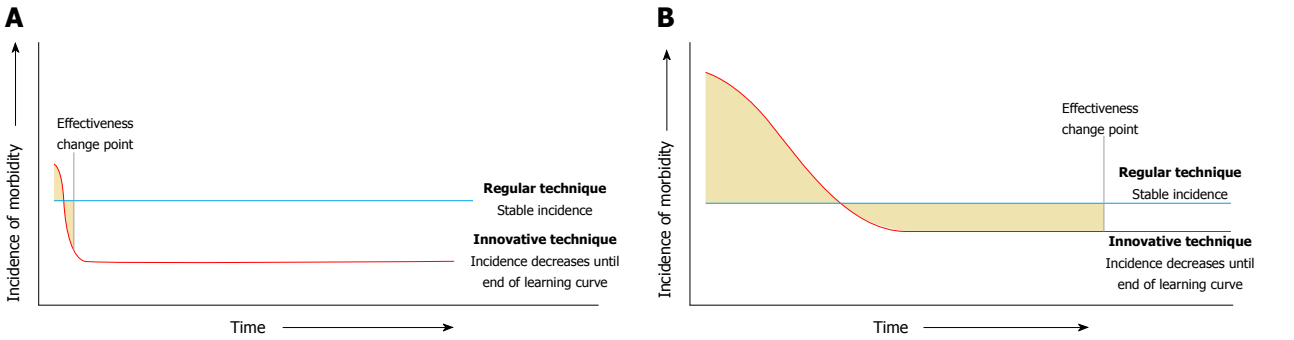

Figure 1 Scenarios in which the differences in the impact that learning curves can have on the effectiveness of an innovative intervention is described. A: Learning curves can be neglected in case of a short learning curve and large difference in relative effectiveness between the regular technique and the innovative technique. B: If the learning curve of an innovative technique is substantial and the difference in relative effectiveness is small, learning curves can have a large impact on when an innovative technique becomes effective.

learning associated morbidity, but no studies have been published that support this hypothesis. Together with data from studies comparing the effectiveness of different approaches of MIE, data on differences in learning curves can be used by clinicians to decide which approach is best to implement in their practice.

SAFE IMPLEMENTATION PROGRAMS

Implementation of increasingly complex innovative procedures require increasingly effective and safe implementation programs to prevent learning associated morbidity. Standardized training programs have been described to be effective for surgical procedures[20-22]. Although the implementation of a new, technically challenging surgical procedure probably requires a multidisciplinary and multifaceted approach, there is currently very little robust evidence on how an implementation program should be designed and what factors make them effective[23]. In addition, the effectiveness of interventions aimed at safer implementation has not been adequately compared to implementation without these interventions. For example, proctorship is widely used to shorten the learning curve and ensure safe implementation of a new technique, but to the best of our knowledge, it's effectiveness has not been compared to implementation without a proctor.

Research that focuses on identification of factors that are associated with shorter learning curves and lower learning associated morbidity is important. Recently, we investigated whether surgeon age and surgeon volume were associated with the length of learning curves in patients undergoing open esophagectomy using a Swedish national esophagectomy registry[24]. In this study, younger surgeons and higher volume surgeons had shorter learning curves compared to older surgeons and lower volume surgeons. Although this study has its limitations, this is the first evidence that suggests that selecting surgeons and training them in high volume facilities may be beneficial to patients and enable safer implementation.

Safe implementation of MIE

For MIE, fundamental items of a safe implementation program have been established by expert opinion[25]. However, although all fundamental requirements of safe implementation were met, our group of 4 European expert centers found a significant learning curve effect after implementation of MIE: anastomotic leakage decreased from 28.9% to well below 5%[8]. Thirty-six patients (10.1% of all patients operated during the learning curve that took a mean of 119 cases to complete) experienced learning associated anastomotic leakage. The fact that significant learning associated anastomotic leakage occurred underlines the need for more research regarding safe implementation.

However, these data should be interpreted with care. Although learning associated morbidity was high in this study, centers switched anastomotic techniques from a cervical anastomosis (McKeown) to an intrathoracic anastomosis (Ivor Lewis) and the incidence of anastomotic leakage did not change initially, since it was already higher in patients with a cervical anastomosis. Therefore, it did not seem unethical to proceed with implementation of Ivor Lewis TMIE in these centers at that time. These data also show that innovation can ultimately be associated with a favorable outcome, since the national incidence of intrathoracic anastomotic leakage was around 17% in the Netherlands at the time the study was performed[26]. In our opinion, some learning associated morbidity is inevitable and in general, this can be justified if morbidity during learning curves does not exceed the morbidity associated with the old procedure. However, shortening learning curves and reducing learning associated morbidity remain important goals that can be beneficial to a significant number of patients.

PIONEERING

For surgeons, pioneering with new procedures, proper training of the surgical team prior to implementation of a new procedure may not be possible. Pioneering

surgeons should describe the development and refinement of new procedures according to the Idea, Development, Exploration, Assessment, Long-term monitoring (IDEAL) framework[27]. According to the IDEAL framework, surgical innovation starts with the Idea (IDEAL stage Ⅰ) in which proof of concept and feasibility are investigated. In the Development (IDEAL stage Ⅱa) and Exploration (IDEAL stage Ⅱb) stages, the procedure is developed and refined. Innovations are compared to old techniques in the Assessment (IDEAL stage 3) and Long-term study (IDEAL stage IV) phases regarding short- and long-term outcome. IDEAL stage Ⅲ and Ⅳ are further characterized by a stable surgical technique and the development of standardized training programs that can be followed by other surgeons. It is plausible that surgeons that start pioneering new techniques (*i.e.* implement innovations in IDEAL stage Ⅱa or Ⅱb) have longer learning curves that are associated with more learning associated morbidity than surgeons that implement innovations after the surgical technique has been refined.

However, it is currently not uncommon for contemporary surgeons to implement surgical procedures in IDEAL stage Ⅱa or Ⅱb. The patient's desire to be operated by the newest procedures and the surgeon's desire to offer the newest surgical innovations may contribute to a surgeon's decision to pioneer with procedures of which it has not yet been determined how to optimally perform key steps or to implement procedures of which the relative effectiveness has not been established adequately and no standardized training programs exist.

Although pioneering surgeons are the cornerstone of surgical progress and their innovations have led to beneficial outcomes for numerous patients, it has become apparent that pioneering with technically challenging procedures can be hazardous. Although currently no guidelines exist, pioneering should probably be reserved for the absolute experts in the field with extensive experience of similar procedures. A solid outcome registration and regular multidisciplinary outcome meetings in which the results and refinements of the new procedure are discussed may contribute to safer pioneering, but consensus is lacking.

CONCLUSION

Although surgical innovation is important in improving patient outcome, the problem of learning curves and learning associated morbidity is increasing with ongoing surgical innovation and increasing complexity of newly implemented procedures. More insight in amendable factors determining the efficiency of surgical learning and safe implementation programs may increase patient safety and lead to better outcomes in the current surgical era.

REFERENCES

1 **Hopper AN**, Jamison MH, Lewis WG. Learning curves in surgical practice. *Postgrad Med J* 2007; **83**: 777-779 [PMID: 18057179 DOI: 10.1136/pgmj.2007.057190]

2 **Ramsay CR**, Grant AM, Wallace SA, Garthwaite PH, Monk AF, Russell IT. Assessment of the learning curve in health technologies. A systematic review. *Int J Technol Assess Health Care* 2000; **16**: 1095-1108 [PMID: 11155830 DOI: 10.1017/S0266462300103149]

3 **Wright TP**. Factors affecting the cost of airplanes. *J Aeronaut Sci* 1936; **3**: 122–128 [DOI: 10.2514/8.155]

4 **Harrysson IJ**, Cook J, Sirimanna P, Feldman LS, Darzi A, Aggarwal R. Systematic review of learning curves for minimally invasive abdominal surgery: a review of the methodology of data collection, depiction of outcomes, and statistical analysis. *Ann Surg* 2014; **260**: 37-45 [PMID: 24670849 DOI: 10.1097/SLA.0000000000000596]

5 **Khan N**, Abboudi H, Khan MS, Dasgupta P, Ahmed K. Measuring the surgical 'learning curve': methods, variables and competency. *BJU Int* 2014; **113**: 504-508 [PMID: 23819461 DOI: 10.1111/bju.12197]

6 **Mackenzie H**, Markar SR, Askari A, Ni M, Faiz O, Hanna GB. National proficiency-gain curves for minimally invasive gastrointestinal cancer surgery. *Br J Surg* 2016; **103**: 88-96 [PMID: 26578089 DOI: 10.1002/bjs.9963]

7 **Markar SR**, Mackenzie H, Lagergren P, Hanna GB, Lagergren J. Surgical Proficiency Gain and Survival After Esophagectomy for Cancer. *J Clin Oncol* 2016; **34**: 1528-1536 [PMID: 26951311 DOI: 10.1200/JCO.2015.65.2875]

8 **van Workum F**, Stenstra MHBC, Berkelmans GHK, Slaman AE, van Berge Henegouwen MI, Gisbertz SS, van den Wildenberg FJH, Polat F, Irino T, Nilsson M, Nieuwenhuijzen GAP, Luyer MD, Adang EM, Hannink G, Rovers MM, Rosman C. Learning Curve and Associated Morbidity of Minimally Invasive Esophagectomy: A Retrospective Multicenter Study. *Ann Surg* 2017 Epub ahead of print [PMID: 28857809 DOI: 10.1097/SLA.0000000000002469]

9 **Lichtenstein IL**, Shulman AG, Amid PK, Montllor MM. The tension-free hernioplasty. *Am J Surg* 1989; **157**: 188-193 [PMID: 2916733 DOI: 10.1016/0002-9610(89)90526-6]

10 **EU Hernia Trialists Collaboration**. Mesh compared with non-mesh methods of open groin hernia repair: systematic review of randomized controlled trials. *Br J Surg* 2000; **87**: 854-859 [PMID: 10931018 DOI: 10.1046/j.1365-2168.2000.01539.x]

11 **Dankelman J**. Increasing complexity of medical technology and consequences for training and for outcome of care. Accessed August 24, 2018 Available from: URL: http://apps.who.int/iris/handle/10665/70455

12 **Veldkamp R**, Kuhry E, Hop WC, Jeekel J, Kazemier G, Bonjer HJ, Haglind E, Påhlman L, Cuesta MA, Msika S, Morino M, Lacy AM; COlon cancer Laparoscopic or Open Resection Study Group (COLOR). Laparoscopic surgery versus open surgery for colon cancer: short-term outcomes of a randomised trial. *Lancet Oncol* 2005; **6**: 477-484 [PMID: 15992696 DOI: 10.1016/S1470-2045(05)70221-7]

13 **Biere SS**, van Berge Henegouwen MI, Maas KW, Bonavina L, Rosman C, Garcia JR, Gisbertz SS, Klinkenbijl JH, Hollmann MW, de Lange ES, Bonjer HJ, van der Peet DL, Cuesta MA. Minimally invasive versus open oesophagectomy for patients with oesophageal cancer: a multicentre, open-label, randomised controlled trial. *Lancet* 2012; **379**: 1887-1892 [PMID: 22552194 DOI: 10.1016/S0140-6736(12)60516-9]

14 **Mariette M**, Meunier B, Pezet, Dalban C, Collet D, Thomas PA, Brigand C, Perniceni T, Carrere N, Bonnetain F, Piessen G. Hybrid minimally invasive versus open oesophagectomy for patients with oesophageal cancer: A multicenter, open-label, randomized phase III controlled trial, the MIRO trial. *J Clin Oncol* 2015; **3** Suppl3: Abstr5 [DOI: 10.1200/jco.2015.33.3_suppl.5]

15 **Roh HF**, Nam SH, Kim JM. Robot-assisted laparoscopic surgery versus conventional laparoscopic surgery in randomized controlled trials: A systematic review and meta-analysis. *PLoS One* 2018; **13**: e0191628 [PMID: 29360840 DOI: 10.1371/journal.pone.0191628]

16 **Straatman J**, van der Wielen N, Cuesta MA, Daams F, Roig Garcia J, Bonavina L, Rosman C, van Berge Henegouwen MI, Gisbertz SS, van der Peet DL. Minimally Invasive Versus Open Esophageal Resection: Three-year Follow-up of the Previously Reported Randomized Controlled Trial: the TIME Trial. *Ann Surg* 2017; **266**:

232-236 [PMID: 28187044 DOI: 10.1097/SLA.0000000000002171]
17 **Guo W**, Zou YB, Ma Z, Niu HJ, Jiang YG, Zhao YP, Gong TQ, Wang RW. One surgeon's learning curve for video-assisted thoracoscopic esophagectomy for esophageal cancer with the patient in lateral position: how many cases are needed to reach competence? *Surg Endosc* 2013; **27**: 1346-1352 [PMID: 23093242 DOI: 10.1007/s00464-012-2614-8]
18 **Lin J**, Kang M, Chen C, Lin R, Zheng W, Zhug Y, Deng F, Chen S. Thoracolaparoscopy oesophagectomy and extensive two-field lymphadenectomy for oesophageal cancer: introduction and teaching of a new technique in a high-volume centre. *Eur J Cardiothorac Surg* 2013; **43**: 115-121 [PMID: 22518035 DOI: 10.1093/ejcts/ezs151]
19 **Mu JW**, Gao SG, Xue Q, Mao YS, Wang DL, Zhao J, Gao YS, Huang JF, He J. Updated experiences with minimally invasive McKeown esophagectomy for esophageal cancer. *World J Gastroenterol* 2015; **21**: 12873-12881 [PMID: 26668512 DOI: 10.3748/wjg.v21.i45.12873]
20 **Fleshman J**, Marcello P, Stamos MJ, Wexner SD; American Society of Colon and Rectal Surgeons (ASCRS); Society of American Gastrointestinal and Endoscopic Surgeons (SAGES). Focus Group on Laparoscopic Colectomy Education as endorsed by The American Society of Colon and Rectal Surgeons (ASCRS) and The Society of American Gastrointestinal and Endoscopic Surgeons (SAGES). *Dis Colon Rectum* 2006; **49**: 945-949 [PMID: 16649114 DOI: 10.1007/s10350-006-0559-5]
21 **Schout BM**, Hendrikx AJ, Scherpbier AJ, Bemelmans BL. Update on training models in endourology: a qualitative systematic review of the literature between January 1980 and April 2008. *Eur Urol* 2008; **54**: 1247-1261 [PMID: 18597924 DOI: 10.1016/j.eururo.2008.06.036]
22 **Larsen CR**, Soerensen JL, Grantcharov TP, Dalsgaard T, Schouenborg L, Ottosen C, Schroeder TV, Ottesen BS. Effect of virtual reality training on laparoscopic surgery: randomised controlled trial. *BMJ* 2009; **338**: b1802 [PMID: 19443914 DOI: 10.1136/bmj.b1802]
23 **Harris C**, Garrubba M, Allen K, King R, Kelly C, Thiagarajan M, Castleman B, Ramsey W, Farjou D. Development, implementation and evaluation of an evidence-based program for introduction of new health technologies and clinical practices in a local healthcare setting. *BMC Health Serv Res* 2015; **15**: 575 [PMID: 26707549 DOI: 10.1186/s12913-015-1178-4]
24 **Gottlieb-Vedi E**, Mackenzie H, van Workum F, Rosman C, Lagergren P, Markar S, Lagergren J. Surgeon Volume and Surgeon Age in Relation to Proficiency Gain Curves for Prognosis Following Surgery for Esophageal Cancer. *Ann Surg Oncol* 2018; Epub ahead of print [PMID: 30324469 DOI: 10.1245/s10434-018-6869-8]
25 **Visser E**, van Rossum PSN, van Veer H, Al-Naimi K, Chaudry MA, Cuesta MA, Gisbertz SS, Gutschow CA, Hölscher AH, Luyer MDP, Mariette C, Moorthy K, Nieuwenhuijzen GAP, Nilsson M, Räsänen JV, Schneider PM, Schröder W, Cheong E, van Hillegersberg R. A structured training program for minimally invasive esophagectomy for esophageal cancer- a Delphi consensus study in Europe. *Dis Esophagus* 2018; **31** [PMID: 29121243 DOI: 10.1093/dote/dox124]
26 **Gooszen JAH**, Goense L, Gisbertz SS, Ruurda JP, van Hillegersberg R, van Berge Henegouwen MI. Intrathoracic versus cervical anastomosis and predictors of anastomotic leakage after oesophagectomy for cancer. *Br J Surg* 2018; **105**: 552-560 [PMID: 29412450 DOI: 10.1002/bjs.10728]
27 **McCulloch P**, Altman DG, Campbell WB, Flum DR, Glasziou P, Marshall JC, Nicholl J; Balliol Collaboration, Aronson JK, Barkun JS, Blazeby JM, Boutron IC, Campbell WB, Clavien PA, Cook JA, Ergina PL, Feldman LS, Flum DR, Maddern GJ, Nicholl J, Reeves BC, Seiler CM, Strasberg SM, Meakins JL, Ashby D, Black N, Bunker J, Burton M, Campbell M, Chalkidou K, Chalmers I, de Leval M, Deeks J, Ergina PL, Grant A, Gray M, Greenhalgh R, Jenicek M, Kehoe S, Lilford R, Littlejohns P, Loke Y, Madhock R, McPherson K, Meakins J, Rothwell P, Summerskill B, Taggart D, Tekkis P, Thompson M, Treasure T, Trohler U, Vandenbroucke J. No surgical innovation without evaluation: the IDEAL recommendations. *Lancet* 2009; **374**: 1105-1112 [PMID: 19782876 DOI: 10.1016/S0140-6736(09)61116-8]

P- Reviewer: Wang Y, Watson DI **S- Editor**: Ma RY **L- Editor**: A
E- Editor: Yin SY

World Journal of Gastroenterology

Submit a Manuscript: http://www.f6publishing.com

World J Gastroenterol 2018 November 28; 24(44): 4979-4988

DOI: 10.3748/wjg.v24.i44.4979

ISSN 1007-9327 (print) ISSN 2219-2840 (online)

MINIREVIEWS

Glutathione depleting drugs, antioxidants and intestinal calcium absorption

Luciana Moine, María Rivoira, Gabriela Díaz de Barboza, Adriana Pérez, Nori Tolosa de Talamoni

Luciana Moine, María Rivoira, Gabriela Díaz de Barboza, Adriana Pérez, Nori Tolosa de Talamoni, Laboratorio "Dr. Fernando Cañas", Cátedra de Bioquímica y Biología Molecular, Facultad de Ciencias Médicas, INICSA (CONICET-Universidad Nacional de Córdoba), Córdoba 5000, Argentina

ORCID number: Luciana Moine (0000-0002-0350-8956); María Rivoira (0000-0002-7316-1564); Gabriela Díaz de Barboza (0000-0003-0617-8005); Adriana Pérez (0000-0002-5415-3139); Nori Tolosa de Talamoni (0000-0001-5570-2024).

Author contributions: Moine L, Rivoira M, Díaz de Barboza G, Pérez A and Tolosa de Talamoni NT participated in information collection, analysis, information organization, writing, figure design, and final editing.

Conflict-of-interest statement: No conflicts of interest, financial or otherwise, are declared by the authors.

Manuscript source: Invited manuscript

Corresponding author to: Nori Tolosa de Talamoni, PhD, Professor, Laboratorio "Dr. Fernando Cañas", Cátedra de Bioquímica y Biología Molecular, Facultad de Ciencias Médicas, INICSA (CONICET-Universidad Nacional de Córdoba), Pabellón Argentina, 2do. Piso, Ciudad Universitaria, Córdoba 5000, Argentina. ntolosa@biomed.fcm.unc.edu.ar
Telephone: +54-351-4333024

Received: August 28, 2018
Peer-review started: August 28, 2018
First decision: October 9, 2018
Revised: October 24, 2018
Accepted: Novmeber 2, 2018
Article in press: Novmeber 2, 2018
Published online: November 28, 2018

Abstract

Glutathione (GSH) is a tripeptide that constitutes one of the main intracellular reducing compounds. The normal content of GSH in the intestine is essential to optimize the intestinal Ca^{2+} absorption. The use of GSH depleting drugs such as DL-buthionine-S,R-sulfoximine, menadione or vitamin K_3, sodium deoxycholate or diets enriched in fructose, which induce several features of the metabolic syndrome, produce inhibition of the intestinal Ca^{2+} absorption. The GSH depleting drugs switch the redox state towards an oxidant condition provoking oxidative/nitrosative stress and inflammation, which lead to apoptosis and/or autophagy of the enterocytes. Either the transcellular Ca^{2+} transport or the paracellular Ca^{2+} route are altered by GSH depleting drugs. The gene and/or protein expression of transporters involved in the transcellular Ca^{2+} pathway are decreased. The flavonoids quercetin and naringin highly abrogate the inhibition of intestinal Ca^{2+} absorption, not only by restoration of the GSH levels in the intestine but also by their anti-apoptotic properties. Ursodeoxycholic acid, melatonin and glutamine also block the inhibition of Ca^{2+} transport caused by GSH depleting drugs. The use of any of these antioxidants to ameliorate the intestinal Ca^{2+} absorption under oxidant conditions associated with different pathologies in humans requires more investigation with regards to the safety, pharmacokinetics and pharmacodynamics of them.

Key words: Glutathione; Transcellular and paracellular Ca^{2+}pathways; DL-buthionine-S,R-sulfoximine; Fructose rich diet; Menadione; Sodium deoxycholate; Glutamine; Ursodeoxycholic acid; Melatonin; Quercetin; Naringin

Core tip: The normal content of glutathione (GSH) in the intestine is essential to optimize the intestinal Ca^{2+} absorption. The use of GSH depleting drugs such as DL-buthionine-S,R-sulfoximine, menadione or vitamin K_3, sodium deoxycholate or diets enriched in fructose, which induce several features of the metabolic syndrome, produce inhibition of the intestinal Ca^{2+} absorption. The flavonoids quercetin and naringin highly abrogate the inhibition of intestinal Ca^{2+} absorption, not only by restoration of the GSH levels in the intestine but also by their anti-apoptotic properties. Ursodeoxycholic acid, melatonin and glutamine also block the inhibition of Ca^{2+} transport caused by GSH depleting drugs.

Moine L, Rivoira M, Díaz de Barboza G, Pérez A, Tolosa de Talamoni N. Glutathione depleting drugs, antioxidants and intestinal calcium absorption. *World J Gastroenterol* 2018; 24(44): 4979-4988 Available from: URL: http://www.wjgnet.com/1007-9327/full/v24/i44/4979.htm DOI: http://dx.doi.org/10.3748/wjg.v24.i44.4979

INTRODUCTION

Ca^{2+} absorption is one of the most important intestinal functions since the intestine is the only entrance gate of the cation into the body. This physiological process together with the renal Ca^{2+} reabsorption and the bone Ca^{2+} resorption maintain the Ca^{2+} homeostasis. An appropriate Ca^{2+} homeostasis preserves bone integrity, metabolic balance and avoids epithelial cancers such as breast, colon and prostate cancer[1-3]. A poor intestine absorption caused by infection, inflammation or a pathology in the intestine morphology may cause an adverse Ca^{2+} balance[4], which under chronic conditions leads to a deleterious bone mineralization. The intestinal Ca^{2+} absorption occurs along the entire intestine, but the small intestine is responsible for about 90% of overall Ca^{2+} absorption, and the order of Ca^{2+} absorption rate is duodenum > jejunum > ileum. The colon is only responsible for less than 10% of the total Ca^{2+} absorbed, but it appears to become important under pathological conditions[5].

Ca^{2+} is absorbed in the intestine by active and passive transport systems. The transcellular Ca^{2+} absorption is an active process and occurs *via* cation influx into the enterocyte, intracellular shuttling, and basolateral extrusion[6]. Ca^{2+} absorption can also occur *via* a passive, paracellular route, where the movement of the cation between epithelial cells is made through tight junction (TJ) proteins, which facilitate or block the Ca^{2+} movement[7]. The active transport of Ca^{2+} is mainly regulated by the biologically active form of vitamin D, $1,25(OH)_2D_3$ (calcitriol)[8], by previous activation of a vitamin D receptor (VDR)[9]. When VDR was deleted specifically in the intestine (VDR^{int-}) of mice, the intestinal Ca^{2+} absorption was decreased, the bone mineralization is inhibited and bone fractures were increased[10]. Thus, intestinal VDR is not only essential for intestinal Ca^{2+} absorption, but also for bone formation.

As previously reported, the transcellular Ca^{2+} movement involves the participation of transient receptor potential vanilloid type 6 (TRPV6) and transient receptor potential vanilloid type 5 in the step across the brush border membrane from enterocytes, calbindin D_{9k} (CB D_{9k}) as a ferry from one pole to the other pole of the cells and the plasma membrane Ca^{2+}-ATPase ($PMCA_{1b}$) and the Na^+/Ca^{2+} exchanger (NCX1) for cation extrusion[11]. The molecules involved in the paracellular Ca^{2+} movement are not completely known, but there is certain evidence that the proteins of the TJ such as claudin-2 and claudin-12 facilitate the Ca^{2+} transport[12,13]. In contrast, either gene or protein expression of cadherin-17 are decreased in mice´s and rat´s intestines during low Ca intake[14], as well as in Caco-2 cells after treatment with calcitriol[15].

When Ca^{2+} intake is low, the cation entry occurs through the transcellular pathway; whereas high luminal Ca^{2+} content (> 2-6 mmol/L) switches on the paracellular route due to a short sojourn time in the intestine and a down-regulation of molecules involved in the transcellular pathway[16,17]. The expression of paracellular TJ genes seems to be regulated by the calbindin protein, which suggests that the active and passive Ca^{2+} transport pathways may work cooperatively[18]. A reduction in more than 70% in the active intestinal Ca^{2+} absorption, 55% in CB D_{9k} expression and 90% in TRPV6 expression was observed in VDR null mice[19].

Although calcitriol is the main regulator of intestinal Ca^{2+} absorption, other hormones also contribute to altering this process as parathyroid hormone, glucocorticoids, estrogen, growth hormone, etc. In addition, many dietary and pharmacological compounds also modify the intestinal Ca^{2+} transport[20]. We have demonstrated that the normal content of the tripeptide glutathione (GSH) in enterocytes is essential for an optimal intestinal Ca^{2+} absorption, which was proved either in birds or in mammals[21,22]. GSH depletion produced by different ways generates a low GSH/glutathione disulfide (GSSG) ratio leading to oxidative stress and apoptosis of enterocytes by exacerbation of reactive oxygen species (ROS) production[23]. Clausen *et al*[24] have reported that GSH plays an important role in the opening of the TJ of intestinal epithelia enhancing the paracellular transport. In this review we will analyze the role of GSH in the intestine, the molecular mechanisms by which GSH depleting drugs inhibit the intestinal Ca^{2+} absorption and the prevention or restoration of these effects by drugs that act through normalization of intestinal GSH content.

GSH SYNTHESIS AND ITS PHYSIOLOGICAL ROLE IN THE INTESTINE

The intestinal mucosa comprises the surface monolayer

of self-renewing epithelial cells and the lamina propria with the vascular, immune and structural components[25]. In the small intestine there are invaginations called crypts of Lieberkuhn and prominences into the lumen called villi with differentiated cells. The crypts contain proliferative stem cells and Paneth cells responsible for the innate immunity and antibacterial defense and for providing essential signals to intestinal stem cells. The intestinal epithelium is a single heterogeneous layer of different cells: enterocytes (80% of total cells), enteroendocrine cells (1% of all epithelial cells), Goblet cells (4% in duodenum, secretory cells) and tuft cells (secretory cell type). They originate in the crypts, migrate toward the villi during differentiation and then suffer spontaneous apoptosis and shedding when reaching the villus tip after terminal differentiation[26]. Only enterocytes are involved in the Ca^{2+} transport from the intestinal lumen to the lamina propria. Although Ca^{2+} uptake occurs in all enterocytes, the mature cells from the tip and the middle part of the villi are mainly involved in the transcellular Ca^{2+} movement. Ca^{2+} uptake is stimulated by calcitriol or low Ca diets either in the mature enterocytes or in the undifferentiated cells from the crypt, but the most differentiated cells exhibit a higher response[27]. The GSH content in the intestine is in the millimolar range as occurs in other cells[28,29]; however, the tripeptide concentration varies according to the degree of maturation of cells. Surprisingly, mature enterocytes have lower GSH content than the immature cells[30]. GSH exists as the biologically active reduced-thiol form, and its oxidation to GSSG is associated with oxidative stress (OS). The GSH/GSSG ratio is around 100/1; when GSSG increases, this ratio decreases causing an oxidative shift in the cellular redox state[31]. Intestinal GSH redox homeostasis is maintained by *de novo* synthesis[32], regeneration from GSSG[33] and GSH uptake that derives from the dietary intake and mainly from the biliary output because the bile is enriched in GSH (1-2 mmol/L)[34,35]. The dietary GSH comes from fresh fruits, vegetables, and many types of meat, but the luminal GSH is lower (250 μmol/L in rats) than that from the intracellular compartment[36]. In the enterocytes and in the proximal tubular cells from kidney, the enzyme γ-glutamyl transpeptidase plays an important role in GSH homeostasis. It is located in the outer surface of plasma membranes of epithelial cells and cleaves the extracellular GSH to glutamate and cysteinyl-glycine, which is subsequently hydrolyzed by a dipeptidase to yield the constituent amino acids[37]. The biosynthesis of GSH occurs in the cytosolic compartment through two consecutive adenosine triphosphate (ATP)-dependent reactions. First, the glutamate cysteine ligase (GCL) catalyzes the formation of a dipeptide constituted by glutamate and cysteine, and then the GSH synthetase catalyzes the addition of glycine to form GSH[38], the former being the rate-limiting step. GCL has a catalytic subunit and a modulatory subunit. The control of GCL function is regulated at transcriptional levels of both subunits and through product feedback[39]. The γ-glutamyl cycle comprises the enzymatic reactions involved in the intracellular GSH synthesis and the extracellular GSH degradation, which could be considered as a mechanism to preserve cellular GSH homeostasis in transport epithelial cells. The reduction of GSSG by glutathione reductase (GR) to form GSH depends on the supply of the reductant nicotinamide adenine dinucleotide phosphate, which is provided by the pentose phosphate shunt[40]. The redox couple GSH/GSSG assures a redox environment that allows the maintenance of the gut microbiota, the adequate nutrient absorption, the reversal of oxidant-induced epithelium damage and the modulation of intestinal cell transformation and apoptosis[41]. The regulation of the GSH metabolism by the gut microbiota in mice has also been suggested[42], but it needs further investigation. GSH from the intestinal lumen plays different important roles such as reduction of dietary disulfides, detoxification of xenobiotics, metabolism of peroxidized lipids and maintenance of the mucus fluidity[29,34,41]. Tsunada *et al*[43] have shown that chronic administration of lipid peroxides interferes with the regulation of enterocyte death and proliferation *in vivo*; these disruptive effects were reversed by GSH supplementation after normalization of GSH/GSSG redox balance (Figure 1).

Intracellular GSH is distributed in different compartments. Cytosolic GSH is the source of GSH pool of the mitochondria, endoplasmic reticulum and nucleus. The GSH/GSSG ratio in the cytoplasm varies between 30/1 to 100/1, whereas in the endoplasmic reticulum (ER) is between 3/1 and 1/1, which indicates that in ER the system GSH/GSSH is more oxidized than that from the cytoplasm. The steady-state redox potential of the GSH/GSSG system is about -330 mmol/L to -300 mmol/L in the mitochondrial matrix and -260 mmol/L to -200 mmol/L in the cytoplasm. The endoplasmic reticular GSH/GSSG redox potential is about -150 mmol/L, which is in midway between cytoplasmic and plasma values[44]. The nuclear GSH/GSSG redox potential remains unknown but there is certain evidence that it can be somewhat more reducing than that from the cytoplasm. Proliferative cells have more negative steaty-state redox potential and differentiated cells have more positive cells and cells undergoing apoptosis and necrosis have a more oxidized steady-state potential (around -170 mmol/L to -150 mmol/L)[45]. In other words, the cellular compartments have different GSH/GSSG ratios, and the life cell cycle is also associated with different thiol redox potentials, which can alter the cellular functions. Since enterocytes show different degrees of differentiation and then suffer apoptosis and shedding in a range of 4-7 d, the redox potential of GSH/GSSG couple must change quite rapidly in order to facilitate the variety of functions of those cells during the lifespan.

GSH DEPLETION AND THE INTESTINAL CALCIUM ABSORPTION

Many years ago, Mårtensson *et al*[46] demonstrated that

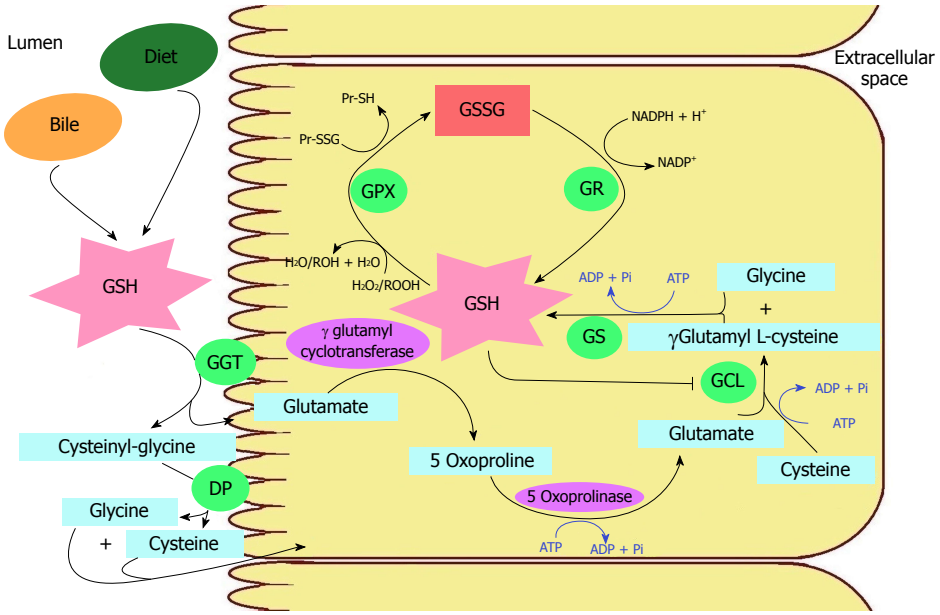

Figure 1 Intestinal glutathione metabolism. The γ-glutamyl cycle comprises the enzymatic reactions involved in the extracellular glutathione (GSH) degradation and the intracellular GSH synthesis: The enzymes γ-glutamyl transpeptidase and dipeptidase, localized in plasma membrane of enterocytes, cleave the extracellular GSH to their constituent amino acids. Within the enterocytes the GSH is synthesized *de novo* by two reactions that consume adenosine triphosphate that are catalyzed by glutamate cysteine ligase and glutathione synthetase, sequentially. In the redox couple that ensures the maintenance of the cellular redox state participates the enzymes glutathione peroxidase and glutathione reductase. GSH: Glutathione; GSSG: Glutathione disulfide; GGT: γ-glutamyl transpeptidase; GCL: Glutamate cysteine ligase; GS: Glutathione synthetase; GR: Glutathione reductase; GPX: Glutathione peroxidase; DP: Dipeptidase.

GSH was required for intestinal function. They observed that chronic depletion of mucosal GSH by buthionine sulfoximine (BSO), a specific inhibitor of GCL[47], caused severe degeneration of epithelial cells from jejunum and colon, which was prevented by oral GSH or GSH monoester. We have shown that BSO alters the Ca^{2+} transfer from intestinal lumen-to-blood in vitamin D supplemented chicks but does not affect that of vitamin D-deficient chicks, which indicate that the effects of BSO on intestinal Ca^{2+} absorption were dependent on the vitamin D status of the animal. The reversibility of this inhibition was proved by adding GSH monoester, an indication that intestinal GSH is essential to have an optimal intestinal Ca^{2+} absorption[21]. At that time, the molecular mechanisms involved in the effect of BSO on the intestinal Ca^{2+} absorption remained unknown. Later on, we have demonstrated that GSH depleting drugs inhibit the intestinal Ca^{2+} transport not only in birds but also in mammals[48]. The tripeptide depletion might increase the oxidation of sulfhydryl groups that are important to maintain the functionality of proteins involved in the Ca^{2+} transport, such as occurs with the $PMCA_{1b}$[21]. In addition, other GSH depleting drug such as vitamin K_3 or menadione (MEN) causes inhibition of intestinal Ca^{2+} absorption, which is related to OS, as judged by a decrease in GSH content and an increment in the total carbonyl group content. This inhibitory effect of MEN on intestinal Ca^{2+} absorption begins in half an hour, lasts for several hours and finishes after 10 h of treatment[49]. The quinone inhibits two enzymes presumably involved in Ca^{2+} transcellular pathway such as the intestinal alkaline phosphatase (IAP), located in the brush border membrane, and $PMCA_{1b}$, protein that carries Ca^{2+} outside the cell, as mentioned above. The enzyme inhibition might be due to alterations produced by ROS, which are triggered by GSH depletion caused by its consumption in the redox cycle of the quinone[50]. When MEN is metabolized, it may undergo one or two-electron reduction. If it suffers one-electron reduction, there is formation of a very unstable semiquinone radical, which reacts rapidly with molecular oxygen resulting in regeneration of the parent compound and production of a superoxide anion that yields H_2O_2 *via* enzymatic or spontaneous dismutation. Two-electron reduction of MEN produces a hydroquinone, a pathway that constitutes a detoxification mechanism[51]. In both cases, GSH is the electron donor, which explains the tripeptide depletion after MEN treatment. Since the intestinal Ca^{2+} absorption is an active process, which requires ATP that is mainly provided by the mitochondria, we have analyzed the functionality of these organelles in the intestinal mucosa when animals were treated with MEN. In fact, we have detected that MEN produces mitochondrial dysfunction caused by GSH depletion, which alters the mitochondrial permeability resulting in the release of cytochrome c and DNA fragmentation, biomarkers of apoptosis through the intrinsic pathway. In other words, mitochondrial dysfunction is also involved in the mechanisms by which MEN inhibits transiently the intestinal Ca^{2+} absorption[49]. Later on, the system FASL/FAS/caspase-3, indicators of apoptosis *via* the extrinsic pathway, was also demonstrated to be activated by MEN[52].

Sodium deoxycholate (NaDOC) is another GSH depleting drug that produces OS, as indicated by ROS generation and mitochondrial swelling leading to inhibition of intestinal Ca^{2+} absorption[53]. The effect of

Table 1 Glutathione depletion and the intestinal calcium absorption

	Oxidative stress markers	Effect on intestinal Ca^{2+} absorption
BSO	↓GSH	↓Ca^{2+} transfer from lumen-to-blood
MEN	↓GSH ↑ROS and protein carbonyl ↑Mn^{2+}-SOD and GPX Mitochondrial dysfunction	↓Ca^{2+} transfer from lumen-to-blood ↓IAP and PMCA1b activities
NaDOC	↓GSH ↑ROS Mitochondrial swelling. ↑SOD, CAT and GPX ↑NO• ↑iNOS protein	↓Intestinal Ca^{2+}absorption ↓mRNA PMCA1b ↓PMCA1b, CB_{D28k} and NCX1 protein expression
FRD	↓GSH ↑O_2^- ↑protein carbonyl and nitrotyrosine content ↓SOD and CAT ↑NO•	↓Intestinal Ca^{2+} absorption ↓IAP activity ↓TRPV6, PMCA1b, CBD9k, CLDN 2, CLDN12 and VDR protein expression

BSO: DL-buthionine-*S*,*R*-sulfoximine; CAT: Catalase; CB_{D28k}: Calbindin D28k; CB_{D9k}: Calbindin D9k; CLDN 2: Claudin 2; CLDN12: Claudin 12; FRD: Fructose rich diet; GPX: Glutathione peroxidase. GSH: Glutathione; IAP: Intestinal alkaline phosphatase. MEN: menadione. Mn^{2+}-SOD: Mn^{2+}-superoxide dismutase. NaDOC: sodium deoxycholate.NCX1: Na^+/Ca^{2+} exchanger; NO•: Nitric oxide; PMCA1b: Plasma membrane Ca^{2+}ATPase; SOD: Superoxide dismutase; TRPV6: Transient receptor potential vanilloid type 6; VDR: Vitamin D receptor.

NaDOC is time and dose-dependent and is higher in mature enterocytes[53,22]. NaDOC exerts its effect altering the transcellular Ca^{2+} pathway; the gene and protein expression of $PMCA_{1b}$ and the protein expressions of calbindin D_{28k} (CB D_{28k}) and NCX1 are decreased by this hydrophobic bile salt. NaDOC is a major component of the bile; in high concentrations it provokes liver damage during cholestasis and promotes colon carcinogenesis in experimental animals[54,55]. The molecular mechanisms by which NaDOC alters the protein expression of molecules involved in the intestinal Ca^{2+} absorption seem to be also related to nitrosative stress, as indicated by increment in NO• content and in induced nitric oxide synthase (iNOS) protein expression, and apoptosis, as shown by enhancement of the system FASL/FAS/caspase-8/caspase-3. In addition, an increase in acidic vesicular organelles (AVOs) and in LC3 Ⅱ protein expression produced by NaDOC means that autophagy might be another mechanism triggered by this bile salt associated with the inhibition of the intestinal Ca^{2+} absorption[22] (Table 1).

The administration of fructose rich diets (FRD) to normal rats, which induce several features of the metabolic syndrome, inhibit the intestinal Ca^{2+} absorption and induce vitamin D insufficiency[56,57]. In our laboratory, we have found that the VDR protein expression is also diminished by the FRD[58]. Since $1,25(OH)_2D_3$ and its receptor are depleted, the inhibition in the cation transport could be explained due to $1,25(OH)_2D_3$ is the main stimulator of the intestinal Ca^{2+} absorption. FRD alter both the transcellular and the paracellular pathways. The protein expression of TRPV6, CB D_{9k} and $PMCA_{1b}$ as well as the enzyme activity of IAP are lower in animals fed FRD than in rats fed a normal diet. Similarly, the protein expressions of Claudin-2 and Claudin-12, molecules located in intestinal TJ, are also decreased in rats fed FRD[58]. The intestinal GSH levels are decreased by the FRD, which would explain the increment in the superoxide anion and in the protein carbonyl content. This scenario is worsened by a decrease in the activities of superoxide dismutase and catalase, enzymes of the antioxidant defense, which result in impairment of the redox equilibrium contributing to altering the intestinal Ca^{2+} absorption. Other authors have also demonstrated that FRD decrease the GSH content and the antioxidant enzyme activities as well as vitamin C and vitamin E levels in rat liver and skeletal muscle[59]. In addition, we have demonstrated that FRD increase the NO• content and the nitrosylation of proteins of 22 and 38 kDa from rat intestine. He *et al*[60] have demonstrated that FRD increase the expression of inducible NO• synthase in the liver. Kannappan *et al*[59] have shown that FRD augment nitrosothiols in the plasma, liver and skeletal muscle. All these findings indicate that an intake rich in fructose triggers nitrosative stress in a variety of tissues.

The inflammation is another mechanism triggered by FRD in rat intestine, as suggested by an increment in the intestinal protein expression of nuclear factor (NF)-κB and interleukin (IL)-6. NF-κB is a transcription factor that controls over 100 genes activated direct or indirectly by inflammation[61]; IL-6 is a cytokine, whose gene has a promotor region with a site of binding for NF-κB. In addition, IL-6 has been suggested to be associated with metabolic syndrome and each of its components and it could be added as a biomarker of progression of that condition[62]. Therefore, the inhibition of the intestinal Ca^{2+} absorption by FRD is also mediated through the enhancement of inflammatory molecules[58].

In conclusion, any drug or disease associated with intestinal GSH depletion causes inhibition of intestinal Ca^{2+} absorption. This response is mediated by OS/nitrosative stress and inflammation, which could lead to cell death of enterocytes with capability to transport Ca^{2+} across the cells and in the paracellular route.

REVERSION/PREVENTION OF THE INHIBITION OF INTESTINAL CALCIUM ABSORPTION CAUSED BY GSH DEPLETION

The first approaches to revert or prevent the inhibition

Table 2 Antioxidants that preserve/ restore the inhibition of intestinal Ca^{2+} absorption caused by glutathione depletion

Drugs	Normalized OS markers	Effect on inhibition of ICaA	Normalized component of ICaA	Apoptosis markers	References
GSH monoester	GSH total	Restoration			Tolosa de Talamoni *et al*[21]
MEL	GSH, $^{\cdot}O^{2-}$ Protein carbonyl SOD, CAT and GPX activities iNOS gene and protein expression	Prevention restoration	PMCA1b, CB_{D9k}, NCX1, CLDN 2 and CLD 12 protein expression	↓TUNEL index ↓Caspase 3 activity/ protein expression	Carpentieri *et al*[80] Areco *et al*[81]
QT	GSH total. GPX activity	Prevention		↓Caspase 3 activity ↓ FAS, ↓FASL. Blocks mit swelling	Marchionatti *et al*[52]
GLN	GSH, $^{\cdot}O_2^{-}$. Protein carbonyl SOD and CAT activity	Prevention restoration	CB_{D28k} and PMCA1b protein expression.	↓TUNEL index. ↓FAS, ↓FASL ↓Caspase-3 activity	Moine *et al*[88]
NAR	GSH, $^{\cdot}O^{2-}$ NO• Protein carbonyl and nitrotyrosine content. SOD and CAT activity	Prevention	IAP activity (partially) PMCA1b, CB_{D9k}, NCX1, VDR, CLDN2 and CLD12 protein expression		Rodríguez *et al*[58]
UDCA	GSH, NO• protein carbonyl SOD activity iNOS protein expression	Increase restoration	IAP activity ↑PMCA1b, CB_{D28k}, NCX1, VDR gene and protein expression	↓Mit swelling ↓FAS, ↓FASL gene/ protein content Caspase 8 protein content Caspase 3 activity	Rodríguez *et al*[22,48]

CAT: Catalase; CB_{D28k}: Calbindin D28k; CB_{D9k}: Calbindin D9k; CLDN 2: Claudin 2; CLDN12: Claudin 12; GLN: Glutamine; GPX: Glutathione peroxidase; GSH: Glutathione; IAP: Intestinal alkaline phosphatase; ICaA: Intestinal Ca^{2+} absorption; MEL: Melatonin; MEN: Menadione; Mit: Mitochondrial; NAR: Naringin; NCX1: Na^{+}/Ca^{2+}exchanger; NO: Nitric oxide; OS: Oxidative stress; PMCA1b: Plasma membrane Ca^{2+}-ATPase; QT: Quercetin; SOD: Superoxide dismutase; TRPV6: Transient receptor potential vanilloid type 6; UDCA: Ursodeoxycholic acid; VDR: Vitamin D receptor.

of intestinal Ca^{2+} absorption caused by GSH depletion consisted in the use of GSH monoester in order to replenish the intestine with the tripeptide[21]. In fact, this treatment leads to the normalization of the intestinal Ca^{2+} absorption. In addition, other strategies were also assayed because the intestinal GSH depletion could be generated not only by drugs but also by pathological conditions such as cholestasis and metabolic syndrome[58,63].

Since GSH depletion causes exacerbation of ROS production, inflammation, apoptosis and autophagy, the reversion or prevention was thought to be blocked by flavonoids, molecules derived from natural sources with antioxidant, anti-inflammatory and antiapoptotic properties. Flavonoids are a class of phenolic metabolites produced by plants and fungi[64]. Among them, quercetin (QT) is largely present in fruit, red wine, tea, vegetables and aromatic plants[65], and exhibits all the biological properties mentioned above. Hence, QT is considered as a potential therapeutic agent for different diseases such as cancer, hypertension, inflammation, diabetes, thrombosis[66-68]. Inoue *et al*[69] have suggested that QT might improve the intestinal Ca^{2+} absorption because they have demonstrated in Caco-2 cells that QT increases the gene expression of TRPV6, which is a VDR target gene. We did not find that QT alone ameliorates the Ca^{2+} transport in the intestine, but we demonstrated that QT blocks the inhibition of the intestinal Ca^{2+} absorption caused by MEN *via* GSH depletion. Similarly, QT by itself does not change the intestinal GSH content, but it prevents the GSH depletion produced by the quinone[52]. Boots *et al*[70] have also observed that the effects of QT supplementation in patients with sarcoidosis appear to be more pronounced when the baseline levels of oxidative (malondialdehyde) and inflammatory (tumor necrosis factor α, IL-8, IL-10) markers are increased. So, it appears that the extent of the QT effects depends on the baseline of OS and inflammation. The protective mechanisms of QT on the intestinal Ca^{2+} absorption under oxidant conditions could be summarized in: (1) Normalization of intestinal redox state, (2) blockage of alterations in the mitochondrial membrane permeability (swelling), and (3) interference with the FASL/FAS/caspase-3 cascade activation. Taken together, it could be concluded that QT might be useful to prevent the inhibition of intestinal Ca^{2+} absorption caused by pro-oxidants or conditions that deplete GSH leading to OS and apoptosis[52].

Naringin (NAR) is another flavonoid that abrogates the inhibition of intestinal Ca^{2+} absorption caused by oxidant conditions such as an experimental metabolic syndrome produced in rats by FRD[58]. NAR is chemically known as naringenin 7-O-neohesperidoside and is present in different citrus being responsible for the bitterness in grapefruit, which is one of the richest sources of this flavonoid[71]. NAR has been demonstrated to increase the GSH content either in the liver or in the intestine from mice exposed to whole-body irradiation[72]. A meta-analysis also showed that NAR restores the GSH content in different parts of brain in various neurological ailments in rodents[73]. We have demonstrated that NAR (40 mg/kg bw) can protect the intestinal Ca^{2+} absorption by blocking all the alterations in the redox state of the intestinal mucosa caused under oxidant conditions such as the intake of FRD by rats[58]. With regard to GSH, NAR

not only blocked its depletion produced by FRD but also increased almost twice the normal intestinal GSH content by a mechanism that needs to be clarified. NAR was able to abrogate all the described alterations provoked by FRD in rats through its anti-oxidant, anti-nitrergic and anti-inflammatory properties. The use of NAR to ameliorate the intestinal Ca^{2+} transport under oxidant conditions associated with different pathologies holds a remarkable potential, but there are some obstacles in NAR clinical translation related to the extensive *in vivo* metabolism, low bioavailability and irregular absorption[74]. On the other hand, it has been demonstrated that various phenolic antioxidants exhibit pro-oxidant properties at high doses[75]. In fact, both flavonoids, quercetin and naringin, have antioxidant and pro-oxidant effects[76].

Melatonin (MEL) is one of the natural human antioxidant that has gained increasing attention. MEL is a hormone secreted by the pineal gland and other tissues such as bone marrow, skin and gastrointestinal tract. MEL is a lipophilic antioxidant of broad spectrum that has a high membrane permeability[77]. The molecular mechanisms triggered by MEL seem to be different from those of the classical antioxidants such as vitamin C, vitamin E and GSH; however, MEL synergizes with them in the scavenging of free radicals. The classical antioxidants undergo redox cycling so they have the potential to promote oxidation or prevent it. In contrast, MEL does not display redox cycling, thus, it does not stimulate oxidation; therefore it could be considered as a suicidal or terminal antioxidant. MEL may interact with free radicals forming several stable end products, which are excreted in the urine[78]. MEL content is 400 times larger in the intestine than in the pineal gland[79], but the physiological significance of this is not very clear. Similarly to QT, MEL alone does not affect the intestinal Ca^{2+} absorption, but it avoids or reverses the inhibitory effect of MEN or BSO[80,81]. The GSH depletion caused by MEN was also prevented by MEL, counteracting the oxidative stress and apoptosis provoked by the quinone. MEL protects either the intestinal transcellular Ca^{2+} pathway or the paracellular Ca^{2+} route, but only under oxidant conditions. The modulation of transporters of Ca^{2+} by MEL has also been reported in pancreatic acinar cells[82] and in rat pituitary GH3 cells[83]. In conclusion, MEL could be a drug for reversal of impaired intestinal Ca^{2+} absorption produced by OS and apoptosis that occurs under pathophysiological conditions such as aging, celiac disease, intestinal bowel disease, cancer or other gut disorders, or by GSH depleting drugs (Table 2).

Since the amino acid glutamine (GLN) in the intestine is a fuel and a source of glutamate, substrate for GSH synthesis[84,85], and it has antioxidant and antiapoptotic properties[86], and has the advantage of being an oral nutritional supplement[87], we have thought that it could be used to prevent or reverse the intestinal Ca^{2+} absorption inhibited by GSH depleting drugs. Similarly to other antioxidants, GLN alone does not modify the intestinal Ca^{2+} absorption but it reverses the inhibition of the intestinal cation transport caused by MEN. The GLN protective action is dose and time dependent and also occurs when it is administered previous to MEN treatment. The normalization of the protein expression of CB D_{28k} and $PMCA_{1b}$ by GLN indicates that this amino acid protects the transcellular Ca^{2+} pathway. The protection may be achieved because GLN restores the intestinal GSH content, normalizes the enzymatic activities of the antioxidant defense system and decreases the activation of the apoptotic pathway FASL/FAS/Caspase-3[88]. In other words, the antioxidant and antiapoptotic properties of GLN facilitate the normalization of the intestinal Ca^{2+} absorption under oxidant conditions. Whether GLN alters or not the intestinal Ca^{2+} paracelluar route and/or other mechanisms are involved in the protection of the intestinal Ca^{2+} absorption is under investigation.

Ursodeoxycholic acid (UDCA) is a minor component of the bile and has hydrophilic properties[48]. It is known that UDCA blocks the reactive oxygen species formation, the mitochondrial dysfunction and the death receptor induced apoptosis[89]. It has been widely used for treatment of cholestatic liver diseases, mainly primary biliary cirrhosis (PBC)[90]. In our laboratory, we have explored the possibility that UDCA could prevent the inhibition of intestinal Ca^{2+} absorption caused by NaDOC, a hydrophobic bile acid that causes GSH depletion in the duodenum, as mentioned in the previous section. Verma *et al*[91] have demonstrated that UDCA therapy enhances fractional Ca^{2+} absorption in PBC. In agreement with these data, we have observed that UDCA alone improves the intestinal Ca^{2+} absorption by increasing the amount of Ca^{2+} transporters involved in the transcellular Ca^{2+} pathway *via* activation of the VDR gene and protein expression. The effect of UDCA on Ca^{2+} uptake by enterocytes has been shown to depend on the degree of differentiation of these cells, being higher in mature enterocytes. When UDCA is given simultaneously with NaDOC, the intestinal Ca^{2+} absorption is similar to that from the control animals, which means that UDCA prevents the inhibition in the Ca^{2+} transport caused by NaDOC. Although UDCA alone decreases FASL and FAS protein expression without changing the Caspase-8 protein expression and caspase-3 activity, it avoids the apoptotic effects of NaDOC through normalization of the protein expression of FASL, FAS, Caspase-8 and the enzyme activity of Caspase-3. Similarly, UDCA *per se* does not alter the intestinal NO• content, but it abrogates the increase in NO• and in iNOS protein expression provoked by NaDOC. In addition, UDCA avoids efficiently the enhancement in LC3Ⅱ protein expression and in the number of AVOs in enterocytes caused by NaDOC, which means that UDCA attenuates the biomarkers of autophagy[22]. The physiological significance of this response is not quite clear and needs to be clarified.

CONCLUSION

The Ca^{2+} entrance to the organism is very important to maintain the Ca^{2+}-dependent functions and the correct mineralization of the skeleton. An optimal intestinal

Ca^{2+} absorption is reached when the GSH content in the intestine is in the normal range. Conditions associated with intestinal GSH depletion arising from administration of certain drugs or different diseases may inhibit the intestinal Ca^{2+} transport. This response could be prevented or restored by using flavonoids (QT, NAR), MEL, UDCA or GLN, which block the effects of the GSH depletion mainly through their antioxidant, antiapoptotic and anti-inflammatory properties. However, the use of these drugs to improve the intestinal Ca^{2+} absorption under oxidant conditions associated with different pathologies in humans requires more investigation with regards to the safety, pharmacokinetics and the pharmacodynamics of them.

REFERENCES

1 **Cianferotti L**, Gomes AR, Fabbri S, Tanini A, Brandi ML. The calcium-sensing receptor in bone metabolism: from bench to bedside and back. *Osteoporos Int* 2015; **26**: 2055-2071 [PMID: 26100412 DOI: 10.1007/s00198-015-3203-1]

2 **Bartlett PJ**, Gaspers LD, Pierobon N, Thomas AP. Calcium-dependent regulation of glucose homeostasis in the liver. *Cell Calcium* 2014; **55**: 306-316 [PMID: 24630174 DOI: 10.1016/j.ceca.2014.02.007]

3 **Farfariello V**, Iamshanova O, Germain E, Fliniaux I, Prevarskaya N. Calcium homeostasis in cancer: A focus on senescence. *Biochim Biophys Acta* 2015; **1853**: 1974-1979 [PMID: 25764980 DOI: 10.1016/j.bbamcr.2015.03.005]

4 **Krupa-Kozak U**, Markiewicz LH, Lamparski G, Juśkiewicz J. Administration of Inulin-Supplemented Gluten-Free Diet Modified Calcium Absorption and Caecal Microbiota in Rats in a Calcium-Dependent Manner. *Nutrients* 2017; **9** [PMID: 28684691 DOI: 10.3390/nu9070702]

5 **Jongwattanapisan P**, Suntornsaratoon P, Wongdee K, Dorkkam N, Krishnamra N, Charoenphandhu N. Impaired body calcium metabolism with low bone density and compensatory colonic calcium absorption in cecectomized rats. *Am J Physiol Endocrinol Metab* 2012; **302**: E852-E863 [PMID: 22275757 DOI: 10.1152/ajpendo.00503.2011]

6 **Beggs MR**, Alexander RT. Intestinal absorption and renal reabsorption of calcium throughout postnatal development. *Exp Biol Med* (Maywood) 2017; **242**: 840-849 [PMID: 28346014 DOI: 10.1177/1535370217699536]

7 **Alexander RT**, Rievaj J, Dimke H. Paracellular calcium transport across renal and intestinal epithelia. *Biochem Cell Biol* 2014; **92**: 467-480 [PMID: 25386841 DOI: 10.1139/bcb-2014-0061]

8 **Norman AW**. Intestinal calcium absorption: a vitamin D-hormone-mediated adaptive response. *Am J Clin Nutr* 1990; **51**: 290-300 [PMID: 2407100 DOI: 10.1093/ajcn/51.2.290]

9 **Uenishi K**, Tokiwa M, Kato S, Shiraki M. Stimulation of intestinal calcium absorption by orally administrated vitamin D3 compounds: a prospective open-label randomized trial in osteoporosis. *Osteoporos Int* 2018; **29**: 723-732 [PMID: 29273827 DOI: 10.1007/s00198-017-4351-2]

10 **Lieben L**, Masuyama R, Torrekens S, Van Looveren R, Schrooten J, Baatsen P, Lafage-Proust MH, Dresselaers T, Feng JQ, Bonewald LF, Meyer MB, Pike JW, Bouillon R, Carmeliet G. Normocalcemia is maintained in mice under conditions of calcium malabsorption by vitamin D-induced inhibition of bone mineralization. *J Clin Invest* 2012; **122**: 1803-1815 [PMID: 22523068 DOI: 10.1172/JCI45890]

11 **Diaz de Barboza G**, Guizzardi S, Tolosa de Talamoni N. Molecular aspects of intestinal calcium absorption. *World J Gastroenterol* 2015; **21**: 7142-7154 [PMID: 26109800 DOI: 10.3748/wjg.v21.i23.7142]

12 **Fujita H**, Sugimoto K, Inatomi S, Maeda T, Osanai M, Uchiyama Y, Yamamoto Y, Wada T, Kojima T, Yokozaki H, Yamashita T, Kato S, Sawada N, Chiba H. Tight junction proteins claudin-2 and -12 are critical for vitamin D-dependent Ca2+ absorption between enterocytes. *Mol Biol Cell* 2008; **19**: 1912-1921 [PMID: 18287530 DOI: 10.1091/mbc.E07-09-0973]

13 **Chiba H**, Osanai M, Murata M, Kojima T, Sawada N. Transmembrane proteins of tight junctions. *Biochim Biophys Acta* 2008; **1778**: 588-600 [PMID: 17916321 DOI: 10.1016/j.bbamem.2007.08.017]

14 **Benn BS**, Ajibade D, Porta A, Dhawan P, Hediger M, Peng JB, Jiang Y, Oh GT, Jeung EB, Lieben L, Bouillon R, Carmeliet G, Christakos S. Active intestinal calcium transport in the absence of transient receptor potential vanilloid type 6 and calbindin-D9k. *Endocrinology* 2008; **149**: 3196-3205 [PMID: 18325990 DOI: 10.1210/en.2007-1655]

15 **Christakos S**, Dhawan P, Ajibade D, Benn BS, Feng J, Joshi SS. Mechanisms involved in vitamin D mediated intestinal calcium absorption and in non-classical actions of vitamin D. *J Steroid Biochem Mol Biol* 2010; **121**: 183-187 [PMID: 20214989 DOI: 10.1016/j.jsbmb.2010.03.005]

16 **Bronner F**. Mechanisms of intestinal calcium absorption. *J Cell Biochem* 2003; **88**: 387-393 [PMID: 12520541 DOI: 10.1002/jcb.10330]

17 **Wasserman RH**. Vitamin D and the dual processes of intestinal calcium absorption. *J Nutr* 2004; **134**: 3137-3139 [PMID: 15514288 DOI: 10.1093/jn/134.11.3137]

18 **Hwang I**, Yang H, Kang HS, Ahn C, Hong EJ, An BS, Jeung EB. Alteration of tight junction gene expression by calcium- and vitamin D-deficient diet in the duodenum of calbindin-null mice. *Int J Mol Sci* 2013; **14**: 22997-23010 [PMID: 24264043 DOI: 10.3390/ijms141122997]

19 **Xue Y**, Fleet JC. Intestinal vitamin D receptor is required for normal calcium and bone metabolism in mice. *Gastroenterology* 2009; **136**: 1317-1327, e1-e2 [PMID: 19254681 DOI: 10.1053/j.gastro.2008.12.051]

20 **Areco V**, Rivoira MA, Rodriguez V, Marchionatti AM, Carpentieri A, Tolosa de Talamoni N. Dietary and pharmacological compounds altering intestinal calcium absorption in humans and animals. *Nutr Res Rev* 2015; **28**: 83-99 [PMID: 26466525 DOI: 10.1017/S0954422415000050]

21 **Tolosa de Talamoni N**, Marchionatti A, Baudino V, Alisio A. Glutathione plays a role in the chick intestinal calcium absorption. *Comp Biochem Physiol A Physiol* 1996; **115**: 127-132 [PMID: 8916550]

22 **Rodríguez VA**, Rivoira MA, Pérez Adel V, Marchionatti AM, Tolosa de Talamoni NG. Ursodeoxycholic and deoxycholic acids: Differential effects on intestinal Ca(2+) uptake, apoptosis and autophagy of rat intestine. *Arch Biochem Biophys* 2016; **591**: 28-34 [PMID: 26707246 DOI: 10.1016/j.abb.2015.12.006]

23 **Xiao Y**, Cui J, Shi YH, Sun J, Wang ZP, Le GW. Effects of duodenal redox status on calcium absorption and related genes expression in high-fat diet-fed mice. *Nutrition* 2010; **26**: 1188-1194 [PMID: 20444574 DOI: 10.1016/j.nut.2009.11.021]

24 **Clausen AE**, Kast CE, Bernkop-Schnürch A. The role of glutathione in the permeation enhancing effect of thiolated polymers. *Pharm Res* 2002; **19**: 602-608 [PMID: 12069161 DOI: 10.1023/A:1015345827091]

25 **Neish AS**. Redox signaling mediated by the gut microbiota. *Free Radic Res* 2013; **47**: 950-957 [PMID: 23937589 DOI: 10.3109/10715762.2013.833331]

26 **van der Flier LG**, Clevers H. Stem cells, self-renewal, and differentiation in the intestinal epithelium. *Annu Rev Physiol* 2009; **71**: 241-260 [PMID: 18808327 DOI: 10.1146/annurev.physiol.010908.163145]

27 **Centeno VA**, Díaz de Barboza GE, Marchionatti AM, Alisio AE, Dallorso ME, Nasif R, Tolosa de Talamoni NG. Dietary calcium deficiency increases Ca2+ uptake and Ca2+ extrusion mechanisms in chick enterocytes. *Comp Biochem Physiol A Mol Integr Physiol* 2004; **139**: 133-141 [PMID: 15528161 DOI: 10.1016/j.cbpb.2004.08.002]

28 **Meister A**, Anderson ME. Glutathione. *Annu Rev Biochem* 1983; **52**: 711-760 [PMID: 6137189 DOI: 10.1146/annurev.bi.52.070183.003431]

29 **Circu ML**, Aw TY. Intestinal redox biology and oxidative stress. *Semin Cell Dev Biol* 2012; **23**: 729-737 [PMID: 22484611 DOI: 10.1016/j.semcdb.2012.03.014]

30 **Venoji R**, Amirtharaj GJ, Kini A, Vanaparthi S, Venkatraman A, Ramachandran A. Enteral glutamine differentially regulates Nrf 2 along the villus-crypt axis of the intestine to enhance glutathione levels. *J Gastroenterol Hepatol* 2015; **30**: 1740-1747 [PMID: 26095579 DOI: 10.1111/jgh.13019]

31 **Smith IC**, Vigna C, Levy AS, Denniss SG, Rush JW, Tupling AR. The effects of buthionine sulfoximine treatment on diaphragm contractility and SERCA pump function in adult and middle aged rats. *Physiol Rep* 2015; **3** [PMID: 26371231 DOI: 10.14814/phy2.12547]

32 **Aw TY**, Wierzbicka G, Jones DP. Oral glutathione increases tissue glutathione in vivo. *Chem Biol Interact* 1991; **80**: 89-97 [PMID: 1913980 DOI: 10.1016/0009-2797(91)90033-4]

33 **Shan XQ**, Aw TY, Jones DP. Glutathione-dependent protection against oxidative injury. *Pharmacol Ther* 1990; **47**: 61-71 [PMID: 2195557 DOI: 10.1016/0163-7258(90)90045-4]

34 **Aw TY**. Biliary glutathione promotes the mucosal metabolism of luminal peroxidized lipids by rat small intestine in vivo. *J Clin Invest* 1994; **94**: 1218-1225 [PMID: 8083363 DOI: 10.1172/JCI117439]

35 **Samiec PS**, Dahm LJ, Jones DP. Glutathione S-transferase in mucus of rat small intestine. *Toxicol Sci* 2000; **54**: 52-59 [PMID: 10746931 DOI: 10.1093/toxsci/54.1.52]

36 **Jones DP**, Coates RJ, Flagg EW, Eley JW, Block G, Greenberg RS, Gunter EW, Jackson B. Glutathione in foods listed in the National Cancer Institute's Health Habits and History Food Frequency Questionnaire. *Nutr Cancer* 1992; **17**: 57-75 [PMID: 1574445 DOI: 10.1080/01635589209514173]

37 **Circu ML**, Aw TY. Glutathione and modulation of cell apoptosis. *Biochim Biophys Acta* 2012; **1823**: 1767-1777 [PMID: 22732297 DOI: 10.1016/j.bbamcr.2012.06.019]

38 **Wu G**, Fang YZ, Yang S, Lupton JR, Turner ND. Glutathione metabolism and its implications for health. *J Nutr* 2004; **134**: 489-492 [PMID: 14988435 DOI: 10.1093/jn/134.3.489]

39 **Soltaninassab SR**, Sekhar KR, Meredith MJ, Freeman ML. Multi-faceted regulation of gamma-glutamylcysteine synthetase. *J Cell Physiol* 2000; **182**: 163-170 [PMID: 10623879 DOI: 10.1002/(SICI)1097-4652(200002)182:2<163::AID-JCP4>3.0.CO;2-1]

40 **Meister A**, Tate SS. Glutathione and related gamma-glutamyl compounds: biosynthesis and utilization. *Annu Rev Biochem* 1976; **45**: 559-604 [PMID: 9027 DOI: 10.1146/annurev.bi.45.070176.003015]

41 **Circu ML**, Aw TY. Redox biology of the intestine. *Free Radic Res* 2011; **45**: 1245-1266 [PMID: 21831010 DOI: 10.3109/10715762.2011.611509]

42 **Mardinoglu A**, Shoaie S, Bergentall M, Ghaffari P, Zhang C, Larsson E, Bäckhed F, Nielsen J. The gut microbiota modulates host amino acid and glutathione metabolism in mice. *Mol Syst Biol* 2015; **11**: 834 [PMID: 26475342 DOI: 10.15252/msb.20156487]

43 **Tsunada S**, Iwakiri R, Fujimoto K, Aw TY. Chronic lipid hydroperoxide stress suppresses mucosal proliferation in rat intestine: potentiation of ornithine decarboxylase activity by epidermal growth factor. *Dig Dis Sci* 2003; **48**: 2333-2341 [PMID: 14714622 DOI: 10.1023/B:DDAS.0000007872.66693.6c]

44 **Jones DP**, Go YM. Redox compartmentalization and cellular stress. *Diabetes Obes Metab* 2010; **12** Suppl 2: 116-125 [PMID: 21029308 DOI: 10.1111/j.1463-1326.2010.01266.x]

45 **Go YM**, Ziegler TR, Johnson JM, Gu L, Hansen JM, Jones DP. Selective protection of nuclear thioredoxin-1 and glutathione redox systems against oxidation during glucose and glutamine deficiency in human colonic epithelial cells. *Free Radic Biol Med* 2007; **42**: 363-370 [PMID: 17210449 DOI: 10.1016/j.freeradbiomed.2006.11.005]

46 **Mårtensson J**, Jain A, Meister A. Glutathione is required for intestinal function. *Proc Natl Acad Sci USA* 1990; **87**: 1715-1719 [PMID: 2308931 DOI: 10.1073/pnas.87.5.1715]

47 **Nishizawa S**, Araki H, Ishikawa Y, Kitazawa S, Hata A, Soga T, Hara T. Low tumor glutathione level as a sensitivity marker for glutamate-cysteine ligase inhibitors. *Oncol Lett* 2018; **15**: 8735-8743 [PMID: 29928324 DOI: 10.3892/ol.2018.8447]

48 **Rodríguez V**, Rivoira M, Marchionatti A, Pérez A, Tolosa de Talamoni N. Ursodeoxycholic and deoxycholic acids: A good and a bad bile acid for intestinal calcium absorption. *Arch Biochem Biophys* 2013; **540**: 19-25 [PMID: 24096173 DOI: 10.1016/j.abb.2013.09.018]

49 **Marchionatti AM**, Perez AV, Diaz de Barboza GE, Pereira BM, Tolosa de Talamoni NG. Mitochondrial dysfunction is responsible for the intestinal calcium absorption inhibition induced by menadione. *Biochim Biophys Acta* 2008; **1780**: 101-107 [PMID: 18053815 DOI: 10.1016/j.bbagen.2007.10.020]

50 **Marchionatti AM**, Díaz de Barboza GE, Centeno VA, Alisio AE, Tolosa de Talamoni NG. Effects of a single dose of menadione on the intestinal calcium absorption and associated variables. *J Nutr Biochem* 2003; **14**: 466-472 [PMID: 12948877 DOI: 10.1016/S0955-2863(03)00078-0]

51 **Chiou TJ**, Tzeng WF. The roles of glutathione and antioxidant enzymes in menadione-induced oxidative stress. *Toxicology* 2000; **154**: 75-84 [PMID: 11118672 DOI: 10.1016/S0300-483X(00)00321-8]

52 **Marchionatti AM**, Pacciaroni A, Tolosa de Talamoni NG. Effects of quercetin and menadione on intestinal calcium absorption and the underlying mechanisms. *Comp Biochem Physiol A Mol Integr Physiol* 2013; **164**: 215-220 [PMID: 23000882 DOI: 10.1016/j.cbpa.2012.09.007]

53 **Rivoira MA**, Marchionatti AM, Centeno VA, Díaz de Barboza GE, Peralta López ME, Tolosa de Talamoni NG. Sodium deoxycholate inhibits chick duodenal calcium absorption through oxidative stress and apoptosis. *Comp Biochem Physiol A Mol Integr Physiol* 2012; **162**: 397-405 [PMID: 22561666 DOI: 10.1016/j.cbpa.2012.04.016]

54 **Lamireau T**, Zoltowska M, Levy E, Yousef I, Rosenbaum J, Tuchweber B, Desmoulière A. Effects of bile acids on biliary epithelial cells: proliferation, cytotoxicity, and cytokine secretion. *Life Sci* 2003; **72**: 1401-1411 [PMID: 12527037 DOI: 10.1016/S0024-3205(02)02408-6]

55 **Farhana L**, Nangia-Makker P, Arbit E, Shango K, Sarkar S, Mahmud H, Hadden T, Yu Y, Majumdar AP. Bile acid: a potential inducer of colon cancer stem cells. *Stem Cell Res Ther* 2016; **7**: 181 [PMID: 27908290 DOI: 10.1186/s13287-016-0439-4]

56 **Douard V**, Asgerally A, Sabbagh Y, Sugiura S, Shapses SA, Casirola D, Ferraris RP. Dietary fructose inhibits intestinal calcium absorption and induces vitamin D insufficiency in CKD. *J Am Soc Nephrol* 2010; **21**: 261-271 [PMID: 19959720 DOI: 10.1681/ASN.2009080795]

57 **Douard V**, Patel C, Lee J, Tharabenjasin P, Williams E, Fritton JC, Sabbagh Y, Ferraris RP. Chronic high fructose intake reduces serum 1,25 (OH)2D3 levels in calcium-sufficient rodents. *PLoS One* 2014; **9**: e93611 [PMID: 24718641 DOI: 10.1371/journal.pone.0093611]

58 **Rodríguez V**, Rivoira M, Guizzardi S, Tolosa de Talamoni N. Naringin prevents the inhibition of intestinal Ca^{2+} absorption induced by a fructose rich diet. *Arch Biochem Biophys* 2017; **636**: 1-10 [PMID: 29122589 DOI: 10.1016/j.abb.2017.11.002]

59 **Kannappan S**, Palanisamy N, Anuradha CV. Suppression of hepatic oxidative events and regulation of eNOS expression in the liver by naringenin in fructose-administered rats. *Eur J Pharmacol* 2010; **645**: 177-184 [PMID: 20655900 DOI: 10.1016/j.ejphar.2010.07.015]

60 **He S**, Rehman H, Wright GL, Zhong Z. Inhibition of inducible nitric oxide synthase prevents mitochondrial damage and improves survival of steatotic partial liver grafts. *Transplantation* 2010; **89**: 291-298 [PMID: 20145519 DOI: 10.1097/TP.0b013e3181c99185]

61 **Boone DL**, Dassopoulos T, Lodolce JP, Chai S, Chien M, Ma A. Interleukin-2-deficient mice develop colitis in the absence of CD28 costimulation. *Inflamm Bowel Dis* 2002; **8**: 35-42 [PMID: 11837936 DOI: 10.1097/00054725-200201000-00005]

62 **Srikanthan K**, Feyh A, Visweshwar H, Shapiro JI, Sodhi K. Systematic Review of Metabolic Syndrome Biomarkers: A Panel for Early Detection, Management, and Risk Stratification in the West Virginian Population. *Int J Med Sci* 2016; **13**: 25-38 [PMID: 26816492 DOI: 10.7150/ijms.13800]

63 **Wang P**, Gong G, Wei Z, Li Y. Ethyl pyruvate prevents intestinal inflammatory response and oxidative stress in a rat model of extrahepatic cholestasis. *J Surg Res* 2010; **160**: 228-235 [PMID: 19628226 DOI: 10.1016/j.jss.2009.03.027]

64 **Xiao J**. Dietary flavonoid aglycones and their glycosides: Which show better biological significance? *Crit Rev Food Sci Nutr* 2017; **57**: 1874-1905 [PMID: 26176651 DOI: 10.1080/10408398.2015.1032400]

65 **Patel RV**, Mistry BM, Shinde SK, Syed R, Singh V, Shin HS.

Therapeutic potential of quercetin as a cardiovascular agent. *Eur J Med Chem* 2018; **155**: 889-904 [PMID: 29966915 DOI: 10.1016/j.ejmech.2018.06.053]

66 **Kasmi S**, Bkhairia I, Harrabi B, Mnif H, Marrakchi R, Ghozzi H, Kallel C, Nasri M, Zeghal K, Jamoussi K, Hakim A. Modulatory effects of quercetin on liver histopathological, biochemical, hematological, oxidative stress and DNA alterations in rats exposed to graded doses of score 250. *Toxicol Mech Methods* 2018; **28**: 12-22 [PMID: 28679351 DOI: 10.1080/15376516.2017.1351507]

67 **Zhou J**, Fang L, Liao J, Li L, Yao W, Xiong Z, Zhou X. Investigation of the anti-cancer effect of quercetin on HepG2 cells in vivo. *PLoS One* 2017; **12**: e0172838 [PMID: 28264020 DOI: 10.1371/journal.pone.0172838]

68 **Kleemann R**, Verschuren L, Morrison M, Zadelaar S, van Erk MJ, Wielinga PY, Kooistra T. Anti-inflammatory, anti-proliferative and anti-atherosclerotic effects of quercetin in human in vitro and in vivo models. *Atherosclerosis* 2011; **218**: 44-52 [PMID: 21601209 DOI: 10.1016/j.atherosclerosis.2011.04.023]

69 **Inoue J**, Choi JM, Yoshidomi T, Yashiro T, Sato R. Quercetin enhances VDR activity, leading to stimulation of its target gene expression in Caco-2 cells. *J Nutr Sci Vitaminol* (Tokyo) 2010; **56**: 326-330 [PMID: 21228504 DOI: 10.3177/jnsv.56.326]

70 **Boots AW**, Drent M, de Boer VC, Bast A, Haenen GR. Quercetin reduces markers of oxidative stress and inflammation in sarcoidosis. *Clin Nutr* 2011; **30**: 506-512 [PMID: 21324570 DOI: 10.1016/j.clnu.2011.01.010]

71 **Cavia-Saiz M**, Busto MD, Pilar-Izquierdo MC, Ortega N, Perez-Mateos M, Muñiz P. Antioxidant properties, radical scavenging activity and biomolecule protection capacity of flavonoid naringenin and its glycoside naringin: a comparative study. *J Sci Food Agric* 2010; **90**: 1238-1244 [PMID: 20394007 DOI: 10.1002/jsfa.3959]

72 **Jagetia GC**, Reddy TK. Modulation of radiation-induced alteration in the antioxidant status of mice by naringin. *Life Sci* 2005; **77**: 780-794 [PMID: 15936352 DOI: 10.1016/j.lfs.2005.01.015]

73 **Viswanatha GL**, Shylaja H, Moolemath Y. The beneficial role of Naringin- a citrus bioflavonoid, against oxidative stress-induced neurobehavioral disorders and cognitive dysfunction in rodents: A systematic review and meta-analysis. *Biomed Pharmacother* 2017; **94**: 909-929 [PMID: 28810519 DOI: 10.1016/j.biopha.2017.07.072]

74 **Lavrador P**, Gaspar VM, Mano JF. Bioinspired bone therapies using naringin: applications and advances. *Drug Discov Today* 2018; **23**: 1293-1304 [PMID: 29747006 DOI: 10.1016/j.drudis.2018.05.012]

75 **Wong WS**, McLean AE. Effects of phenolic antioxidants and flavonoids on DNA synthesis in rat liver, spleen, and testis in vitro. *Toxicology* 1999; **139**: 243-253 [PMID: 10647924 DOI: 10.1016/S0300-483X(99)00136-5]

76 **Vargas AJ**, Burd R. Hormesis and synergy: pathways and mechanisms of quercetin in cancer prevention and management. *Nutr Rev* 2010; **68**: 418-428 [PMID: 20591109 DOI: 10.1111/j.1753-4887.2010.00301.x]

77 **Yu H**, Dickson EJ, Jung SR, Koh DS, Hille B. High membrane permeability for melatonin. *J Gen Physiol* 2016; **147**: 63-76 [PMID: 26712850 DOI: 10.1085/jgp.201511526]

78 **Tan DX**, Manchester LC, Reiter RJ, Qi WB, Karbownik M, Calvo JR. Significance of melatonin in antioxidative defense system: reactions and products. *Biol Signals Recept* 2000; **9**: 137-159 [PMID: 10899700 DOI: 10.1159/000014635]

79 **Bubenik GA**. Gastrointestinal melatonin: localization, function, and clinical relevance. *Dig Dis Sci* 2002; **47**: 2336-2348 [PMID: 12395907 DOI: 10.1023/A:1020107915919]

80 **Carpentieri A**, Marchionatti A, Areco V, Perez A, Centeno V, Tolosa de Talamoni N. Antioxidant and antiapoptotic properties of melatonin restore intestinal calcium absorption altered by menadione. *Mol Cell Biochem* 2014; **387**: 197-205 [PMID: 24234419 DOI: 10.1007/s11010-013-1885-2]

81 **Areco V**, Rodriguez V, Marchionatti A, Carpentieri A, Tolosa de Talamoni N. Melatonin not only restores but also prevents the inhibition of the intestinal Ca(2+) absorption caused by glutathione depleting drugs. *Comp Biochem Physiol A Mol Integr Physiol* 2016; **197**: 16-22 [PMID: 26970583 DOI: 10.1016/j.cbpa.2016.03.005]

82 **Huai J**, Shao Y, Sun X, Jin Y, Wu J, Huang Z. Melatonin ameliorates acute necrotizing pancreatitis by the regulation of cytosolic Ca2+ homeostasis. *Pancreatology* 2012; **12**: 257-263 [PMID: 22687382 DOI: 10.1016/j.pan.2012.02.004]

83 **Yoo YM**, Jeung EB. Melatonin-induced calbindin-D9k expression reduces hydrogen peroxide-mediated cell death in rat pituitary GH3 cells. *J Pineal Res* 2010; **48**: 83-93 [PMID: 20041988 DOI: 10.1111/j.1600-079X.2009.00730.x]

84 **Wang AL**, Niu Q, Shi N, Wang J, Jia XF, Lian HF, Liu Z, Liu CX. Glutamine ameliorates intestinal ischemia-reperfusion Injury in rats by activating the Nrf2/Are signaling pathway. *Int J Clin Exp Pathol* 2015; **8**: 7896-7904 [PMID: 26339354]

85 **Newsholme P**, Lima MM, Procopio J, Pithon-Curi TC, Doi SQ, Bazotte RB, Curi R. Glutamine and glutamate as vital metabolites. *Braz J Med Biol Res* 2003; **36**: 153-163 [PMID: 12563517 DOI: 10.1590/S0100-879X2003000200002]

86 **Jiang Q**, Chen J, Liu S, Liu G, Yao K, Yin Y. l-Glutamine Attenuates Apoptosis Induced by Endoplasmic Reticulum Stress by Activating the IRE1α-XBP1 Axis in IPEC-J2: A Novel Mechanism of l-Glutamine in Promoting Intestinal Health. *Int J Mol Sci* 2017; **18** [PMID: 29206200 DOI: 10.3390/ijms18122617]

87 **Chaudhry KK**, Shukla PK, Mir H, Manda B, Gangwar R, Yadav N, McMullen M, Nagy LE, Rao R. Glutamine supplementation attenuates ethanol-induced disruption of apical junctional complexes in colonic epithelium and ameliorates gut barrier dysfunction and fatty liver in mice. *J Nutr Biochem* 2016; **27**: 16-26 [PMID: 26365579 DOI: 10.1016/j.jnutbio.2015.08.012]

88 **Moine L**, Díaz de Barboza G, Pérez A, Benedetto M, Tolosa de Talamoni N. Glutamine protects intestinal calcium absorption against oxidative stress and apoptosis. *Comp Biochem Physiol A Mol Integr Physiol* 2017; **212**: 64-71 [PMID: 28732794 DOI: 10.1016/j.cbpa.2017.07.006]

89 **Perez MJ**, Briz O. Bile-acid-induced cell injury and protection. *World J Gastroenterol* 2009; **15**: 1677-1689 [PMID: 19360911 DOI: 10.3748/wjg.15.1677]

90 **Úriz M**, Sáez E, Prieto J, Medina JF, Banales JM. Ursodeoxycholic acid is conjugated with taurine to promote secretin-stimulated biliary hydrocholeresis in the normal rat. *PLoS One* 2011; **6**: e28717 [PMID: 22194894 DOI: 10.1371/journal.pone.0028717]

91 **Verma A**, Maxwell JD, Ang L, Davis T, Hodges S, Northfield TC, Zaidi M, Pazianas M. Ursodeoxycholic acid enhances fractional calcium absorption in primary biliary cirrhosis. *Osteoporos Int* 2002; **13**: 677-682 [PMID: 12181628 DOI: 10.1007/s001980200092]

P- Reviewer: Kan L, Marcos M, Polonikov AV, Yu XJ
S- Editor: Wang XJ **L- Editor**: A **E- Editor**: Yin SY

World Journal of Gastroenterology

Submit a Manuscript: http://www.f6publishing.com

World J Gastroenterol 2018 November 28; 24(44): 4989-5004

DOI: 10.3748/wjg.v24.i44.4989

ISSN 1007-9327 (print) ISSN 2219-2840 (online)

ORIGINAL ARTICLE

Basic Study

Different distributions of interstitial cells of Cajal and platelet-derived growth factor receptor-α positive cells in colonic smooth muscle cell/interstitial cell of Cajal/platelet-derived growth factor receptor-α positive cell syncytium in mice

Chen Lu, Xu Huang, Hong-Li Lu, Shao-Hua Liu, Jing-Yu Zang, Yu-Jia Li, Jie Chen, Wen-Xie Xu

Chen Lu, Xu Huang, Hong-Li Lu, Yu-Jia Li, Wen-Xie Xu, Department of Physiology, Shanghai Jiao Tong University School of Medicine, Shanghai 200240, China

Shao-Hua Liu, Department of Anesthesiology, Ren Ji Hospital Affiliated to Shanghai Jiao Tong University School of Medicine, Shanghai 201112, China

Jing-Yu Zang, Jie Chen, Department of Pediatric Surgery, Xin Hua Hospital Affiliated to Shanghai Jiao Tong University School of Medicine, Shanghai 200092, China

ORCID number: Chen Lu (0000-0001-8020-0501); Xu Huang (0000-0002-8640-5177); Hong-Li Lu (0000-0001-5374-8336); Shao-Hua Liu (0000-0001-8359-3758); Jing-Yu Zang (0000-0002-6646-9341); Yu-Jia Li (0000-0001-8614-2234); Jie Chen (0000-0003-2308-0130); Wen-Xie Xu (0000-0003-3040-4340).

Author contributions: Lu C designed and performed the majority of experiments; Huang X, Lu HL, and Liu SH contributed new reagents and analytic tools; Zang JY, Li YJ, and Chen J analyzed the data; Xu WX wrote and edited the manuscript.

Supported by The National Natural Science Foundation of China, No. 31671192 and No. 31571180; and Foundation of Xin Hua Hospital, No. JZPI201708.

Institutional review board statement: This research was approved by the Ethics Committee of Shanghai Jiao Tong University School of Medicine.

Institutional animal care and use committee statement: The protocol was approved by the Committee on the Ethics of Animal Experiments of Shanghai Jiao Tong University School of Medicine (Permit Number: Hu 686-2009).

Conflict-of-interest statement: To the best of our knowledge, no conflict of interest exists.

Data sharing statement: No additional data is available.

ARRIVE guidelines statement: The authors have read the ARRIVE guidelines and prepared the manuscript accordingly.

Manuscript source: Unsolicited manuscript

Corresponding author to: Wen-Xie Xu, PhD, Professor, Department of Physiology, Shanghai Jiao Tong University School of Medicine, 800 Dongchuan Road, Shanghai 200240, China. wenxiexu@sjtu.edu.cn
Telephone: +86-21-34205639
Fax: +86-21-34205639

Received: August 24, 2018
Peer-review started: August 24, 2018
First decision: October 5, 2018
Revised: November 7, 2018
Accepted: November 7, 2018
Article in press: November 7, 2018
Published online: November 28, 2018

Abstract

AIM

To investigate the distribution and function of interstitial

cells of Cajal (ICCs) and platelet-derived growth factor receptor-α positive (PDGFRα$^+$) cells in the proximal and distal colon.

METHODS

The comparison of colonic transit in the proximal and distal ends was performed by colonic migrating motor complexes (CMMCs). The tension of the colonic smooth muscle was examined by smooth muscle spontaneous contractile experiments with both ends of the smooth muscle strip tied with a silk thread. Intracellular recordings were used to assess electrical field stimulation (EFS)-induced inhibitory junction potentials (IJP) on the colonic smooth muscle. Western blot analysis was used to examine the expression levels of ICCs and PDGFRα in the colonic smooth muscle.

RESULTS

Treatment with NG-nitro-L-arginine methyl ester hydrochloride (L-NAME) significantly increased the CMMC frequency and spontaneous contractions, especially in the proximal colon, while treatment with MRS2500 increased only distal CMMC activity and smooth muscle contractions. Both CMMCs and spontaneous contractions were markedly inhibited by NPPB, especially in the proximal colon. Accordingly, CyPPA sharply inhibited the distal contraction of both CMMCs and spontaneous contractions. Additionally, the amplitude of stimulation-induced nitric oxide (NO)/ICC-dependent slow IJPs (sIJPs) by intracellular recordings from the smooth muscles in the proximal colon was larger than that in the distal colon, while the amplitude of electric field stimulation-induced purinergic/PDGFRα-dependent fast IJPs (fIJPs) in the distal colon was larger than that in the proximal colon. Consistently, protein expression levels of c-Kit and anoctamin-1 (ANO1) in the proximal colon were much higher, while protein expression levels of PDGFRα and small conductance calcium-activated potassium channel 3 (SK3) in the distal colon were much higher.

CONCLUSION

The ICCs are mainly distributed in the proximal colon and there are more PDGFRα$^+$ cells are in the distal colon, which generates a pressure gradient between the two ends of the colon to propel the feces to the anus.

Key words: Interstitial cells of Cajal; Platelet-derived growth factor receptor-α positive cells; Smooth muscle cell/interstitial cell of Cajal/platelet-derived growth factor receptor-α positive cell syncytium; Nitric oxide; Purine

Core tip: The different distributions of interstitial cells of Cajal (ICCs) and platelet-derived growth factor receptor-α positive (PDGFRα$^+$) cells in the different parts of the colon result in a pressure gradient in the colon that propels the feces to the anus. Nitric oxide (NO) is mainly involved in the regulation of contraction through ICCs, and purine mainly participates in relaxation through PDGFRα$^+$ cells. The regulation of the inhibitory transmitter NO and purine through the two kinds of interstitial cells (ICCs and PDGFRα$^+$ cells) is very important for rhythmic colonic migrating motor complexes, which are the main driving force underlying colon transit.

Lu C, Huang X, Lu HL, Liu SH, Zang JY, Li YJ, Chen J, Xu WX. Different distributions of interstitial cells of Cajal and platelet-derived growth factor receptor-α positive cells in colonic smooth muscle cell/interstitial cell of Cajal/platelet-derived growth factor receptor-α positive cell syncytium in mice. *World J Gastroenterol* 2018; 24(44): 4989-5004 Available from: URL: http://www.wjgnet.com/1007-9327/full/v24/i44/4989.htm DOI: http://dx.doi.org/10.3748/wjg.v24.i44.4989

INTRODUCTION

In the gastrointestinal (GI) tract, smooth muscle cell/interstitial cell of Cajal/platelet-derived growth factor receptor-α positive cell (SIP) syncytium consists of interstitial cells of Cajal (ICCs), platelet-derived growth factor receptor-α positive cells (PDGFRα$^+$ cells), and smooth muscle cells (SMCs). ICCs and PDGFRα$^+$ cells are involved in the smooth muscle contraction. Remodeling or damaging of these cells can result in a variety of motor disorders[1]. Cells in the SIP syncytium express many kinds of receptors and ion channels, and conductance changes in any type of cell can induce the excitability or relaxation of the smooth muscle. Although there have been several studies of ICCs and PDGFRα$^+$ cells in the GI tract regarding their location, morphology, function and more, most studies have focused on the small intestine and stomach, with few concerning the colon[2,3]. Therefore, in the present study, we explored the distributions of the two kinds of interstitial cells along with their ion channels and transmission mechanisms for inducing contraction and diastolic reactions at both ends of the colon.

ICCs were first suggested to be GI pacemaker cells in the late 1970s based on electrophysiological and ultrastructural observations[4]. Anoctamin-1 (ANO1), a very important functional protein in ICCs, is a calcium-activated chloride channel that produces pacemaker currents[5]. Another interstitial cell type, PDGFRα$^+$ cells, referred to as "fibroblast-like" cells, express specific small conductance calcium-activated potassium channel 3 (SK3)[6]. When the SK3 channel is activated, large amounts of K^+ flow out, causing hyperpolarization and subsequent relaxation of PDGFRα$^+$ cells and downstream SMCs[7]. Consequently, the motility of smooth muscles depends on the balance between excitatory regulation from ICCs and inhibitory regulation from PDGFRα$^+$ cells.

Colonic motility requires the coordination of the enteric nervous system (ENS) and SIP syncytium. The ENS, consisting of excitatory motor neurons and inhibitory motor neurons (IMNs), including nitric oxide synthase (NOS) and purine neurons, is involved in the regulation of

colonic movement[8-10]. Mañé *et al*[11] have reported that nitric oxide (NO) is responsible for continuous smooth muscle relaxation, while purine neurons are responsible for transient relaxation, which may be dominant in colonic propulsion. In addition, colonic migrating motor complexes (CMMCs) known as the main form of the colonic transmission, have been demonstrated that their generation require two conditions: the activation of cholinergic motor neurons and the release of inhibitory neurotransmitters (mainly NO and purines), both of which can act on the SIP syncytium to regulate colonic transmission[12].

It has been reported that electrical field stimulation (EFS) can induce changes in the membrane potential mediated by inhibitory neurotransmitters called the inhibitory junction potential (IJP), and subsequent relaxation reaction[13,14]. IJPs are composed of two components: a fast-transient hyperpolarization (fIJP) and a subsequent slow and sustained hyperpolarization (sIJP)[6,12]. The release of NO is closely related to ICCs, which can influence the generation of spontaneous contractions and the initiation of sIJPs through ICCs[15-17]. On the other hand, fIJPs have been shown to be mediated by purines specifically through the P2Y1 receptor on PDGFRα^+ cells[7,14].

Based on these previous reports, we sought to characterize the mechanism of the ENS and SIP in the regulation of colon motility, especially distributions of ICCs and PDGFRα^+ cells in the proximal and distal colon according to the response of CMMC, smooth muscle contraction, and intracellular recoding for the blockers of neurotransmitters.

MATERIALS AND METHODS

Ethical statement

All animals were obtained from the Experimental Animal Center of Shanghai Jiao Tong University School of Medicine. This research rigorously complied with the rules of the Guide for the Care and Use of Laboratory Animals of the Science and Technology Commission of China (STCC Publication No. 2, revised 1988). The protocol was approved by the Committee on the Ethics of Animal Experiments of Shanghai Jiao Tong University School of Medicine (Permit Number: Hu 686-2009). All operations were performed under anesthesia using isopentane, and every manipulation of the experimental animals was performed while simultaneously attempting to maximally relieve any suffering.

Animals

Adult male ICR mice were obtained from the Experimental Animal Center of Shanghai Jiao Tong University School of Medicine. The mice, aged 35 d and weighing approximately 30 g, were housed at 22 ℃ under a 12 h light/dark cycle with free access to water and food.

CMMC experiments

Mice were sacrificed under general anesthesia induced by inhalant isoflurane overdose followed by cervical dislocation. Then, the abdomen was opened along the ventral midline, and the colon was exposed, removed quickly, and placed into Krebs solution continuously bubbling with a carbonated mixture (5% CO_2 and 95% O_2). The Krebs solution contained the following components (all concentrations in mmol/L): NaCl, 121.9; $NaHCO_3$, 15.5; KCl, 5.9; $MgSO_4$, 1.2; KH_2PO_4, 1.2; glucose, 11.5; and $CaCl_2$, 2.4. The entire colon was fixed in a Sylgard base dish with impalpable steel pins. The mesentery was carefully removed along the boundary line of the enterocoel under a dissecting microscope. All fecal pellets in the colon were artificially expelled with a 1-mL injector; this procedure was repeated to expel every pellet. This procedure must be performed with care to minimize intestinal damage. The empty colon was gently washed with 5 mL of warm Krebs solution, and a glass capillary tube was inserted through the lumen and linked to an artificial fecal pellet. The capillary was attached to the floor of the silica gel plate using U-shaped pins at the oral and anal end. A rectangular organ filled with 20 mL of warm Krebs solution (36.5 ± 0.5 ℃) was also constantly inundated with carbon-oxygen gas. Then, the colon specimen was gently perfused with warm Krebs solution and left to stabilize for 30-40 min to secure the recovery of the colonic contraction activity. A silk thread (USP 5/0) was attached to both ends of the colon. The mechanical activity of the CMMCs was recorded using an isometric force transducer (RM6240C, Chengdu Instrument Factory, China) linked to an amplifier device. A tension of 0.1 g was applied to the empty colon, which was equilibrated for at least 40 min before the addition of the experimental drugs.

Preparation of smooth muscle tissue and isometric tension measurement

The entire colon full of fecal pellets was isolated as described above. The colon was cut along the mesentery, which is on the colonic circular axis; the pellets were flushed out with Krebs solution; the colon was pinned to a Sylgard dish with the mucosa facing upwards; and the mucosa and submucosa were removed carefully under a dissecting microscope. Smooth muscle strips (approximately 2 mm × 8 mm) were obtained by cutting along the circular axis from the fresh smooth muscle tissue. A silk thread (USP 5/0) was attached to both ends of the muscle strips and attached along the circular axis into 10 mL organ baths containing warm (37 ℃) Krebs solution filled with 95% O_2 and 5% CO_2. The recording device was the same as that for the CMMCs above. A tension of 0.3 g was applied to the muscle strip, and it was equilibrated for at least 40 min before the recovery of its contraction activity.

Western blot analysis

Protein samples were extracted from the colonic smooth muscle tissues and lysed in radioimmunoprecipitation assay (RIPA) buffer (1:10; P0013, Beyotime Chemical Co., Jiangsu, China) and PMSF (1:100) solution. The

suspended material was centrifuged at 12000 rpm for 15 min at 4 ℃, mixed with 4 × loading buffer, and then boiled for 5 min in a 100 ℃ water bath. The protein concentration of the supernatant was calculated using the bicinchoninic acid (BCA) protein assay method (P0010, Beyotime Chemical Co., Jiangsu, China). Protein (30 μg/lane) was subjected to 7.5% sodium dodecyl sulfate-polyacrylamide gel electrophoresis (SDS-PAGE) and then transferred from the polyacrylamide gel to polyvinylidene difluoride (PVDF) membranes using an E-Blotter unit (Bio-Rad) for 120 min. Then, the PVDF membranes were blocked in 5% nonfat milk for 2 h and incubated with rabbit c-Kit and PDGFR-α monoclonal antibodies (1:1000; #3074, #3174, Cell Signaling Technology, United States) and with mouse anti-tubulin antibody (1:1000; AT819, Beyotime Chemical Co., Jiangsu, China) overnight at 4 ℃. The blots were then washed five times (5 min per wash) with Tris-HCl-buffered saline including 0.1% Tween-20 (TBST) and then incubated with secondary antibodies, including either anti-rabbit IgG HRP-linked antibody (1:1000; 7074; Cell Signaling Technology) or anti-mouse IgG HRP-linked antibody (1:1000; 7076; Cell Signaling Technology) for 2 h at room temperature. Protein signal detection was performed using an enhanced chemiluminescence agent (ECL reagents). The signals of the blots were analyzed using Quantity One software.

Intracellular microelectrode recording and electrical stimulation

Based on the operation above, smooth muscle tissue (approximately 20 mm × 8 mm) was isolated from the empty colon, fixed facing forward and up onto the base of a Sylgard-covered chamber, and constantly filled with warm (37 ℃) Krebs solution, 95% O_2, and 5% CO_2. The tissue was equilibrated for approximately 2 h before the recording started. The muscle tissue was maintained at 37 ± 0.5 ℃ through continuous perfusion with warm Krebs solution. Experimental procedures were carried out in the presence of nifedipine (1 μmol/L) to minimize the muscle contraction and maintain the cellular implements. Circular muscle cells were inserted using glass microelectrodes (80-100 MΩ) filled with KCl. Membrane potential was recorded with a Duo 773 (WPI Inc., Sarasota, FL, United States). EFS was made under a consistent voltage, pulse width, and duration (50 V, 0.5 ms, and 5 s, respectively) by two parallel platinum electrodes using a square-wave stimulator (YC-2 stimulator; Chengdu, China). The sIJPs and fIJPs of the smooth muscle were recorded in the presence and absence of various drugs, such as receptor antagonists or agonists in Krebs solution.

Drugs

Tetrodotoxin (TTX) was obtained from Absin Biochemical Company. Atropine was purchased from Sigma-Aldrich. Apamin, NG-Nitro-L-arginine methyl ester hydrochloride (L-NAME), NPPB, MRS2500, and CyPPA were obtained from Tocris Bioscience (Ellisville, MO, United States).

Statistical analysis

The data are described as the mean ± SE. The analysis of data differences between groups was performed using one-way analysis of variance (ANOVA), followed by the Bonferroni's post-hoc test or using the Student' s unpaired *t*-test when needed. *P*-values less than 0.05 were considered to represent significant differences between groups, and *n*-values correspond to the number of animals that were used in the indicated experiments.

RESULTS

Regulatory effects of the ENS/Ach/NO for ANO1 channels in ICCs on CMMCs and spontaneous contractions

Effects of TTX and atropine on CMMCs and spontaneous contractions: To demonstrate the role of the ENS in colonic transit, we used a Na^+ channel antagonist, TTX (0.4 μmol/L), to block neurons. TTX abolished the large amplitude contractions of CMMCs, and only the fast oscillating contractions remained. The contractions were decreased from 100% in controls to 30% ± 2.6% in the proximal colon and 21% ± 4.7% in the distal part ($^aP < 0.05$; $n = 6$, meaning the number of animals used and the same below; Figure 1A and C). Interestingly, the basal tone and frequencies of the burst-like contractions in both ends of the colon were markedly increased by TTX, indicating that the generation of CMMCs in the colon was significantly mediated by the ENS, while the increased basal tone and frequencies of the remaining contractions in the presence of TTX are likely generated directly by ICCs because the dominant effects of the ENS on ICCs were limited by TTX. In addition, the effects of TTX were significantly different between the proximal and distal colon. To further confirm the effects of TTX on the colonic contractions, we observed that TTX significantly increased the rate of spontaneous contractions from 100% in controls to 149% ± 4.2% in the proximal colon and 124% ± 5.4% in the distal part ($^aP < 0.05$; $n = 7$; Figure 1B and D). Moreover, there were significant differences in proximal and distal colon with TTX administration, respectively ($^cP < 0.05$; Figure 1A-D).

To explain the differences of TTX above, we further compared the roles of the excitatory neurons and inhibitory neurons in regulating colonic motility. First, atropine was employed to block acetylcholine (Ach), released by cholinergic neurons. We found that, similar to the effects of TTX, atropine (100 μmol/L) abolished the large amplitude contractions of CMMCs, and only the burst-like contractions (*e.g.*, ICC pacemaking activity) remained in both parts of the colon. Overall, CMMCs were significantly suppressed, from 100% in controls to 21% ± 1.9% in the proximal colon and 39% ± 3.7% in the distal part ($^aP < 0.05$; $n = 5$; Figure 1E and G). Similarly, spontaneous contractions were also partially decreased by atropine treatment, from 100% in controls to 57% ± 1.8% in the proximal colon and 74% ± 3.9% in the distal part ($^aP < 0.05$; $n = 7$; Figure 1F and H). Interestingly, significant

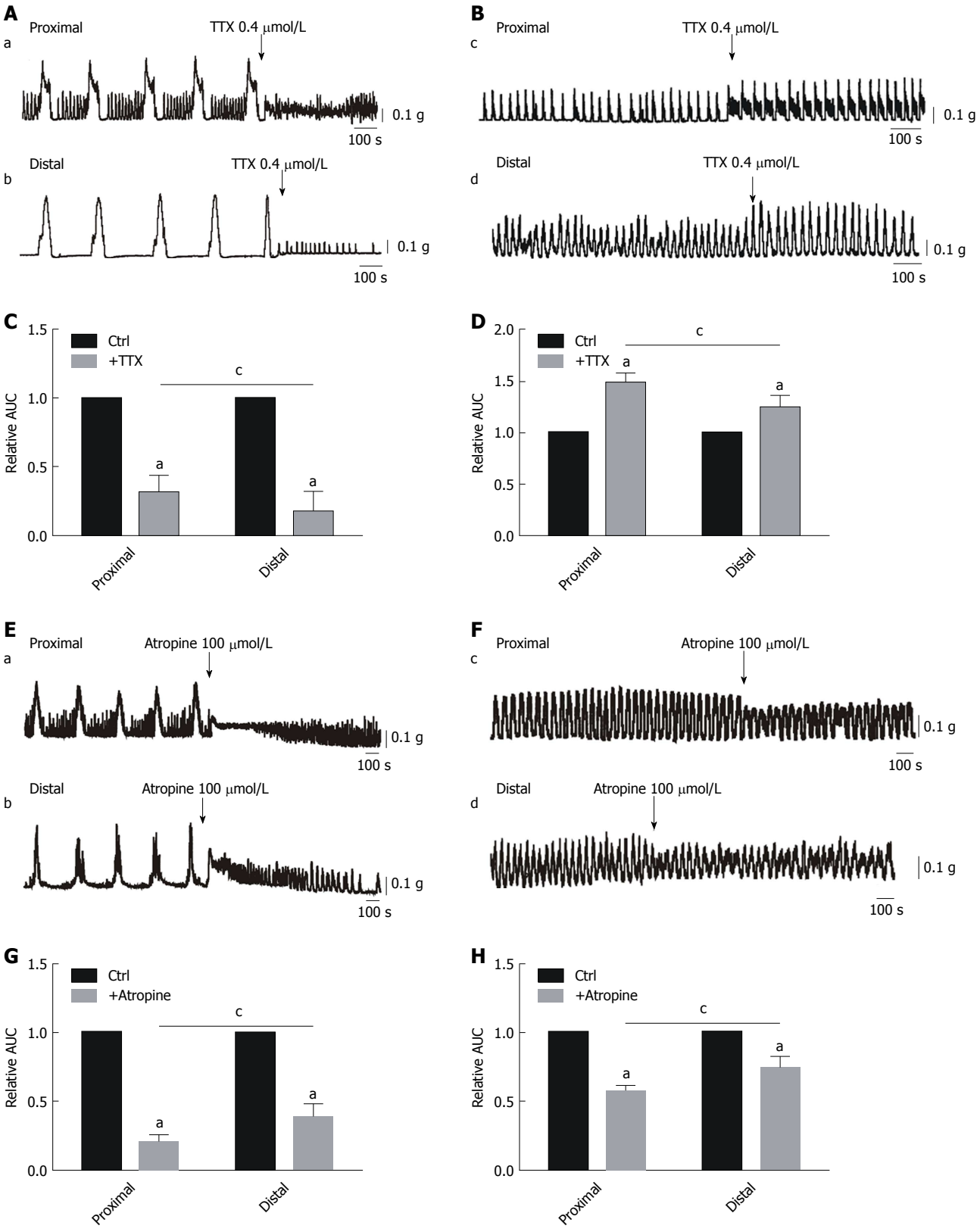

Figure 1 Effects of tetrodotoxin and atropine on smooth muscle contractions of the colon. A and C: Inhibitory effects of tetrodotoxin (TTX) treatment on colonic migrating motor complexes (CMMCs) in the proximal and distal colon, and summary data of the area under the curve (AUC) at 300 s. It is worth noting that AUC measurements can demonstrate the sum of both the amplitudes and frequencies. The data are normalized to the control value (before the application of TTX) (n = 6; $^{a}P < 0.05$ *vs* control; $^{c}P < 0.05$ *vs* proximal colon). B and D: Enhanced effects of TTX on spontaneous contractions in the proximal and distal colon of mice and summary of the contractile responses to TTX, as indicated by the AUC at 200 s, in the smooth muscle tissues of the proximal and distal colon of mice. The data are normalized to the control value (before the application of TTX) (n = 7; $^{a}P < 0.05$ *vs* control; $^{c}P < 0.05$ vs proximal colon). E and G: Responses of CMMCs to atropine in the proximal and distal colon and summary of data as indicated by the AUC at 300 s. The data are normalized to the control value (before the application of atropine) (n = 5; $^{a}P < 0.05$ *vs* control; $^{c}P < 0.05$ *vs* proximal colon). F and H: Inhibitory effects of atropine on spontaneous contraction in the proximal and distal colon and summary of data showing contractile responses to atropine as indicated by the AUC at 200 s. The data are normalized to the control value (before the application of atropine) (n = 7; $^{a}P < 0.05$ *vs* control; $^{c}P < 0.05$ *vs* proximal colon). TTX: Tetrodotoxin; AUC: Area under the curve.

differences remained between the proximal and distal ends treated with atropine in the CMMC and muscle strip experiments ($^{c}P < 0.05$; Figure 1E-H). These results suggest that Ach may play a regulatory role for ICCs.

Effects of L-NAME and NPPB on CMMCs and spontaneous contractions: To characterize the effects of NO on colonic motility, L-NAME (100 μmol/L), a nonspecific inhibitor of NOS, was employed in the present study. We found that CMMCs, especially their frequency, were significantly enhanced by L-NAME, from 100% in controls to 172% ± 4.6% in the proximal colon and 145% ± 4.4% in the distal part ($^{a}P < 0.05$; $n = 7$; Figure 2A and C). Similarly, spontaneous contractions became larger and faster after administration with L-NAME, from 100% in controls to 170% ± 11.5% in the proximal colon and 150% ± 4.0% in the distal part ($^{a}P < 0.05$; $n = 7$; Figure 2E-H). Importantly, we also found that the effects of L-NAME on both CMMCs and spontaneous contractions were more significant in the proximal colon than in the distal part, respectively ($^{c}P < 0.05$; Figure 2E-H). Based on these results, we confirmed that NO contributes substantially to the regulation of CMMC frequency and suggest that there may be more ICCs in the proximal colon than in the distal part.

To further confirm that ICCs have distinct distributions between different parts of the colon, NPPB, a blocker of ANO1 channels, was applied. NPPB treatment (3 μmol/L) significantly inhibited CMMCs, from 100% in controls to 22% ± 2.7% in the proximal colon and 46 ± 4.3% in the distal part ($^{a}P < 0.05$; $n = 5$; Figure 2E and G). The effects of NPPB were much more significant in the proximal part than in the distal part ($^{c}P < 0.05$; $n = 5$; Figure 2E and G). Furthermore, spontaneous contractions were also decreased by NPPB treatment, from 100% in controls to 19% ± 3.4% in the proximal colon and 48% ± 3.7% in the distal part ($^{a}P < 0.05$; $n = 5$; Figure 2F and H). However, the inhibitory effect of NPPB was much more significant in the proximal part than in the distal part of the colon ($^{c}P < 0.05$; $n = 5$; Figure 2F and H).

Regulatory effects of purine for SK3 channels in PDGFRα^{+} cells on CMMCs and spontaneous contractions

Effects of MRS-2500 treatment on CMMCs and spontaneous contractions: In subsequent experiments, to further investigate the role of PDGFRα^{+} cells in the regulation of colonic motility. First, MRS2500 was used (1 μmol/L; an antagonist of P2Y1) on CMMCs and spontaneous contractions. We found that in the proximal colon, MRS2500 had no significant effect on either CMMCs or spontaneous contractions (Figure 3A and B). However, in the distal colon, both CMMCs and spontaneous contractions were increased by MRS2500, reaching 143% ± 2.4% for CMMCs and 130% ± 4.2% for spontaneous contractions ($^{a}P < 0.05$; $n = 8$; Figure 3A-D). MRS2500 had a markedly stronger effect in the distal colon compared to the proximal part ($^{c}P < 0.05$; $n = 8$; Figure 3A-D), which indicates that there is an obvious difference between the two ends. Similarly, this effect may result from different distributions of PDGFRα^{+} cells in these colonic regions.

Effects of apamin and CyPPA on CMMCs and spontaneous contractions: To test the above hypothesis, we determined the effects of apamin (300 nmol/L; an SK3 channel antagonist) on colonic motility. We can observe that apamin significantly enhanced CMMCs, from 100% in controls to 126% ± 0.4% in the proximal colon and 148% ± 2.1% in the distal part ($^{a}P < 0.05$; $n = 7$; Figure 4A and C). Similar results were obtained for spontaneous contractions, which were increased from 100% in controls to 127% ± 1.6% in the proximal colon and 159% ± 3.4% in the distal part ($^{a}P < 0.05$; $n = 7$; Figure 4B and D). Similar to MRS2500 treatment, the effects of apamin in the distal colon were stronger than those in the proximal part ($^{c}P < 0.05$; $n = 7$; Figure 4A-D).

Subsequently, CyPPA (3 μmol/L), an SK3 channel agonist, was also used in the present study. We found that the effects of CyPPA were completely opposite of those observed with apamin treatment. CyPPA markedly inhibited CMMCs, from 100% in controls to 39% ± 1.7% in the proximal colon and 25% ± 2.2% in the distal part ($^{a}P < 0.05$; $n = 7$; Figure 4E and G). Clearly, the effects of CyPPA were much more significant in the distal part than in the proximal part of the colon ($^{c}P < 0.05$; $n = 7$; Figure 4E and G). Moreover, spontaneous contractions were also inhibited by CyPPA, from 100% in controls to 54% ± 4.1% in the proximal colon and 19% ± 3.6% in the distal part ($^{a}P < 0.05$; $n = 7$; Figure 4F and H). Therefore, CyPPA significantly inhibited both CMMCs and spontaneous contractions in both ends. Moreover, the effects of this drug in the distal colon were markedly stronger than those in the proximal part ($^{c}P < 0.05$; $n = 8$; Figure 4E-H).

Effects of ICC/ANO1 and PDGFRα^{+}/SK3 on colonic membrane potentials of smooth muscle tissue

Effects of ANO1 and SK3 antagonists on resting membrane potentials of colonic smooth muscle tissues: It is well-established that smooth muscle contraction and relaxation result from membrane depolarization and hyperpolarization[18]. To further evaluate the distributions of the two interstitial cell type, we first detected the average resting membrane potential (RMP) of colonic circular muscle cells in the proximal colon, which was 42.2 ± 1.92 mV, less than that in the distal part, which was 53.2 ± 2.86 mV ($^{a}P < 0.05$; $n = 12$; Figure 5A). Furthermore, NPPB induced membrane hyperpolarization in both parts of the colon, showing a greater extent in the proximal colon than in the distal part (9.17 ± 1.19 mV in the proximal colon and 4.67 ± 0.56 mV in the distal colon, $^{a}P < 0.05$; $n = 6$, Figure 5B and D). Nevertheless, apamin induced membrane depolarization, which was more marked in the distal

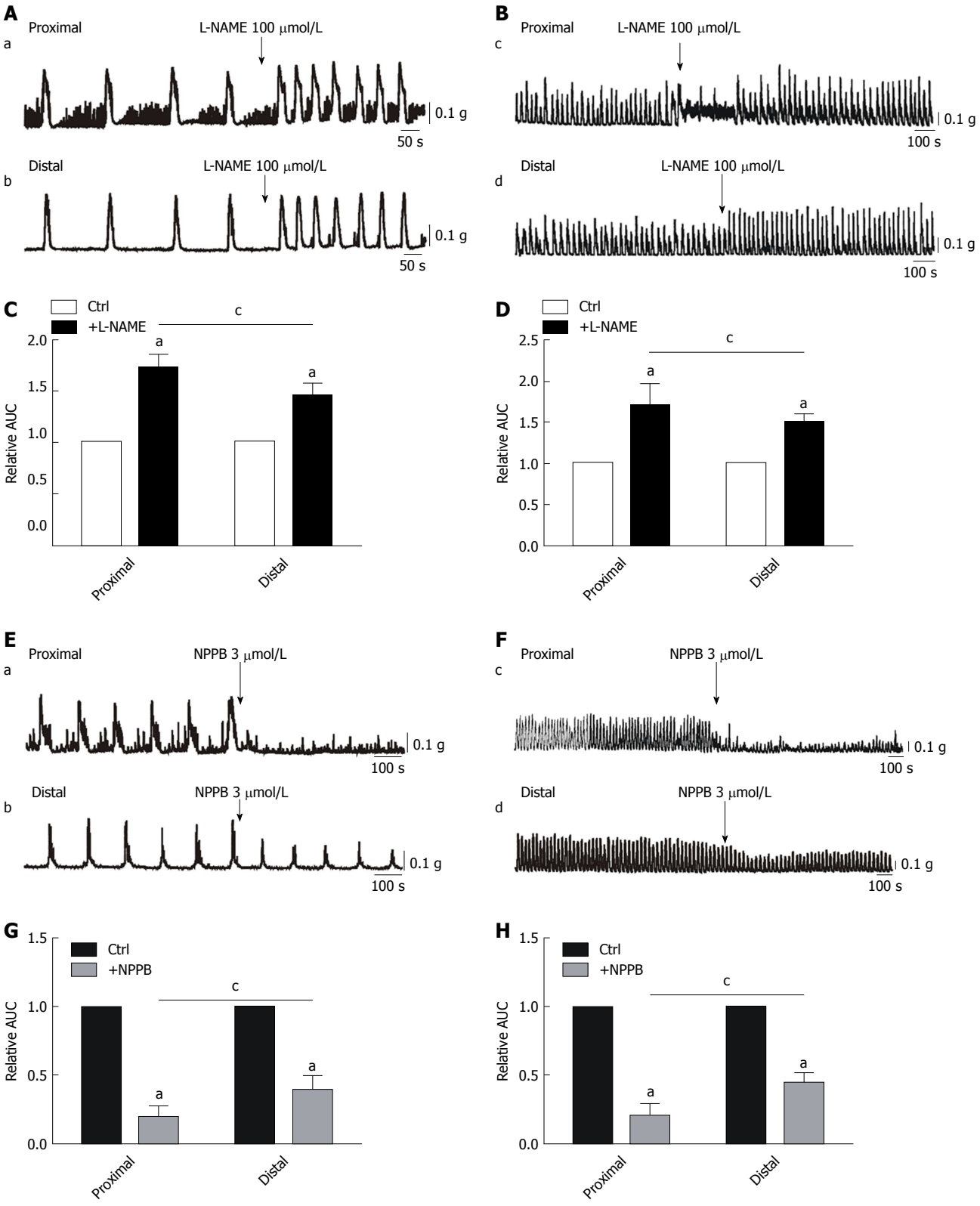

Figure 2 Effects of L-NAME and NPPB on smooth muscle contractions of the colon. A and C: Increased effects of L-NAME on colonic migrating motor complexes (CMMCs) in the proximal and distal colon and summary data of the area under the curve (AUC) at 300 s. The data are normalized to the control value (before the application of L-NAME) (n = 7; ^{a}P < 0.05 *vs* control; ^{c}P < 0.05 *vs* proximal colon). B and D: Enhanced effects of L-NAME on spontaneous contraction in the proximal and distal colon of mice and summary of the contractile responses to L-NAME as indicated by the AUC at 200 s. The data are normalized to the control value (before the application of L-NAME) (n = 7; ^{a}P < 0.05 *vs* control; ^{c}P < 0.05 *vs* proximal colon). E and G: Responses of CMMCs to NPPB in the proximal and distal colon and the summary of data as indicated by the AUC at 300 s. The data are normalized to the control value (before the application of NPPB) (n = 5; ^{a}P < 0.05 *vs* control; ^{c}P < 0.05 *vs* proximal colon). F and H: Inhibitory effects of NPPB (3 μmol/L) on spontaneous contraction in the proximal and distal colon and summary of the data showing contractile responses to NPPB as indicated by the AUC at 200 s. The data are normalized to the control value (before the application of NPPB) (n = 5; ^{a}P < 0.05 *vs* control; ^{c}P < 0.05 *vs* proximal colon). AUC: Area under the curve.

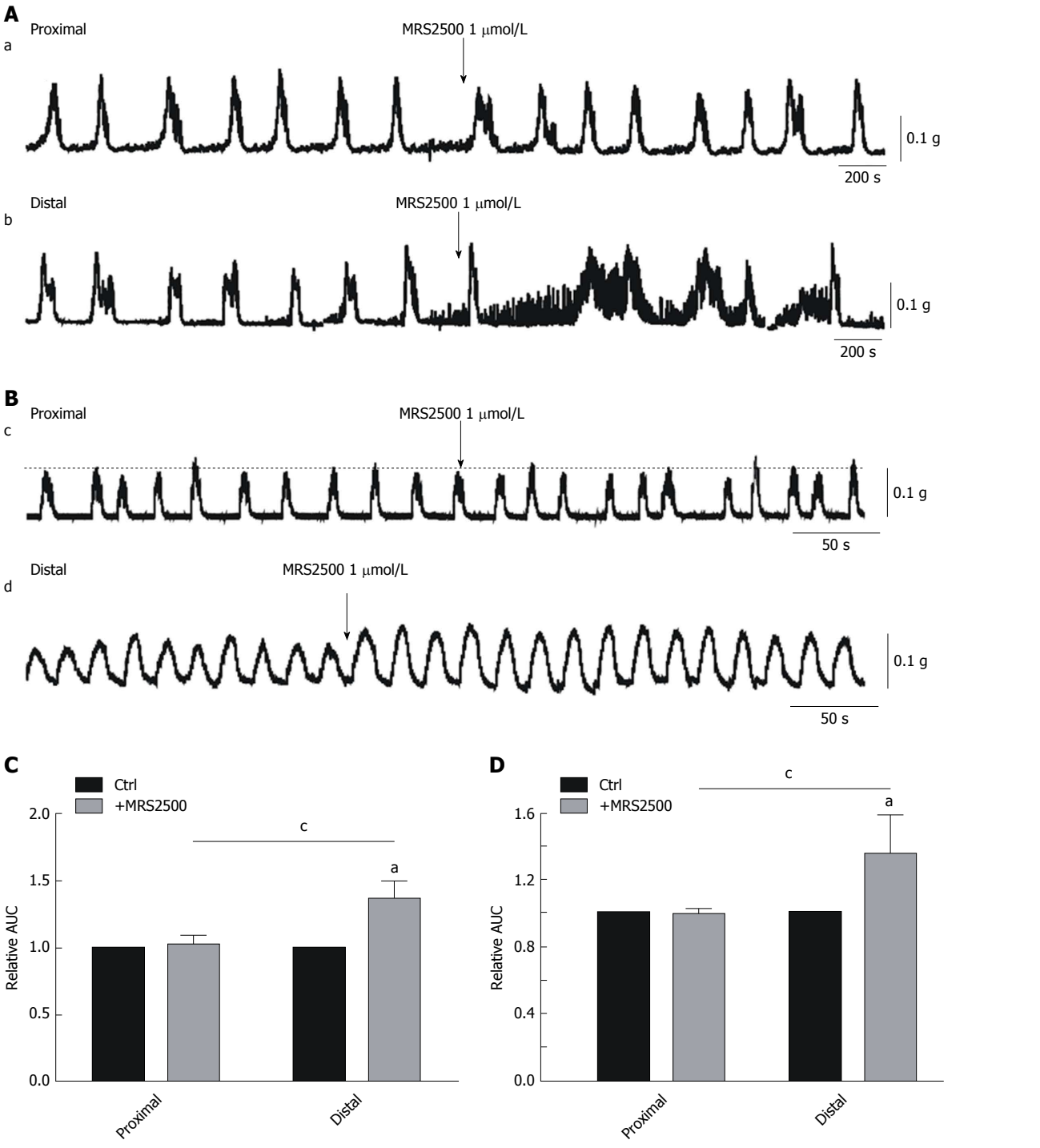

Figure 3 Effects of MRS2500 on smooth muscle contractions in the colon. A and C: Effects of MRS2500 on colonic migrating motor complexes (CMMCs) in the proximal and distal colon and summary of the area under the curve (AUC) at 300 s. The data are normalized to the control value (before the application of MRS2500) (n = 8; $^{a}P < 0.05$ *vs* control; $^{c}P < 0.05$ *vs* proximal colon). B and D: Representative traces illustrating the effects of the P2Y1 antagonist MRS2500 on the contractions of colonic smooth muscles in the proximal and distal colon of mice and summary of the contractile responses to MRS2500 as indicated by the AUC at 200 s. The data are normalized to the control value (before the application of MRS2500) (n = 8; $^{a}P < 0.05$ *vs* control; $^{c}P < 0.05$ *vs* proximal colon). AUC: Area under the curve.

colon than in the proximal part (7.10 ± 1.36 mV in the proximal colon and 11.07 ± 1.01 mV in the distal colon, $^{a}P < 0.05$; n = 5; Figure 5C and E).

Postjunctional potentials evoked by EFS in colonic smooth muscle tissues: Consequently, we used EFS to evaluate the response of membrane potentials to determine whether there were differences between the proximal and distal colon. We observed that EFS (50 V; 3, 6, and 9 Hz; 5 s) induced IJPs including fIJPs and sIJPs in both ends of the colon. The average amplitude of the fIJPs was larger in the distal colon than in the proximal part (6.70 ± 0.39, 11.8 ± 0.33, and 18.86 ± 0.53 mV in the proximal colon, n = 8; 11.24 ± 0.35, 14.58 ± 0. 34,

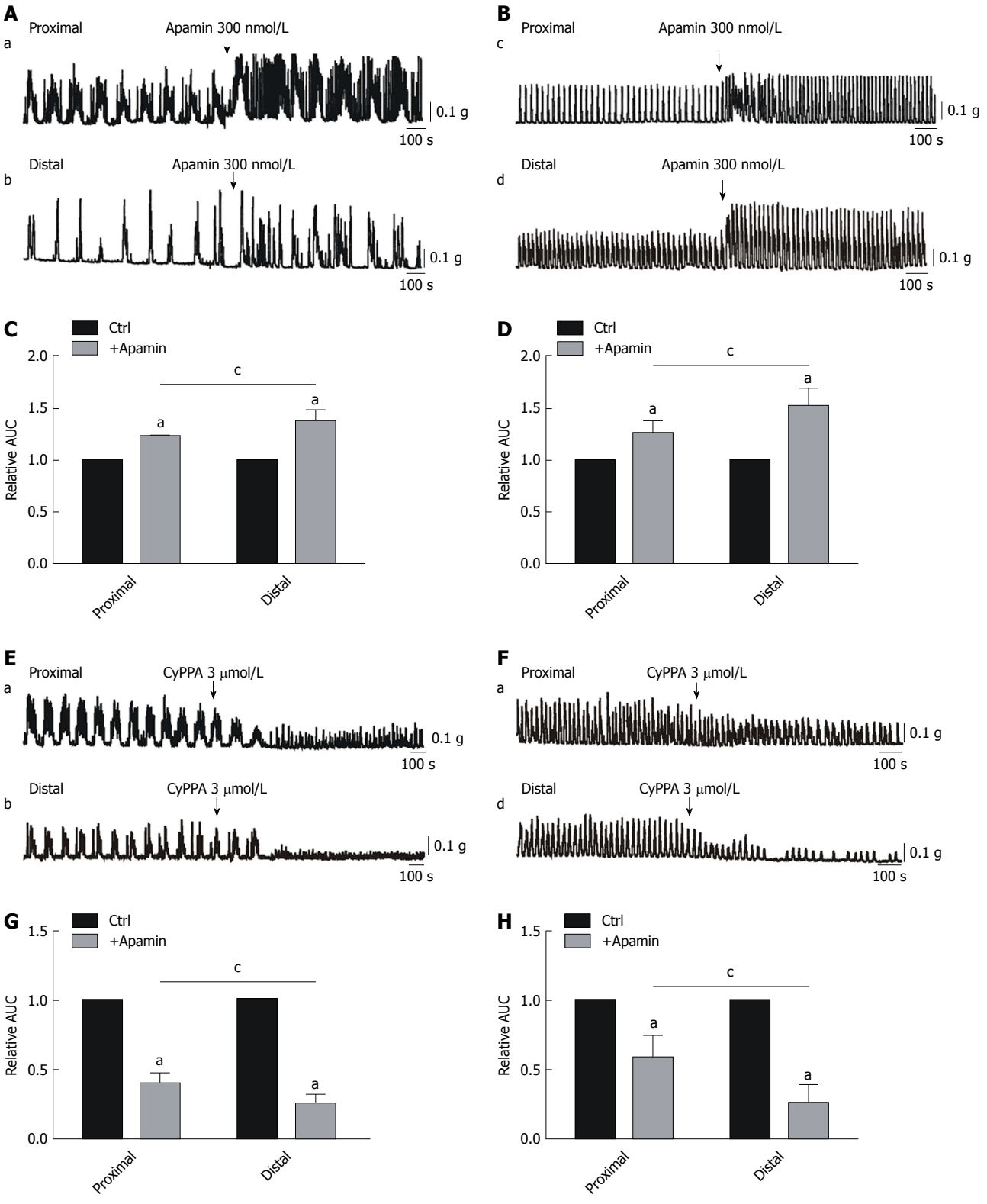

Figure 4 Effects of small conductance calcium-activated potassium channel 3 channel antagonist and agonist treatment on smooth muscle contractions in the murine colon. A and C: Responses of colonic migrating motor complexes (CMMCs) to small conductance calcium-activated potassium channel 3 (SK3) channel antagonist treatment in the proximal and distal colon and summary of the CMMC responses to apamin as indicated by the area under the curve (AUC) at 300 s. The data are normalized to the control value (before the application of apamin) (n = 7; ^{a}P < 0.05 *vs* control; ^{c}P < 0.05 *vs* proximal colon). B and D: Enhanced effects of apamin (300 nmol/L) on spontaneous contractions in the proximal and distal colon and summary of the data showing contractile responses to apamin as indicated by the AUC at 200 s. The data are normalized to control (before the application of apamin) (n = 7; ^{a}P < 0.05 *vs* control; ^{c}P < 0.05 *vs* proximal colon). E and G: Responses of CMMCs to SK3 channel agonist treatment in the proximal and distal colon and summary of the CMMC responses to CyPPA as indicated by the AUC at 300 s. The data are normalized to the control value (before the application of CyPPA) (n = 7; ^{a}P < 0.05 *vs* control; ^{c}P < 0.05 *vs* proximal colon). F and H: Inhibitory effects of CyPPA on spontaneous contractions in the proximal and distal colon and summary of the data showing contractile responses to CyPPA as indicated by the AUC at 200 s. The data are normalized to the control value (before the application of CyPPA) (n = 7; ^{a}P < 0.05 *vs* control; ^{c}P < 0.05 *vs* proximal colon). AUC: Area under the curve.

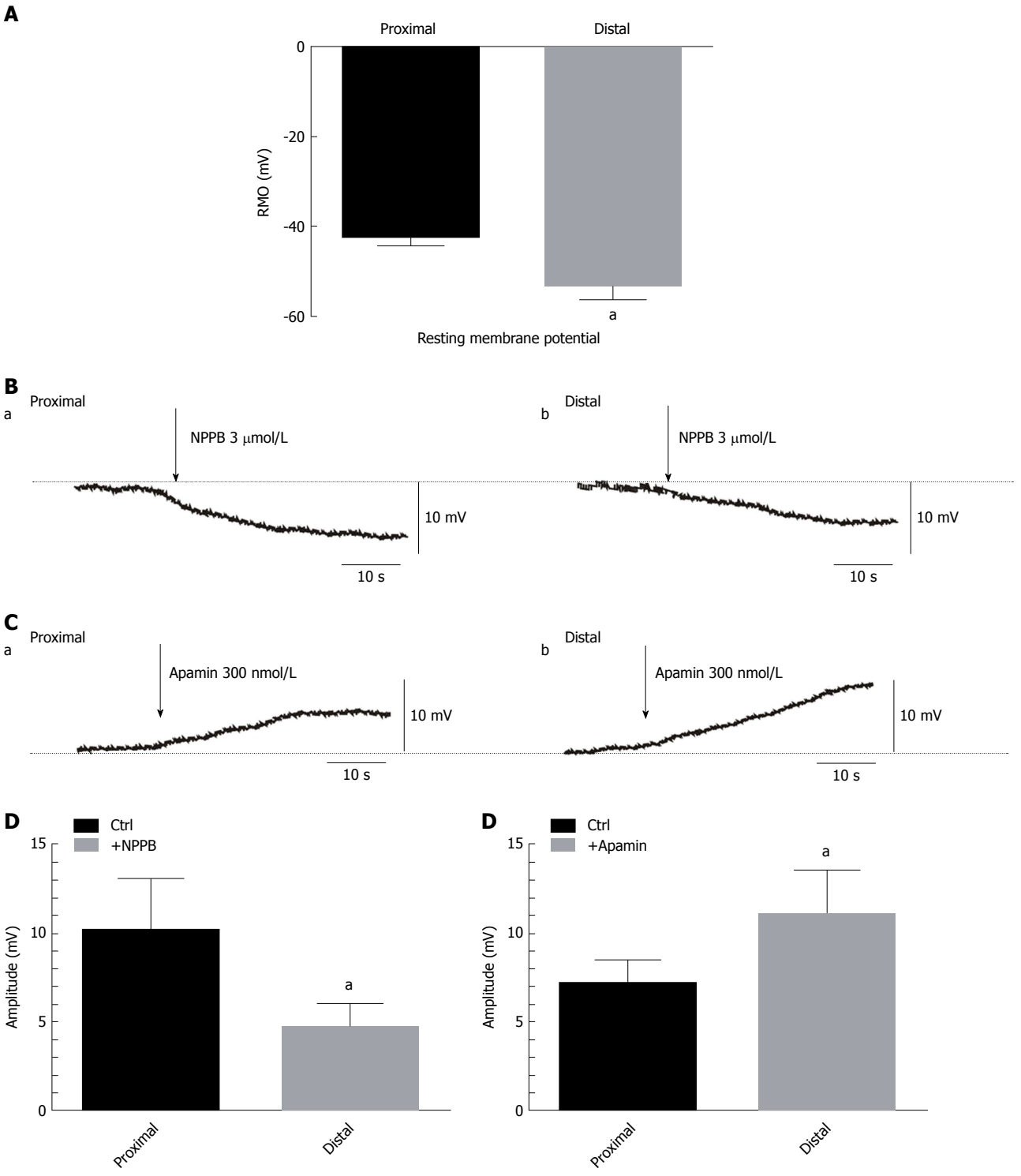

Figure 5 Effects of anoctamin-1 and small conductance calcium-activated potassium channel 3 channel antagonist treatment on membrane potentials in the murine colon. A: Summary of the resting membrane potentials of colonic smooth muscle cells from the proximal and distal colon of mice (n = 12; $^{a}P < 0.05$). B: Responses of membrane potentials to anoctamin-1 (ANO1) antagonist treatment (NPPB, 3 μmol/L, arrow). C: Responses of membrane potentials to SK3 antagonist treatment (apamin, 300 nmol/L, arrow). D and E: Summary of data showing the average effects of NPPB and apamin on membrane potentials in colonic smooth muscle cells from both ends of the colon (NPPB n = 6; apamin n = 5; $^{a}P < 0.05$). RMP: Resting membrane potentials.

and 23.60 ± 0.45 mV in the distal colon, n = 8; $^{a}P < 0.05$, Figure 6A-C), while the amplitude of sIJPs was more obvious in the proximal colon than in the distal parts (2.94 ± 0.17, 7.8 ± 0.25, and 3.60 ± 0.51 mV in the proximal colon, n = 8; 1.34 ± 0. 24, 5.14 ± 0.15, and 9.98 ± 0.56 mV in the distal part, n = 8; $^{a}P < 0.05$, Figure 6A, B, and D). These results further confirm that there is indeed a difference in the distribution of ICC and PDGFRα+ cells in the proximal and distal colon.

Changes in purine-dependent fIJPs and NO-dependent sIJPs in colonic smooth muscle tissues: For the purpose of illustrating the distribution of PDGFRα^{+} cells at both ends of the colon, L-NAME (100 μmol/L) and

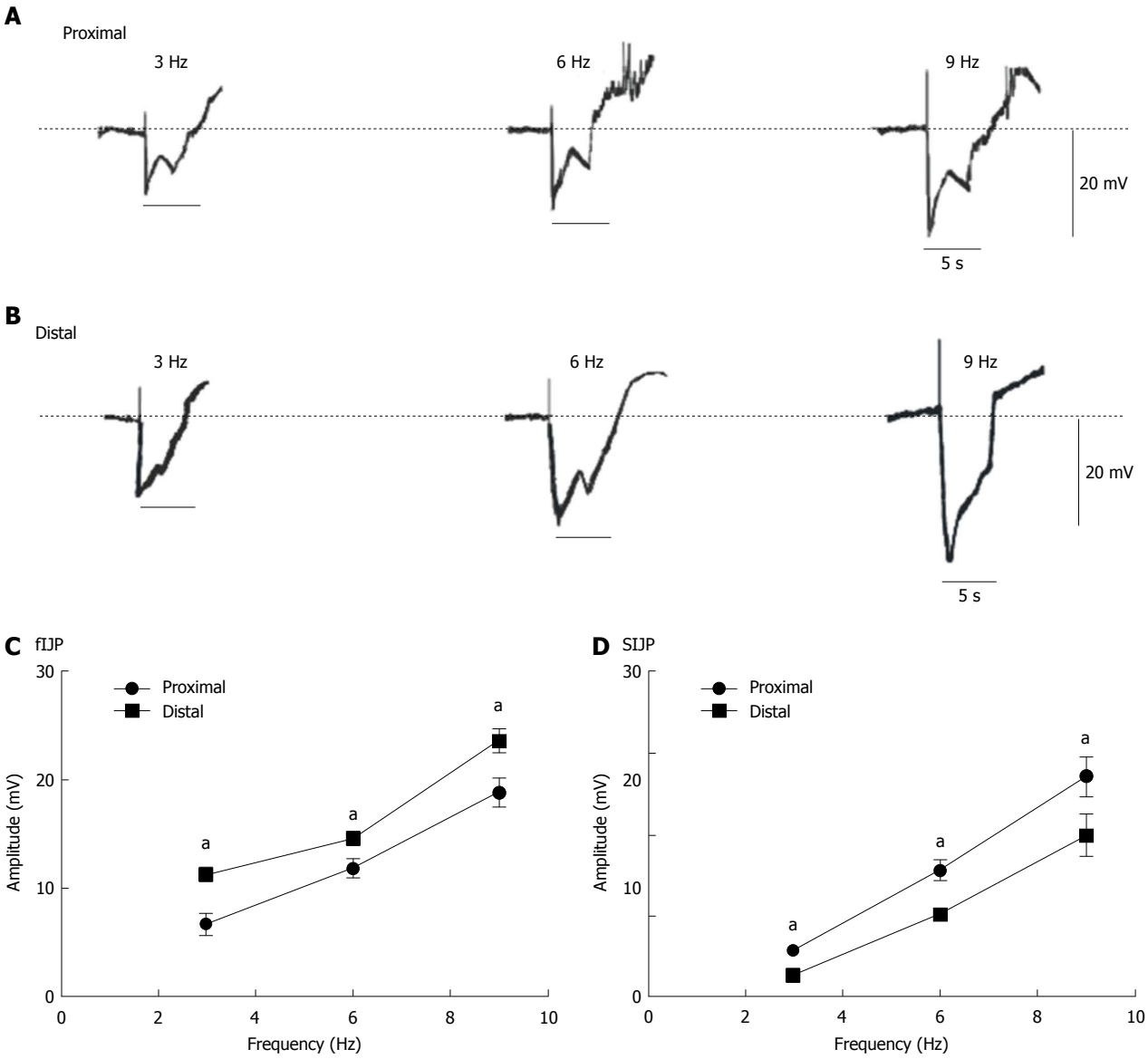

Figure 6 Membrane potentials evoked by electrical field stimulation in normal colonic proximal and distal muscles. A: Electrical field stimulation (EFS) from the proximal colon at different frequencies (50 V; 3, 6, and 9 Hz for 5 s; black bars in each panel) elicited biphasic hyperpolarization comprising a peak component followed by sustained hyperpolarization. B: EFS from the proximal colon at different frequencies (50 V; 3, 6, and 9 Hz for 5 s; black bars in each panel). C and D: Summary of data showing the average amplitude of fast inhibitory junction potentials and slow inhibitory junction potentials at both ends of the colon (n = 8; $^{a}P < 0.05$). fIJP: Fast inhibitory junction potential; sIJP: Slow inhibitory junction potential.

atropine (1 μmol/L) were used to block NO and Ach to solely observe the EFS response to purine. We found that the amplitude of the sIJPs significantly attenuated and almost all that remains were the fIJPs. The amplitudes of fIJPs in the distal colonic muscles remained stronger than those in the proximal colon (*i.e.*, 6.78 ± 0. 27, 9.20 ± 0. 49, and 18.00 ± 0.71 mV; $^{a}P < 0.05$; n = 7; Figure 7A and C). In the distal colon, the mean amplitudes were separately 12.44 ± 0. 47, 15.80 ± 0.73, and 24.22 ± 0.54 mV ($^{a}P < 0.05$; n =8; Figure 7B and C). These results indicate that the distal colon has more PDGFRα^{+} cells and stronger fIJPs primarily elicited by purine and induces relaxation.

To explore the distribution of ICCs at both ends of the colon, MRS2500 (1 μmol/L) and atropine (1 μmol/L) were used to block purines and Ach to solely observe the EFS response to NO. The addition of MRS2500 and atropine almost fully eliminated the fIJPs, leaving only the sIJPs. The amplitudes of sIJPs (with EFS 3, 6, and 9 Hz) in the proximal colon appeared much larger than those in the distal colon (*i.e.*, 3.12 ± 0.33, 5.54 ± 0.39, and 10.18 ± 0.40 mV, Figure 7E and F); in the proximal colon, the mean amplitudes of sIJPs were 5.54 ± 0. 43, 9.32 ± 0.53, and 14.8 ± 0.37 mV, respectively ($^{a}P < 0.05$; n = 7; Figure 7D and F). These results confirm that the proximal colon has a greater distribution of ICCs and stronger sIJPs elicited by NO, inducing stimulation by ICCs.

Expression levels of c-Kit and PDGFRα in colonic smooth muscle tissues

Finally, we examined the density of ICC, ANO1, PDGFRα,

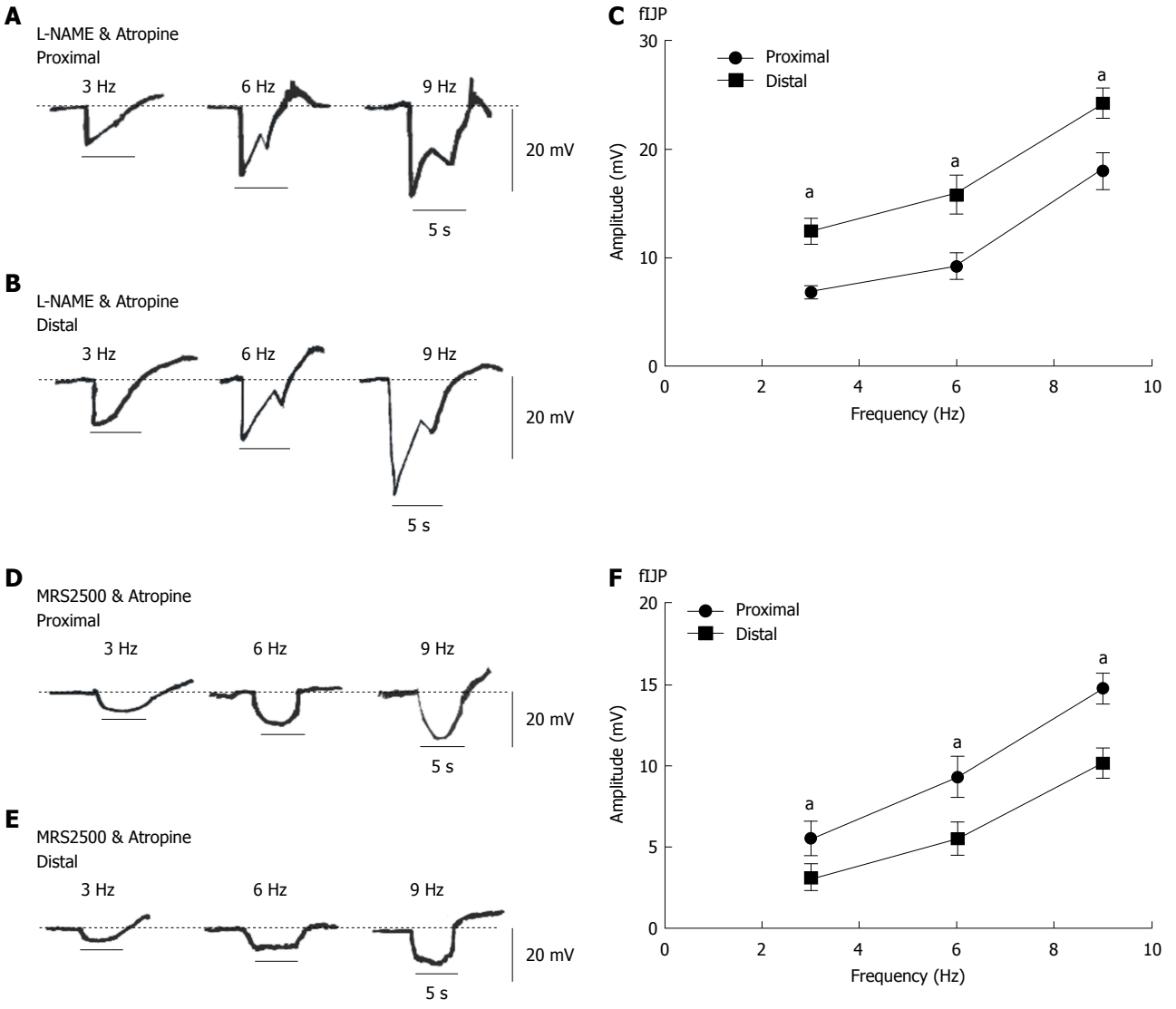

Figure 7 Fast inhibitory junction potential and slow inhibitory junction potential elicited by electrical field stimulation in smooth muscles of the proximal and distal colon. A and B: Atropine and L-NAME treatment blocked excitatory junction potentials (EJPs) and decreased slow inhibitory junction potentials (sIJPs) but had no effect on fast IJPs (fIJPs) in colonic muscles from both ends. D and E: Atropine and MRS2500 treatment blocked EJPs and decreased fIJPs but had no effect on sIJPs in colonic muscles from both ends. C and F: Summary of data showing the average amplitude of fIJPs and sIJPs (in the presence of atropine and L-NAME, n = 8; in the presence of atropine and MRS2500, n = 7; $^{a}P < 0.05$). fIJP: Fast inhibitory junction potential; sIJP: Slow inhibitory junction potential.

and SK3 in the smooth muscle tissues of the colon. We found that the expression levels of c-Kit and ANO1 were much higher in the proximal colon (97.7% ± 10.9% and 35.7% ± 4.3%, respectively), while those in the distal end were lower (58.2% ± 6.5% and 19% ± 3.6%, respectively [$^{a}P < 0.05$; n = 8; Figure 8A and C (c-Kit) and Figure 8B and D (ANO1)]. Additionally, the expression of the PDGFRα protein in the colonic muscle layer was significantly increased, from 54.8% ± 5.0% to 77.6% ± 3.2% in the proximal and distal ends, respectively; similarly, the expression of SK3 in the colonic muscle layer ranged from 36.2% ± 4.1% to 61.4% ± 3.1%, respectively, in the proximal and distal ends [$^{a}P < 0.05$; n = 8; Figure 8E and F (PDGFRα) and Figure 8E and G (SK3)]. These protein expression data directly show that the proximal colon has more ICCs and that the distal colon has more PDGFRα^{+} cells.

DISCUSSION

This study focused on the distribution and function of ICCs and PDGFRα^{+} cells at both ends of the colon and the role of NO and purines on colonic dynamic transmission. This finding may have clinical implications in studying and treating colonic dysmotility of inflammatory bowel disease (IBD) and irritable bowel syndrome (IBS). It has previously been established that the large intestine has many different motor patterns, including segmental activity, antiperistaltic and peristaltic waves, and tonic inhibition[19,20]. Regardless of transmission form, it is necessary to produce pressure gradient to ensure that feces are propelled from the proximal to distal colon. Therefore, we divided the colon into two segments to separately study its transmitting mechanism. Based on previous reports, the speed of fecal pellet propulsion

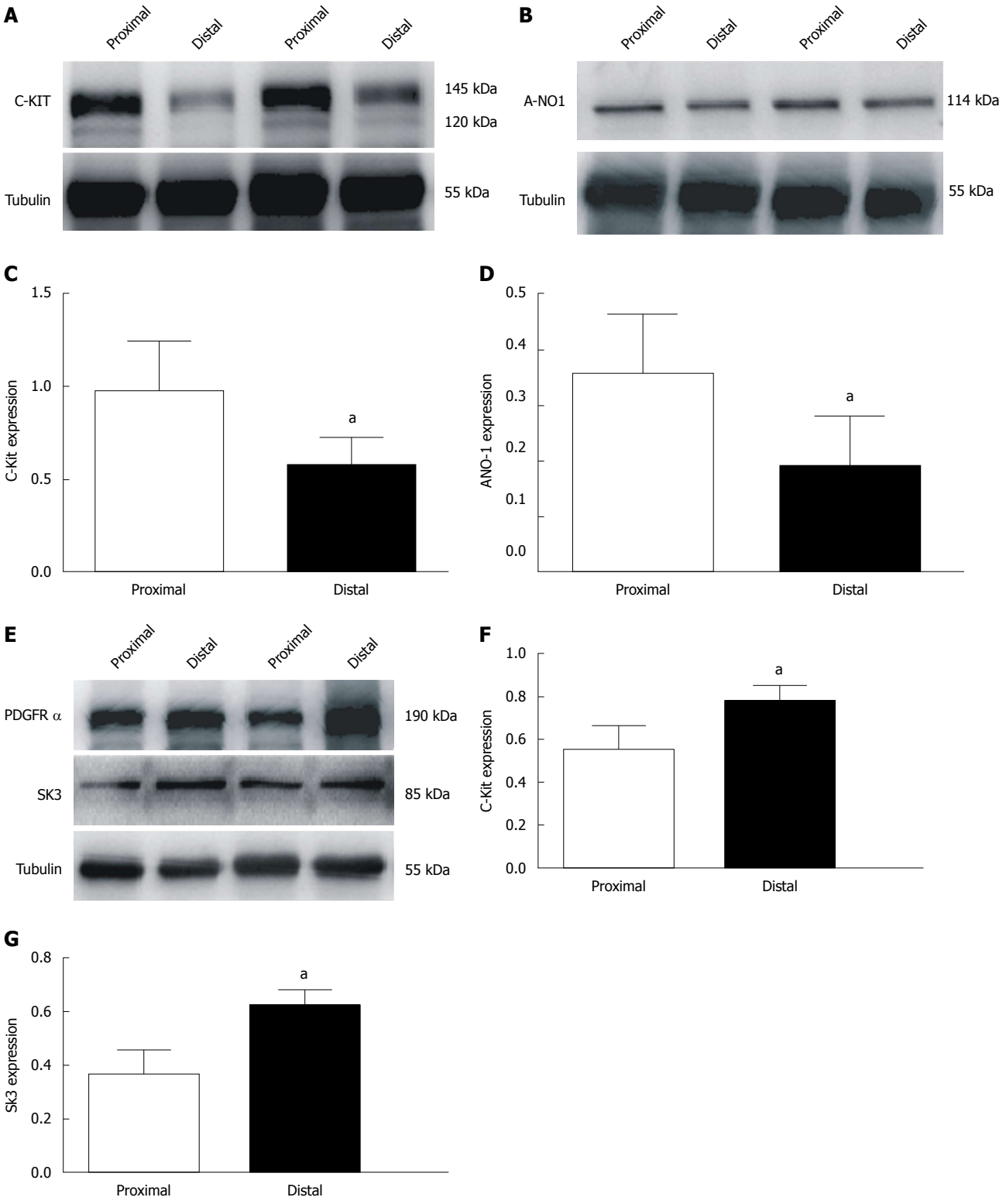

Figure 8 Expression levels of c-Kit/anoctamin-1 and platelet-derived growth factor receptor-α/small conductance calcium-activated potassium channel 3 in proximal and distal smooth muscles of the colon. A and B: Western blot analysis of interstitial cells of Cajal (ICCs) and anoctamin-1 (ANO1) in both ends of the colon. C and D: Summary of data analyzed using densitometric quantification (ICC, ANO1 $n = 8$, $^{a}P < 0.05$). E: Western blot analysis of platelet-derived growth factor receptor-α and small conductance calcium-activated potassium channel 3 in both ends of the colon. F and G: Summary of data analyzed using densitometric quantification ($n = 8$, $^{a}P < 0.05$). ANO1: Anoctamin-1; SK3: Small conductance calcium-activated potassium channel 3.

along the murine colon is the same as the conduction velocity of the CMMC contraction, indicating that CMMCs drive the pellets forward[21].

In our study, we found that the large amplitude contraction of CMMCs was almost completely inhibited when the ENS or cholinergic neurons were blocked; instead,

irregular contractions with much higher frequencies were recorded. Notably, in the CMMC experiments (treatment with TTX), the distal colon had more obvious drug effect, while in smooth muscle contraction experiment, the drug effect of proximal colon was more prominent in the presence of TTX or atropine (Figure 1). These results suggested that even though CMMC was almost abolished by TTX, the spontaneous contractions of the smooth muscle were significantly increased by TTX treatment. Therefore, we speculate that in the ENS, inhibitory neurons play a dominant role in spontaneous contractions of the colon. Moreover, the small irregular contraction waves in atropine may result from the pacemaker activity of ICCs and CMMCs are initiated by excitatory cholinergic neurons through ICCs. In the past several years, pacemaker function of ICCs and the ENS network have generally been considered as separate systems in colonic transit. However, new findings have reported that the pacemaker network in the colon consists of both ICC-MY (interstitial cells of Cajal of myenteric plexus) and ICC-IM (intramuscular interstitial cells of Cajal) and that this network is activated *via* cholinergic KV7.5 channel inhibition in ICC-IM[22]. Even though colonic motor transit has been confirmed by the cooperation of ICC networks with the ENS[23], information regarding the transit mechanism by which ICCs sequentially function remain unclear. Therefore, we primarily focused on the regulation of murine colonic contractile activity by nitrergic and purinergic neurons.

Based on the finding of nitrergic signaling through ICCs to regulate colonic spontaneous contraction and CMMCs (described above), we used L-NAME and NPPB to block NO and ANO1 in ICCs, respectively, to observe whether there are functional differences between the two ends of the colon (Figure 2). Our results showed that the AUC (equaling the frequencies and amplitudes) of CMMCs and spontaneous contractions in the smooth muscle were significantly increased in the presence of L-NAME or NPPB, indicating that NO is involved in regulating the frequency of CMMC through ICCs to maintain normal colonic transit. Moreover, the proximal colon has larger amplitude and higher frequencies in the presence of these two drugs, indicating that there are more ICCs in this part of the colon.

In addition to NO, purine is also considered to be involved in inhibitory regulation of smooth muscle contractions through another kind of interstitial cells-PDGFRα^+ cells[24]. Burnstock *et al*[7] first proposed that adenosine triphosphate (ATP) or purine was a main inhibitory neurotransmitter in the GI tract in 1970. Additionally, it may promote the release of glutamate (an inhibitory neurotransmitter) by binding to presynaptic metabotropic P2Y receptors[25]. Recent studies have proven that purinergic receptors (P2Y1) and SK3 channels are expressed in PDGFRα^+ cells responsible for nerve-mediated relaxation in the GI tract[24]. Compared to other classical neurotransmitters, the role of purinergic signaling in colonic transmission is not well understood or appreciated. Therefore, our results (Figures 3 and 4) proved that the amplitudes and frequencies of CMMCs and spontaneous contractions in the distal colon were markedly changed when P2Y1 receptors and SK3 channels were blocked by MRS2500 and apamin, respectively, or SK3 was activated by CyPPA, illustrating that purines help to maintain regular colonic transmission by inhibiting contractions. Moreover, the distal colon showing stronger contractile activity indicates that there may be more PDGFRα^+ cells, resulting from the inhibitory role of purine on PDGFRα^+ cells being eliminated by MRS2500 treatment.

Based on CMMC and smooth muscle contraction experiments, we speculated that ICCs and PDGFRα^+ cells may have different distributions at different ends of the colon. To confirm this hypothesis, we used intracellular recordings to detect whether there exists a difference in the electrophysiological properties between the two ends of the colon. Previous studies have shown that GI motility is regulated by excitatory and IMNs, among which IMNs evoke IJPs, causing muscle relaxation. In the colon, neurotransmitters released by the ENS could activate the conductance of interstitial cells (*i.e.*, ANO1 in ICCs or SK3 channels in PDGFRα^+ cells) to regulate the excitability of SMCs through gap junctions to meditate colonic motility[23,26]. ANO1 regulates sensory signal transduction and smooth muscle contractile activity to generate rhythmic contraction, which is supported by the absence of slow waves in *ANO1* knockout mice[27-29]. Additionally, SK3 channels in PDGFRα^+ cells are activated by purines and produce apamin-sensitive outward currents[30]. These SK3 channels are believed to be involved in inducing membrane hyperpolarization and IJPs. In GI smooth muscle tissues, IJPs have bipolar phases and consist of two main components: fIJP, induced by the release of purines in PDGFRα^+ cells, and sIJP arising from NO through ICCs[31,32], which was also proved in this study (Figures 5-7). More importantly, we also found that the amplitudes of fIJPs induced by purinergic neurons through PDGFRα^+ cells were much higher in the distal colon than in the proximal segment. Furthermore, the amplitude of sIJPs induced mainly by NO through ICCs was much higher in the proximal colon than in the distal part. These results provide concrete functional evidence that ICCs and PDGFRα^+ cells have a different distribution at both ends of the colon.

Finally, we confirmed that more ICCs were distributed in the proximal colon, whereas more PDGFRα^+ cells were distributed in the distal colon using Western blot analysis (Figure 8). We speculate that this distribution difference is responsible for the stronger contractions in the proximal colon and the relatively weaker contractions in the distal part, forming a pressure gradient from the proximal colon to the distal part to propel feces smoothly forward to the anus.

In summary, our findings in the present study provide clear evidence that the ENS regulates colonic motility through cholinergic and nitrergic neurons regulating the spontaneous rhythmic pacemaker activity of ICCs and through purinergic neurons mediating inhibitory ef-

fects on smooth muscle contractions by acting on P2Y1 receptors in PDGFRα$^+$ cells to suppress colonic transit. We further found that inhibitory neuromodulation has a leading role in colonic transmission, which may be associated with the formation of fecal pellets in the colon and full absorption of water and nutrients. Furthermore, the distribution characteristics of more ICCs in the proximal and more PDGFRα$^+$ cells in the distal colon contribute to the formation of a pressure gradient from the oral to anal ends of the colon, which is associated with the roles of ENS-NO/ICCs and purine/PDGFRα$^+$ cells in the regulation of colonic motility. Consequently, an in-depth understanding of the mechanism of colon motility may provide a new direction and target for the study and treatment of diarrhea or constipation in colon motility disorder, such as IBD and IBS.

ARTICLE HIGHLIGHTS

Research background

Interstitial cells of Cajal (ICCs) and PDGFRα$^+$ cells are mainly located in the smooth muscle layer of the colon, which is widely believed to play a critical role in the generation of colonic transit motility. Large numbers of studies have shown that ICCs are mainly responsible for the contraction response of the smooth muscle, while PDGFRα$^+$ cells mainly regulate the relaxation of the smooth muscle. Inhibitory neuronal transmitters [nitric oxide (NO) and purine] can respectively act on ICCs and PDGFRα$^+$ cells to mediate colonic transit, thus propelling feces into the rectum and the anus. However, the distributions of ICC and PDGFRα$^+$ in the colon remain unclear. Therefore, it is an important scientific problem to study the transit mechanism of the proximal and distal colon.

Research motivation

In recent years, the incidence of colonic dysmotility diseases has been increasing year by year, such as inflammatory bowel disease (IBD), irritable bowel syndrome (IBS), and complications of some diseases (*e.g.*, diabetes-induced slow transit constipation), whose main clinical symptoms are diarrhea or constipation. The smooth muscle layer, as the main source of colon power, consists of ICCs, PDGFRα$^+$ cells, and smooth muscle cells (SMCs) contacted by the gap junction. Therefore, it is very significant to study the differential distributions of ICCs and PDGFRα$^+$ cells in the two ends of the colon.

Research objectives

In this study, we for the first time researched the distributions and functions of ICCs and PDGFRα$^+$ cells in the proximal and distal colon. Then, we studied the roles of inhibitory neurotransmitters NO for ICCs and purine for P2Y1 receptor on PDGFRα$^+$ cells in colonic motility transit. This study may represent a future strategy for therapeutic intervention in disorders of colonic motility, such as IBD and IBS, by understanding the distributions and function of NO-ICCs and purine-PDGFRα$^+$ cells at both ends of the colon.

Research methods

First, we compared the isolated colonic transit differences between the proximal and distal colon using colonic migrating motor complexes (CMMCs). Then, we used the smooth muscle contraction experiment, which is the major source of colon motility, to compare the drug differences between the proximal and distal colon by adding the blockers and agonists of anoctamin-1 (ANO1) channels on ICCs and small conductance calcium-activated potassium channel 3 (SK3) channels on PDGFRα$^+$ cells. Subsequently, we compared the membrane potentials of the proximal and distal colon by intracellular recordings. Later, Western blot analysis was used to detect the protein expression of c-Kit, ANO1, PDGFRα, and SK3 in the colon. Finally, we added immunofluorescence methods to visually describe the distributions of ICC and PDGFRα$^+$ cells in the proximal and distal colon.

Research results

Treatment with tetrodotoxin (TTX) to block the enteric nervous system (ENS) in the CMMC experiment almost completely blocked colonic transit. However, in the smooth muscle contraction experiment, when the ENS was blocked, the contraction of the colon was enhanced, suggesting that inhibitory nerve regulation plays critical roles in the transmission of the colon. In addition, when the ANO1 channel on ICCs was blocked by NPPB, the proximal colon showed a more obvious inhibitory role. While the SK3 channels on PDGFRα$^+$ cells were blocked by apamin, there was a more obvious drug effect in the distal colon, indicating that the proximal colon might distribute more ICCs, and the distal colon has more PDGFRα$^+$ cells. Intracellular electrical recording experiments indicated that slow inhibitory junction potentials (sIJP) mediated by the NO-ICC-ANO1 signal pathway was more obvious in the proximal colon, while fast inhibitory junction potentials (fIJP) mediated by purine-PDGFRα$^+$-SK3 was more prominent in the distal colon, indicating that there are more ICCs in the proximal colon and more PDGFRα$^+$ cells in the distal colon from the membrane potential level.

Research conclusions

In this study, we demonstrated that NO has a more obvious effect on the ICCs in the proximal colon, while purine has a more prominent effect on the distal PDGFRα$^+$ cells, indicating that there are more ICC cells in the proximal colon and more PDGFRα$^+$ cells in the distal colon. In addition, NO and purine acting on the SMC/ICC/PDGFRα$^+$ cell (SIP) syncytium (consisting of SMCs, ICCs, and PDGFRα$^+$ cells) are both inhibitory neurotransmitters, suggesting that colonic transit is mainly dominated by inhibitory neuromodulation. Although the stomach and small intestine are dominated by excitatory neuromodulation, this feature of the colon may contribute to the adequate absorption of nutrients and the formation of feces.

Research perspectives

This is the first study to report that the differential distributions of ICCs and PDGFRα$^+$ cells at the two ends of the colon. Our findings have highlighted the effects of inhibitory neuromodulation NO-ICC-ANO1 and purine-PDGFRα$^+$ cells-SK3 on colonic transit. In order to maintain regular colonic transit, the perfect cooperation of NO-ICC and purine-PDGFRα$^+$ cells is required. Therefore, in the future study of colon dynamic disorder such as IBD or IBS, we can start from whether the distribution and function of ICC and PDGFRα$^+$ cells have changed, and then extend to the effect of the ENS, especially inhibitory neuromodulation, on colonic transmission disorder to find the pathogenesis of colonic transit dysfunction. These findings in the present study may provide new insights and strategies for the diagnosis and treatment of gastrointestinal motility disorders.

REFERENCES

1 **Sanders KM**, Ward SM, Koh SD. Interstitial cells: regulators of smooth muscle function. *Physiol Rev* 2014; **94**: 859-907 [PMID: 24987007 DOI: 10.1152/physrev.00037.2013]

2 **Sanders KM**, Koh SD, Ward SM. Interstitial cells of cajal as pacemakers in the gastrointestinal tract. *Annu Rev Physiol* 2006; **68**: 307-343 [PMID: 16460275 DOI: 10.1146/annurev.physiol.68.040504.094718]

3 **Huizinga JD**, Chen JH. Interstitial cells of Cajal: update on basic and clinical science. *Curr Gastroenterol Rep* 2014; **16**: 363 [PMID: 24408748 DOI: 10.1007/s11894-013-0363-z]

4 **Faussone Pellegrini MS**, Cortesini C, Romagnoli P. [Ultrastructure of the tunica muscularis of the cardial portion of the human esophagus and stomach, with special reference to the so-called Cajal's interstitial cells]. *Arch Ital Anat Embriol* 1977; **82**: 157-177 [PMID: 613989]

5 **Bernstein K**, Vink JY, Fu XW, Wakita H, Danielsson J, Wapner R, Gallos G. Calcium-activated chloride channels anoctamin 1 and 2 promote murine uterine smooth muscle contractility. *Am J Obstet Gynecol* 2014; **211**: 688.e1-688.10 [PMID: 24928056 DOI: 10.1016/

j.ajog.2014.06.018]
6 **Song NN**, Lu HL, Lu C, Tong L, Huang SQ, Huang X, Chen J, Kim YC, Xu WX. Diabetes-induced colonic slow transit mediated by the up-regulation of PDGFRα$^+$ cells/SK3 in streptozotocin-induced diabetic mice. *Neurogastroenterol Motil* 2018 Epub ahead of print [PMID: 29521017 DOI: 10.1111/nmo.13326]
7 **Jiménez M**. Platelet-derived growth factor receptor-α-positive cells: new players in nerve-mediated purinergic responses in the colon. *J Physiol* 2015; **593**: 1765-1766 [PMID: 25871557 DOI: 10.1113/JP270259]
8 **Qu ZD**, Thacker M, Castelucci P, Bagyánszki M, Epstein ML, Furness JB. Immunohistochemical analysis of neuron types in the mouse small intestine. *Cell Tissue Res* 2008; **334**: 147-161 [PMID: 18855018 DOI: 10.1007/s00441-008-0684-7]
9 **Foong JP**, Hirst CS, Hao MM, McKeown SJ, Boesmans W, Young HM, Bornstein JC, Vanden Berghe P. Changes in Nicotinic Neurotransmission during Enteric Nervous System Development. *J Neurosci* 2015; **35**: 7106-7115 [PMID: 25948261 DOI: 10.1523/JNEUROSCI.4175-14.2015]
10 **Lu HL**, Huang X, Wu YS, Zhang CM, Meng XM, Liu DH, Kim YC, Xu WX. Gastric nNOS reduction accompanied by natriuretic peptides signaling pathway upregulation in diabetic mice. *World J Gastroenterol* 2014; **20**: 4626-4635 [PMID: 24782615 DOI: 10.3748/wjg.v20.i16.4626]
11 **Mañé N**, Gil V, Martínez-Cutillas M, Clavé P, Gallego D, Jiménez M. Differential functional role of purinergic and nitrergic inhibitory cotransmitters in human colonic relaxation. *Acta Physiol* (Oxf) 2014; **212**: 293-305 [PMID: 25327170 DOI: 10.1111/apha.12408]
12 **Durnin L**, Lees A, Manzoor S, Sasse KC, Sanders KM, Mutafova-Yambolieva VN. Loss of nitric oxide-mediated inhibition of purine neurotransmitter release in the colon in the absence of interstitial cells of Cajal. *Am J Physiol Gastrointest Liver Physiol* 2017; **313**: G419-G433 [PMID: 28705804 DOI: 10.1152/ajpgi.00045.2017]
13 **Hibberd TJ**, Costa M, Travis L, Brookes SJH, Wattchow DA, Feng J, Hu H, Spencer NJ. Neurogenic and myogenic patterns of electrical activity in isolated intact mouse colon. *Neurogastroenterol Motil* 2017; **29**: 1-12 [PMID: 28418103 DOI: 10.1111/nmo.13089]
14 **Zhang Y**, Lomax AE, Paterson WG. P2Y1 receptors mediate apamin-sensitive and -insensitive inhibitory junction potentials in murine colonic circular smooth muscle. *J Pharmacol Exp Ther* 2010; **333**: 602-611 [PMID: 20103587 DOI: 10.1124/jpet.109.160978]
15 **Lies B**, Beck K, Keppler J, Saur D, Groneberg D, Friebe A. Nitrergic signalling via interstitial cells of Cajal regulates motor activity in murine colon. *J Physiol* 2015; **593**: 4589-4601 [PMID: 26227063 DOI: 10.1113/JP270511]
16 **Kaji N**, Horiguchi K, Iino S, Nakayama S, Ohwada T, Otani Y, Firman, Murata T, Sanders KM, Ozaki H, Hori M. Nitric oxide-induced oxidative stress impairs pacemaker function of murine interstitial cells of Cajal during inflammation. *Pharmacol Res* 2016; **111**: 838-848 [PMID: 27468647 DOI: 10.1016/j.phrs.2016.07.030]
17 **Smith TK**, Koh SD. A model of the enteric neural circuitry underlying the generation of rhythmic motor patterns in the colon: the role of serotonin. *Am J Physiol Gastrointest Liver Physiol* 2017; **312**: G1-G14 [PMID: 27789457 DOI: 10.1152/ajpgi.00337.2016]
18 **Blair PJ**, Rhee PL, Sanders KM, Ward SM. The significance of interstitial cells in neurogastroenterology. *J Neurogastroenterol Motil* 2014; **20**: 294-317 [PMID: 24948131 DOI: 10.5056/jnm14060]
19 **Costa M**, Dodds KN, Wiklendt L, Spencer NJ, Brookes SJ, Dinning PG. Neurogenic and myogenic motor activity in the colon of the guinea pig, mouse, rabbit, and rat. *Am J Physiol Gastrointest Liver Physiol* 2013; **305**: G749-G759 [PMID: 24052530 DOI: 10.1152/ajpgi.00227.2013]
20 **Costa M**, Wiklendt L, Simpson P, Spencer NJ, Brookes SJ, Dinning PG. Neuromechanical factors involved in the formation and propulsion of fecal pellets in the guinea-pig colon. *Neurogastroenterol Motil* 2015; **27**: 1466-1477 [PMID: 26251321 DOI: 10.1111/nmo.12646]
21 **Heredia DJ**, Dickson EJ, Bayguinov PO, Hennig GW, Smith TK. Localized release of serotonin (5-hydroxytryptamine) by a fecal pellet regulates migrating motor complexes in murine colon. *Gastroenterology* 2009; **136**: 1328-1338 [PMID: 19138686 DOI: 10.1053/j.gastro.2008.12.010]
22 **Wright GW**, Parsons SP, Loera-Valencia R, Wang XY, Barajas-López C, Huizinga JD. Cholinergic signalling-regulated KV7.5 currents are expressed in colonic ICC-IM but not ICC-MP. *Pflugers Arch* 2014; **466**: 1805-1818 [PMID: 24375291 DOI: 10.1007/s00424-013-1425-7]
23 **Huizinga JD**, Martz S, Gil V, Wang XY, Jimenez M, Parsons S. Two independent networks of interstitial cells of cajal work cooperatively with the enteric nervous system to create colonic motor patterns. *Front Neurosci* 2011; **5**: 93 [PMID: 21833164 DOI: 10.3389/fnins.2011.00093]
24 **Lee H**, Koh BH, Peri LE, Sanders KM, Koh SD. Purinergic inhibitory regulation of murine detrusor muscles mediated by PDGFRα+ interstitial cells. *J Physiol* 2014; **592**: 1283-1293 [PMID: 24396055 DOI: 10.1113/jphysiol.2013.267989]
25 **Patti L**, Raiteri L, Grilli M, Parodi M, Raiteri M, Marchi M. P2X(7) receptors exert a permissive role on the activation of release-enhancing presynaptic alpha7 nicotinic receptors co-existing on rat neocortex glutamatergic terminals. *Neuropharmacology* 2006; **50**: 705-713 [PMID: 16427662 DOI: 10.1016/j.neuropharm.2005.11.016]
26 **Furness JB**. The enteric nervous system and neurogastroenterology. *Nat Rev Gastroenterol Hepatol* 2012; **9**: 286-294 [PMID: 22392290 DOI: 10.1038/nrgastro.2012.32]
27 **Hwang SJ**, Blair PJ, Britton FC, O'Driscoll KE, Hennig G, Bayguinov YR, Rock JR, Harfe BD, Sanders KM, Ward SM. Expression of anoctamin 1/TMEM16A by interstitial cells of Cajal is fundamental for slow wave activity in gastrointestinal muscles. *J Physiol* 2009; **587**: 4887-4904 [PMID: 19687122 DOI: 10.1113/jphysiol.2009.176198]
28 **Cipriani G**, Serboiu CS, Gherghiceanu M, Faussone-Pellegrini MS, Vannucchi MG. NK receptors, Substance P, Ano1 expression and ultrastructural features of the muscle coat in Cav-1(-/-) mouse ileum. *J Cell Mol Med* 2011; **15**: 2411-2420 [PMID: 21535398 DOI: 10.1111/j.1582-4934.2011.01333.x]
29 **Huang F**, Rock JR, Harfe BD, Cheng T, Huang X, Jan YN, Jan LY. Studies on expression and function of the TMEM16A calcium-activated chloride channel. *Proc Natl Acad Sci USA* 2009; **106**: 21413-21418 [PMID: 19965375 DOI: 10.1073/pnas.0911935106]
30 **Iino S**, Nojyo Y. Immunohistochemical demonstration of c-Kit-negative fibroblast-like cells in murine gastrointestinal musculature. *Arch Histol Cytol* 2009; **72**: 107-115 [PMID: 20009347 DOI: 10.1679/aohc.72.107]
31 **Lang RJ**. Do 'fibroblast-like cells' intercede during enteric inhibitory motor neurotransmission in gastrointestinal smooth muscles? *J Physiol* 2011; **589**: 453-454 [PMID: 21285025 DOI: 10.1113/jphysiol.2010.204016]
32 **Yeoh JW**, Corrias A, Buist ML. A mechanistic model of a PDGFRα(+) cell. *J Theor Biol* 2016; **408**: 127-136 [PMID: 27521526 DOI: 10.1016/j.jtbi.2016.08.004]

P- Reviewer: Liu S, Rolle U **S- Editor**: Ma RY
L- Editor: Wang TQ **E- Editor**: Yin SY

World Journal of Gastroenterology

Submit a Manuscript: http://www.f6publishing.com

World J Gastroenterol 2018 November 28; 24(44): 5005-5012

DOI: 10.3748/wjg.v24.i44.5005

ISSN 1007-9327 (print) ISSN 2219-2840 (online)

ORIGINAL ARTICLE

Basic Study

Development of a novel rat model of heterogeneous hepatic injury by injection with colchicine *via* the splenic vein

Yan-Yan Zhang, Chao-Xu Zhang, Yu Li, Xuan Jiang, Yong-Fang Wang, Yang Sun, Jun Wang, Wan-Ying Ji, Yi Liu

Yan-Yan Zhang, Medical Imaging Center,The Affiliated Hospital of Liaoning Traditional Chinese Medical University, Shenyang 110032, Liaoning Province, China

Yan-Yan Zhang, Yong-Fang Wang, Yang Sun, Jun Wang, Wan-Ying Ji, Yi Liu, Department of Radiology, The First Hospital of China Medical University, Shenyang 110001, Liaoning Province, China

Chao-Xu Zhang, Department of Medical Oncology, The First Hospital of China Medical University, Shenyang 110001, Liaoning Province, China

Yu Li, Xuan Jiang, Department of Cardiac Surgery, The First Hospital of China Medical University, Shenyang 110001, Liaoning Province, China

ORCID number: Yan-Yan Zhang (0000-0003-4391-688X); Chao-Xu Zhang (0000-0002-5643-2561); Yu Li (0000-0002-4433-8420); Xuan Jiang (0000-0002-3950-9504); Yong-Fang Wang (0000-0002-4804-3566); Yang Sun (0000-0001-7795-9824); Jun Wang (0000-0003-4405-9867); Wan-Ying Ji (0000-0002-9360-8642); Yi Liu (0000-0002-3442-8713).

Author contributions: Liu Y designed the research; Zhang YY, Li Y, and Jiang X performed the research; Wang YF contributed new reagents or analytic tools; Sun Y, Wang J, and Ji WY analyzed the data; Zhang YY and Zhang CX wrote the paper.

Supported by the Chinese National Natural Science Foundation, No. 81471719.

Institutional review board statement: This study was reviewed and approved by the Ethics Committee of the First Hospital of China Medical University (No. AF-SOP-07-7.1-01).

Institutional animal care and use committee statement: All experimental procedures were performed in accordance with the Guide for the Care and Use of Laboratory Animals published by the National Institutes of Health. This study was approved by the animal care committee of our university.

Conflict-of-interest statement: To the best of our knowledge, no conflict of interest exists.

Data sharing statement: No additional data are available.

ARRIVE guidelines statement: The ARRIVE Guidelines have been adopted.

Manuscript source: Unsolicited manuscript

Corresponding author to: Yi Liu, PhD, Professor, Department of Radiology, The First Hospital of China Medical University, Heping District, No. 155, Nanjing Street, Shenyang 110001, Liaoning Province, China. liuyicmu@sina.cn
Telephone: +86-18740085050
Fax: +86-24-83282859

Received: September 11, 2018
Peer-review started: September 11, 2018
First decision: October 11, 2018
Revised: October 20, 2018
Accepted: November 2, 2018
Article in press: November 2, 2018
Published online: November 28, 2018

Abstract

AIM

To develop a novel rat model of heterogeneous hepatic injury.

METHODS

Seventy male Sprague-Dawley rats were randomly divided into a control group (n = 10) and a colchicine group (n =

60). A 0.25% colchicine solution (0.4 mL/kg) was injected *via* the splenic vein in the colchicine group to develop a rat model of heterogeneous hepatic injury. An equal volume of normal saline was injected *via* the splenic vein in the control group. At days 3, 7, and 14 and weeks 4, 8, and 12 after the operation, at least seven rats of the colchicine group were selected randomly for magnetic resonance imaging (MRI) examinations, and then they were euthanized. Ten rats of the control group underwent MRI examinations at the same time points, and then were euthanized at week 12. T2-weighted images (T2WI) and diffusion weighted imaging (DWI) were used to evaluate the heterogeneous hepatic injury. The heterogeneous injury between the left and right hepatic lobes was assessed on liver sections according to the histological scoring criteria, and correlated with the results of MRI study.

RESULTS

Obvious pathological changes occurred in the hepatic parenchyma in the colchicine group. Hepatic injury scores were significantly different between the left and right lobes at each time point ($P < 0.05$). There was a significant difference in apparent diffusion coefficient (ADC) of DWI and liver-to-muscle ratio (LMR) of T2WI between the left and right lobes of rats in the colchicine group ($P < 0.05$) at each time point, and similar results were observed between the colchicine and control groups. Besides, there was a significant correlation between hepatic injury scores and ADC values or LMR ($r = -0.682$, $P = 0.000$; $r = -0.245$, $P = 0.018$).

CONCLUSION

Injection with colchicine *via* the splenic vein can be used to successfully develop a rat model of heterogeneous hepatic injury. DWI and T2WI may help evaluate the heterogeneous injury among liver lobes.

Key words: Heterogeneous hepatic injury; Rat model; Colchicine; T2-weighted images; Diffusion weighted imaging

Core tip: In this study, injection with colchicine *via* the splenic vein is shown to successfully develop a rat model of heterogeneous hepatic injury. Obvious pathological changes occurred in the hepatic parenchyma in the colchicine group. A significant difference was observed in liver injury scores, apparent diffusion coefficient values, and liver-to-muscle ratios of T2-weighted images (T2WI) between the left and right lobes in the colchicine group ($P < 0.05$). Our study suggested that diffusion weighted imaging and T2WI can be used to evaluate the heterogeneous injury among liver lobes.

Zhang YY, Zhang CX, Li Y, Jiang X, Wang YF, Sun Y, Wang J, Ji WY, Liu Y. Development of a novel rat model of heterogeneous hepatic injury by injection with colchicine *via* the splenic vein. *World J Gastroenterol* 2018; 24(44): 5005-5012 Available from: URL: http://www.wjgnet.com/1007-9327/full/v24/i44/5005.htm DOI: http://dx.doi.org/10.3748/wjg.v24.i44.5005

INTRODUCTION

Heterogeneous hepatic injury is often manifested in patients with hepatic tumors, especially those accompanied by hepatitis and cirrhosis. Estimation of total and regional hepatic function is essential for preventing postoperative liver failure and devising an effective treatment plan for patients with hepatic tumors[1]. The current technological limitations that preclude whole-organ assessment of heterogeneous hepatic injury present a clinical challenge. Unfortunately, the lack of an ideal animal model of heterogeneous hepatic injury has hindered the development of such assessment methods[2]. Therefore, it is urgent to establish a practical and reproducible animal model of heterogeneous hepatic injury to provide a manipulable *in vivo* tool for future development of simple, safe, and effective whole liver assessment methods.

Several animal models have been established to evaluate liver function, but they are limited in their ability to reflect homogeneous hepatic injury. The most popular of these models induce hepatic injury subcutaneous injection with a mixture of CCl_4 and olive oil to induce hepatic injury[3] and daily gavage with colchicine consecutively for 4 wk (in mice)[4].

Colchicine is an antimitotic cytotoxic agent derived from the *Colchicum autumnale* plant. Although the exact mechanism of hepatotoxicity of colchicine remains unclear, in the present study we injected rats with colchicine *via* the splenic vein to develop a practical model of heterogeneous hepatic injury. The heterogeneous injury between the left and right hepatic lobes was assessed on liver sections according to the histological scoring criteria, which was then correlated with the results of magnetic resonance imaging (MRI) using the sequences reported for evaluating hepatic injury[5,6].

MATERIALS AND METHODS

Compliance with ethical requirements

All experimental procedures were performed in accordance with the Guide for the Care and Use of Laboratory Animals published by the National Institutes of Health. This study was approved by the animal care committee of our university.

Animals and grouping

Seventy male Sprague-Dawley rats of SPF grade, weighing 280 ± 20 g, were purchased form Changsheng Laboratory, Benxi, Liaoning (certification number: SCXK-2015-0001). Before the start of experiments, the rats were fed normally in separated cages. The animals were randomly divided into a control group ($n = 10$) and a colchicine group ($n = 60$). All animals were fed a

Figure 1 Development of a rat model of heterogeneous hepatic injury. After anesthesia and splenic vein dissection, 0.25% colchicine at a dose of 0.4 mL/kg was injected *via* the splenic vein.

standard diet before the operation.

Induction of heterogeneous hepatic injury in rats

All rats were fasted for at least 6 hours before the operation. Pentobarbital sodium (1%; 40 mg/kg) was injected intraperitoneally for anesthesia. For rats in the colchicine group, after opening the peritoneal cavity, 0.25% colchicine (Nanjng Zelang Medical Technology Co. Ltd., Nanjing, China; purity: > 98%; injection rate: 0.1 mL/s) was injected at a dose of 0.4 mL/kg *via* the splenic vein. For rats in the control group, the peritoneal cavity was opened similarly and an equal volume of normal saline was injected *via* the splenic vein (Figure 1). After the operation, all animals were fed a normal diet. Twelve rats in the colchicine group died after 24 h and were excluded from further experiments.

MRI procedure

At days 3, 7, and 14 and week 4 after the operation, seven rats of the colchicine group, and at weeks 8 and 12, ten rats of the colchicine group were randomly selected for MRI examinations, and then the rats were euthanized by over-anesthesia. One rat died from an overdose of anesthetic at week 8, and a second one died at week 12. Ten rats of the control group underwent MRI examinations at the same time points, and were euthanized at week 12 after MRI examinations. Liver tissue was fixed in 4% paraformaldehyde.

Prior to MRI examinations, the selected rats were fasted for about 8 h. After anesthesia by intraperitoneal injection with 1% pentobarbital sodium (40 mg/kg), MRI was performed using a GE Signa HDxT 3.0T magnet scanner with a wrist coil. The detailed scanning settings are as follows: T2-weighted images (T2WI): TR, 3840 ms; TE, 85 ms; field of view, 14 cm; NEX, 4; matrix, 256 × 192; slice thickness, 3 mm; flip angle, 90°; scan time, 3 min and 12 s; and diffusion weighted imaging (DWI): b = 500 s/mm^2; TR, 5000 ms; TE, 77.3 ms; field of view, 14 cm; NEX, 2; matrix, 128 × 128; slice thickness, 3 mm; flip angle, 90°; scan time, 40 s.

Image analysis

Image analysis was performed independently by two radiologists with more than 5 years of clinical experience, who were blinded to the histopathologic results. The largest regions of interest (ROIs) as possible were defined in both the left and right lobes of the liver in three successive slices on T2WI and apparent diffusion coefficient (ADC) maps, and the vessels and artifacts were excluded when positioning the ROI. The signal intensities of the erector spinae muscles on T2WI were detected on the same slices simultaneously, and the average values of these measurements on the three successive slices were calculated. Based on the average values, the liver-to-muscle ratio (LMR) on T2WI, ΔLMR (the difference of LMR on T2WI between the left and right lobes of the liver), and ΔADC (the difference of ADC values between the left and right lobes of the liver) were calculated[7,8].

Liver histopathology

Liver tissue was fixed, paraffin-embedded, and sliced (5.0 μm). After conventional hematoxylin and eosin (H&E) staining, the sections were examined under a light microscope. Masson's trichrome staining was used to assess fibrosis. Scoring for liver injury was conducted according to the following criteria: no hepatocellular necrosis, edema, or inflammatory cell infiltration, 0; mild, 1; moderate, 2; severe, 3. Liver fibrosis was scored as no fibrosis, 0; fibrous portal expansion, 1; bridging fibrosis, 2; bridging fibrosis with architectural distortion, 3; liver cirrhosis, 4[9,10].

Statistical analysis

Data are expressed as mean ± standard deviation. Normal distribution was assessed by the Kolmogorov-Smirnov test. Differences in liver injury, ΔLMR, and ΔADC between the two groups were compared using the Student's *t*-test or Mann-Whitney *U*-test. Statistical significance was defined as $P < 0.05$. Correlations between LMR, ADC values, and liver injury scores in the colchicine group were assessed using the Spearman's correlation coefficient by rank test. Statistically significant correlations were defined as $P < 0.05$.

RESULTS

Postoperative status

All animals awoke within 1 h after the operation. Rats in the colchicine group exhibited fatigue, reduced food and water consumption, and slow movement after the operation. Although the activity of rats in the control group was slightly decreased, their general state was normal upon awaking. Rats in the control group all survived the operation. Twelve rats in the colchicine group did not survive the procedure and died after 24 h of the operation. One rat died from an overdose of anesthetic at week 8 wk during the MRI examination, and a second one died at week 12.

Pathology

There were no obvious pathological changes of rat liver tissue in the control group under a light microscope.

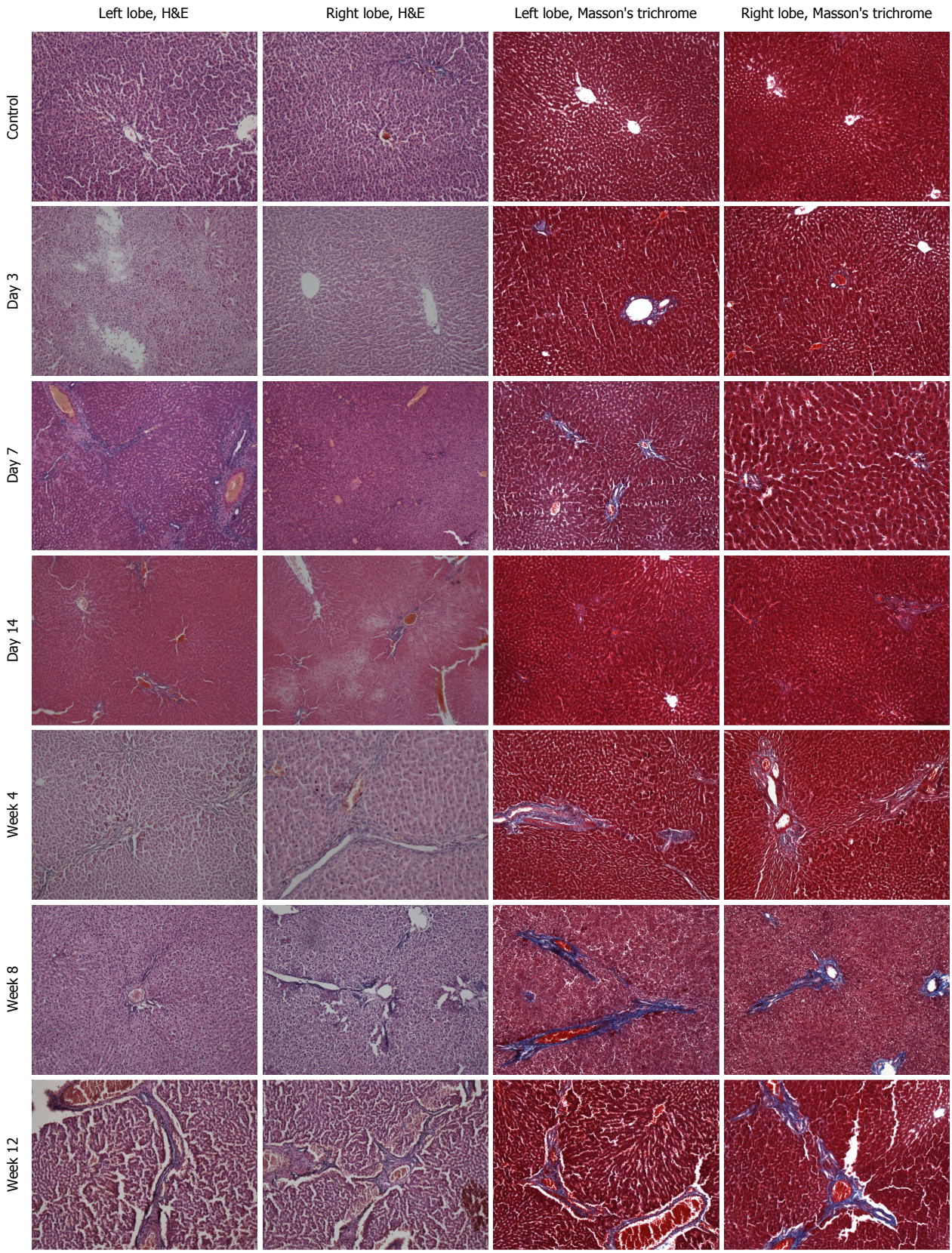

Figure 2 Histopathological changes of the liver (× 100). H&E staining of sections of the left lobe (1st column) and right lobe (2nd column) of the liver, and Masson's trichrome staining of sections of the left lobe (3rd column) and right lobe (4th column) of the liver were performed in the control group (1st row) and at each time point after injection of colchicine (2nd to 7th rows). No obvious pathological changes were observed in the control group. The hepatic injury was different between the left and right lobes at each time point. At day 3 after colchicine injection, there was massive inflammatory cells infiltration, hepatocellular edema, and mild liver necrosis. At day 14, reduced inflammation and increased necrosis were observed, while fibrosis was not detected. At week 4, cholestasis and early fibrosis were observed. At weeks 8 and 12, there was further fibrosis.

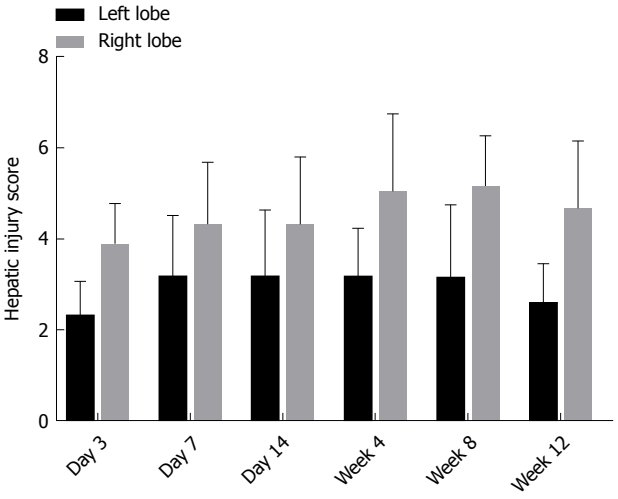

Figure 3 Comparisons of hepatic injury scores between the left and right lobes of rats in the colchicine group at each time point. Difference in hepatic injury between the left and right lobes of colchicine group at each time point was statistically significant ($P < 0.05$).

In the colchicine group, hepatocellular necrosis, inflammatory cell infiltration, hepatocellular edema, and liver fibrosis were observed, accompanied by hepatic cord disappearance and nuclear dissolution. At day 3 after colchicine injection, there was massive inflammatory cell infiltration, hepatocellular edema, and mild liver necrosis, without apparent fibrosis. At day 14, reduced inflammation and increased necrosis were observed, while fibrosis was not detected. At week 4, cholestasis and early fibrosis were observed. At weeks 8 and 12, there was further fibrosis (Figure 2). Based on the scoring criteria[9,10], hepatic injury scores were significantly different between the left and right lobes at each time point ($P < 0.05$, Figure 3).

Results of MRI

ΔADC between the right and left hepatic lobes differed significantly between the colchicine group and the control group ($P < 0.05$; Figure 4A). A statistically significant difference was also noted in ΔLMR between the right and left hepatic lobes from the T2WI of the colchicine group compared to that of the control group at each time point ($P < 0.05$; Figure 4B).

Relationship between pathology scores and MRI variables

The relationship between ADC values and hepatic injury scores is shown in Figure 5A. The ADC values decreased as hepatic injury scores increased, and the correlation was statistically significant ($r = -0.682$; $P = 0.000$). LMR and hepatic injury scores also demonstrated a negative correlation ($r = -0.245$; $P = 0.018$) (Figure 5B).

DISCUSSION

Patients who will undergo liver resection always exhibit heterogeneous hepatic injury induced by chemotherapy, metabolic syndrome, or cirrhosis[1,11-16], and this often leads to postoperative liver failure, which has become the leading cause of mortality after liver resection[17-19]. Therefore, assessment of the uneven distribution of hepatic function and prediction of reserved liver function are essential for preventing postoperative liver failure[12]. The development of a practical animal model of heterogeneous liver injury is the basis for further studies to curtail or eliminate this dire situation. Although there have been some animal models of hepatic injury, such as administration of thioacetamide solution in drinking water and a choline-deficient diet[20] and subcutaneous injection with a mixture of CCl_4 and olive oil[3], these models show homogeneous hepatic injury and cannot be used to investigate the heterogeneous liver injury condition that exists in human patients. Therefore, it is urgent to develop a simple, noninvasive, and reliable method to estimate liver regional function in patients with liver diseases.

In this study, we successfully developed an animal model of heterogeneous liver injury by injection with colchicine *via* the splenic vein in rats. The toxicity of colchicine may affect all cells in the body and causes multi-organ toxicity[21]. Colchicine binds to the intracellular tubule, arresting its polymerization of alpha and beta forms into microtubules. Proteins of the Golgi apparatus, endocytosis, exocytosis, cellular shape, and motility are therefore impaired. Mitosis is also disrupted in metaphase because of compromised microtubule-dependent functions in chromosome separation[22,23]. Colchicine has been used to induce conspicuous hepatotoxicity diseases including liver necrosis and steatosis in animals[4,24]. On the other hand, it was found that portal vein blood, which comes from the superior mesenteric vein and the splenic vein, is unevenly distributed in different lobes of the liver after merging into the portal vein. Thus, we injected rats with colchicine *via* the splenic vein to introduce inhomogeneous hepatic injury, and a statistically significant difference in pathological changes between the left and right hepatic lobes was observed. The histological results showed heterogeneous hepatocellular necrosis, edema, inflammatory cell infiltration, and liver fibrosis after colchicine injection, as well as cord disappearance, fibrous septa collapse, and nuclear dissolution. These findings support the point that this rat model can be used for future studies of hepatic injury, such as quantitative analysis of regional liver function.

In this model, the pathological changes of hepatic parenchyma mirrored the findings of previous studies[6], namely, the decreased inflammation of hepatic parenchyma within 2 wk after colchicine injection and the progressive, irreversible development of fibrosis. The current gold standard for estimation of liver injury is liver biopsy, yet liver specimens obtained by needle biopsy represent only a very small part of the liver parenchyma[25]. Moreover, liver biopsy is associated with the possibility of sampling errors, invasiveness, interobserver variability, and risk of complications. Therefore, liver biopsy is not practicable for estimating inhomogeneous

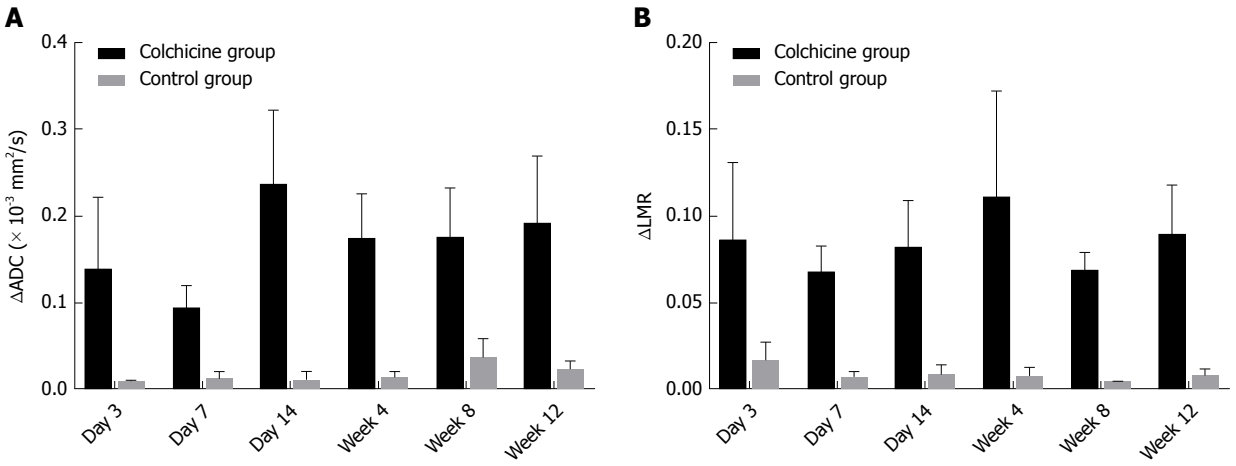

Figure 4 Comparisons of the difference of apparent diffusion coefficient (A) and the difference of liver-to-muscle ratio (B) between the colchicine group and the control group at each time point. Data are expressed as mean ± standard deviation. A statistically significant difference was noted in ΔADC (A) and ΔLMR (B) between the colchicine group and the control group ($P < 0.05$). ADC: Apparent diffusion coefficient; LMR: Liver-to-muscle ratio.

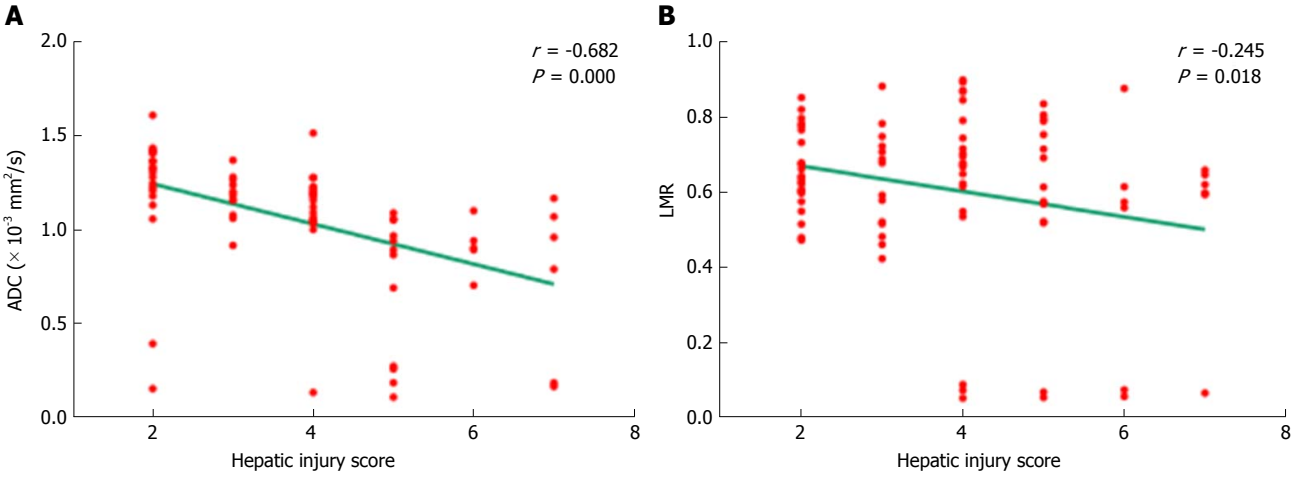

Figure 5 Correlations between magnetic resonance imaging variables and hepatic injury scores based on the scoring criteria. ADC values and LMR decreased as hepatic injury scores increased, and the correlations were statistically significant. ADC: Apparent diffusion coefficient; LMR: Liver-to-muscle ratio.

hepatic injury[26]. In addition, there are currently no serum markers or clinical signs that can accurately assess liver regional function[20].

Recently, several MRI methods have been developed to characterize the processes of various liver diseases and grade the extent of liver disease[27]. In addition, several studies have confirmed the value of magnetic resonance sequences in evaluating liver injury[5,6,28]. Therefore, in this study we used the T2WI and DWI to assess heterogeneous liver injury in our model. The ADC values from DWI can be used to measure the diffusion of random molecular motions[29]. As such, in the early stage of chemical hepatic injury, decreased ADC values may reflect a reduced ratio of extracellular/intracellular water volume caused by cytotoxic intracellular edema, as well as decreased intracellular proton movement resulting from energy loss. As fibrosis progresses, narrowed sinusoids and restricted water mobility caused by accumulation of collagen fibers, glycosaminoglycans, and proteoglycan lead to even lower ADC values for the liver parenchyma. This is similar to other reports showing that the ADC values decreased as liver disease progressed and fibrotic scores increased[30]. A previous study showed that hepatic injury resulted in increased T2 relaxation time and heightened T2WI sensitivity to necrosis[31]. Others also reported that T2WI can be used to monitor *in vivo* hepatotoxicity over time[32]. In our study, the difference of histological changes between the left and right lobes caused by uneven injury was reflected by LMR calculated from T2WI and ADC value from DWI. Both ADC values and LMR decreased as hepatic injury scores increased, and the correlations were statistically significant. The correlation coefficient between the ADC value and hepatic injury score was significantly higher than that between the LMR and hepatic injury score. The results of this study support the notion that both ADC value and LMR are potentially useful for evaluating heterogeneous hepatic injury.

There are several limitations to the present study that must be considered when interpreting or generalizing

our findings. First, the stability of uneven hepatic injury is influenced by individual differences of animals. Second, none of the MRI parameters was obtained over time to evaluate longitudinal changes. Third, although the ADC value from DWI enables noninvasive prediction of heterogeneous hepatic injury, it is limited by its relatively poor spatial resolution. Further studies are needed to explore other techniques such as gadolinium-ethoxybenzyl-diethylenetriamine pentaacetic acid-enhanced MRI, T1 mapping, and T2 mapping for assessing regional liver function in this model[28,33].

In summary, a novel rat model with uneven hepatic injury has been developed by injection with colchicine *via* the splenic vein. Data generated using this model suggested that DWI and T2WI can potentially evaluate heterogeneous injury between liver lobes.

ACKNOWLEDGMENTS

We appreciate the help from Professor Xuyong Lin (Pathology, The First Hospital of China Medical University) for pathology diagnosis.

ARTICLE HIGHLIGHTS

Research background

Heterogeneous hepatic injury is often exhibited in patients who will undergo liver resection, especially those accompanied by hepatitis and cirrhosis. Assessment of uneven hepatic function is essential for preventing postoperative liver failure. Until now, there has been no simple, safe, and effective method to evaluate heterogeneous hepatic injury due to the absence of an ideal animal model.

Research motivation

The development of a practical, reproducible animal model of heterogeneous hepatic injury is the basis for future studies that will ultimately benefit human clinical practice. In the present study, a novel rat model was established by injection with colchicine *via* the splenic vein, aiming at developing a practical model of heterogeneous hepatic injury. The heterogeneous injury between the left and right hepatic lobes was assessed on liver sections according to the histological scoring criteria, which was then correlated with the results of magnetic resonance imaging (MRI) using the sequences reported for evaluating hepatic injury.

Research objectives

To develop a practical rat model of heterogeneous hepatic injury which can be used for the future studies into human clinical parameters, such as quantitative analysis of the regional liver function, by injection with colchicine *via* the splenic vein.

Research methods

Seventy male Sprague-Dawley rats were randomly divided into a control group and a colchicine group. Colchicine (0.25%) was injected *via* the splenic vein to develop a rat model of heterogeneous hepatic injury. An equal volume of normal saline was injected *via* the splenic vein in the control group. After the operation, rats of the colchicine group were selected randomly for MRI examinations. Rats of the control group underwent MRI examinations. T2-weighted images (T2WI) and diffusion weighted imaging (DWI) were used to evaluate the heterogeneous hepatic injury. The heterogeneous injury between the left and right hepatic lobes was assessed on liver sections according to the histological scoring criteria, which was then correlated with the results of MRI study.

Research results

Obvious pathological changes of hepatic parenchyma were observed over time in the colchicine group. Hepatic injury scores were significantly different between the left and right lobes at each time point. There was a significant difference in apparent diffusion coefficient (ADC) of DWI and liver-to-muscle ratio (LMR) of T2WI between the left and right lobes in the colchicine group at each time point, and similar result was also observed between the colchicine and control groups. Besides, there were significant correlations between hepatic injury scores and ADC values or LMR. Some problems, such as the stability of the uneven hepatic injury influenced by individual differences of animals, and longitudinal changes that can be evaluated using MRI parameters obtained over time, remain to be solved.

Research conclusions

In this study, it was found that injection with colchicine *via* the splenic vein can be used to successfully develop a rat model of heterogeneous hepatic injury. The results of this study support that DWI and T2WI can potentially evaluate heterogeneous injury among liver lobes.

Research perspectives

Using this model, future studies are needed to explore other new techniques for assessing the uneven distribution of hepatic function and predicting the reserved liver function.

REFERENCES

1 **Nilsson H**, Karlgren S, Blomqvist L, Jonas E. The inhomogeneous distribution of liver function: possible impact on the prediction of post-operative remnant liver function. *HPB* (Oxford) 2015; **17**: 272-277 [PMID: 25297934 DOI: 10.1111/hpb.12348]

2 **Seyama Y**, Kokudo N. Assessment of liver function for safe hepatic resection. *Hepatol Res* 2009; **39**: 107-116 [PMID: 19208031 DOI: 10.1111/j.1872-034X.2008.00441.x]

3 **Ma C**, Liu A, Wang Y, Geng X, Hao L, Song Q, Sun B, Wang H, Zhao G. The hepatocyte phase of Gd-EOB-DTPA-enhanced MRI in the evaluation of hepatic fibrosis and early liver cirrhosis in a rat model: an experimental study. *Life Sci* 2014; **108**: 104-108 [PMID: 24881519 DOI: 10.1016/j.lfs.2014.05.016]

4 **Guo X**, Lin D, Li W, Wang K, Peng Y, Zheng J. Electrophilicities and Protein Covalent Binding of Demethylation Metabolites of Colchicine. *Chem Res Toxicol* 2016; **29**: 296-302 [PMID: 26845511 DOI: 10.1021/acs.chemrestox.5b00461]

5 **Cassinotto C**, Feldis M, Vergniol J, Mouries A, Cochet H, Lapuyade B, Hocquelet A, Juanola E, Foucher J, Laurent F, De Ledinghen V. MR relaxometry in chronic liver diseases: Comparison of T1 mapping, T2 mapping, and diffusion-weighted imaging for assessing cirrhosis diagnosis and severity. *Eur J Radiol* 2015; **84**: 1459-1465 [PMID: 26032126 DOI: 10.1016/j.ejrad.2015.05.019]

6 **Zhao F**, Wang YX, Yuan J, Deng M, Wong HL, Chu ES, Go MY, Teng GJ, Ahuja AT, Yu J. MR T1ρ as an imaging biomarker for monitoring liver injury progression and regression: an experimental study in rats with carbon tetrachloride intoxication. *Eur Radiol* 2012; **22**: 1709-1716 [PMID: 22752522 DOI: 10.1007/s00330-012-2419-0]

7 **Shimamoto D**, Nishie A, Asayama Y, Ushijima Y, Takayama Y, Fujita N, Shirabe K, Hida T, Kubo Y, Honda H. MR Prediction of Liver Function and Pathology Using Gd-EOB-DTPA: Effect of Liver Volume Consideration. *Biomed Res Int* 2015; **2015**: 141853 [PMID: 26609519 DOI: 10.1155/2015/141853]

8 **Katsube T**, Okada M, Kumano S, Imaoka I, Kagawa Y, Hori M, Ishii K, Tanigawa N, Imai Y, Kudo M, Murakami T. Estimation of liver function using T2* mapping on gadolinium ethoxybenzyl diethylenetriamine pentaacetic acid enhanced magnetic resonance imaging. *Eur J Radiol* 2012; **81**: 1460-1464 [PMID: 21514080 DOI: 10.1016/j.ejrad.2011.03.073]

9 **Lu Y**, Liu P, Fu P, Chen Y, Nan D, Yang X. Comparison of the DWI and Gd-EOB-DTPA-enhanced MRI on assessing the hepatic ischemia and reperfusion injury after partial hepatectomy. *Biomed Pharmacother* 2017; **86**: 118-126 [PMID: 27951418 DOI: 10.1016/j.biopha.2016.11.123]

10 **Tomimaru Y**, Sasaki Y, Yamada T, Eguchi H, Ohigashi H, Ishikawa O, Imaoka S. Fibrosis in non-cancerous tissue is the unique prognostic factor for primary hepatocellular carcinoma without hepatitis B or C viral infection. *World J Surg* 2006; **30**: 1729-1735 [PMID: 16850156

DOI: 10.1007/s00268-005-0123-9]
11 **Tsujino T**, Samarasena JB, Chang KJ. EUS anatomy of the liver segments. *Endosc Ultrasound* 2018; **7**: 246-251 [PMID: 30117487 DOI: 10.4103/eus.eus_34_18]
12 **Nilsson H**, Blomqvist L, Douglas L, Nordell A, Janczewska I, Näslund E, Jonas E. Gd-EOB-DTPA-enhanced MRI for the assessment of liver function and volume in liver cirrhosis. *Br J Radiol* 2013; **86**: 20120653 [PMID: 23403453 DOI: 10.1259/bjr.20120653]
13 **de Graaf W**, Häusler S, Heger M, van Ginhoven TM, van Cappellen G, Bennink RJ, Kullak-Ublick GA, Hesselmann R, van Gulik TM, Stieger B. Transporters involved in the hepatic uptake of (99m)Tc-mebrofenin and indocyanine green. *J Hepatol* 2011; **54**: 738-745 [PMID: 21163547 DOI: 10.1016/j.jhep.2010.07.047]
14 **Arun J**, Jhala N, Lazenby AJ, Clements R, Abrams GA. Influence of liver biopsy heterogeneity and diagnosis of nonalcoholic steatohepatitis in subjects undergoing gastric bypass. *Obes Surg* 2007; **17**: 155-161 [PMID: 17476865 DOI: 10.1007/s11695-007-9041-2]
15 **Merriman RB**, Ferrell LD, Patti MG, Weston SR, Pabst MS, Aouizerat BE, Bass NM. Correlation of paired liver biopsies in morbidly obese patients with suspected nonalcoholic fatty liver disease. *Hepatology* 2006; **44**: 874-880 [PMID: 17006934 DOI: 10.1002/hep.21346]
16 **Ratziu V**, Charlotte F, Heurtier A, Gombert S, Giral P, Bruckert E, Grimaldi A, Capron F, Poynard T; LIDO Study Group. Sampling variability of liver biopsy in nonalcoholic fatty liver disease. *Gastroenterology* 2005; **128**: 1898-1906 [PMID: 15940625 DOI: 10.1053/j.gastro.2005.03.084]
17 **Balzan S**, Belghiti J, Farges O, Ogata S, Sauvanet A, Delefosse D, Durand F. The "50-50 criteria" on postoperative day 5: an accurate predictor of liver failure and death after hepatectomy. *Ann Surg* 2005; **242**: 824-828, discussion 828-discussion 829 [PMID: 16327492]
18 **Capussotti L**, Viganò L, Giuliante F, Ferrero A, Giovannini I, Nuzzo G. Liver dysfunction and sepsis determine operative mortality after liver resection. *Br J Surg* 2009; **96**: 88-94 [PMID: 19109799 DOI: 10.1002/bjs.6429]
19 **Mullen JT**, Ribero D, Reddy SK, Donadon M, Zorzi D, Gautam S, Abdalla EK, Curley SA, Capussotti L, Clary BM, Vauthey JN. Hepatic insufficiency and mortality in 1,059 noncirrhotic patients undergoing major hepatectomy. *J Am Coll Surg* 2007; **204**: 854-862; discussion 862-864 [PMID: 17481498 DOI: 10.1016/j.jamcollsurg.2006.12.032]
20 **Tsuda N**, Matsui O. Signal profile on Gd-EOB-DTPA-enhanced MR imaging in non-alcoholic steatohepatitis and liver cirrhosis induced in rats: correlation with transporter expression. *Eur Radiol* 2011; **21**: 2542-2550 [PMID: 21830099 DOI: 10.1007/s00330-011-2228-x]
21 **Smilde BJ**, Woudstra L, Fong Hing G, Wouters D, Zeerleder S, Murk JL, van Ham M, Heymans S, Juffermans LJ, van Rossum AC, Niessen HW, Krijnen PA, Emmens RW. Colchicine aggravates coxsackievirus B3 infection in mice. *Int J Cardiol* 2016; **216**: 58-65 [PMID: 27140338 DOI: 10.1016/j.ijcard.2016.04.144]
22 **Deng M**, Zhao F, Yuan J, Ahuja AT, Wang YX. Liver T1ρ MRI measurement in healthy human subjects at 3 T: a preliminary study with a two-dimensional fast-field echo sequence. *Br J Radiol* 2012; **85**: e590-e595 [PMID: 22422392 DOI: 10.1259/bjr/98745548]
23 **Unal E**, Idilman IS, Karçaaltıncaba M. Multiparametric or practical quantitative liver MRI: towards millisecond, fat fraction, kilopascal and function era. *Expert Rev Gastroenterol Hepatol* 2017; **11**: 167-182 [PMID: 27937040 DOI: 10.1080/17474124.2017.1271710]
24 **Declèves X**, Niel E, Debray M, Scherrmann JM. Is P-glycoprotein (ABCB1) a phase 0 or a phase 3 colchicine transporter depending on colchicine exposure conditions? *Toxicol Appl Pharmacol* 2006; **217**: 153-160 [PMID: 16978677 DOI: 10.1016/j.taap.2006.08.004]
25 **Fontana RJ**, Lok AS. Noninvasive monitoring of patients with chronic hepatitis C. *Hepatology* 2002; **36**: S57-S64 [PMID: 12407577 DOI: 10.1053/jhep.2002.36800]
26 **Kose S**, Ersan G, Tatar B, Adar P, Sengel BE. Evaluation of Percutaneous Liver Biopsy Complications in Patients with Chronic Viral Hepatitis. *Eurasian J Med* 2015; **47**: 161-164 [PMID: 26644763 DOI: 10.5152/eurasianjmed.2015.107]
27 **Wibmer A**, Nolz R, Trauner M, Ba-Ssalamah A. [Functional MR imaging of the liver]. *Radiologe* 2015; **55**: 1057-1066 [PMID: 26610680 DOI: 10.1007/s00117-015-0032-3]
28 **Poynard T**, Lenaour G, Vaillant JC, Capron F, Munteanu M, Eyraud D, Ngo Y, M'Kada H, Ratziu V, Hannoun L, Charlotte F. Liver biopsy analysis has a low level of performance for diagnosis of intermediate stages of fibrosis. *Clin Gastroenterol Hepatol* 2012; **10**: 657-663.e7 [PMID: 22343514 DOI: 10.1016/j.cgh.2012.01.023]
29 **Slobodnick A**, Shah B, Pillinger MH, Krasnokutsky S. Colchicine: old and new. *Am J Med* 2015; **128**: 461-470 [PMID: 25554368 DOI: 10.1016/j.amjmed.2014.12.010]
30 **Roubille F**, Kritikou E, Busseuil D, Barrere-Lemaire S, Tardif JC. Colchicine: an old wine in a new bottle? *Antiinflamm Antiallergy Agents Med Chem* 2013; **12**: 14-23 [PMID: 23286287 DOI: 10.2174/1871523011312010004]
31 **Shankar S**, Kalra N, Bhatia A, Srinivasan R, Singh P, Dhiman RK, Khandelwal N, Chawla Y. Role of Diffusion Weighted Imaging (DWI) for Hepatocellular Carcinoma (HCC) Detection and its Grading on 3T MRI: A Prospective Study. *J Clin Exp Hepatol* 2016; **6**: 303-310 [PMID: 28003720 DOI: 10.1016/j.jceh.2016.08.012]
32 **Koinuma M**, Ohashi I, Hanafusa K, Shibuya H. Apparent diffusion coefficient measurements with diffusion-weighted magnetic resonance imaging for evaluation of hepatic fibrosis. *J Magn Reson Imaging* 2005; **22**: 80-85 [PMID: 15971188 DOI: 10.1002/jmri.20344]
33 **Lisotti A**, Serrani M, Caletti G, Fusaroli P. EUS liver assessment using contrast agents and elastography. *Endosc Ultrasound* 2018; **7**: 252-256 [PMID: 30117488 DOI: 10.4103/eus.eus_29_18]

P- Reviewer: Kositamongkol P, Lee S, Svein D **S- Editor**: Wang XJ
L- Editor: Wang TQ **E- Editor**: Yin SY

World Journal of Gastroenterology

Submit a Manuscript: http://www.f6publishing.com

World J Gastroenterol 2018 November 28; 24(44): 5013-5024

DOI: 10.3748/wjg.v24.i44.5013

ISSN 1007-9327 (print) ISSN 2219-2840 (online)

ORIGINAL ARTICLE

Basic Study

Involvement of methylation-associated silencing of formin 2 in colorectal carcinogenesis

Dao-Jiang Li, Zhi-Cai Feng, Xiao-Rong Li, Gui Hu

Dao-Jiang Li, Xiao-Rong Li, Gui Hu, Department of Gastrointestinal Surgery, the Third Xiangya Hospital, Central South University, Changsha 410013, Hunan Province, China

Zhi-Cai Feng, Department of Burns and Plastic Surgery, the Third Xiangya Hospital, Central South University, Changsha 410013, Hunan Province, China

ORCID number: Dao-Jiang Li (0000-0003-0986-4190); Zhi-Cai Feng (0000-0003-2485-7466); Xiao-Rong Li (0000-0001-8585-3632); Gui Hu (0000-0002-0901-9686).

Author contributions: Li DJ, Li XR, and Hu G contributed to conceptualization and design of the study, analyzed the data, and coordinated the research; Li DJ and Feng ZC performed the majority of the experiments and analyzed the data; all authors drafted the article and made revisions related to the intellectual content of the manuscript, and approved the final version of the article to be published.

Supported by the National Nature Science Foundation of China, No. 81773130; the Fundamental Research Funds for the Central Universities of Central South University(the Key Projects of Postgraduate Independent Exploration and Innovation of Central South University, No. 2018zzts050); and the New Xiangya Talent Projects of the Third Xiangya Hospital of Central South University, No. JY201508.

Institutional review board statement: This study was reviewed and approved by the Ethics Committee of Central South University. Informed consent was obtained from all individual participants included in the study.

Conflict-of-interest statement: To the best of our knowledge, no conflict of interest exists.

Data sharing statement: No additional data are available.

Manuscript source: Unsolicited manuscript

Corresponding author to: Gui Hu, PhD, Surgeon, Department of Gastrointestinal Surgery, the Third Xiangya Hospital, Central South University, No. 172, Tongzi Po Road, Changsha 410013, Hunan Province, China. xy3zzz@csu.edu.cn.
Telephone:+86-13908472002
Fax: +86-731-88618832

Received: August 20, 2018
Peer-review started: August 20, 2018
First decision: October 11, 2018
Revised: October 14, 2018
Accepted: November 7, 2018
Article in press: November 7, 2018
Published online: November 28, 2018

Abstract

AIM

To investigate whether promoter methylation is responsible for the silencing of formin 2 (*FMN2*) in colorectal cancer (CRC) and to analyze the association between *FMN2* methylation and CRC.

METHODS

We first identified the expression levels and methylation levels of *FMN2* in large-scale human CRC expression datasets, including GEO and TCGA, and analyzed the relationship between the expression and methylation levels. Then, the methylation levels in four CpG regions adjacent to the *FMN2* promoter were assessed by MethylTarget™ assays in CRC cells and in paired colorectal tumor samples and adjacent nontumor tissue samples. Furthermore, we inhibited DNA methylation in CRC cells with 5-Aza-2′-deoxycytidine and assessed the expression of *FMN2* by qRT-PCR. Last, the association between *FMN2* methylation patterns and clinical indicators was analyzed.

RESULTS

A statistically significant downregulation of *FMN2* expression in large-scale human CRC expression datasets was found. Subsequent analysis showed that a high frequency of hypermethylation occurred in the *FMN2* gene promoter in CRC tissues; operating characteristic curve analysis revealed that *FMN2* gene methylation had a good capability for discriminating between CRC and nontumor tissue samples (AUC = 0.8432, $P < 0.0001$). MethylTarget™ assays showed that CRC cells and tissues displayed higher methylation of these CpG regions than nontumor tissue samples. Correlation analysis showed a strong inverse correlation between methylation and *FMN2* expression, and the inhibition of DNA methylation with 5-Aza significantly increased endogenous *FMN2* expression. Analysis of the association between *FMN2* methylation patterns and clinical indicators showed that *FMN2* methylation was significantly associated with age, N stage, lymphovascular invasion, and pathologic tumor stage. Notably, the highest methylation of *FMN2* occurred in tissues from cases of early-stage CRC, including cases with no regional lymph node metastasis (N0), cases in stages Ⅰ and Ⅱ, and cases with no lymphovascular invasion, but the methylation level began to decrease with tumor progression. Additionally, *FMN2* promoter hypermethylation was more common in patients > 60 years old and in colon cancer tissue.

CONCLUSION

FMN2 promoter hypermethylation may be an important early event in CRC, most likely playing a critical role in cancer initiation, and can serve as an ideal diagnostic biomarker in elderly patients with early-stage colon cancer.

Key words: Formin 2; Colorectal cancer; Methylation; Methylation-associated silencing; Early-stage cancer

Core tip: Colorectal cancer (CRC) is the leading cause of cancer death in the world. We identified a statistically significant downregulation of formin 2 (*FMN2*) expression in large-scale human CRC expression datasets and our clinical samples. Then, we first showed that a high frequency of hypermethylation occurred in the *FMN2* gene promoter, which is responsible for the downregulation of *FMN2* expression. Additionally, the highest methylation of *FMN2* occurred in tissues from cases of early-stage CRC and patients > 60 years old. *FMN2* hypermethylation may be an important early event in CRC and can serve as an ideal diagnostic biomarker in elderly patients with early-stage CRC.

Li DJ, Feng ZC, Li XR, Hu G. Involvement of methylation-associated silencing of formin 2 in colorectal carcinogenesis. *World J Gastroenterol* 2018; 24(44): 5013-5024 Available from: URL: http://www.wjgnet.com/1007-9327/full/v24/i44/5013.htm DOI: http://dx.doi.org/10.3748/wjg.v24.i44.5013

INTRODUCTION

Colorectal cancer (CRC) is a common malignancy and a major cause of incidence and mortality in many countries, especially more developed countries[1]. Over the years, researchers have identified CRC as a gradual process that lasts for several years, since it begins as a single mutation in a cell until it becomes a detectable malignancy[2]. Therefore, the main secondary preventive strategy for CRC is the early detection of preneoplastic or neoplastic lesions in the large bowel[3].

Formin 2 (FMN2) is a member of the formin homology protein family; the encoded protein is thought to have essential roles in the organization of the actin cytoskeleton and in cell polarity[4]. More recently, *FMN2* was reported to be involved in cancer, for example, serving as a potential oncogene in leukemia[5]. FMN2 can enhance the expression of the cell cycle inhibitor p21 by preventing its degradation. In addition, *FMN2* is induced by the activation of other oncogenes, hypoxia, and DNA damage[6]. To date, only two studies have explored the relationship between FMN2 and CRC. The first study was in 2012; to identify the genetic determinants of colon tumorigenesis, Liu *et al*[7] and colleagues carried out a genome-wide association study of azoxymethane-induced colon tumorigenesis and subsequently confirmed through fine mapping that *FMN2* is associated with colon tumor susceptibility. Another study[8] assessed the expression of FMN2 in tumor and adjacent nontumor tissue by immunohistochemistry, with results showing that FMN2 was predominantly localized in the cytoplasm of tumor cells; that the rate of positive FMN2 protein expression in the CRC and paracarcinoma tissues was 53.73% (180/335) and 80.90% (271/335), respectively, with a significant difference ($P < 0.05$); and that the level of the FMN2 protein in CRC patients was associated with tumor differentiation, TNM stage, and lymph node metastasis. However, the mechanism leading to the downregulation of FMN2 expression in CRC has not been studied. In this article, we tried to show that the high frequency of hypermethylation occurring in the promoter of the *FMN2* gene in CRC tissues is responsible for the silencing of *FMN2,* and we further explored the association between *FMN2* methylation and clinical indicators. We found that the highest level of *FMN2* methylation occurred in early-stage CRC tissues; thus, FMN2 may provide a new biomarker for the secondary prevention of CRC.

MATERIALS AND METHODS

Cell lines and tissue samples

Human CRC cell lines (SW620 and SW480) were cultured in L15 medium (KeyGEN BioTECH, Nanjing, China) supplemented with 10% fetal bovine serum (FBS) (Biological Industries, Israel), and HCT116 and HT-29 cells were cultured in McCoy's 5A medium (KeyGEN BioTECH, Nanjing, China) supplemented with 10% FBS. Cells were grown in a 5% CO_2 cell culture incubator at 37 ℃.

Table 1 Clinical materials used in this article

No.	Sex	Age	Lymph nodes	TNM	Pathology	Differentiation	MSI	Organ
1	M	67	5 (14)	T4aN2aM0	Adenocarcinoma	Moderate	No	Rectum
2	M	53	0 (22)	T2N0M0	Adenocarcinoma	Moderate	-	Rectum
3	M	72	4 (20)	T4aN2aM0	Adenocarcinoma	Poor	-	Right colon
4	M	52	0 (16)	T3N0M0	Adenocarcinoma	Moderate	-	Rectum
5	M	52	3 (25)	T3N1bM0	Adenocarcinoma	Moderate	-	Sigmoid colon
6	F	57	0 (15)	T4aN0M0	Adenocarcinoma	Moderate	-	Left colon
7	F	51	0 (14)	T4aN0M0	Adenocarcinoma	Moderate	No	Rectum
8	F	66	19 (27)	T3N2bM0	Adenocarcinoma	Poor	No	Rectum
9	F	71	0 (16)	T4bN0M1b	Adenocarcinoma	Moderate	No	Rectum

Table 2 Details of the four CpG regions in the CpG islands of formin 2

Target	TSS	Start	End	Length	Target strand	Distance2TSS
FMN2_1	240255184	240255353	240255531	179	+	169
FMN2_2	240255184	240255809	240256007	199	+	625
FMN2_3	240255184	240256241	240256483	243	+	1057
FMN2_4	240255184	240256757	240257017	261	+	1573

Start: The starting position of the product on the reference genome; TSS: The mRNA transcription initiation site; End: The end position of the product on the reference genome; Length: the product length; Target strand: The product orientation; Distance2TSS: The distance from the product to the TSS.

Table 3 Primers used for the MethylTarget™ assays

Primer name	Primer
FMN2_1_F	GAGGGTYGGGATGGTTTGAG
FMN2_1_R	CCCCCRCTCCCCTTCTTT
FMN2_2F	GAGTGTGYGGATTTTTTTGAGGT
FMN2_2R	AAATATCTAAAAACAAATCCTCTTACTCC
FMN2_3F	GATTTGTTYGAGAGTTTGGTTGT
FMN2_3R	AAACRCATCCTCAAAAACATCCT
FMN2_4F	TTTTTGAGTYGAGGGTTTAGAATTG
FMN2_4R	CACRTTCTAAAAACCATCCRCAAC

Clinical samples were obtained from patients treated at the Third Xiangya Hospital of Central South University (Hunan, China) under informed consent and approval by the Ethics Committee of Central South University (more details about the clinical samples can be found in Table 1).

RNA purification and reverse transcription-PCR

Total RNA was extracted using TRIzol reagent (Invitrogen, United States). The reverse transcription reaction was performed using ReverTra Ace qPCR RT Master Mix with gDNA Remover (TOYOBO, Japan), and this kit includes reagents for reverse transcription and for the removal of genomic DNA (DNase Ⅰ treatment). cDNA was amplified with KOD SYBR® qPCR mix (TOYOBO, Japan) on a LightCycler® 480 Ⅱ system (Roche) according to the manufacturer's instructions (*FMN2* primers: forward, GCGAACGCTGTTGGAGAAG and reverse, CTGATTACACGGTTCCCTGAAG).

Treatment with 5-aza-2'-deoxycytidine

Cells were grown in appropriate culture conditions. For demethylation treatment, colorectal cells were treated with 5-aza-2'-deoxycytidine (5-Aza) (Sigma, United States) for 96 h (5 μmol/L), with daily replacement of the drug and medium. Untreated cells were used as a control group.

DNA extraction and bisulfate treatment

DNA was isolated with an Easypure Genomic DNA kit (TransGen Biotech, Beijing, China) according to the manufacturer's instructions. The DNA concentration was assessed by spectrophotometry and confirmed by gel electrophoresis; DNA was stored at -20 ℃. An EZ DNA Methylation Gold™ Kit (Zymo Research Corporation, CA, United States) was used to convert all unmethylated cytosine to uracils.

DNA methylation analysis

MethylTarget™ assays (targeted bisulfite sequencing) developed by Genesky BioTech (Shanghai, China) were carried out as previously described[9,10]. Briefly, CpG islands adjacent to the promoter region of the *FMN2* gene were analyzed, and based on these CpG islands, four CpG regions from CpG islands in *FMN2* were sequenced (the details, including the relative distance from the transcriptional start site, amplification primers, and product size, of these CpG regions can be found in Tables 2 and 3). Genomic DNA was converted with bisulfite, and PCR was performed to amplify the targeted DNA sequences. The products were sequenced on an Illumina MiSeq benchtop sequencer (Illumina, CA, United States).

Bioinformatics

Cosmic[11], a database cataloguing somatic mutations in human cancer, was used to assess methylation mutations in human cancer tissues. Datasets for CRC, including GEO GSE20842, GSE8671, and GSE4183, as well as TCGA[12], were used to assess the expression level

of *FMN2*. Data about DNA methylation, the patients, and the samples were downloaded from the TCGA database (https://cancergenome.nih.gov/).

Statistical analysis

GraphPad Prism 7 software was used to analyze the data. The methylation and expression levels in normal, adenoma, and cancerous tissues, as well as the methylation level in different clinical materials, were assessed by two-tailed unpaired Student's *t*-tests; box-whisker plots depict the means, 1st and 3rd quartiles, and minimum/maximum. The error bars in the figures represent SDs. Spearman's correlation coefficient (*r*) was used to determine the correlation. Overall survival (OS) and disease-free survival (DFS) were estimated using the Kaplan-Meier method. Receiver operating characteristic curves were constructed based on the level of *FMN2* methylation. The data were considered nonsignificant for $P > 0.05$.

RESULTS

Analysis of FMN2 expression in large-scale human CRC expression datasets

Previous studies demonstrated that *FMN2* is underexpressed in CRC. To further confirm the expression characteristics of *FMN2* in CRC, we expanded our analysis to published, large-scale human CRC expression datasets. GSE20842, which contains 65 paired samples of tumor and mucosal tissue samples from 65 CRC patients, was used to assess *FMN2* expression; we found a statistically significant downregulation of *FMN2* expression from normal colorectal tissue to carcinoma tissue ($P < 0.0001$) (Figure 1A). An identical pattern was observed in human CRC samples from TCGA ($P < 0.0001$); however, it is noteworthy that we found that the expression level of *FMN2* was significantly lower in early-stage CRC tissues (stages Ⅰ + Ⅱ *vs* stages Ⅲ + Ⅳ, $P = 0.02$) (Figure 1B), which indicates that *FMN2* downregulation may be an important early event in CRC. To confirm this finding, GSE8671, which contains 32 colorectal adenoma and corresponding normal colonic mucosa samples, was downloaded to analyze *FMN2* expression; we found a statistically significant downregulation of *FMN2* expression from normal colorectal tissue to adenoma tissue ($P < 0.0001$) (Figure 1C). In addition, we downloaded the GSE4183 dataset, which contains colonic biopsies of 15 patients with CRC, 15 patients with adenoma, and 8 healthy normal controls, to simultaneously assess the reduction of *FMN2* in adenomas and cancer tissues. As shown in Figure 1D**,** adenoma tissues displayed a greater reduction in expression ($P = 0.0002$) than tumor tissues ($P = 0.01$).

High frequency of hypermethylation occurs in the FMN2 gene promoter in CRC tissues

Somatic mutation in cancer is an important reason for the aberrant expression of genes, so the Catalogue of Somatic Mutations in Cancer (COSMIC), the world's largest and most comprehensive resource for exploring the impact of somatic mutations in human cancer, was used to analyze the somatic mutations of *FMN2* in CRC tissues. The result indicated that methylation was the main somatic mutation and that *FMN2* gene promoter hypermethylation occurred in 37.37% of CRC tissues. In addition, COSMIC indicated that *FMN2* methylation mainly occurred in CRC tissues and was the most common somatic mutation among all human tumor tissues and that *FMN2* was one of the top 20 genes with an extremely high frequency of hypermethylation in CRC. Then, *FMN2* gene promoter DNA methylation profiles were downloaded from TCGA; the results revealed a statistically significant hypermethylation of *FMN2* in tumor tissues compared with adjacent nontumor tissue samples ($P < 0.0001$) (Figure 1E). We next assessed the accuracy of the *FMN2* methylation signature for the detection of CRC *via* receiver operating characteristic curve analysis, and the analysis revealed a good capability for discriminating between CRC and nonneoplastic tissue specimens (AUC = 0.8432, 95%CI: 0.8022-0.8841; $P < 0.0001$) (Figure 1F).

Analysis of the features of methylation-associated FMN2 silencing in CRC tissue and cells

The majority of research indicates that promoter hypermethylation is a key mediator underlying the downregulation of gene expression. The high frequency of hypermethylation in the *FMN2* gene promoter and the significant inverse correlation between methylation levels and the expression of *FMN2* in 372 CRC tissues (Figure 2A) remind us that methylation is the main cause of *FMN2* gene silencing. To investigate this topic, nine paired colorectal tumor samples and adjacent nontumor tissue samples (for details, see Table 1) were selected for RT-qPCR and MethylTarget™ assays. We first examined *FMN2* expression using RT-qPCR in these paired samples. A significant reduction in *FMN2* expression was observed in seven of the nine CRC tissues (Figure 2B). Then, based on the CpG islands adjacent to the *FMN2* promoter region, four CpG regions (*FMN2*-1, *FMN2*-2, *FMN2*-3, and *FMN2*-4, the details of which can be found in Table 2) from CpG islands were amplified and sequenced. The result demonstrated that CRC tissues revealed a stronger methylation pattern than noncancerous tissues and identified three CpG regions, namely, *FMN2*-2, *FMN2*-3, and *FMN2*-4, with a statistically significant difference ($P = 0.0069$, $P = 0.0094$, and $P = 0.0005$, respectively) (Figure 2C-F; Table 2). Notably, tumor tissues (cases 1, 3-7, and 9) exhibiting lower *FMN2* expression than the corresponding noncancerous tissues displayed an increase in methylation at these islands compared with the noncancerous tissues, whereas CRC cases 2 and 8, with moderate FMN2 expression, revealed a methylation pattern similar to that of the corresponding noncancerous tissues. Correlation analysis revealed a strong inverse correlation between the methylation of island 2 ($r = -0.86$), island 4 ($r = -0.71$), and island 3 ($r = -0.78$)

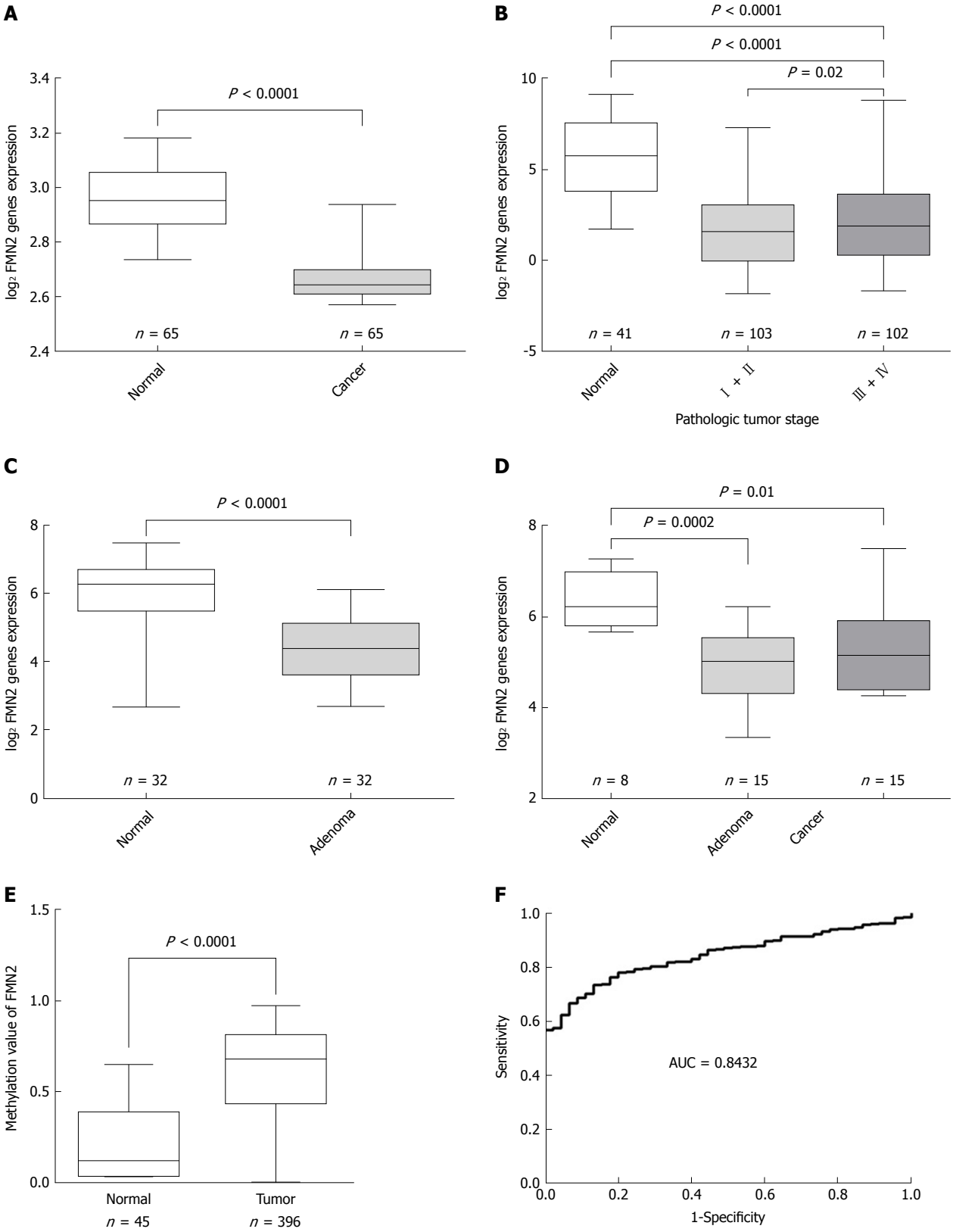

Figure 1 Colorectal tissues show decreased formin 2 expression and a high frequency of hypermethylation in the formin 2 promoter. A: Normalized expression of formin 2 (*FMN2*) mRNA in carcinoma and adjacent normal tissues, presented as box-whisker plots (unpaired *t*-test, GEO: GSE20842); B: Normalized expression of *FMN2* mRNA in tissue from different stages of carcinoma (according to the AJCC Cancer Staging Manual) and in normal tissue, presented as box-whisker plots (unpaired *t*-test, colorectal cancer samples from TCGA); C: Normalized expression of *FMN2* mRNA in adenoma and corresponding normal colonic mucosal tissues, presented as box-whisker plots (unpaired *t*-test, GEO: GSE8671); D: Normalized expression of *FMN2* mRNA in normal, adenoma, and carcinoma tissues, presented as box-whisker plots (unpaired *t*-test, GEO: GSE4183); E: The FMN2 gene shows an increased methylation level in colorectal cancer tissues compared with normal tissues (unpaired *t*-test, colorectal cancer samples from TCGA); F: Receiver operating characteristic curve analysis was used to assess the clinical diagnostic utility of *FMN2* DNA methylation for the prediction of colorectal cancer.

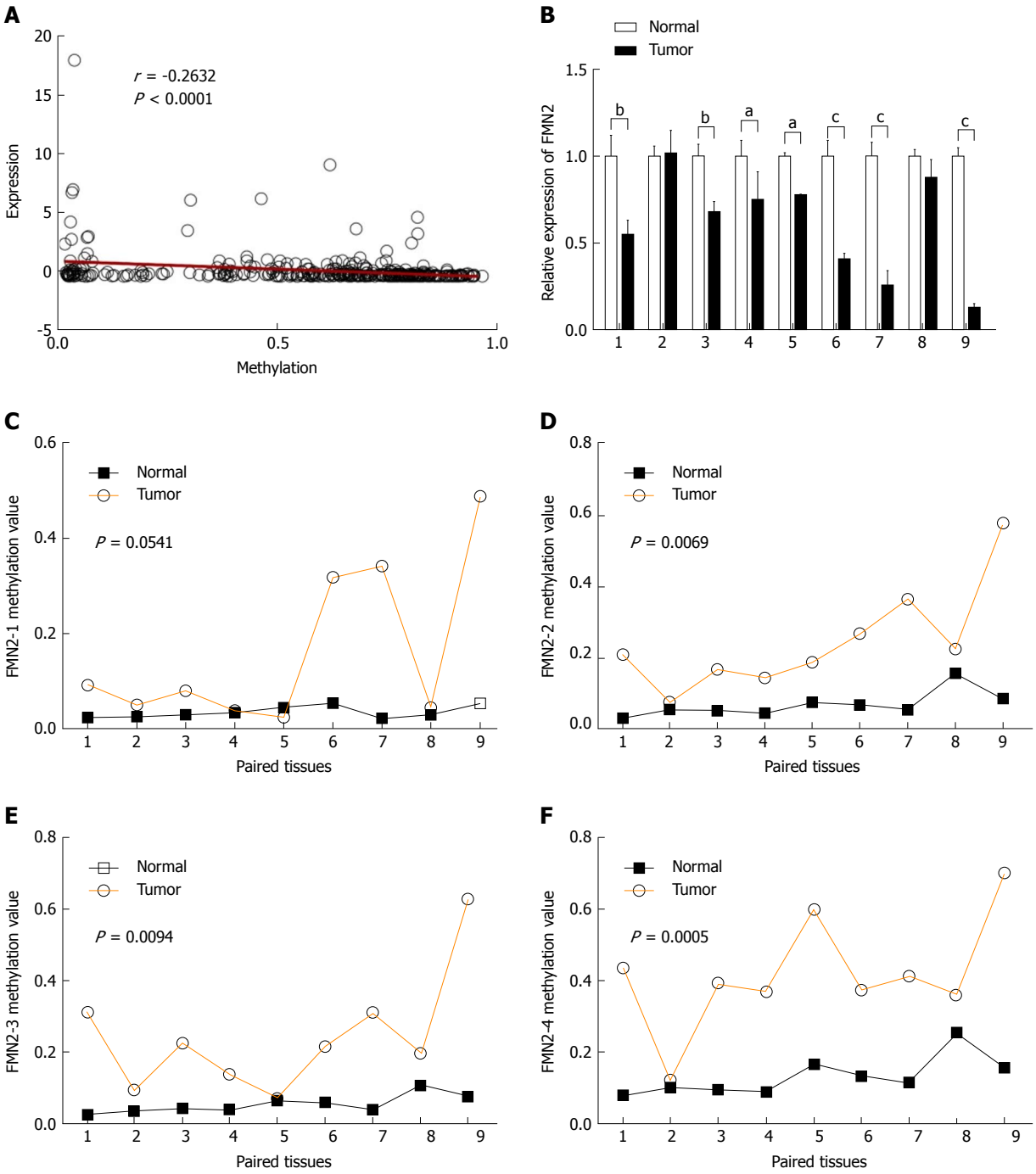

Figure 2 Hypermethylation of formin 2 correlates with decreased expression of formin 2 during colorectal cancer. A: The expression of the formin 2 (*FMN2*) gene is significantly inversely correlated with the methylation level (Pearson correlation analysis); B: Quantitative real-time RT-PCR for *FMN2* was carried out on nine colorectal cancer surgical specimens (filled bars) and paired noncancerous tissues (unfilled bars). The expression levels in the tumor samples were independently calculated relative to those in the nontumor samples, which are normalized to 1. Vertical bar, SD; $^{a}P < 0.05$, $^{b}P < 0.03$, $^{c}P < 0.01$ (unpaired *t*-test); C-F: Results of MethylTarget™ assays on nine paired noncancerous tissues and colorectal cancer tissues. Four CpG regions (*FMN2*-1, *FMN2*-2, *FMN2*-3, and *FMN2*-4) from CpG islands adjacent to the FMN2 promoter were sequenced (unpaired *t*-test. More details about the four CpG regions can be found in Table 2).

and *FMN2* expression (data not shown). In addition, we assessed the methylation level of each CG site in CpG island regions and found that 8 of 14 CG sites in *FMN2*-1 and all CG sites in *FMN2*-2 (13/13), *FMN2*-3 (23/23), and *FMN2*-4 (27/27) revealed a significantly stronger methylation pattern in the tumor tissues than in the corresponding noncancerous tissues (Table 4).

We next wondered whether promoter hypermethylation at these loci and *FMN2* expression are causally related. To answer this question, four CRC cell lines (HCT116, HT29, SW480, and SW620) were selected for MethylTarget™ assays. The result revealed a high level of DNA methylation in all CRC cell lines, whereas only limited methylation was observed in normal colon tissue from a healthy individual (Figure 3A). Then, we treated HCT116, HT29, and SW480 cells with 5-Aza;

Table 4 Methylation level of each CG site in the CpG island regions

Target	Position	Type	*P* value (*t*-test)	OR (L95-U95) (logistic)	C mean	N mean
FMN2_1	25	CG	0.007774578	2.1731 (0.9323-5.0653)	0.17	0.04
FMN2_1	27	CG	0.01061292	1.5266 (0.8980-2.5953)	0.16	0.03
FMN2_1	30	CG	0.1359111	1.3535 (0.7970-2.2986)	0.15	0.03
FMN2_1	32	CG	0.01875771	1.7416 (0.8662-3.5016)	0.16	0.04
FMN2_1	35	CG	0.03998355	1.2722 (0.8959-1.8068)	0.18	0.05
FMN2_1	38	CG	0.01419169	1.6993 (0.8462-3.4125)	0.16	0.03
FMN2_1	46	CG	0.003990128	2.2454 (0.9140-5.5161)	0.15	0.02
FMN2_1	90	CG	0.1134924	1.3103 (0.6401-2.6825)	0.16	0.03
FMN2_1	108	CG	0.06252571	1.2532 (0.7873-1.9948)	0.17	0.04
FMN2_1	114	CG	0.1134924	1.1858 (0.8641-1.6273)	0.18	0.05
FMN2_1	117	CG	0.05030852	1.3499 (0.8867-2.0550)	0.19	0.04
FMN2_1	123	CG	0.01061292	2.2247 (0.9162-5.4017)	0.16	0.03
FMN2_1	126	CG	0.09391197	1.2852 (0.7471-2.2110)	0.16	0.03
FMN2_1	134	CG	0.01875771	2.4645 (0.6195-9.8050)	0.16	0.02
FMN2_2	27	CG	0.000493624	1.3442 (1.0433-1.7321)	0.28	0.07
FMN2_2	51	CG	0.01419169	1.2762 (0.9670-1.6843)	0.17	0.04
FMN2_2	63	CG	0.007774578	1.4062 (0.9872-2.0030)	0.37	0.25
FMN2_2	70	CG	0.000781571	1.3753 (1.0378-1.8226)	0.24	0.05
FMN2_2	74	CG	0.000493624	1.3079 (1.0283-1.6636)	0.31	0.07
FMN2_2	78	CG	0.000287947	1.3676 (1.0603-1.7639)	0.25	0.05
FMN2_2	81	CG	0.00185109	1.3630 (0.9664-1.9224)	0.21	0.05
FMN2_2	107	CG	0.000493624	1.3025 (0.9942-1.7063)	0.24	0.06
FMN2_2	131	CG	0.007774578	1.2706 (0.9662-1.6708)	0.15	0.03
FMN2_2	137	CG	0.002756067	1.3002 (0.9986-1.6928)	0.21	0.05
FMN2_2	143	CG	0.00123406	1.3743 (1.0297-1.8341)	0.20	0.04
FMN2_2	164	CG	0.000287947	1.3527 (1.0108-1.8101)	0.29	0.07
FMN2_2	170	CG	0.00123406	1.2431 (1.0019-1.5424)	0.28	0.08
FMN2_3	24	CG	0.005635541	1.3854 (0.9994-1.9207)	0.20	0.05
FMN2_3	31	CG	0.005635541	1.4241 (0.9731-2.0841)	0.23	0.04
FMN2_3	47	CG	0.002756067	1.3776 (0.9695-1.9574)	0.24	0.06
FMN2_3	50	CG	0.003990128	1.3787 (1.0219-1.8599)	0.22	0.05
FMN2_3	57	CG	0.00123406	1.3592 (1.0212-1.8091)	0.25	0.06
FMN2_3	60	CG	0.003990128	1.5630 (0.9433-2.5897)	0.19	0.04
FMN2_3	68	CG	0.00185109	1.3474 (1.0273-1.7673)	0.23	0.06
FMN2_3	75	CG	0.00123406	1.3787 (0.9962-1.9082)	0.26	0.06
FMN2_3	80	CG	0.00123406	1.3582 (0.9518-1.9380)	0.24	0.05
FMN2_3	92	CG	0.00185109	1.3665 (0.9746-1.9159)	0.23	0.05
FMN2_3	98	CG	0.00123406	1.3200 (0.9414-1.8509)	0.27	0.06
FMN2_3	105	CG	0.000781571	1.4801 (0.9296-2.3566)	0.22	0.04
FMN2_3	107	CG	0.007774578	1.2402 (1.0141-1.5168)	0.21	0.05
FMN2_3	119	CG	0.00123406	1.4326 (0.9810-2.0921)	0.19	0.04
FMN2_3	131	CG	0.000493624	1.7790 (0.9589-3.3006)	0.22	0.04
FMN2_3	147	CG	0.007774578	1.3343 (0.9443-1.8856)	0.20	0.04
FMN2_3	153	CG	0.000493624	1.5405 (0.9677-2.4523)	0.22	0.05
FMN2_3	158	CG	8.23E-05	1.9417 (0.8981-4.1979)	0.31	0.08
FMN2_3	170	CG	4.11E-05	1714240.0000 (0.0000-Inf)	0.32	0.08
FMN2_3	174	CG	4.11E-05	11577516733.0000 (0.0000-Inf)	0.34	0.08
FMN2_3	183	CG	0.000287947	1.6836 (0.9224-3.0731)	0.28	0.06
FMN2_3	187	CG	0.000287947	1.4526 (0.9861-2.1399)	0.27	0.06
FMN2_3	203	CG	0.000781571	1.4980 (0.9815-2.2861)	0.25	0.05
FMN2_4	36	CG	0.003990128	1.1409 (1.0248-1.2702)	0.41	0.14
FMN2_4	42	CG	0.002756067	1.2068 (1.0353-1.4068)	0.38	0.12
FMN2_4	47	CG	0.000781571	1.2264 (1.0309-1.4589)	0.37	0.10
FMN2_4	61	CG	0.005386639	1.1552 (1.0206-1.3075)	0.38	0.10
FMN2_4	66	CG	0.0003108	243.9222 (0.0000-Inf)	0.40	0.09
FMN2_4	69	CG	8.23E-05	1.7294 (0.6520-4.5874)	0.42	0.09
FMN2_4	72	CG	0.003990128	1.2209 (1.0296-1.4477)	0.4	0.13
FMN2_4	80	CG	4.11E-05	2515571.0000 (0.0000-Inf)	0.48	0.18
FMN2_4	84	CG	0.00185109	1.2366 (1.0241-1.4931)	0.39	0.12
FMN2_4	94	CG	0.002756067	1.2121 (1.0363-1.4178)	0.38	0.12
FMN2_4	98	CG	0.003990128	1.1618 (1.0236-1.3186)	0.36	0.11
FMN2_4	110	CG	0.00185109	1.1712 (1.0253-1.3378)	0.44	0.19
FMN2_4	123	CG	0.000781571	1.2218 (1.0321-1.4463)	0.40	0.10
FMN2_4	127	CG	0.00185109	1.2220 (1.0324-1.4464)	0.39	0.11
FMN2_4	131	CG	8.23E-05	1.3179 (1.0259-1.6931)	0.38	0.08
FMN2_4	136	CG	0.003990128	1.1979 (1.0209-1.4054)	0.34	0.09
FMN2_4	150	CG	4.11E-05	1217702.0000 (0.0000-Inf)	0.54	0.22

FMN2_4	152	CG	0.003990128	1.1644 (1.0196-1.3297)	0.39	0.12
FMN2_4	166	CG	0.000164541	1.3446 (0.9896-1.8269)	0.45	0.16
FMN2_4	168	CG	0.001710676	1.2557 (1.0089-1.5628)	0.44	0.16
FMN2_4	176	CG	4.11E-05	26059.6300 (0.0000-Inf)	0.52	0.21
FMN2_4	186	CG	0.000781571	1.1735 (1.0224-1.3469)	0.54	0.2
FMN2_4	189	CG	0.003990128	1.1348 (1.0221-1.2600)	0.49	0.18
FMN2_4	213	CG	0.00185109	1.1572 (1.0241-1.3076)	0.47	0.14
FMN2_4	221	CG	0.002756067	1.1534 (1.0276-1.2947)	0.45	0.13
FMN2_4	234	CG	0.00185109	1.1981 (1.0181-1.4099)	0.32	0.08
FMN2_4	236	CG	0.000493624	1.2631 (1.0149-1.5720)	0.36	0.08

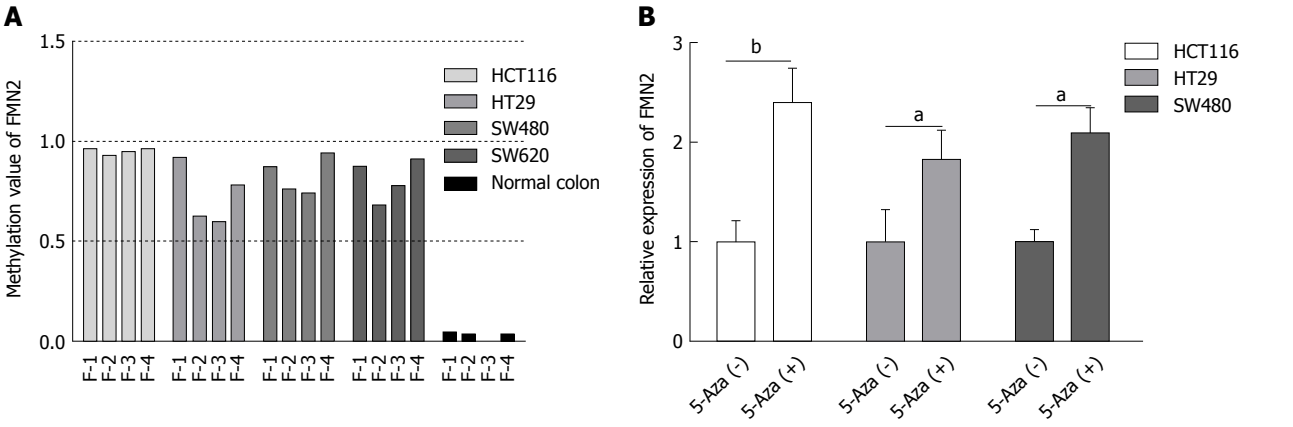

Figure 3 Promoter hypermethylation and formin 2 expression are causally related. A: Results of MethylTarget™ assays on four colorectal cancer cell lines and normal colon cells from a healthy individual; B: The inhibition of DNA methylation with 5-Aza significantly increased the endogenous *FMN2* expression (unpaired *t*-test).

the inhibition of DNA methylation by 5-Aza significantly increased the endogenous *FMN2* expression (Figure 3B).

FMN2 promoter hypermethylation is an early event in CRC

To analyze the clinicopathological significance of *FMN2* promoter methylation, we divided the patients into a high-methylation group and a low-methylation group according to the median value of methylation. The association between clinicopathological factors and *FMN2* methylation was analyzed (Table 5). High FMN2 methylation was associated with age (P = 0.0006), N stage (P = 0.0293), pathologic tumor stage (P = 0.0161), and lymphovascular invasion (P = 0.0180). Notably, the association analysis showed that the highest methylation level of *FMN2* occurred in tissues from cases of early-stage CRC, including cases with no regional lymph node metastasis (N0), cases in stages Ⅰ and Ⅱ, and cases with no lymphovascular invasion; the methylation level began to decrease with tumor progression. To understand our conclusions more intuitively, we then performed unpaired *t*-tests based on the pathological data. An identical pattern is shown in Figure 4A-C; DNA methylation of the *FMN2* gene increased from normal tissues to cancer tissues, reaching the highest level in early-stage cancer (N0, stages Ⅰ and Ⅱ, and no lymphovascular invasion) and decreasing stepwise in advanced-stage carcinomas. However, it is worth noting that the methylation level of *FMN2* in advanced-stage carcinomas is still significantly higher than that in normal tissue (P < 0.0001). Additionally, we analyzed the methylation level of *FMN2* according to the primary tumor site, and the result showed that there were statistically significant differences among the means (P < 0.0001) and that tumors located in the sigmoid colon and rectum had a relatively low *FMN2* methylation level (Figure 4D). Furthermore, we found that *FMN2* promoter hypermethylation was not associated with OS or DFS (Figure 4E and F). All these results indicated that *FMN2* promoter hypermethylation mainly occurred in elderly and early-stage patients with colon cancer.

DISCUSSION

In this article we first reported that a high frequency of hypermethylation occurred in the promoter of the *FMN2* gene in CRC tissues and that hypermethylation was responsible for the silencing of *FMN2*, which suggests that the epigenetic silencing of *FMN2* may be an important event in CRC. To the best of our knowledge, although *FMN2* was one of the top 20 genes with an extremely high frequency of hypermethylation in CRC (COSMIC, https://cancer.sanger.ac.uk/cosmic), this study is the first and only to investigate the regulation of the *FMN2* gene by methylation.

Previously, studies and investigations of publicly available datasets in FireBrowse (http://firebrowse.org/) have demonstrated differential *FMN2* RNA expression in human tumors, depending on the tumor type. For example, *FMN2* is overexpressed in approximately 95% of pre-B acute lymphoblastic leukemias[5] but is underexpressed in kidney renal clear cell carcinoma

Table 5 Relationship between formin 2 methylation levels and clinicopathological data

Factor	No.	*FMN2*		*P* value
		Low, *n* (%)	High, *n* (%)	
Age (yr)				
< 60	136	66 (45.83)	70 (28.69)	0.0006[1]
⩾ 60	252	78 (54.17)	174 (71.31)	
Gender				
Male	210	72 (50.00)	138 (56.56)	0.2105
Female	178	72 (50.00)	106 (43.44)	
Height (cm)				
< 170	138	52 (48.60)	86 (47.25)	0.8250
⩾ 170	151	55 (51.40)	96 (52.75)	
Weight (kg)				
< 80	156	56 (49.12)	100 (51.55)	0.6812
⩾ 80	152	58 (50.88)	94 (48.45)	
T				
T1	11	5 (3.47)	6 (2.47)	0.4830
T2	54	16 (11.11)	38 (15.71)	
T3	270	106 (73.61)	164 (67.77)	
T4	51	17 (11.81)	34 (14.05)	
N				
N0	212	69 (47.92)	143 (59.34)	0.0293[1]
N1 + N2	173	75 (52.08)	98 (40.66)	
M				
M0	264	98 (80.33)	166 (85.13)	0.2651
M1	53	24 (19.67)	29 (14.87)	
Stage				
Ⅰ + Ⅱ	197	62 (45.26)	135 (58.19)	0.0161[1]
Ⅲ + Ⅳ	172	75 (54.74)	97 (41.81)	
Lymphovascular invasion				
Yes	231	77 (60.63)	154 (72.99)	0.0180[1]
No	107	50 (39.37)	57 (27.01)	
Vascular invasion				
Yes	78	31 (24.80)	47 (22.71)	0.6627
No	254	94 (75.20)	160 (77.29)	
Perineural invasion				
Yes	59	20 (24.39)	39 (26.53)	0.7225
No	170	62 (75.61)	108 (73.47)	
Tumor status				
Tumor-free	246	86 (71.07)	160 (77.29)	0.2094
Tumor-present	82	35 (28.93)	47 (22.71)	
KRAS mutation				
Yes	28	8 (42.11)	20 (54.05)	0.3972
No	28	11 (57.89)	17 (45.95)	

[1]Indicates a statistically significant result. TNM stage was defined according to the AJCC Cancer Staging Manual. Tumor status: The state or condition of an individual's neoplasm at a particular point in time.

(FireBrowse); the mechanism underlying these phenomena has not been studied. In our research, we identified that *FMN2* is underexpressed in CRC tissues and were the first to explore the underlying mechanism. Epigenetic modifications of DNA, such as DNA promoter hypermethylation, have critical roles in mediating gene expression in mammalian development and human disease[13]. Methylation-mediated silencing of some genes in CRC has been reported in previous studies; for example, *Lgr5* methylation, by effecting *Lgr5* expression and CRC stem cell differentiation, may serve as a novel prognostic marker in CRC patients[14]. *SMYD3* promoter hypomethylation suppressed *SMYD3* expression and was associated with the risk of CRC[15]. Based on the fact that a high frequency of hypermethylation occurred in the *FMN2* gene promoter in CRC tissues, we found that both the downregulation of *FMN2* expression and the high frequency of hypermethylation occurred at the earliest stages of carcinogenesis; furthermore, these parameters had a significant inverse correlation in both our study and in published, large-scale human CRC electronic datasets. We also carried out MethylTarget™ assays in paired CRC tissues and inhibited DNA methylation with 5-Aza in CRC cells, which identified that hypermethylation and *FMN2* expression are causally related.

It is particularly important to determine which CpG islands adjacent to the promoter affect the expression of a gene, because this knowledge can provide directions for future research and potential targets for treatment. For example, Tavazoie SF[16] found that the *Mest/miR-335* promoter contained three CpG islands upstream of the transcriptional start site; among these CpG islands, island 3 demonstrated a strong inverse correlation between methylation and miR-335 expression

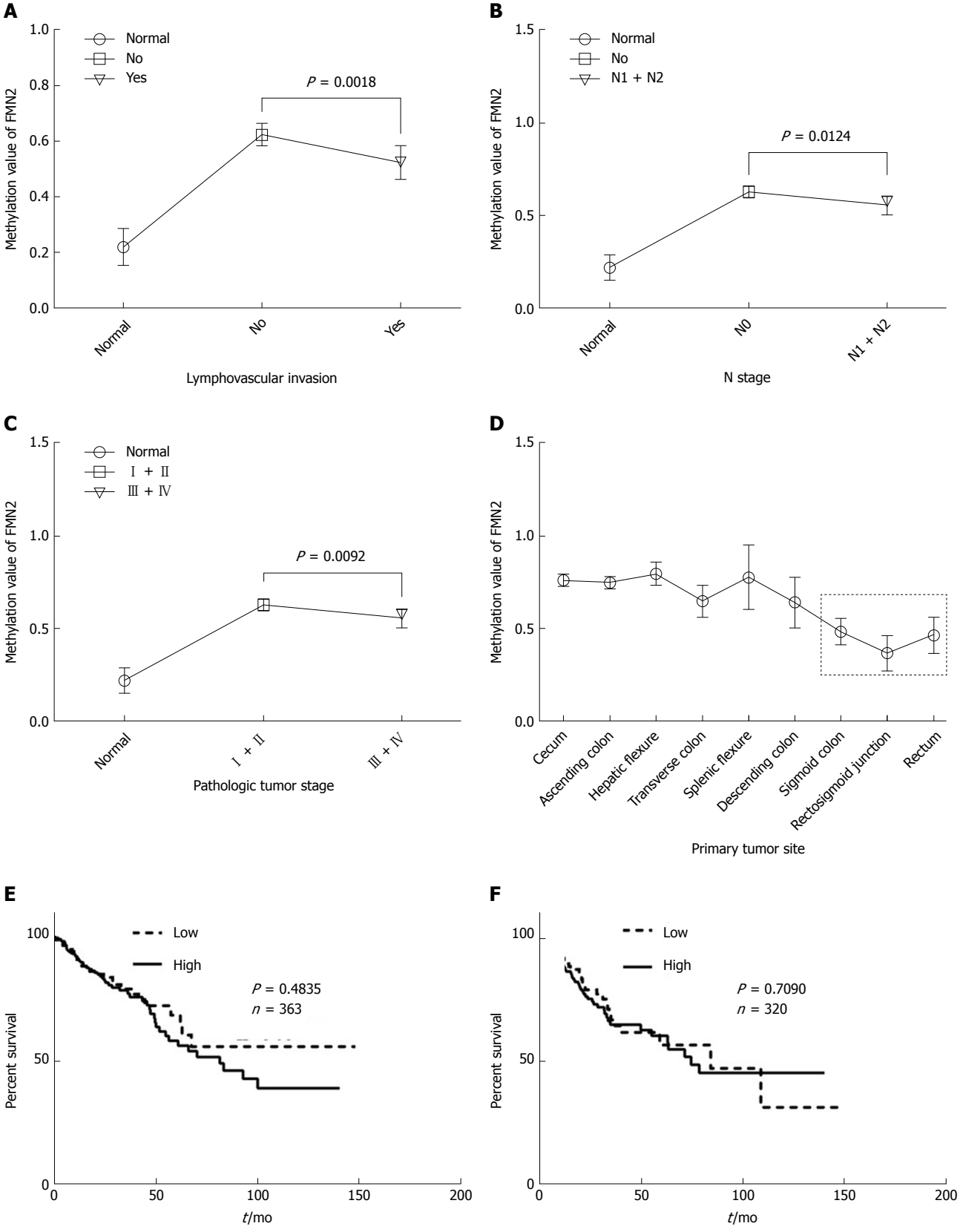

Figure 4 Formin 2 promoter hypermethylation mainly occurs in early-stage colon cancer patients. A: Formin 2 (*FMN2*) promoter methylation level in colorectal cancer (CRC) tissues with (yes) and without (no) lymphovascular invasion, presented as column means with 95%CI, mean connected. (unpaired *t*-test; normal: *n* = 45, CRC tissues with and without lymphovascular invasion: *n* = 231 and *n* = 107, respectively); B: *FMN2* promoter methylation level in CRC tissues with (N1 + N2) and without (N0) regional lymph node metastasis, presented as column means with 95%CI, mean connected (unpaired *t*-test, Normal: *n* = 45, CRC tissues with and without regional lymph node metastasis: *n* = 212 and *n* = 173, according to the AJCC Cancer Staging Manual); C: FMN2 promoter methylation level in CRC tissues from different stages, presented as column means with 95%CI, mean connected (unpaired *t*-test; Normal: *n* = 45, Stages Ⅰ + Ⅱ: *n* = 197, Stages Ⅲ + Ⅳ: *n* = 172, according to the AJCC Cancer Staging Manual); D: *FMN2* promoter methylation level in different organ sites, presented as column means with 95%CI, mean connected; E and F: *FMN2* hypermethylation has no effect on the overall survival or disease-free survival of CRC patients.

(r^2 = -0.81). The methylation status of island 3 plays a key role in inhibiting miR-335 expression. An identical pattern was observed in our study; we found that although the methylation status of *FMN2*-2, -3 and -4 was significantly increased in the eight CRC tissues, the methylation of *FMN2*-1 was not significantly higher than that in the paired nontumor tissues. All these findings suggest that during CRC progression, *FMN2* expression may be mainly mediated by the methylation of a specific CpG island region in the *FMN2* promoter.

In addition, we found that the hypermethylation of *FMN2* was significantly associated with age, N stage, pathologic tumor stage, and lymphovascular invasion. Notably, the association analysis showed that the highest methylation level of *FMN2* occurred in tissues from cases of early-stage CRC, including cases with no regional lymph node metastasis (N0), cases in stages Ⅰ and Ⅱ, and cases with no lymphovascular invasion and that the methylation level began to decrease with tumor progression. Identical results have been reported in previous research. In endometrial tumorigenesis, Schneider-Stock[17] found that DNA methylation of the *APC* gene increased from atypical hyperplasia (23.5%) to endometrial carcinoma, reaching its highest level of 77.4% in early-stage cancer (FIGO stages Ⅰ and Ⅱ) and decreasing stepwise to 24.2% in advanced-stage carcinomas (FIGO stages Ⅲ and Ⅳ). Epigenetic inactivation of the candidate tumor suppressor *USP44* is a frequent and early event in colorectal neoplasia[18], and *P16* methylation is an early event in cervical carcinogenesis[19]. All these studies, along with ours, have identified that DNA hypermethylation can be an early event in tumorigenesis. Hypermethylation most likely plays a critical role in cancer initiation, and creates an environment conducive to the overwhelming accumulation of simultaneous genetic and epigenetic mutations[20]. Additionally, we identified that patients younger than 60 years and patients with tumors located in the sigmoid colon and rectum exhibit relatively low *FMN2* methylation levels, which indicates that the methylation-associated silencing of *FMN2* may be involved in specific patients. In addition, Grady[21] identified that the patterns of DNA methylation in the colon vary by anatomical location, patient gender, and patient age.

In summary, we identified that the RNA expression of *FMN2* is reduced in CRC tissues and were the first to reveal that the hypermethylation of specific CpG islands adjacent to the *FMN2* promoter is the mechanism underlying *FMN2* silencing. Although the *FMN2* methylation is significantly stronger in tumor tissues than in paired nontumor tissues, the methylation level begins to decrease with tumor progression, which suggests that DNA hypermethylation is an early event in CRC tumorigenesis and can serve as a biomarker for the detection of CRC.

ARTICLE HIGHLIGHTS

Research background

Colorectal cancer (CRC) is a critical contributor to cancer mortality and morbidity, and some critical genes and pathways were important in the initiation and progression of CRC. Recent studies have shown that formin 2 (*FMN2*) may be down-regulated in CRC. Whether *FMN2* is abnormally expressed in CRC and what causes its abnormal expression are unclear. Revealing the role of FMN2 in CRC may provide potential therapeutic targets.

Research motivation

Epigenetic modifications of DNA, especially promoter hypermethylation, have critical roles in mediating some gene expression in the initiation and progression of CRC. Whether abnormal DNA methylation changes can occur in the promoter of the *FMN2* gene in CRC and whether such changes can be responsible for the silencing of *FMN2* are poorly known. So the main topic in this article is to try to solve this question that epigenetic silencing of *FMN2* may be an important event in CRC. All can provide the basis and direction for future research.

Research objectives

This study focuses on whether FMN2 is underexpressed in CRC, and whether methylation changes occur in CpG islands located in the promoter region of *FMN2*. If changes occur, what are the characteristics of fragments and CpG sites in these CpG islands? What is the core fragment of the change? Does methylation change silence the expression of *FMN2*, and is there a correlation between methylation changes in *FMN2* and clinical indicators of CRC? The answers to these questions can better explain the role of FMN2 in CRC.

Research methods

Large-scale human CRC expression datasets, including GEO and TCGA, were used to assess the expression levels and methylation levels of *FMN2* in CRC. Then, the mRNA levels of *FMN2* in our own clinical samples was analyzed by real-time quantitative polymerase chain reaction, and the methylation levels in four CpG regions adjacent to the *FMN2* promoter were assessed by MethylTarget™ assays in CRC cells and in paired colorectal tumor samples and adjacent nontumor tissue samples. Furthermore, we performed demethylation treatment in CRC cells with 5-Aza-2'-deoxycytidine and assessed the expression of *FMN2* by qRT-PCR. Last, the association between *FMN2* methylation patterns and clinical indicators was analyzed.

Research results

FMN2 is underexpressed in CRC, and the most obvious low expression occurs in early colon cancer tissues. Subsequent analysis coming from large-scale human CRC datasets showed that *FMN2* was one of the top 20 genes with an extremely high frequency of hypermethylation in CRC, methylation was the main somatic mutation, and *FMN2* gene promoter hypermethylation occurred in 37.37% of CRC tissues. Our own experiments confirmed that CRC cells and tissues displayed higher methylation levels in CpG regions of *FMN2* than nontumor tissue samples. Correlation analysis showed a strong inverse correlation between methylation and *FMN2* expression. Treatment of CRC cells with demethylation reagent, 5-Aza-2'-deoxycytidine, can significantly increase endogenous *FMN2* expression. The highest methylation of *FMN2* occurred in tissues from cases of early-stage CRC, including cases with no regional lymph node metastasis (N0), cases in stages I and II, and cases with no lymphovascular invasion. Additionally, *FMN2* promoter hypermethylation was more common in patients > 60 years and in colon cancer tissue.

Research conclusions

In this article we confirmed the low expression of *FMN2* in CRC and first reported that a high frequency of hypermethylation occurred in the promoter of the *FMN2* gene in CRC tissues and that hypermethylation was responsible for the silencing of *FMN2*. It is worth noting that we found that the low expression and hypermethylation of *FMN2* occurred more prominently in early colon cancer tissues, which suggests that DNA hypermethylation leading to the low expression of the *FMN2* gene may be an important early event in CRC, most likely playing a critical role in cancer initiation, and can serve as an ideal diagnostic biomarker in elderly patients with early-stage colon cancer.

Research perspectives

In the era of big data, the rational use of tumor databases such as TCGA, GEO, and COSMIC can provide us with valuable information. The emergence of some new technologies can provide more accurate data for our experiments.

For example, MethylTarget™ assays developed by Genesky BioTech used in this article can be used very well for methylation analysis. Involvement of the methylation-associated silencing of *FMN2* in colorectal carcinogenesis may be a valuable research direction. Future research can select more clinical specimens to explore whether it can be used as a good clinical diagnostic index, and can also develop demethylation treatment. The article on the relationship between *FMN2* and CRC is rare, so further study investigating whether FMN2 participates in the process of colorectal carcinogenesis and its underlying mechanisms are very important.

REFERENCES

1 **Siegel RL**, Miller KD, Jemal A. Cancer statistics, 2018. *CA Cancer J Clin* 2018; **68**: 7-30 [PMID: 29313949 DOI: 10.3322/caac.21442]

2 **Zeuner A**, Todaro M, Stassi G, De Maria R. Colorectal cancer stem cells: from the crypt to the clinic. *Cell Stem Cell* 2014; **15**: 692-705 [PMID: 25479747 DOI: 10.1016/j.stem.2014.11.012]

3 **Roncucci L**, Mariani F. Prevention of colorectal cancer: How many tools do we have in our basket? *Eur J Intern Med* 2015; **26**: 752-756 [PMID: 26499755 DOI: 10.1016/j.ejim.2015.08.019]

4 **Faix J**, Grosse R. Staying in shape with formins. *Dev Cell* 2006; **10**: 693-706 [PMID: 16740473 DOI: 10.1016/j.devcel.2006.05.001]

5 **Charfi C**, Voisin V, Levros LC Jr, Edouard E, Rassart E. Gene profiling of Graffi murine leukemia virus-induced lymphoid leukemias: identification of leukemia markers and Fmn2 as a potential oncogene. *Blood* 2011; **117**: 1899-1910 [PMID: 21135260 DOI: 10.1182/blood-2010-10-311001]

6 **Yamada K**, Ono M, Perkins ND, Rocha S, Lamond AI. Identification and functional characterization of FMN2, a regulator of the cyclin-dependent kinase inhibitor p21. *Mol Cell* 2013; **49**: 922-933 [PMID: 23375502 DOI: 10.1016/j.molcel.2012.12.023]

7 **Liu P**, Lu Y, Liu H, Wen W, Jia D, Wang Y, You M. Genome-wide association and fine mapping of genetic loci predisposing to colon carcinogenesis in mice. *Mol Cancer Res* 2012; **10**: 66-74 [PMID: 22127497 DOI: 10.1158/1541-7786.MCR-10-0540]

8 **Chen Wenping**, Shi Hai, Zhou Yi, Li Xiaohua, Chu Dake, Liu Zhaoxu. Expression and significance of Formin2 protein in colorectal cancer. *Chinese J of Dig Surge* **2015**: 335-338 [DOI:10.3760/cma.j.issn.1673-9752.2015.04.015]

9 **Zhou S**, Zhang Y, Wang L, Zhang Z, Cai B, Liu K, Zhang H, Dai M, Sun L, Xu X, Cai H, Liu X, Lu G, Xu G. CDKN2B methylation is associated with carotid artery calcification in ischemic stroke patients. *J Transl Med* 2016; **14**: 333 [PMID: 27905995 DOI: 10.1186/s12967-016-1093-4]

10 **Pu W**, Wang C, Chen S, Zhao D, Zhou Y, Ma Y, Wang Y, Li C, Huang Z, Jin L, Guo S, Wang J, Wang M. Targeted bisulfite sequencing identified a panel of DNA methylation-based biomarkers for esophageal squamous cell carcinoma (ESCC). *Clin Epigenetics* 2017; **9**: 129 [PMID: 29270239 DOI: 10.1186/s13148-017-0430-7]

11 **Forbes SA**, Beare D, Boutselakis H, Bamford S, Bindal N, Tate J, Cole CG, Ward S, Dawson E, Ponting L, Stefancsik R, Harsha B, Kok CY, Jia M, Jubb H, Sondka Z, Thompson S, De T, Campbell PJ. COSMIC: somatic cancer genetics at high-resolution. *Nucleic Acids Res* 2017; **45**: D777-D783 [PMID: 27899578 DOI: 10.1093/nar/gkw1121]

12 **Cancer Genome Atlas Network**. Comprehensive molecular characterization of human colon and rectal cancer. *Nature* 2012; **487**: 330-337 [PMID: 22810696 DOI: 10.1038/nature11252]

13 **Schübeler D**. Function and information content of DNA methylation. *Nature* 2015; **517**: 321-326 [PMID: 25592537 DOI: 10.1038/nature14192]

14 **Su S**, Hong F, Liang Y, Zhou J, Liang Y, Chen K, Wang X, Wang Z, Wang Z, Chang C, Han W, Gong W, Qin H, Jiang B, Xiong H, Peng L. Lgr5 Methylation in Cancer Stem Cell Differentiation and Prognosis-Prediction in Colorectal Cancer. *PLoS One* 2015; **10**: e0143513 [PMID: 26599100 DOI: 10.1371/journal.pone.0143513]

15 **Li B**, Pan R, Zhou C, Dai J, Mao Y, Chen M, Huang T, Ying X, Hu H, Zhao J, Zhang W, Duan S. SMYD3 promoter hypomethylation is associated with the risk of colorectal cancer. *Future Oncol* 2018; **14**: 1825-1834 [PMID: 29969917 DOI: 10.2217/fon-2017-0682]

16 **Png KJ**, Yoshida M, Zhang XH, Shu W, Lee H, Rimner A, Chan TA, Comen E, Andrade VP, Kim SW, King TA, Hudis CA, Norton L, Hicks J, Massagué J, Tavazoie SF. MicroRNA-335 inhibits tumor reinitiation and is silenced through genetic and epigenetic mechanisms in human breast cancer. *Genes Dev* 2011; **25**: 226-231 [PMID: 21289068 DOI: 10.1101/gad.1974211]

17 **Ignatov A**, Bischoff J, Ignatov T, Schwarzenau C, Krebs T, Kuester D, Costa SD, Roessner A, Semczuk A, Schneider-Stock R. APC promoter hypermethylation is an early event in endometrial tumorigenesis. *Cancer Sci* 2010; **101**: 321-327 [PMID: 19900189 DOI: 10.1111/j.1349-7006.2009.01397.x]

18 **Sloane MA**, Wong JW, Perera D, Nunez AC, Pimanda JE, Hawkins NJ, Sieber OM, Bourke MJ, Hesson LB, Ward RL. Epigenetic inactivation of the candidate tumor suppressor USP44 is a frequent and early event in colorectal neoplasia. *Epigenetics* 2014; **9**: 1092-1100 [PMID: 24837038 DOI: 10.4161/epi.29222]

19 **Huang LW**, Pan HS, Lin YH, Seow KM, Chen HJ, Hwang JL. P16 methylation is an early event in cervical carcinogenesis. *Int J Gynecol Cancer* 2011; **21**: 452-456 [PMID: 21436693 DOI: 10.1097/IGC.0b013e31821091ea]

20 **Taby R**, Issa JP. Cancer epigenetics. *CA Cancer J Clin* 2010; **60**: 376-392 [PMID: 20959400 DOI: 10.3322/caac.20085]

21 **Kaz AM**, Wong CJ, Dzieciatkowski S, Luo Y, Schoen RE, Grady WM. Patterns of DNA methylation in the normal colon vary by anatomical location, gender, and age. *Epigenetics* 2014; **9**: 492-502 [PMID: 24413027 DOI: 10.4161/epi.27650]

P- Reviewer: Bordonaro M, Leon J, Noda H **S- Editor**: Wang XJ
L- Editor: Wang TQ **E- Editor**: Yin SY

World Journal of Gastroenterology

Submit a Manuscript: http://www.f6publishing.com

World J Gastroenterol 2018 November 28; 24(44): 5025-5033

DOI: 10.3748/wjg.v24.i44.5025

ISSN 1007-9327 (print) ISSN 2219-2840 (online)

ORIGINAL ARTICLE

Retrospective Cohort Study

Timing of upper gastrointestinal endoscopy does not influence short-term outcomes in patients with acute variceal bleeding

Jeong-Ju Yoo, Young Chang, Eun Ju Cho, Ji Eun Moon, Sang Gyune Kim, Young Seok Kim, Yun Bin Lee, Jeong-Hoon Lee, Su Jong Yu, Yoon Jun Kim, Jung-Hwan Yoon

Jeong-Ju Yoo, Sang Gyune Kim, Young Seok Kim, Department of Gastroenterology and Hepatology, Soonchunhyang University school of Medicine, Bucheon 14584, South Korea

Young Chang, Eun Ju Cho, Yun Bin Lee, Jeong-Hoon Lee, Su Jong Yu, Yoon Jun Kim, Jung-Hwan Yoon, Department of Internal Medicine and Liver Research Institute, Seoul National University College of Medicine, Seoul 03080, South Korea

Ji Eun Moon, Department of Biostatistics, Clinical Trial Center, Soonchunhyang University Bucheon Hospital, Bucheon 14584, South Korea

ORCID number: Jeong-Ju Yoo (0000-0002-7802-0381); Young Chang (0000-0001-7752-7618); Eun Ju Cho (0000-0002-2677-3189); Ji Eun Moon (0000-0002-0887-703X); Sang Gyune Kim (0000-0001-8694-777X); Young Seok Kim (0000-0002-7113-3623); Yun Bin Lee (0000-0002-3193-9745); Jeong-Hoon Lee (0000-0002-0315-2080); Su Jong Yu (0000-0001-8888-7977); Yoon Jun Kim (0000-0001-9141-7773); Jung-Hwan Yoon (0000-0002-9128-3610).

Author contributions: All authors helped to perform the research; Yoo JJ and Chang Y contributed equally as co-first authors; Yoo JJ and Chang Y did the manuscript writing, drafting conception and design, and data analysis; Moon JE did the manuscript writing, and data analysis; Kim SG, Kim YS, Lee YB, Lee JH, Yu SJ, Kim YJ, and Yoon JH made contribution to the manuscript writing; Cho EJ made contribution to the manuscript writing, conception drafting and design.

Institutional review board statement: The study protocol was approved by the Institutional Review Board of each hospital, and also conformed to the ethical guidelines of the World Medical Association Declaration of Helsinki (H-1801-057-914, SCH 2018-06-013).

Informed consent statement: Patients were not required to give informed consent to the study because the analysis used anonymous clinical data that were obtained after each patient agreed to treatment by written consent.

Conflict-of-interest statement: All authors have no conflict of interest with respect to the subjects described in this article.

Data sharing statement: No additional data are available.

STROBE statement: The authors have read the STROBE Statement-checklist of items, and the manuscript was prepared and revised according to the STROBE Statement-checklist of items.

Manuscript source: Unsolicited manuscript

Corresponding author to: Eun Ju Cho, MD, PhD, Assistant Professor, Department of Internal Medicine and Liver Research Institute, Seoul National University College of Medicine, 101 Daehak-no, Jongno-gu, Seoul 03080, South Korea. creatio3@snu.ac.kr
Telephone: +82-2-20722228
Fax: +82-2-7436701

Received: August 30, 2018
Peer-review started: August 30, 2018
First decision: October 14, 2018
Revised: October 15, 2018
Accepted: November 13, 2018
Article in press: November 13, 2018

Published online: November 28, 2018

Abstract

AIM

To examine the association between the timing of endoscopy and the short-term outcomes of acute variceal bleeding in cirrhotic patients.

METHODS

This retrospective study included 274 consecutive patients admitted with acute esophageal variceal bleeding of two tertiary hospitals in Korea. We adjusted confounding factors using the Cox proportional hazards model and the inverse probability weighting (IPW) method. The primary outcome was the mortality of patients within 6 wk.

RESULTS

A total of 173 patients received urgent endoscopy (*i.e.*, ≤ 12 h after admission), and 101 patients received non-urgent endoscopy (> 12 h after admission). The 6-wk mortality rate was 22.5% in the urgent endoscopy group and 29.7% in the non-urgent endoscopy group, and there was no significant difference between the two groups before (P = 0.266) and after IPW (P = 0.639). The length of hospital stay was statistically different between the urgent group and non-urgent group (P = 0.033); however, there was no significant difference in the in-hospital mortality rate between the two groups (8.1% *vs* 7.9%, P = 0.960). In multivariate analyses, timing of endoscopy was not associated with 6-wk mortality (hazard ratio, 1.297; 95% confidence interval, 0.806-2.089; P = 0.284).

CONCLUSION

In cirrhotic patients with acute variceal bleeding, the timing of endoscopy may be independent of short-term mortality.

Key words: Cirrhosis; Endoscopy; Upper gastrointestinal bleeding; Gastroesophageal varices; Timing

Core tip: Most guidelines recommend performing endoscopy for acute variceal bleeding within 12 h. However, the evidence level for this recommendation is very low. We found that, after inverse probability weighting matching, compared to non-urgent endoscopy, performing endoscopy within 12 h of admission (so-called urgent endoscopy) was not associated with short-term prognosis, including overall survival at 6 wk or transplant-free survival at 6 wk. Rather, age, hepatocellular carcinoma, model for end-stage liver disease score, and degree of ascites were related to short-term mortality. These results indicate that, in cirrhotic patients with acute variceal bleeding, the timing of endoscopy does not appear to be associated with short-term prognosis.

Yoo JJ, Chang Y, Cho EJ, Moon JE, Kim SG, Kim YS, Lee YB, Lee JH, Yu SJ, Kim YJ, Yoon JH. Timing of upper gastrointestinal endoscopy does not influence short-term outcomes in patients with acute variceal bleeding. *World J Gastroenterol* 2018; 24(44): 5025-5033 Available from: URL: http://www.wjgnet.com/1007-9327/full/v24/i44/5025.htm DOI: http://dx.doi.org/10.3748/wjg.v24.i44.5025

INTRODUCTION

Variceal bleeding is a common complication of cirrhosis of the liver, and in patients with cirrhosis, is found to be the cause of 60%-65% of bleeding episodes[1]. It increases the risk of mortality by approximately 15%-20%. Many guidelines recommend a standardized treatment of acute variceal bleeding[2-5]. Endoscopic procedures and endoscopic hemostasis techniques, *e.g.*, band ligation, are considered very important in the treatment of such patients[6], with most guidelines recommending that emergency endoscopy be performed within 12 h of hospital arrival[4-6].

However, this recommendation appears to be based on "expert opinion", rather than on the level of evidence, which is in fact very low. For example, one survey showed significant variability in gastoenterologists' opinion of the timing of emergency endoscopy following variceal bleeding[7]. Moreover, there is little related research to date to support this current recommendation of endoscopy within 12 h of hospital arrival[8,9]. However, providing better evidence by clinically performing a randomized controlled trial on these acutely ill patients is problematic, because of their unstable vital signs and the ethical problems that would arise from this type of study.

Compared to other medical treatments such as vasoactive agents, endoscopy is a relatively invasive procedure and both the risk and benefit to the patient need to be considered. If unnecessary endoscopies are frequently performed, medical staff fatigue may increase dramatically, and so may the medical costs[10]. Moreover, if endoscopy is performed too early, the examination may be may not be adequate; for example it may be marred by remnant blood clots *etc*. As well, the risk of a procedure-related complication tends to increase when endoscopy is performed too early in patients with unstable condition compared to when performed in a more stable state[10,11]. To date, a gold standard recommended timing of endoscopy in patients with acute variceal bleeding has not been clearly determined.

The aim of this study was to examine the association between the timing of endoscopy and clinical outcomes in acute esophageal variceal bleeding.

MATERIALS AND METHODS

Patients

We collected the data of cirrhotic patients undergoing routine clinical care in either of two tertiary hospitals

(Seoul National University Hospital and Soon Chun Hyang University Bucheon Hospital) between January 2011 and December 2015. The inclusion criteria were as follows: (1) Cirrhotic patients admitted *via* the emergency room (ER) with upper gastrointestinal bleeding (UGIB), and diagnosed through endoscopy with acute variceal bleeding; and (2) aged over 19 years. Exclusion criteria were as follows: (1) Patients who did not undergo endoscopic examination during ER stay (n = 38); (2) UGIB from other than variceal bleeding (*e.g.*, peptic ulcer bleeding, portal hypertensive gastropathy bleeding) (n = 165); or (3) if endoscopy had been performed within 7 d prior to admission (n = 7). In total, 484 patients met the inclusion criteria and 210 patients were excluded as above. Finally, 274 patients were analyzed.

Standard of care and endoscopic procedure

When a cirrhotic patient with UGIB arrived at the ER of each hospital, adequate fluid resuscitation, a prophylactic antibiotic, and a vasoactive drug with terlipressin were immediately administered at the time of admission. If peptic ulcer bleeding could not be ruled out, a proton pump inhibitor was also administrated. An emergency medical specialist first examined the patient, and consulted a gastrointestinal (GI) specialist about whether an endoscopy was to be performed. Then, the GI specialist determined the timing of the endoscopy, considering each patient's age, presence of comorbidities such as renal failure or cardiopulmonary disease, presence of hepatic encephalopathy, hemodynamic instability, and laboratory abnormalities including anemia, lactic acidosis and coagulopathy. If patients did not exhibit poor clinical factors or they had signs of hepatic encephalopathy more than grade Ⅲ, delayed endoscopic examination was considered. (In both hospitals, a GI specialist with technical expertise in the use of endoscopic devices is on call 24 h a day, 7 d a week.) Therapeutic endoscopy was performed using standard video-endoscopes (GIF-Q260 or GIF-Q290; Olympus, Tokyo, Japan). When EVL failed, salvage treatments including endoscopic variceal obturation (EVO) using n-butyl-2-cyanoacrylate (NBC), insertion of a Sengstaken-Blakemore (SB) tube, transjugular intrahepatic portosystemic shunt, variceal embolization, or a combination of multiple treatment modalities were performed. When EVO was performed, NBC (Histoacryl®; B. Braun Dexon, Spangenberg, Germany) was mixed with ethiodized oil (Lipiodol; Guerbert, Roissy, France) and was injected as a bolus dose of 0.5-2 mL, depending on the amount of bleeding.

Data collection

Two independent reviewers (Yoo JJ and Chang Y), each with more than 5 years of endoscopic experience, screened medical records and endoscopic reports to confirm that each case was of a true acute gastroesophageal variceal bleeding. If a patient was admitted more than once during the study period due to variceal bleeding, the earliest visit was selected for inclusion in the analysis. Demographics, relevant medical history, any comorbid conditions, and relevant laboratory findings at the time of admission were collected. Two widely-studied UGIB prognostic scores of each of the patients, namely the Glasgow-Blatchford score (GBS) and the Rockall score, were also calculated[12,13]. If the patient had died during the study period, the cause of death was evaluated from hospital records, where possible.

Definitions

Time to endoscopy was defined as the time interval from the hospital arrival to the initial endoscopic examination[14]. Urgent endoscopy was defined according to the guidelines as an endoscopic examination performed within 12 h of admission, and non-urgent endoscopy defined as one performed after 12 h[5].

The primary outcome for this study was the 6-wk mortality rate following variceal bleeding. The secondary outcomes were: 6-wk mortality or transplantation rates, hospital admission duration, in-hospital mortality, and re-bleeding rate.

Statistical analysis

Only the patients with complete data were analyzed in this study. Frequencies with percentages and means with standard deviations were used for descriptive statistics. Statistical differences between the groups were investigated using the χ^2 test or Fisher's exact test for categorical variables and the Student's t test or Mann-Whitney U test for continuous variables. Cumulative 6-wk survival and transplant-free survival (TFS) rates after acute variceal bleeding were estimated using the Kaplan-Meier method, and differences between the curves were compared using the log-rank test. In patients with loss to follow-up, the data were censored on the last date on which their survival status was known. The effect of endoscopic timing on clinical outcomes was assessed using the Cox proportional hazards regression model. If multicollinearity occurred between the individual components in the univariate analysis, only the most relevant prognostic parameter was included in the final multivariable model. The inverse probability weighting method based on propensity score was applied so as to correct baseline differences between the two groups (urgent endoscopy *vs* non-urgent endoscopy). A P-value less than 0.05 was considered significant. Hazard ratios (HRs) and 95% confidence intervals (CIs) were also calculated. All statistical analyses were performed using R (version 3.3.3, The R Foundation for Statistical Computing, Vienna, Austria), or PASW version 18.0 statistical software (SPSS Inc.; Chicago, IL, United States).

RESULTS

Baseline characteristics

The baseline characteristics of the patients enrolled in the study are reported in Table 1. The mean age of the

Table 1 Baseline characteristics of patients before and after inverse probability weighting *n* (%)

Characteristics	Unweighted				Inverse probability weighting			
	All patients (*n* = 274)	Urgent endoscopy (*n* = 173)	Non-urgent endoscopy (*n* = 101)	*P* value	All patients (*n* = 272)	Urgent endoscopy (*n* = 172)	Non-urgent endoscopy (*n* = 100)	*P* value
Demographics								
Age (yr)	58.05 ± 12.10	57.62 ± 12.09	58.77 ± 12.22	0.45	58.14 ± 0.85	58.17 ± 1.03	58.10 ± 1.34	0.971
Sex (male)	207 (75.5)	128 (74.0)	79 (78.2)	0.469	205 (74.6)	127 (37.2)	78 (37.4)	0.956
Hepatocellular carcinoma	149 (54.4)	97 (56.1)	52 (51.5)	0.452	148 (54.8)	97 (27.8)	51 (27.0)	0.830
Prior variceal upper GI bleeding	179 (65.3)	110 (63.6)	69 (68.3)	0.511	178 (65.7)	109 (32.3)	69 (33.5)	0.713
Prior non-variceal upper GI bleeding	8 (2.9)	2 (1.2)	6 (5.9)	0.055	8 (2.9)	2 (1.4)	6 (1.5)	0.890
Initial hepatic encephalopathy				< 0.001				0.939
None	241 (88.0)	164 (94.8)	77 (76.2)		239 (88.6)	163 (44.5)	76 (44.4)	
Grade Ⅰ-Ⅱ	16 (5.8)	5 (2.9)	11 (10.9)		16 (5.4)	5 (2.5)	11 (2.9)	
Grade Ⅲ-Ⅳ	17 (6.2)	4 (2.3)	13 (12.9)		17 (5.7)	4 (2.6)	13 (3.1)	
Initial ascites				0.067				0.994
None	111 (40.5)	77 (44.5)	34 (33.7)		111 (41.1)	77 (20.3)	34 (20.8)	
Mild	77 (28.1)	50 (28.9)	27 (26.7)		76 (29.4)	49 (14.7)	27 (14.7)	
Moderate to severe	86 (31.4)	46 (26.6)	40 (39.6)		85 (29.5)	46 (14.6)	39 (14.9)	
Etiology				0.985				0.930
HBV	137 (50.0)	86 (49.8)	51 (50.5)		136 (49.7)	86 (24.4)	50 (25.33)	
HCV	25 (9.1)	16 (9.2)	9 (8.9)		25 (9.4)	16 (5.4)	9 (4.0)	
Alcohol	69 (25.2)	43 (24.9)	26 (25.7)		68 (24.0)	42 (12.3)	26 (12.7)	
Others	43 (15.7)	28 (16.2)	15 (14.9)		43 (16.0)	28 (8.0)	15 (8.0)	
Vital signs								
Systolic blood pressure (mm Hg)	117 ± 26	116 ± 26	120 ± 26	0.221	118 ± 2	116 ± 2	119 ± 3	0.408
Heart rate (beat/min)	95 ± 18	96 ± 19	94 ± 17	0.551	95 ± 1	95 ± 1	95 ± 2	0.827
Laboratory values								
Hemoglobin	9.2 ± 2.5	9.0 ± 2.5	9.6 ± 2.5	0.044	9.1 ± 0.2	8.8 ± 0.2	9.3 ± 0.3	0.105
Platelet count (10^3/mL)	117 + 79	118 ± 78	114 ± 80	0.701	118 ± 5	119 ± 6	118 ± 8	0.917
Total bilirubin	3.8 ± 5.8	3.5 ± 5.3	4.5 ± 6.5	0.148	3.7 ± 0.4	3.6 ± 0.5	3.8 ± 0.5	0.817
Serum albumin	2.9 ± 0.6	2.9 ± 0.6	2.9 ± 0.7	0.702	3.0 ± 0.1	3.0 ± 0.1	4.0 ± 0.1	0.736
Prothromin time (INR)	1.6 ± 1.8	1.4 ± 0.6	1.8 ± 2.9	0.046	1.6 ± 0.1	1.5 ± 0.1	1.7 ± 0.2	0.157
Serum creatinine	1.3 ± 1.5	1.4 ± 1.8	1.2 ± 1.0	0.24	1.2 ± 0.1	1.4 ± 0.1	1.1 ± 0.1	0.07
MELD score	15.9 ± 7.8	15.4 ± 6.9	16.9 ± 9.2	0.112	15.6 ± 0.5	15.6 ± 0.5	15.6 ± 0.8	0.964
Prognostic scores								
Glasgow-Blatchford score	9.1 ± 3.5	9.2 ± 3.3	9.1 ± 3.9	0.818	9.3 ± 0.2	9.3 ± 0.3	9.3 ± 0.4	0.907
Rockall score	3.9 ± 1.4	4.0 ± 1.4	3.6 ± 1.5	0.021	3.4 ± 0.1	3.9 ± 0.1	3.9 ± 0.2	0.875
Endoscopy								
Time to endoscopy, hours, median (IQR)	12.7 (2.8-16.5)	4.0 (2.1-6.8)	19.5 (15.0-35.5)	< 0.001	12.5 (2.8-16.4)	4.0 (2.2-6.8)	19.5 (15.1-35.4)	< 0.001

Data are expressed as mean ± standard deviation or number (percentage), unless otherwise stated. GI: Gastrointestinal; HBV: Hepatitis B virus; HCV: Hepatitis C virus; INR: International normalized ratio; MELD: Model for end-stage liver disease.

patients was 58.05 ± 12.10 years, and 75.5% (207) were male. The proportion of patients with hepatocellular carcinoma (HCC) was 54.4% (149). Sixty-five percent of the patients had experienced variceal bleeding prior to the study period. Chronic hepatitis B virus (HBV) infection was the most common etiology of cirrhosis, followed by alcohol use and other causes. Sixty percent of patients presented with any grade of ascites.

At the time of hospital arrival, the heart rate of the patients was found to be abnormally high, with an average of 95 beat per minute, and their mean systolic pressure was 116 ± 26 mmHg. They showed deteriorated liver function with a mean model for end-stage liver disease (MELD) score of 15.9 ± 7.8 points. The mean Glasgow-Blatchford score was 9.1 ± 3.5 points, suggesting a poor prognosis.

Patients underwent endoscopic examination at an average of 9.1 ± 3.5 h after arrival at the hospital. Based on the timing of the endoscopy, patients were divided into an urgent endoscopy group (< 12 h) and a non-urgent endoscopy group (≥ 12 h). The baseline characteristics of the two groups were similar and there was no significant difference in the MELD scores (15.4 ± 6.9 *vs* 16.9 ± 9.2; *P* = 0.088) between the two groups.

Impact of endoscopic timing on outcomes

The 6-wk mortality rate was 22.5% in the urgent endoscopy group and 29.7% in the non-urgent endoscopy group, and there were no significant differences between the two groups (*P* = 0.266, Figure 1). After IPW, the baseline characteristics were well balanced between the two groups (Tables 1). The IPW-adjusted analysis also showed that both groups did not differ in terms of the risk of death (*P* = 0.639). The 6-wk mortality or transplantation rate was slightly lower in the urgent group but with marginal significance (*P* = 0.060, Figure 2). However, after IPW there was no significant difference between the two groups (*P* = 0.532).

Table 2 Clinical outcomes of the patients *n* (%)

Outcomes	All patients (*n* = 274)	Urgent endoscopy (*n* = 173)	Non-urgent endoscopy (*n* = 101)	*P* value
Hospital admission duration, days, median (IQR)	4.0 (3.0-9.5)	4.0 (2.0-9.0)	4.0 (3.0-11.0)	0.033
In-hospital mortality	22 (8.0)	14 (8.1)	8 (7.9)	0.960
Re-bleeding rate	60 (21.9)	35 (20.2)	25 (24.8)	0.449
Six-week mortality	69 (25.2)	39 (22.5)	30 (29.7)	0.197
Liver transplantation	25 (9.1)	14 (8.1)	11 (10.9)	0.515

Data are expressed as number (percentage), unless otherwise stated. IQR: Interquartile range.

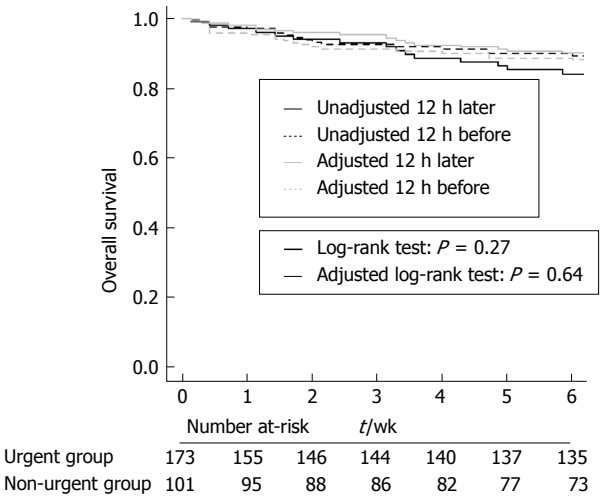

Figure 1 Comparison of 6-wk survival in the urgent and the non-urgent endoscopy groups. Kaplan-Meier survival plot stratified by timing of endoscopy of all patients. The dotted line indicates urgent endoscopy and the solid line indicates non-urgent endoscopy. The black line is the unadjusted cumulative survival graph before inverse probability weighting (IPW), and the gray line is the adjusted after the IPW correction.

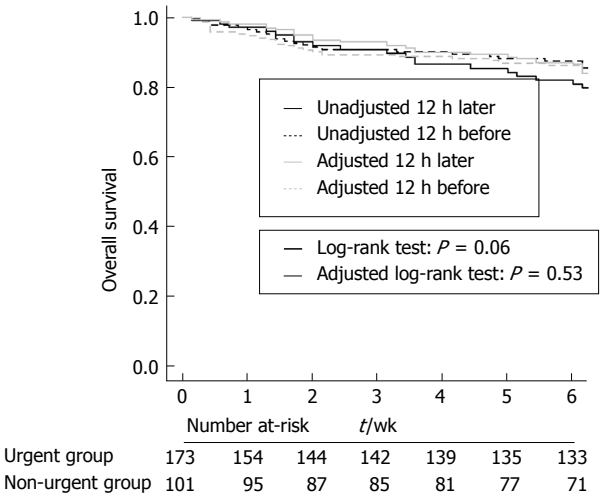

Figure 2 Comparison of 6-wk transplant-free survival in the urgent and the non-urgent endoscopy groups. Kaplan-Meier survival plot stratified by timing of endoscopy of all patients. The dotted line indicates urgent endoscopy and the solid line indicates non-urgent endoscopy. The black line is the unadjusted cumulative graph before inverse probability weighting (IPW), and the gray line is the adjusted after the IPW correction.

Other clinical outcomes

Other clinical outcomes are described in Table 2. Although the median hospital admission duration was similar in both groups, significant differences observed in the mean rank scores (*i.e.*, Mann-Whitney *U* test), suggesting that the data for the non-urgent group were more right skewed ($P = 0.033$)[15]. However, there was no significant difference in the in-hospital mortality rate between the urgent group and the non-urgent group (8.1% *vs* 7.9%; $P = 0.960$).

The rate of variceal re-bleeding within 6 wk was 10.4% in the urgent group and 12.9% in the non-urgent group, which was statistically nonsignificant ($P = 0.557$). The Kaplan-Meier analysis of time to re-bleeding also showed no significant difference between the two groups either before or after IPW matching ($P = 0.538$ and 0.631, respectively; Figure 3).

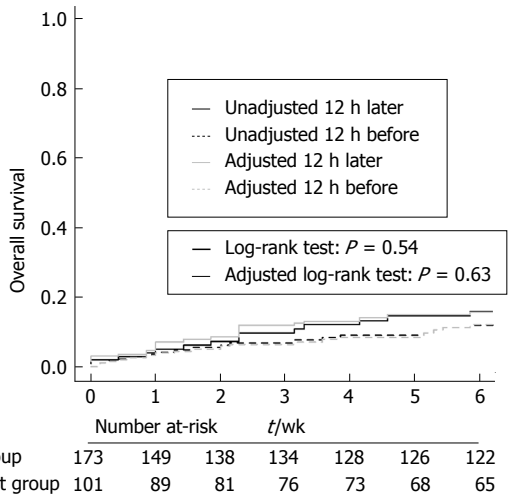

Figure 3 Comparison of 6-wk re-bleeding rate in the urgent and the non-urgent endoscopy groups. Kaplan-Meier survival plot stratified by timing of endoscopy of all patients. The dotted line indicates urgent endoscopy and the solid line indicates non-urgent endoscopy. The black line is the unadjusted cumulative graph before inverse probability weighting (IPW), and the gray line is the adjusted after the IPW correction.

Predictors of 6-wk mortality

Finally, we analyzed clinical predictors associated with 6-wk mortality (Table 3). Compared with non-urgent endoscopy, urgent endoscopy was not independently associated with short-term mortality [adjusted hazard ratio (aHR): 1.297; 95% confidence interval (CI): 0.806-2.089; $P = 0.284$). On the other hand, the following were independent risk factors of 6-wk mortality: advanced age (aHR: 1.035; 95%CI: 1.011-1.0059;

Table 3 Cox proportional hazards model for 6-wk mortality

Variable	Univariable		Multivariable	
	HR (95%CI)	*P* value	HR (95%CI)	*P* value
Age	1.037 (1.016-1.059)	< 0.001	1.035 (1.011-1.059)	0.004
Sex				
Female	1			
Male	0.946 (0.543-1.664)	0.845		
Etiology				
Non-viral	1		1	
Viral	0.536 (0.319-0.902)	0.019	0.683 (0.384-1.214)	0.194
Hepatocellular carcinoma	2.442 (1.439-4.142)	0.001	1.929 (1.072-3.469)	0.028
Diabetes Mellitus	0.535 (0.292-0.978)	0.042	0.423 (0.225-0.795)	0.008
Hypertension	0.994 (0.521-1.894)	0.984		
Prior variceal upper GI bleeding	0.916 (0.561-1.497)	0.726		
Prior non-variceal upper GI bleeding	3.92E-8 (0-INF)	0.996		
Systolic blood pressure	1.003 (0.994-1.012)	0.489		
Heart rate	1.005 (0.992-1.018)	0.477		
MELD score[1]	1.062 (1.041-1.083)	< 0.001	1.049(1.024-1.074)	< 0.001
ALT	1.001 (0.999-1.002)	0.123		
Serum creatinine[1]	1.075 (1.013-1.197)	0.018		
Serum total bilirubin[1]	1.047 (1.012-1.083)	0.007		
Prothrombin time[1]	1.128 (1.043-1.221)	0.003		
Initial hepatic encephalopathy				
None	1		1	
Grade Ⅰ-Ⅱ	1.393 (0.558-3.477)	0.477	0.555 (0.200-1.537)	0.257
Grade Ⅲ-Ⅳ	2.229 (1.062-4.677)	0.034	0.969 (0.449-2.088)	0.935
Initial ascites				
None	1		1	
Mild	2.064 (1.003-4.250)	0.049	1.604 (0.766-3.361)	0.210
Moderate to severe	4.675 (2.494-8.766)	< 0.001	3.346 (1.715-6.527)	< 0.001
Glasgow-Blatchford score	0.980 (0.917-1.047)	0.550		
Rockall score	1.138 (0.968-1.338)	0.118		
Timing of endoscopy				
Non-urgent (≥ 12 h)	1			
Urgent (< 12 h)	1.297 (0.806-2.088)	0.284		

[1]Considering the multicollinearity between model for end-stage liver disease (MELD) score and its individual components, only MELD score, the most relevant prognostic parameter in cirrhosis, was included in the final multivariable model. HR: Hazard ratio; GI: Gastrointestinal; MELD: Model for end-stage liver disease; ALT: Alanine aminotransferase.

P = 0.004), high MELD score (aHR: 1.049; 95%CI: 1.024-1.074; *P* < 0.001), and the presence of ascites. In particular, the grade of ascites showed dose-dependency. When the ascites was present to a more than moderate degree, the 6-wk mortality was increased 3.346-fold compared to when there was no ascites. Also, the presence of HCC (aHR: 1.929; 95%CI: 1.072-3.469; *P* = 0.028) increased the risk of short-term mortality in variceal bleeding patients. However, the GBS and Rockall scores were not significantly associated with 6-wk mortality in patients with acute variceal bleeding. Similar results were obtained when the factors predicting transplantation or death were analyzed (Supplementary Table 1).

DISCUSSION

The decision as to when to perform endoscopy in patients with acute variceal bleeding has always been controversial. Guidelines have traditionally recommended that endoscopy be performed within 12 h of admission, but to date there has been little actual supporting evidence for this[4,5,16]. Our study analyzed relatively large numbers of patients, and concluded that, despite the existing guidelines, the timing of endoscopy was not associated with short-term survival or mortality in patients with variceal bleeding.

Studies on the optimal timing of endoscopy in patients with acute variceal bleeding have taken place mostly at a time in the past when sclerotherapy was the mainstream treatment. Several randomized control trials reported at this time have concluded that, if endoscopy was performed early, clinical indices did not improve significantly[17,18]. In studies, including some meta-analyses, endoscopic treatment was recommended only when pharmacotherapy fails[19]. However, band ligation therapy has completely replaced sclerotherapy nowadays[20,21]. Moreover, it is now widely acknowledged that combination therapy is superior to pharmaco- or endoscopic monotherapy for acute variceal bleeding[22,23]. Paradoxically, however, in the age of band ligation, there has been little research so far on the optimal timing of endoscopy.

To date, there have been two relatively large-scale studies on the optimal timing of the endoscopy of variceal bleeding patients in the "band ligation era". In a

study published in Taiwan, early endoscopy (*i.e.*, < 15 h) reduced in-hospital mortality, but did not have a significant impact on mortality[9]. Another study published in Canada showed that time-to-endoscopy did not appear to be associated with mortality[8]. Both studies exhibited selection bias, in that only hemodynamically stable patients were included. The authors suggested that in-hospital mortality was increased due to delays in time-to-endoscopy, but the baseline MELD score was higher in those patients with higher in-hospital mortality (16.5 *vs* 11.2)[9]. In other words, it is difficult to tell whether these patients' increased in-hospital mortality was due to underlying liver disease or because of the delayed time-to-endoscopy. Finally, both studies analyzed the door-to-endoscopy time as a continuous variable, and therefore showed results that were not significant.

In our study, to overcome these limitations, we conducted IPW for baseline correction and analyzed "door-to-scope" time as a 12-h categorical variable according to the existing guidelines. Considering the degree to which the various factors that influence the timing of endoscopy may impact the clinical outcomes, it was essential to conduct the IPW. In fact, clinicians tend to perform endoscopy more quickly if the patient shows unstable features, and in this situation, the effect of endoscopy on survival is likely to be underestimated.

So, when is the appropriate time to do endoscopy in variceal bleeding? Research to date shows it is more complicated than just "the sooner the better". In the Taiwan study, the authors divided endoscopic timing into several stages, but they failed to prove "the sooner, the better" concept[9]. Although we have not described it in this study, we analyzed the results of a door-to-endoscopy time of 6 h, but we failed to demonstrate a benefit with more urgent endoscopy. It seems that timing of endoscopy and clinical outcomes, including mortality, shows a non-linear correlation. For example, in peptic ulcer bleeding patients, the correlation between the timing of endoscopy and clinical outcomes is *U*-shaped, and we consider it likely to be similar in variceal bleeding patients[24]. This phenomenon is believed to be due to the fact that basic resuscitation (*e.g.*, adequate hydration, antibiotics) influences the patient's outcome in the early stages of treatment[4,5,25]. If the patient is transported too early in order to undergo an endoscopic procedure, it may interfere with basic resuscitation during the critical early period of management, leading to a bad prognosis. Also, if the endoscopy is performed too soon, the quality of endoscopic examination may be suboptimal, due to poor preparation. In clinical practice, we sometimes find that delayed endoscopy, after using vasoactive drugs, is actually faster and safer.

In our study, the median door-to-endoscopy time in the non-urgent group was 19.5 h which was much longer than the recommended time. Although most guidelines recommend that endoscopy should be performed within 12 h of presentation, various clinical and facility factors may hamper guideline implementation in the real clinical settings[4,5,26,27]. To overcome these baseline imbalances, we used IPW method. After IPW, there were no significant differences in the short-term outcomes between two groups.

When it comes to studies of endoscopy, it is important to consider the selection of appropriate outcomes. Previous studies have focused primarily on long-term prognosis, such as overall survival or all-cause mortality. These studies have failed to show a reduction in mortality in urgent endoscopy. However, since the long-term prognosis of patients with variceal bleeding is mainly related to their basal liver function, it is unreasonable to associate a single-point endoscopy with a long-term prognosis. Indeed, in our data and in the Canadian studies, the most common cause of death was liver cirrhosis, not the bleeding itself (Supplementary Table 2). For this reason, unlike other studies, in our study we changed the endpoint to overall survival at 6 wk or TFS at 6 ws. We consider short-term outcomes to be more appropriate than long-term outcomes in demonstrating the precise effect of endoscopic timing on prognosis. In fact, the Barveno guideline recommends 6-wk mortality rather than OS as an outcome[5].

Consistent with previous reports, the length of hospital stay was statistically different between the urgent group and non-urgent group[10,28-30]. It may be due to more accurate diagnosis and earlier hemostasis of the bleeding source by urgent endoscopy, leading to decrease in the subsequent resource use including the length of stay and total hospitalization costs.

There are some limitations to our study. First, as with other studies, our study may be confounded by unmeasured factors because of its retrospective design. Clearly there are ethical difficulties in enrolling acute variceal bleeding patients into RCTs; nevertheless retrospective studies can be of benefit in providing reliable and practical information. Second, where there is no weekend rounder, the results of this study may be difficult to apply. Another issue to consider is that previous research refers to geographic variability in prognosis of UGIB patients.

In conclusion, we demonstrated that endoscopic timing may not affect the clinical outcomes of patients with esophageal variceal bleeding, especially in short-term outcomes. Therefore it is necessary to perform endoscopy at an appropriate time, depending on each patient's condition. A prospective study, or a meta-analysis involving a greater number of centers in different countries, will assist in establishing a more accurate optimal timing for endoscopy.

ARTICLE HIGHLIGHTS

Research background

The optimal timing of emergency endoscopy in acute variceal bleeding remains unclear. Most guidelines recommend performing endoscopy for acute variceal bleeding within 12 h of admission. However, the evidence level for this recommendation is very low, with few relevant studies to date to justify it

Research motivation

Determining the appropriate endoscopic timing is a very important issue, and

both the risk and benefit to the patient need to be considered. We hypothesized that the earlier the endoscopy was performed, the better the short-term prognosis of the cirrhotic patients with variceal bleeding.

Research objectives

The aim of this study was to examine the association between the timing of endoscopy and the short-term prognosis of acute variceal bleeding in cirrhotic patients.

Research methods

We performed a retrospective study of cirrhotic patients with variceal bleeding. Patients were divided into two groups according to the time of endoscopy. Urgent endoscopy group was defined as performing endoscopy before 12 h of admission and non-urgent endoscopy group after 12 h of admission. The inverse probability weighting (IPW) method based on propensity score was applied to correct baseline differences between the two groups, and compared short-term prognosis between the two groups.

Research results

In 274 patients, 173 patients received urgent endoscopy, and 101 patients received non-urgent endoscopy. After IPW method, short term prognosis including 6-wk mortality rate or 6-wk transplantation rate was not different between the two groups. In multivariate analyses, timing of endoscopy was not associated with 6-wk mortality. Other factors associated with 6-wk mortality were age, hepatocellular carcinoma, MELD score, and degree of ascites.

Research conclusions

Timing of endoscopy may not affect the clinical short-term outcomes of patients with esophageal variceal bleeding.

Research perspectives

Because this is a retrospective study, a prospective study to determine the appropriate timing of endoscopy considering risk and benefit is needed for the future.

REFERENCES

1 **Garcia-Tsao G**, Sanyal AJ, Grace ND, Carey WD; Practice Guidelines Committee of American Association for Study of Liver Diseases; Practice Parameters Committee of American College of Gastroenterology. Prevention and management of gastroesophageal varices and variceal hemorrhage in cirrhosis. *Am J Gastroenterol* 2007; **102**: 2086-2102 [PMID: 17727436 DOI: 10.1111/j.1572-0241.2007.01481.x]

2 **Villanueva C**, Piqueras M, Aracil C, Gómez C, López-Balaguer JM, Gonzalez B, Gallego A, Torras X, Soriano G, Sáinz S, Benito S, Balanzó J. A randomized controlled trial comparing ligation and sclerotherapy as emergency endoscopic treatment added to somatostatin in acute variceal bleeding. *J Hepatol* 2006; **45**: 560-567 [PMID: 16904224 DOI: 10.1016/j.jhep.2006.05.016]

3 **Abraldes JG**, Villanueva C, Bañares R, Aracil C, Catalina MV, Garci A-Pagán JC, Bosch J; Spanish Cooperative Group for Portal Hypertension and Variceal Bleeding. Hepatic venous pressure gradient and prognosis in patients with acute variceal bleeding treated with pharmacologic and endoscopic therapy. *J Hepatol* 2008; **48**: 229-236 [PMID: 18093686 DOI: 10.1016/j.jhep.2007.10.008]

4 **Garcia-Tsao G**, Abraldes JG, Berzigotti A, Bosch J. Portal hypertensive bleeding in cirrhosis: Risk stratification, diagnosis, and management: 2016 practice guidance by the American Association for the study of liver diseases. *Hepatology* 2017; **65**: 310-335 [PMID: 27786365 DOI: 10.1002/hep.28906]

5 **de Franchis R**, Baveno VI Faculty. Expanding consensus in portal hypertension: Report of the Baveno VI Consensus Workshop: Stratifying risk and individualizing care for portal hypertension. *J Hepatol* 2015; **63**: 743-752 [PMID: 26047908 DOI: 10.1016/j.jhep.2015.05.022]

6 **Seo YS**. Prevention and management of gastroesophageal varices. *Clin Mol Hepatol* 2018; **24**: 20-42 [PMID: 29249128 DOI: 10.3350/cmh.2017.0064]

7 **Cheung J**, Wong W, Zandieh I, Leung Y, Lee SS, Ramji A, Yoshida EM. Acute management and secondary prophylaxis of esophageal variceal bleeding: a western Canadian survey. *Can J Gastroenterol* 2006; **20**: 531-534 [PMID: 16955150 DOI: 10.1155/2006/203217]

8 **Cheung J**, Soo I, Bastiampillai R, Zhu Q, Ma M. Urgent vs. non-urgent endoscopy in stable acute variceal bleeding. *Am J Gastroenterol* 2009; **104**: 1125-1129 [PMID: 19337243 DOI: 10.1038/ajg.2009.78]

9 **Hsu YC**, Chung CS, Tseng CH, Lin TL, Liou JM, Wu MS, Hu FC, Wang HP. Delayed endoscopy as a risk factor for in-hospital mortality in cirrhotic patients with acute variceal hemorrhage. *J Gastroenterol Hepatol* 2009; **24**: 1294-1299 [PMID: 19682197 DOI: 10.1111/j.1440-1746.2009.05903.x]

10 **Lee JG**, Turnipseed S, Romano PS, Vigil H, Azari R, Melnikoff N, Hsu R, Kirk D, Sokolove P, Leung JW. Endoscopy-based triage significantly reduces hospitalization rates and costs of treating upper GI bleeding: a randomized controlled trial. *Gastrointest Endosc* 1999; **50**: 755-761 [PMID: 10570332 DOI: 10.1016/S0016-5107(99)70154-9]

11 **Schacher GM**, Lesbros-Pantoflickova D, Ortner MA, Wasserfallen JB, Blum AL, Dorta G. Is early endoscopy in the emergency room beneficial in patients with bleeding peptic ulcer? A "fortuitously controlled" study. *Endoscopy* 2005; **37**: 324-328 [PMID: 15824941 DOI: 10.1055/s-2004-826237]

12 **Rockall TA**, Logan RF, Devlin HB, Northfield TC. Risk assessment after acute upper gastrointestinal haemorrhage. *Gut* 1996; **38**: 316-321 [PMID: 8675081 DOI: 10.1136/gut.38.3.316]

13 **Blatchford O**, Murray WR, Blatchford M. A risk score to predict need for treatment for upper-gastrointestinal haemorrhage. *Lancet* 2000; **356**: 1318-1321 [PMID: 11073021 DOI: 10.1016/S0140-6736(00)02816-6]

14 **Kumar NL**, Cohen AJ, Nayor J, Claggett BL, Saltzman JR. Timing of upper endoscopy influences outcomes in patients with acute nonvariceal upper GI bleeding. *Gastrointest Endosc* 2017; **85**: 945-952.e1 [PMID: 27693643 DOI: 10.1016/j.gie.2016.09.029]

15 **Hart A**. Mann-Whitney test is not just a test of medians: differences in spread can be important. *BMJ* 2001; **323**: 391-393 [PMID: 11509435 DOI: 10.1136/bmj.323.7309.391]

16 **Thabut D**, Bernard-Chabert B. Management of acute bleeding from portal hypertension. *Best Pract Res Clin Gastroenterol* 2007; **21**: 19-29 [PMID: 17223494 DOI: 10.1016/j.bpg.2006.07.010]

17 **Escorsell A**, Ruiz del Arbol L, Planas R, Albillos A, Bañares R, Calès P, Pateron D, Bernard B, Vinel JP, Bosch J. Multicenter randomized controlled trial of terlipressin versus sclerotherapy in the treatment of acute variceal bleeding: the TEST study. *Hepatology* 2000; **32**: 471-476 [PMID: 10960437 DOI: 10.1053/jhep.2000.16601]

18 **Escorsell A**, Bordas JM, del Arbol LR, Jaramillo JL, Planas R, Bañares R, Albillos A, Bosch J. Randomized controlled trial of sclerotherapy versus somatostatin infusion in the prevention of early rebleeding following acute variceal hemorrhage in patients with cirrhosis. Variceal Bleeding Study Group. *J Hepatol* 1998; **29**: 779-788 [PMID: 9833916 DOI: 10.1016/S0168-8278(98)80259-6]

19 **D'Amico G**, Pagliaro L, Pietrosi G, Tarantino I. Emergency sclerotherapy versus vasoactive drugs for bleeding oesophageal varices in cirrhotic patients. *Cochrane Database Syst Rev* 2010; CD002233 [PMID: 20238318 DOI: 10.1002/14651858.CD002233.pub2]

20 **Cremers I**, Ribeiro S. Management of variceal and nonvariceal upper gastrointestinal bleeding in patients with cirrhosis. *Therap Adv Gastroenterol* 2014; **7**: 206-216 [PMID: 25177367 DOI: 10.1177/1756283X14538688]

21 **Dai C**, Liu WX, Jiang M, Sun MJ. Endoscopic variceal ligation compared with endoscopic injection sclerotherapy for treatment of esophageal variceal hemorrhage: a meta-analysis. *World J Gastroenterol* 2015; **21**: 2534-2541 [PMID: 25741164 DOI: 10.3748/wjg.v21.i8.2534]

22 **Augustin S**, González A, Genescà J. Acute esophageal variceal bleeding: Current strategies and new perspectives. *World J Hepatol* 2010; **2**: 261-274 [PMID: 21161008 DOI: 10.4254/wjh.v2.i7.261]

23 **Sung JJ**, Chung SC, Yung MY, Lai CW, Lau JY, Lee YT, Leung VK, Li MK, Li AK. Prospective randomised study of effect of octreotide on rebleeding from oesophageal varices after endoscopic ligation.

Lancet 1995; **346**: 1666-1669 [PMID: 8551824 DOI: 10.1016/S0140-6736(95)92840-5]
24 **Laursen SB**, Leontiadis GI, Stanley AJ, Møller MH, Hansen JM, Schaffalitzky de Muckadell OB. Relationship between timing of endoscopy and mortality in patients with peptic ulcer bleeding: a nationwide cohort study. *Gastrointest Endosc* 2017; **85**: 936-944.e3 [PMID: 27623102 DOI: 10.1016/j.gie.2016.08.049]
25 **Bernard B**, Grangé JD, Khac EN, Amiot X, Opolon P, Poynard T. Antibiotic prophylaxis for the prevention of bacterial infections in cirrhotic patients with gastrointestinal bleeding: a meta-analysis. *Hepatology* 1999; **29**: 1655-1661 [PMID: 10347104 DOI: 10.1002/hep.510290608]
26 **European Association for the Study of the Liver**. EASL Clinical Practice Guidelines for the management of patients with decompensated cirrhosis. *J Hepatol* 2018; **69**: 406-460 [PMID: 29653741 DOI: 10.1016/j.jhep.2018.03.024]
27 **Sarin SK**, Kumar A, Angus PW, Baijal SS, Chawla YK, Dhiman RK, Janaka de Silva H, Hamid S, Hirota S, Hou MC, Jafri W, Khan M, Lesmana LA, Lui HF, Malhotra V, Maruyama H, Mazumder DG, Omata M, Poddar U, Puri AS, Sharma P, Qureshi H, Raza RM, Sahni P, Sakhuja P, Salih M, Santra A, Sharma BC, Shah HA, Shiha G, Sollano J; APASL Working Party on Portal Hypertension. Primary prophylaxis of gastroesophageal variceal bleeding: consensus recommendations of the Asian Pacific Association for the Study of the Liver. *Hepatol Int* 2008; **2**: 429-439 [PMID: 19669318 DOI: 10.1007/s12072-008-9096-8]
28 **Cooper GS**, Chak A, Way LE, Hammar PJ, Harper DL, Rosenthal GE. Early endoscopy in upper gastrointestinal hemorrhage: associations with recurrent bleeding, surgery, and length of hospital stay. *Gastrointest Endosc* 1999; **49**: 145-152 [PMID: 9925690 DOI: 10.1016/S0016-5107(99)70478-5]
29 **Cooper GS**, Kou TD, Wong RC. Use and impact of early endoscopy in elderly patients with peptic ulcer hemorrhage: a population-based analysis. *Gastrointest Endosc* 2009; **70**: 229-235 [PMID: 19329112 DOI: 10.1016/j.gie.2008.10.052]
30 **Lim LG**, Ho KY, Chan YH, Teoh PL, Khor CJ, Lim LL, Rajnakova A, Ong TZ, Yeoh KG. Urgent endoscopy is associated with lower mortality in high-risk but not low-risk nonvariceal upper gastrointestinal bleeding. *Endoscopy* 2011; **43**: 300-306 [PMID: 21360421 DOI: 10.1055/s-0030-1256110]

P- Reviewer: Cholongitas E, Karatapanis S, Stanciu C
S- Editor: Wang XJ **L- Editor**: A **E- Editor**: Yin SY

World Journal of Gastroenterology

Submit a Manuscript: http://www.f6publishing.com

World J Gastroenterol 2018 November 28; 24(44): 5034-5045

DOI: 10.3748/wjg.v24.i44.5034

ISSN 1007-9327 (print) ISSN 2219-2840 (online)

ORIGINAL ARTICLE

Retrospective Cohort Study

Risk factors and prediction score for chronic pancreatitis: A nationwide population-based cohort study

Yen-Chih Lin, Chew-Teng Kor, Wei-Wen Su, Yu-Chun Hsu

Yen-Chih Lin, Wei-Wen Su, Yu-Chun Hsu, Division of Gastroenterology, Department of Internal Medicine, Changhua Christian Hospital, Changhua 50006, Taiwan

Chew-Teng Kor, Internal Medicine Research Center, Changhua Christian Hospital, Changhua 50006, Taiwan

ORCID number: Yen-Chih Lin (0000-0001-7094-1170); Chew-Teng Kor (0000-0002-0285-243X); Wei-Wen Su (0000-0001-5554-5938); Yu-Chun Hsu (0000-0002-0714-2250).

Author contributions: All the authors solely contributed to this paper.

Institutional review board statement: The study was reviewed and approved for publication by our Institutional Reviewer.

Informed consent statement: The data of our study cohort was obtained retrospectively from the Taiwan National Health Insurance Research Database, hence informed consent statement is unnecessary.

Conflict-of-interest statement: All the Authors have no conflict of interest related to the manuscript.

Data sharing statement: The original anonymous dataset is available on request from the corresponding author at 144315@cch.org.tw

STROBE statement: The authors have read the STROBE Statement-checklist of items, and the manuscript was prepared and revised according to the STROBE Statement-checklist of items.

Manuscript source: Unsolicited manuscript

Corresponding author to: Yen-Chih Lin, MD, Attending Doctor, Division of Gastroenterology, Department of Internal Medicine, Changhua Christian Hospital, No.135 Nanhsiao Street, Changhua 50006, Taiwan. 144315@cch.org.tw
Telephone: +886-4-7238595
Fax: +886-4-7232942

Received: September 8, 2018
Peer-review started: September 10, 2018
First decision: October 24, 2018
Revised: October 29, 2018
Accepted: November 9, 2018
Article in press: November 9, 2018
Published online: November 28, 2018

Abstract

AIM

To explore the risk factors of developing chronic pancreatitis (CP) in patients with acute pancreatitis (AP) and develop a prediction score for CP.

METHODS

Using the National Health Insurance Research Database in Taiwan, we obtained large, population-based data of 5971 eligible patients diagnosed with AP from 2000 to 2013. After excluding patients with obstructive pancreatitis and biliary pancreatitis and those with a follow-up period of less than 1 year, we conducted a multivariate analysis using the data of 3739 patients to identify the risk factors of CP and subsequently develop a scoring system that could predict the development of CP in patients with AP. In addition, we validated the scoring system using a validation cohort.

RESULTS

Among the study subjects, 142 patients (12.98%) devel-

oped CP among patients with RAP. On the other hand, only 32 patients (1.21%) developed CP among patients with only one episode of AP. The multivariate analysis revealed that the presence of recurrent AP (RAP), alcoholism, smoking habit, and age of onset of < 55 years were the four important risk factors for CP. We developed a scoring system (risk score 1 and risk score 2) from the derivation cohort by classifying the patients into low-risk, moderate-risk, and high-risk categories based on similar magnitudes of hazard and validated the performance using another validation cohort. Using the prediction score model, the area under the curve (AUC) [95% confidence interval (CI)] in predicting the 5-year CP incidence in risk score 1 (without the number of AP episodes) was 0.83 (0.79, 0.87), whereas the AUC (95%CI) in risk score 2 (including the number of AP episodes) was 0.84 (0.80, 0.88). This result demonstrated that the risk score 2 has somewhat better prediction performance than risk score 1. However, both of them had similar performance between the derivation and validation cohorts.

CONCLUSION

In the study,we identified the risk factors of CP and developed a prediction score model for CP.

Key words: Chronic pancreatitis; Acute pancreatitis; Prediction score; Endoscopic ultrasound; Recurrent acute pancreatitis

Core tip: In this large number, nationwide population-based cohort study, we concluded that the presence of recurrent acute pancreatitis (RAP), along with alcohol consumption, age of onset, and smoking habit are 4 important risk factors of chronic pancreatitis (CP). We developed a novel prediction score model for CP with excellent discrimination and successfully validated this model in our study. Using this scoring system, a clinician can predict the outcome of a patient with AP episode easily and arrange further examination such as pancreatic functional test or endoscopic ultrasound after the acute stage for the high-risk category to diagnose CP as early as possible (incidence rate of CP about 31 per 1000 person-years in high-risk group, based on our study) since CP is an important risk factor of pancreatic cancer.

Lin YC, Kor CT, Su WW, Hsu YC. Risk factors and prediction score for chronic pancreatitis: A nationwide population-based cohort study. *World J Gastroenterol* 2018; 24(44): 5034-5045 Available from: URL: http://www.wjgnet.com/1007-9327/full/v24/i44/5034.htm DOI: http://dx.doi.org/10.3748/wjg.v24.i44.5034

INTRODUCTION

Acute pancreatitis (AP) and chronic pancreatitis (CP) are common diseases with a worldwide prevalence. These diseases have become an important public health issue in several countries because of the high mortality rates and a considerable burden being laid on the healthcare system. AP is an inflammatory condition of the pancreas that has been considered as a self-limiting disease, with an incidence ranging from 5 to 10 per 100000 to 70-80 per 100000 in western countries, which appears to have increased in recent years[1]. In contrast, CP involves a persistent destructive, inflammatory process that eventually leads to an irreversible damage to the endocrine and exocrine functions of the pancreas, and the subsequent development of diabetes mellitus and frequent hospitalizations have become one of the burdens of public health. CP has a poor prognosis, with the mortality rate being approximately two-fold higher than that in the general population. Furthermore, a worldwide epidemiological survey conducted in 1993 revealed that the standardized incidence rate of pancreatic cancer is as high as 26-fold in patients with CP, suggesting that the risk of pancreatic cancer is significantly higher in subjects with CP[2].

An emerging consensus is that AP and CP are a continuum of diseases, and the intermediate stage between them is recurrent AP (RAP)[3]. Several studies have discussed about the natural course of pancreatitis as well as the risk factors and protective factors that contribute to the transition from AP to RAP and CP, although the majority of them have been conducted in western countries[3,4]. The major risk factors for CP include smoking, in addition to alcohol consumption. Moreover, it has been reported that cigarette smoking accelerates the progression of alcoholic CP[5,6]. Furthermore, a recent study has revealed that alcohol consumption of > 13.5 g/d and cigarette use of > 5.5 cigarettes/d are associated with the development of CP[7]. Because only a small proportion of patients with AP progress to CP, and CP has been proven to be an important risk factor of pancreatic duct adenocarcinoma (PDAC), it is critical to predict the development of CP in a patient with AP. However, till date, no prediction scores for CP have been addressed in the English literature, although there were some prognosis scores for CP and AP[8,9]. Therefore, in this population-based, large-scale cohort study, we developed and validated a scoring system for predicting CP using data from the National Health Insurance Research Database (NHIRD) in Taiwan.

MATERIALS AND METHODS

Data source

We obtained data from the Taiwan NHIRD. The NHIRD is one of the most comprehensive databases in the world and includes all claims data from the National Health Insurance program, such as demographic data, number of ambulatory cases, records of clinic visits, hospital admissions, dental services, prescriptions, and disease status. The National Health Insurance program, which

was initiated by the government of Taiwan in March 1995, covers > 99% of the total population or approximately 23 million people. Diagnostic codes used in the NHIRD for identifying diseases are based on the International Classification of Diseases, Ninth Revision, Clinical Modification (ICD-9-CM), which has been proven to be highly accurate and valid[10-12]. This study was exempted from full review and was approved by the Institutional Review Board of the Changhua Christian Hospital (approval number: 171112).

Study population

A total of 5971 patients with one or more episodes of AP (ICD-9-CM code 577.0) recorded in the inpatient claims data from 2000 to 2013 were identified from the database. A 4-year look-back period was applied from 1996 to 1999 to ensure that all cases in our cohort were newly diagnosed and to reduce false incident cases. Patients with a previous diagnosis of AP during the look-back period were excluded. Patients who had CP before the index date, those aged < 18 or > 100 years, those with a follow-up duration of < 1 year, and those with biliary pancreatitis or obstructive pancreatitis[13] (such as pancreatic cancer and pancreas divisum) were also excluded because these patients rarely progress to CP. Accordingly, 3739 patients with nonobstructive, nonbiliary AP were identified for subsequent analysis. Next, we developed a model to predict the progress to CP in randomly selected two-thirds of this cohort (derivation cohort) and validated the model in the remaining one-third of this cohort (validation cohort).

Outcome measures and relevant variables

Outcomes and comorbidities were identified based on ICD-9-CM codes. CP was defined using ICD-9-CM codes (ICD-9-CM code 577.1).

To avoid over-estimation of CP by ICD-9-CM coding alone,we excluded all patients without abdominal computed tomography (CT) or abdominal magnetic resonance imaging (MRI) performed within 3 mo before the diagnosis of CP.

Patients were followed up from the index date (*i.e.*, the date of first AP diagnosis) to the date when they withdrew from the insurance program or to the end of 2013. Major comorbid diseases diagnosed before the index date were defined as baseline comorbidities based on claims data. These comorbidities included obesity, hypertension, hyperlipidemia, diabetes mellitus, alcoholism [alcohol use-related codes: ICD-9-CM codes 291, 303, 305.0, 357.5, 571.0, 571.1, 571.2, and 790.3 (V11.3)], smoking habit (smoking-related codes: ICD-9-CM 305.1, V15.82, 491, 492, 493, and 496), and chronic kidney disease. If the patients with AP enrolled in our study have drinking-related coding or smoking-related coding during their follow-up period after the first AP episode, we considered them have drinking or smoking habit. To evaluate the effects of socioeconomic factors on disease development, monthly income, and place of residence of patients were recorded. To quantify baseline comorbidities, Charlson's comorbidity index (CCI) score was used. The history of long-term use of medications that have been reported as possible risk factors for AP, including statins, angiotensin-converting enzyme inhibitors, prednisolone, hydrochlorothiazide, sex hormones, and metformin, was also evaluated.

Statistical analysis

Demographic and clinical characteristics of the study patients are summarized as proportions and mean ± standard derivation (SD) values. The chi-square test and the *t* test were used to compare the distributions of discrete and continuous variables, respectively. The risk of CP in patients with nonobstructive, nonbiliary AP was estimated using the Cox proportional hazards model. Variables in the Cox model included the presence of RAP or the number of episodes of AP, smoking, alcohol consumption, age, gender, all comorbidities, CCI scores, and long-term use of medications. The significant β coefficients from the Cox model with backward selection procedure were used to construct an integer-based risk score for stratifying the risk of progress to CP. The referent for each variable was assigned a value of 0, and the coefficients for the other variables were calculated by dividing by the smallest coefficient in the model and then rounding to the nearest integer. Individual scores were assigned by summing the individual risk factor scores, and the cumulative incidence rate of each risk score was calculated. For easy application in clinical practice, the total risk scores were classified into low-risk category, moderate-risk category, and high-risk category based on similar magnitudes of hazard.

Within the derivation cohort, the discrimination was assessed using the time-dependent area under the receiver operating characteristic (ROC) curve. The internal validation of this risk score was conducted by 1000 bootstrap simulations. The bootstrap simulations in the derivation cohort were carried out by sampling with replacement for 1000 iterations. Each bootstrap sample was of the same size as the derivation cohort, the computed risk score, and the generated area under the ROC. Furthermore, we validated the risk score externally using the remaining one-third of the random sample. The risk score model was applied, and the discrimination was assessed by a time-dependent ROC curve analysis.

All statistical analyses were performed using SAS 9.4 software (SAS Institute Inc., Cary, NC, United States). Two-tailed *P* values of < 0.05 were considered to be statistically significant.

RESULTS

Characteristics of the study population

The flowchart depicted in Figure 1 describes the patient selection process, while Table 1 shows the characteristics of the study patients. A total of 3739 patients were identified as newly diagnosed nonobstructive, nonbiliary

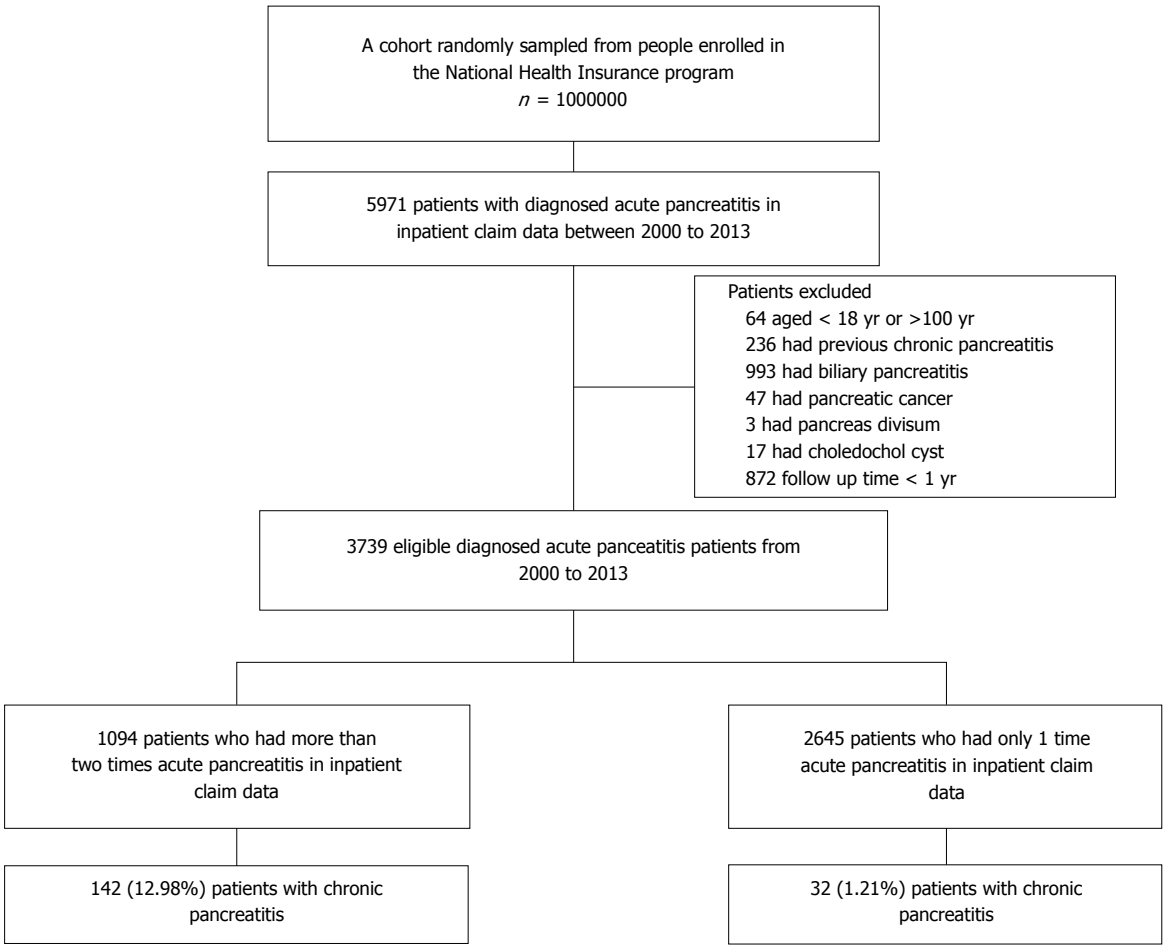

Figure 1 Flowchart of patient selection process.

AP cases. Among these patients, 174 (4.65%) developed CP during the mean follow-up period of 6.13 ± 3.53 years. The mean age at the first onset of nonbiliary, nonobstructive AP was 53.04 ± 17.00 years. In addition, according to the inpatient claims data, 1094 patients had more than one episode of nonbiliary, nonobstructive AP, whereas 2645 patients had only one episode of disease attack. Regarding the behavior-related variables, 21.56% and 33.73% of patients had alcohol-use-related codes and smoking-related codes, respectively. After a random sampling, the derivationcohort consisted of 2493 patients, and the validation cohort consisted of 1246 patients, and the baseline characteristics and demographic variables were comparable between both cohorts (Table 1). The prevalence of CP was similar between the derivation and validation cohorts, at 113 (4.53%) and 61 (4.90%), respectively (Table 1).

Risk score construction for predicting CP

Table 2 shows the results of the multivariate Cox proportional hazard analysis. From the Cox model, four variables, including smoking habit, age < 55 years, alcohol consumption, and RAP/number of episodes of AP, were associated with risks of CP (all $P < 0.05$). Due to the insignificance associated with the risk of CP, comorbidities and history of medication use were excluded from the final model after performing a backward elimination procedure. The risk score based on these factors was constructed as shown in Table 3. Two scoring systems, namely risk score 1 and risk score 2, were separately developed based on the presence or absence of RAP (point 5 if RAP is present) or the number of AP episodes (point 4 for two episodes, point 5 for three episodes, and point 7 for more than three episodes), as well as alcohol-use-related codes (point 3), age < 55 years (point 2), and smoking-related codes (point 1).

Personalized risk prediction

The total score for each patient was calculated by summing each risk factor point. The risk scores 1 and 2 ranged between 0-11 and 0-13, respectively (Table 3). Figure 2 shows the time-dependent ROC curve assessing the discrimination for predicting CP using the risk score at different endpoints of time. The risk score 1 had excellent discrimination for predicting the 3-year, 5-year, and overall time period CP incidence, with the area under the ROC curve of 0.84, 0.84, and 0.79, respectively. The 95% confidence intervals (CIs) yielded by the 1000 bootstrap simulation validation were 0.80-0.88, 0.81-0.87, and 0.75-0.83, respectively (Figure 2A-C, solid line). The risk score 2 also had excellent discrimination for predicting the 3-year, 5-year, and

Table 1 Demographic characteristics of 3739 patients *n* (%)

	Total	Derivationcohort	Validation cohort	*P* value
Sample size	3739	2493	1246	
Age, yr	53.04 ± 17	52.98 ± 17.08	53.18 ± 16.84	0.735
Gender, male	2400 (64.19)	1590 (63.78)	810 (65.01)	0.460
Monthly income, NTD	15423.5 ± 13018.5	15405.6 ± 13071.9	15459.1 ± 12916.2	0.906
Geographic location				
Northern Taiwan	1619 (43.3)	1085 (43.52)	534 (42.86)	0.725
Central Taiwan	780 (20.86)	518 (20.78)	262 (21.03)	0.893
Southern Taiwan	1183 (31.64)	790 (31.69)	393 (31.54)	0.957
Eastern Taiwan and Islands	157 (4.2)	100 (4.01)	57 (4.57)	0.470
Charlson's comorbidity index score	2.55 ± 2.21	2.56 ± 2.22	2.52 ± 2.19	0.574
Comorbidities				
Obesity	17 (0.45)	11 (0.44)	6 (0.48)	0.863
Hypertension	1456 (38.94)	984 (39.47)	472 (37.88)	0.348
Hyperlipidemia	1048 (28.03)	698 (28)	350 (28.09)	0.953
Diabetes mellitus	994 (26.58)	658 (26.39)	336 (26.97)	0.709
Chronic kidney disease	498 (13.32)	332 (13.32)	166 (13.32)	0.996
Alcohol use-related codes	806 (21.56)	533 (21.38)	273(21.91)	0.710
Smoking related codes	1261 (33.73)	849 (34.06)	412 (33.07)	0.546
Long-term medication use				
Statin	569 (15.22)	385 (15.44)	184 (14.77)	0.588
Angiotensin-converting enzyme inhibitor	472 (12.62)	327 (13.12)	145 (11.64)	0.199
Prednisolone	74 (1.98)	56 (2.25)	18 (1.44)	0.097
Hydrochlorothiazide	41 (1.1)	29 (1.16)	12 (0.96)	0.580
Sex hormone	180 (4.81)	129 (5.17)	51 (4.09)	0.145
Metformin	434 (11.61)	290 (11.63)	144 (11.56)	0.946
Number of episode RAP				
1	2645 (70.74)	1769 (70.96)	876 (70.3)	0.707
2	599 (16.02)	403 (16.17)	196 (15.73)	0.768
3	234 (6.26)	153 (6.14)	81 (6.5)	0.718
⩾ 4	261 (6.98)	168 (6.74)	93 (7.46)	0.452
Outcomes				
Chronic pancreatitis	174 (4.65)	113 (4.53)	61 (4.90)	0.619
Follow-up duration, yr	6.13 ± 3.53	6.12 ± 3.52	6.17 ± 3.57	0.685

RAP: Recurrent acute pancreatitis; NTD: New Taiwan Dollars.

overall time period CP incidence, with the area under the ROC curve of 0.85, 0.85, and 0.80, respectively. The 95%CIs yielded by the 1000 bootstrap simulation validation were 0.81-0.89, 0.82-0.88, and 0.75-0.84, respectively (Figure 2A-C, dashed line).

Risk stratification

As the risk score increased, the incidence rate as well as the hazard of CP increased (Supplementary Table 1). On the basis of similar magnitudes of hazard, the risk score 1 of 0-5 was classified as a low-risk category, the risk score 1 of 6-7 was classified as a moderate-risk category, and the risk score 1 of > 7 was classified as a high-risk category. Figure 3 presents the incidence rates for CP over the risk category. As demonstrated in Figure 3A, the incidence rates of CP using risk score 1 were 1.27, 7.89, and 31.37 per 1000 person-years for the low-, moderate-, and high-risk categories, respectively. The hazards of CP were 6.14 (3.05, 12.35) and 23.93 (13.4, 42.73) for the moderate- and high-risk categories, respectively (Supplementary Table 1 and Figure 4).

Similarly, the values of 0-5, 6-7, and 8-13 in risk score 2 (which includes the number of AP episodes) were classified as low-, moderate-, and high-risk categories, respectively. The incidence rates of CP were 1.30, 9.26, and 32.22 per 1000 person-years for the low-, moderate-, and high-risk categories, respectively (Figure 3B). The hazards of CP were 7.08 (3.54, 14.14) and 24.15 (13.76, 42.38) for the moderate- and high-risk categories, respectively (Figure 4).

Validation cohort

The validation cohort was used to test the risk scores. The risk scores were calculated for each patient in the validation cohort, and they were successfully classified as low-, moderate-, and high-risk categories according to the score stratifications in the derivation cohort. As the risk category increased, the incidence rate as well as the hazard of CP increased (Figures 3 and 4). The areas under the ROC curve in risk score 1 at 3-, 5-, and overall year were 0.81, 0.83, and 0.82, respectively. The 95%CIs yielded by the 1000 bootstrap resamplings were 0.76-0.86, 0.79-0.87, and 0.78-0.87, respectively (Figure 3D-F, solid line). In risk score 2, the areas under the ROC curve at 3-, 5-, and overall year were 0.82, 0.84, and 0.83, respectively. The 95%CIs were 0.77-0.87, 0.80-0.88, and 0.78-0.87, respectively (Figure 3D-F, dashed line). This result demonstrated that the risk score had similar performance between the derivation and

Table 2 Adjusted hazard ratio and 95% confidence interval for chronic pancreatitis associated with recurrent acute pancreatitis, smoking, comorbidities, and medication use

	Adjusted $HR^{full\ model}$ (95%CI)	*P* value	Adjusted $HR^{backward\ model}$ (95%CI)	*P* value	Adjusted $HR^{backward+episode}$ (95%CI)	*P* value
Smoking related codes	1.57 (1.07, 2.32)	0.022	1.53 (1.04, 2.25)	0.029	1.48 (1.01, 2.17)	0.047
RAP	8.96 (5.37, 14.93)	< 0.001	8.65 (5.2, 14.38)	< 0.001		
1 episode					1	
2 episode					5.03 (2.75, 9.22)	< 0.001
3 episode					8.47 (4.36, 16.45)	< 0.001
> 3 episode					15.64 (8.91, 27.47)	< 0.001
Geographic location						
Northern Taiwan	1					
Central Taiwan	0.53 (0.28, 0.99)	0.047				
Southern Taiwan	1.45 (0.94, 2.23)	0.090				
Eastern Taiwan and Islands	1.2 (0.57, 2.53)	0.626				
Age category						
Age < 55	2.67 (1.35, 5.29)	0.005	2.43 (1.31, 4.49)	0.005	2.04 (1.06, 3.93)	0.033
Age ⩾ 55	1		1		1	
Gender, male	1.31 (0.72, 2.41)	0.381				
Income	1.1 (0.86, 1.41)	0.440				
CCI	0.96 (0.84, 1.1)	0.576				
Hypertension	1.14 (0.7, 1.84)	0.601				
Hyperlipidemia	0.82 (0.5, 1.35)	0.435				
Diabetes mellitus	0.73 (0.39, 1.35)	0.314				
Chronic kidney disease	1.64 (0.79, 3.39)	0.181				
Alcohol use-related codes	3.06 (1.83, 5.12)	< 0.001	3.10 (1.96, 4.92)	< 0.001	2.66 (1.66, 4.25)	< 0.001
Statin	0.97 (0.43, 2.16)	0.937				
Angiotensin-converting enzyme inhibitor	1.05 (0.42, 2.63)	0.922				
Prednisolone	1.28 (0.28, 5.85)	0.751				
Sex hormone	1.64 (0.52, 5.2)	0.398				
Metformin	2.09 (0.83, 5.29)	0.120				

RAP: Recurrent acute pancreatitis; HR: Hazard ratio; CI: Confidence interval; CCI: Charlson's comorbidity index.

Table 3 Risk score for progression to chronic pancreatitis after acute pancreatitis

	Model coefficient	Risk factor point[1]
Risk Score 1		
Smoking related codes	0.43	1
Age of onset < 55	0.89	2
Alcohol use-related codes	1.13	3
RAP (present or not)	2.16	5
Risk Score 2		
Smoking related codes	0.39	1
Age of onset < 55	0.71	2
Alcohol use-related codes	0.98	3
Numbers of RAP		
2 episode	1.62	4
3 episode	2.14	5
> 3 episode	2.75	7
	Total	13

[1]Risk score was calculated by dividing each model coefficient by the smallest coefficient in the model and rounding the ratio to the integer. RAP: Recurrent acute pancreatitis.

validation cohorts.

DISCUSSION

In this study, we identified RAP, alcohol consumption, age of onset of < 55 years, and smoking habit as the four major risk factors for developing CP during the mean follow-up period of 6.13 ± 3.53 years in the setting of adult patients with episodes of nonbiliary, nonobstructive AP. To our knowledge, this is the first population-based, large-scale cohort study to explore the risk factors for CP in the Chinese ethnic population[14,15]. Furthermore, we developed the first prediction score model for CP, which is simple and useful in the clinical practice (Table 3).

The natural history of AP is still under debate, and the rate of progression from AP to CP varies and depends on the etiology of pancreatitis, with a mean interval of 3.5-5.5 years reported in the English literature[4,16-19]. In our population-based cohort study, the rate of progression from AP to CP was 4.65% during the mean follow-up period of 6.13 ± 3.53 years (Table 1). This prevalence is similar to that reported by a prospective study conducted in Germany, with the rate of progression from AP to CP occurring in approximately 4% of all patients during a 20-year period[4]. In our cohort, 12.8% (142/1094) of patients with RAP (nonobstructive, nonbiliary etiology) developed CP during the follow-up period, whereas only 1.2% (32/2645) of patients with only one episode of AP (nonobstructive, nonbiliary etiology) developed CP during the follow-up period (Figure 1). In a meta-analysis conducted in 2015 by Sankaran *et al*[3], it was observed 10% of patients with a first episode of AP and 36% of patients with RAP developed CP regardless of the etiology. In our study, the incidence of CP was much higher among patients who survived a second attack of

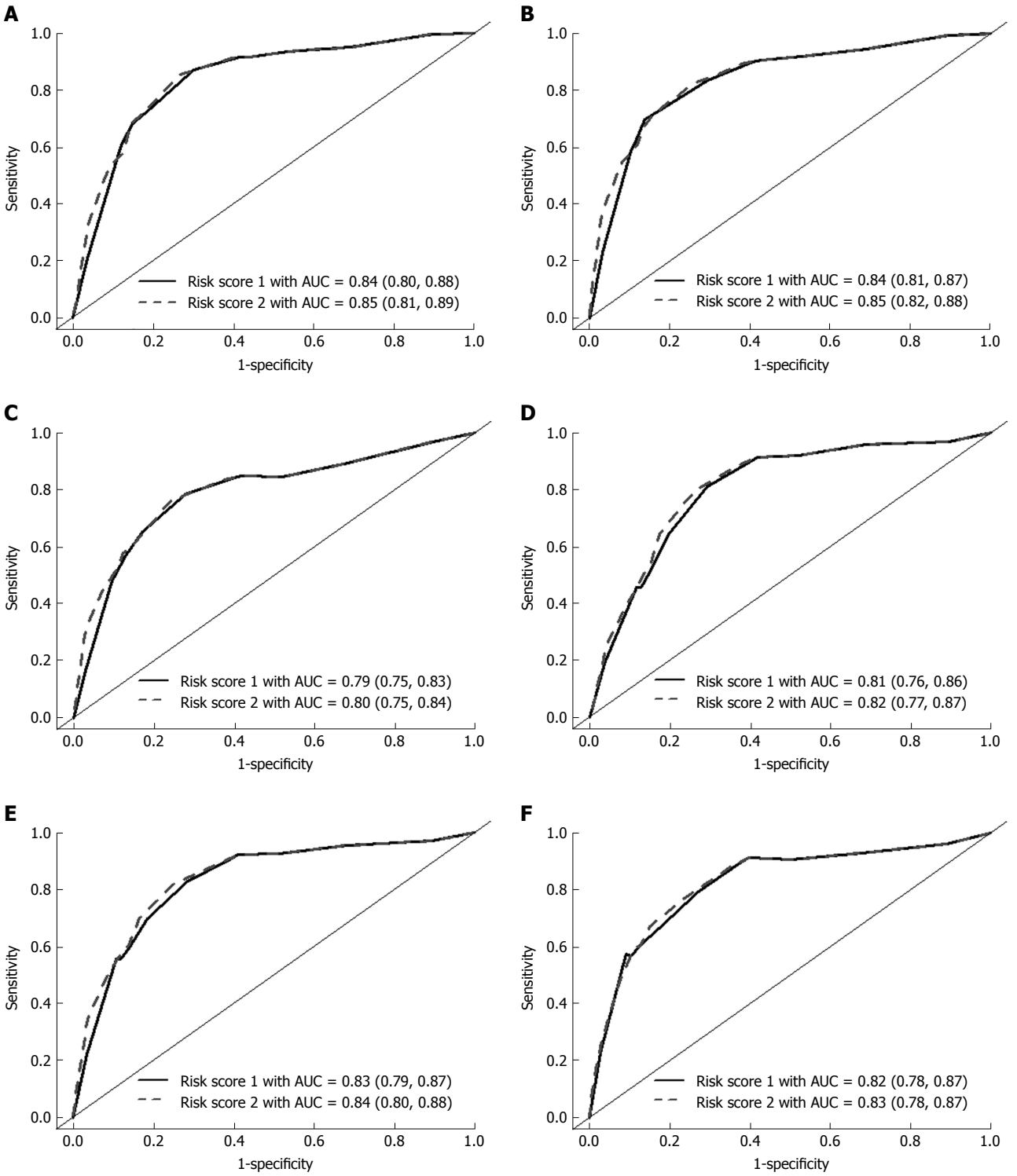

Figure 2 Area under the curve and 95% confidence interval at different time endpoints for risk score in derivation and validation cohorts. Data are presented as area under the curve (95% confidence interval). A: Discrimination of risk score 1 and risk score 2 for predicting 3-year chronic pancreatitis incidence in derivation cohort. B: Discrimination of risk score 1 and risk score 2 for predicting 5-year chronic pancreatitis incidence in derivation cohort. C: Discrimination of risk score 1 and risk score 2 for predicting overall chronic pancreatitis incidence in derivation cohort. D: Discrimination of risk score 1 and risk score 2 for predicting 3-year chronic pancreatitis incidence in validation cohort. E: Discrimination of risk score 1 and risk score 2 for predicting 5-year chronic pancreatitis incidence in validation cohort. F: Discrimination of risk score 1 and risk score 2 for predicting overall chronic pancreatitis incidence in validation cohort. AUC: Area under the curve; ROC: Receiver operating characteristic.

AP than among those with only one attack of AP (aHR: 8.65; 95%CI: 5.2-13.38; $P < 0.001$), consistent with several studies on Caucasians[3,4]

Our multivariate analysis revealed that the risk of progression to CP was higher among patients with RAP, alcoholics, smokers, and younger patients with age of onset of < 55 years, as assessed using alcohol-use-related codes and smoking-related codes as surrogates

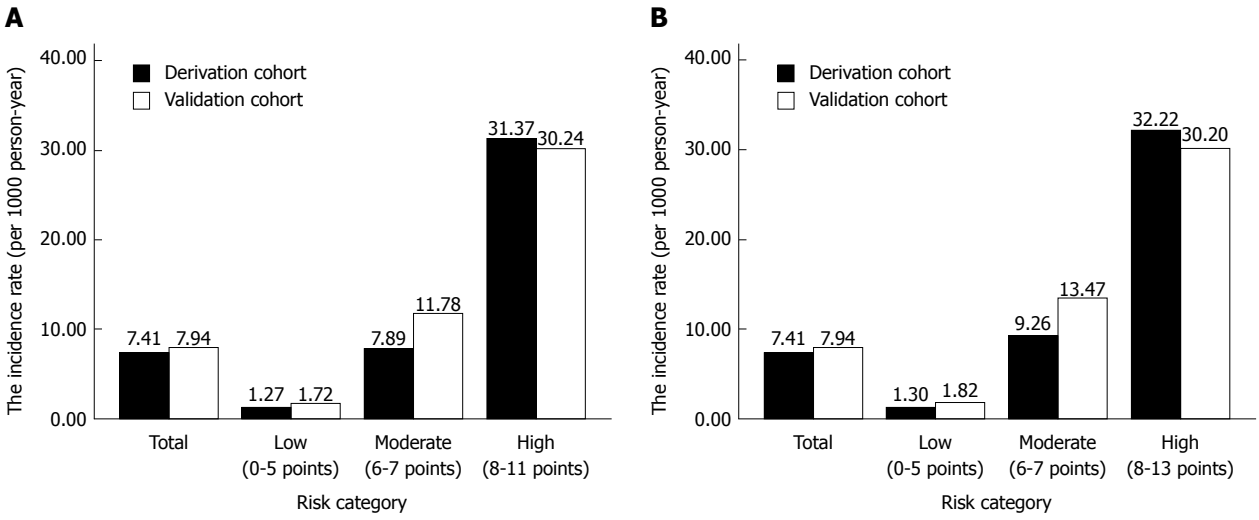

Figure 3 Risk category strata and associated chronic pancreatitis incidence rates in derivation and validation cohorts. A: Risk category strata and associated chronic pancreatitis incidence rates in derivation and validation cohorts, risk score 1. B: Risk category strata and associated chronic pancreatitis incidence rates in derivation and validation cohorts, risk score 2.

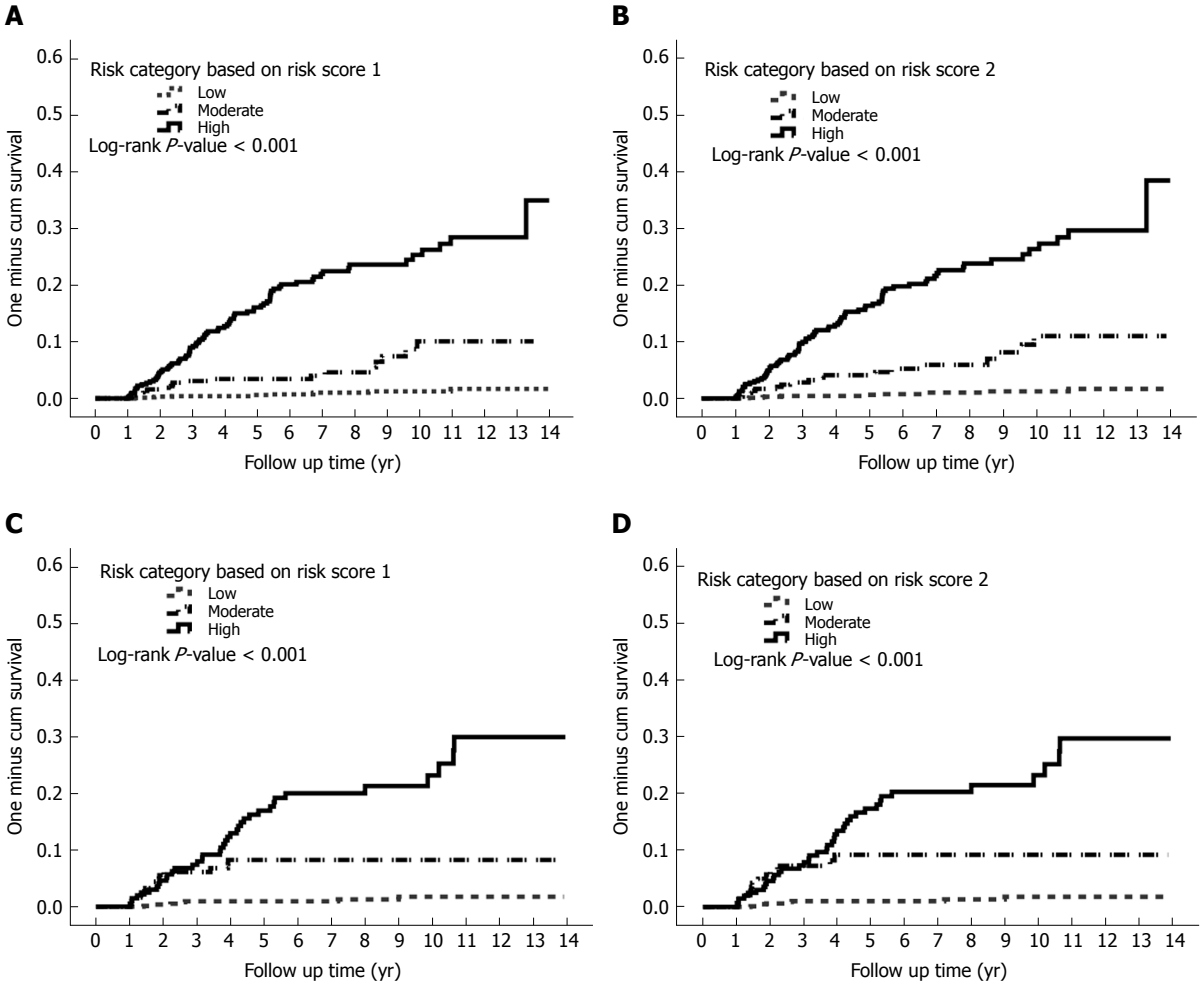

Figure 4 One minus Kaplan-Meier curve for chronic pancreatitis incidence for risk category in derivation and validation cohorts. A: One minus Kaplan-Meier curve for chronic pancreatitis for risk category based on risk score 1 in derivation cohort. B: One minus Kaplan-Meier curve for chronic pancreatitis for risk category based on risk score 2 in derivation cohort. C: One minus Kaplan-Meier curve for chronic pancreatitis for risk category based on risk score 1 in validation cohort. D: One minus Kaplan-Meier curve for chronic pancreatitis for risk category based on risk score 2 in validation cohort.

for alcohol consumption and smoking habit, respectively. Recently, a majority of physicians have recognized that smoking habit[5,20] is also an important risk factor for the development of CP along with RAP[3,4,18] and alcohol

consumption[21,22]. In our population-based cohort study, the multivariate analysis reconfirmed that in addition to alcohol consumption and RAP, cigarette smoking was an independent risk factor for CP also in the Chinese ethnic population (aHR: 1.53; 95%CI: 1.04-2.25; $P = 0.029$).

Patients with RAP were assigned the highest score in our prediction model (Table 3). Patients with RAP in our cohort may represent a susceptible population possessing gene mutations or unfavorable alleles of the *PRSS1, CFTR, SPINK1, CTRC, and CASR genes*, making them more susceptible to environmental factors such as exposure to alcohol or cigarette smoking[16,22-27]. Volker *et al*[16] have reported that an interaction between the environmental and genetic factors (*i.e.*, *N34S* + alcohol or *PRSS1* + smoking) further increased the probability of the development of CP. In addition, Polonikov *et al*[22] have shown that cigarette smokers with the -408CC genotype have an increased risk for AP [odds ratio (OR): 2.07], whereas nonsmoker carriers do not have the disease risk. Genetic risk factors are not rare among patients with CP, and approximately 25% of patients with CP exhibit some genetic risk factors[16]. We hypothesized that a proportion of patients with RAP possess some genetic disorders, and the interaction between genetic and environmental factors, such as a smoking habit and alcohol consumption, accelerates the progression of CP. Thus, although a majority of patients with genetic risk factors display a very slow progression of the natural disease course and always present with RAP in their early life[16], environmental factors such as cigarette smoking may trigger or accelerate the development of CP in the background of genetic disorders.

We found that the age of onset of < 55 years is one of the risk factors for developing CP in this study. In a cross-sectional study, younger age (OR: 0.80; 95%CI: 0.68-0.94) was found to be independently associated with an increased risk of developing recurrent pancreatitis[28]. In other words, that study demonstrated that age is a protective factor of recurrence. In a prospective study with a 30-year follow-up conducted by the Danish registries, it was observed that the risk of progression to CP decreased with increasing age in a dose-dependent manner with 2% less risk per year of age[29], suggesting that the age of onset is an important issue while evaluating the possibility of developing CP. Similar to our study cohort with an etiology of nonobstructive, nonbiliary pancreatitis, Peter layer *et al*[29] published an article on Gastroenterology that disclosed that patients with early-onset and late-onset idiopathic CP had a median age at onset of symptoms of 19 and 56 years, respectively, whereas the majority of patients with alcoholic CP had a median age of onset of 43.9 years, suggesting that most of the patients with nonobstructive, nonbiliary CP have the disease onset in their middle age. The result of that study is consistent with our finding that the age of onset of < 55 years is one of the risk factors for developing CP.

In general, CP involves a persistent destructive, inflammatory process that eventually leads to an "irreversible" damage to the endocrine and exocrine functions of the pancreas. In contrast, early CP is a disease entity that propagated in 2009, and it has been reported that the disease course could be reversed if adequate intervention is taken[30]. Using our prediction score model for CP, we were able to stratify our patients into different categories and arrange further examinations such as pancreatic functional test or endoscopic ultrasound after acute stage for the high-risk category (incidence rate of about 31 per 1000 person-years, based on our study) to detect CP[31] as early as possible and determine the optimal follow-up interval for the patients with AP with a nonbiliary, nonobstructive etiology.

Limitations of this study

First, the definition of the disease was based on ICD-9-CM codes assigned by the NHIRD[32,33]. However, the NHIRD data regarding the diagnosis of AP and other comorbidities have been used in relevant studies on AP and have been proved to be reliable[34-38]. Moreover, to ensure the diagnosis of AP, we enrolled only hospitalized patients with a diagnosis of AP and excluded all the outpatients and patients with prior CP, biliary pancreatitis, and obstructive pancreatitis to avoid overestimation of the cases with AP. To ensure the objective of the diagnosis of CP, patients with CP included in our study were also required to have undergone comprehensive imaging studies such as dynamic abdominal CT or abdominal MRI within 3 mo before the diagnosis of CP. In other words, the diagnosis of CP in our study was not only dependent on ICD-9-CM coding, but it was also reconfirmed by a CT or MRI study.

Second, the personal behaviors of smoking habit and alcohol consumption were based on ICD-9-CM codes, which may have underestimated the actual prevalence of smoking and alcohol consumption. However, the prevalence of alcohol consumption and smoking habit in our study is very close to that reported by another national population-based study in Taiwan, which also used the alcohol-use-related codes and smoking-related codes as surrogates of alcohol consumption and smoking habit, respectively[38]. Considering that the aim of our study was to investigate the weighting of patients' behaviors and the number of AP episodes to the development of CP, the information extracted based on the ICD-9-CM codes was sufficient for our purpose. In addition, because we used conservative statistical methods to analyze the data, the impact of alcohol consumption and cigarette smoking could only be underestimated and not overestimated. Third, due to potential bias, the results derived from a prospective cohort study are generally of a lower statistical quality than those from perspective studies. Fourth, Because we have excluded those with biliary pancreatitis and obstructive pancreatitis at the begining, the prediction score which we developed can not be applied in patients with biliary pancreatitis or obstructive pancreatitis. Howerer, to assess the reliability of our results, we included the patients with biliary pancreatitis and obstructive pancreatitis in the sensitivity analysis.

The results of sensitivity analysis were consistent with those of our primary analyses, indicating the robustness of our study result (Supplementary Table 2).

In conclusion, the presence of RAP, alcohol consumption, age of onset of < 55 years, and smoking habit were found to be the important risk factors for the development of CP in our large, population-based cohort study in Taiwan. Using these parameters, we developed a simple predicting score model for CP, which could be applied easily when a clinician encounters a patient with nonbiliary, nonobstructive AP (most of them may belong to "toxic metabolic" or "idiopathic pancreatitis" according to the TIGAR-O classification). Unless more reliable biomarkers for CP are identified, we believe that this predicting score model could help clinicians in terms of decision-making, early detection of CP, and most importantly reversing the early CP and prevent the development of PDAC.

ARTICLE HIGHLIGHTS

Research background

Chronic pancreatitis (CP) involves a persistent destructive, inflammatory process that eventually leads to an irreversible damage to the endocrine and exocrine functions of the pancreas. CP has complications and poor prognosis, with the mortality rate being approximately two-fold higher than that in the general population.Incidence rate of pancreatic cancer is as high as 26-fold in patients with CP, suggesting that the risk of pancreatic cancer is significantly higher in subjects with CP. Therefore, It is critical to predict CP in patients with acute pancreatitis (AP).

Research motivation

The treatment option of CP is limited. We considered that the prediction of CP in high risk population and the early intervention in high risk category may decrease the disease burden and avoid the subsequent malignant change.

Research objectives

AP, recurrent AP (RAP), and CP are a continuum of diseases. However, only a small proportion of patients with AP progress to CP. It is critical to predict CP in patients with AP since CP is an important risk factor of pancreatic duct adenocarcinoma (PDAC).

Research methods

A total of 5971 patients with one or more episodes of AP (ICD-9-CM code 577.0) recorded in the inpatient claims data from 2000 to 2013 were identified from the database. A 4-year look-back period was applied from 1996 to 1999 to ensure that all cases in our cohort were newly diagnosed and to reduce false incident cases. Eventually, 3739 patients with nonobstructive, nonbiliary AP were included for subsequent analysis. Next, we developed a model to predict the progress to CP in randomly selected two-thirds of this cohort (derivation cohort) and validated the model in the remaining one-third of this cohort (validation cohort). Outcomes and comorbidities were identified based on ICD-9-CM codes. CP was defined using ICD-9-CM codes (ICD-9-CM code 577.1), and abdominal computed tomography (CT) or abdominal magnetic resonance imaging (MRI) performed within 3 mo before the diagnosis of CP was also considered as essential to diagnose clinical CP. The risk of CP in patients with nonobstructive, nonbiliary AP was estimated using the Cox proportional hazards model. The significant β coefficients from the Cox model with backward selection procedure were used to construct an integer-based risk score for stratifying the risk of progress to CP. The referent for each variable was assigned a value of 0, and the coefficients for the other variables were calculated by dividing by the smallest coefficient in the model and then rounding to the nearest integer. Individual scores were assigned by summing the individual risk factor scores, and the cumulative incidence rate of each risk score was calculated. For easy application in clinical practice, the total risk scores were classified into low-risk category, moderate-risk category, and high-risk category based on similar magnitudes of hazard.

Research results

The multivariate analysis revealed that the presence of RAP, alcoholism, smoking habit, and age of onset of < 55 years were the four important risk factors for CP. We developed a scoring system from the derivation cohort by classifying the patients into low-risk, moderate-risk, and high-risk categories based on similar magnitudes of hazard and validated the performance using another validation cohort. Using this score, we could predict the development of CP in high risk population and arrange further intervention in high risk category. However, For the lack of reliable biomarkers for predicting CP at present, we didn't include biomarkers in our variables. In the future, if more sensitive biomarkers for CP could be identified, the biomarkers should be added into the prediction model to improve the predictive value.

Research conclusions

The presence of RAP, along with alcohol consumption, age of onset, and smoking habit have a high prediction value of CP. We developed a novel prediction score model for CP with excellent discrimination and also successfully validated this model in our study. Using this scoring system, a clinician can predict the outcome of a patient with AP and arrange further examination such as endoscopic ultrasound for the high-risk category(incidence rate of about 31 per 1000 person-years in high risk group), in order to early diagnosis of CP and the subsequent pancreatic cancer. Furthemore, healthcare providers can use this scoring system for assessing patient education in terms of alcohol and smoking abstinence,because the treatment option of CP is extremely limited.

Research perspectives

We confirmed that RAP, alcohol drinking, age of onset and smoking habit are important risk factors for CP in Chinese population. Using this score,we could predict the development of CP in high risk population and arrange further intervention in high risk category.For the lack of reliable biomarkers for predicting CP at present, we didn't include biomarkers in our variables analysis. In the future, if more sensitive biomarkers for CP could be identified, the biomarkers should be added into the prediction model to improve the predictive value for CP in patients with AP episode.

REFERENCES

1 **Banks PA**. Epidemiology, natural history, and predictors of disease outcome in acute and chronic pancreatitis. *Gastrointest Endosc* 2002; **56**: S226-S230 [PMID: 12447272 DOI: 10.1067/mge.2002.129022]

2 **Lowenfels AB**, Maisonneuve P, Cavallini G, Ammann RW, Lankisch PG, Andersen JR, Dimagno EP, Andrén-Sandberg A, Domellöf L. Pancreatitis and the risk of pancreatic cancer. International Pancreatitis Study Group. *N Engl J Med* 1993; **328**: 1433-1437 [PMID: 8479461 DOI: 10.1056/NEJM199305203282001]

3 **Sankaran SJ**, Xiao AY, Wu LM, Windsor JA, Forsmark CE, Petrov MS. Frequency of progression from acute to chronic pancreatitis and risk factors: a meta-analysis. *Gastroenterology* 2015; **149**: 1490-1500.e1 [PMID: 26299411 DOI: 10.1053/j.gastro.2015.07.066]

4 **Lankisch PG**, Breuer N, Bruns A, Weber-Dany B, Lowenfels AB, Maisonneuve P. Natural history of acute pancreatitis: a long-term population-based study. *Am J Gastroenterol* 2009; **104**: 2797-2805; quiz 2806 [PMID: 19603011 DOI: 10.1038/ajg.2009.405]

5 **Maisonneuve P**, Lowenfels AB, Müllhaupt B, Cavallini G, Lankisch PG, Andersen JR, Dimagno EP, Andrén-Sandberg A, Domellöf L, Frulloni L, Ammann RW. Cigarette smoking accelerates progression of alcoholic chronic pancreatitis. *Gut* 2005; **54**: 510-514 [PMID: 15753536 DOI: 10.1136/gut.2004.039263]

6 **Yadav D**, Hawes RH, Brand RE, Anderson MA, Money ME, Banks PA, Bishop MD, Baillie J, Sherman S, DiSario J, Burton FR, Gardner TB, Amann ST, Gelrud A, Lawrence C, Elinoff B, Greer JB, O'Connell M, Barmada MM, Slivka A, Whitcomb DC; North American Pancreatic Study Group. Alcohol consumption, cigarette

smoking, and the risk of recurrent acute and chronic pancreatitis. *Arch Intern Med* 2009; **169**: 1035-1045 [PMID: 19506173 DOI: 10.1001/archinternmed.2009.125]
7 **Di Leo M**, Leandro G, Singh SK, Mariani A, Bianco M, Zuppardo RA, Goni E, Rogger TM, Di Mario F, Guslandi M, De Cobelli F, Del Maschio A, Testoni PA, Cavestro GM. Low Alcohol and Cigarette Use Is Associated to the Risk of Developing Chronic Pancreatitis. *Pancreas* 2017; **46**: 225-229 [PMID: 27846144 DOI: 10.1097/MPA.0000000000000737]
8 **Whitlock TL**, Tignor A, Webster EM, Repas K, Conwell D, Banks PA, Wu BU. A scoring system to predict readmission of patients with acute pancreatitis to the hospital within thirty days of discharge. *Clin Gastroenterol Hepatol* 2011; **9**: 175-180; quiz e18 [PMID: 20832502 DOI: 10.1016/j.cgh.2010.08.017]
9 **Beyer G**, Mahajan UM, Budde C, Bulla TJ, Kohlmann T, Kuhlmann L, Schütte K, Aghdassi AA, Weber E, Weiss FU, Drewes AM, Olesen SS, Lerch MM, Mayerle J. Development and Validation of a Chronic Pancreatitis Prognosis Score in 2 Independent Cohorts. *Gastroenterology* 2017; **153**: 1544-1554.e2 [PMID: 28918191 DOI: 10.1053/j.gastro.2017.08.073]
10 **Cheng CL**, Kao YH, Lin SJ, Lee CH, Lai ML. Validation of the National Health Insurance Research Database with ischemic stroke cases in Taiwan. *Pharmacoepidemiol Drug Saf* 2011; **20**: 236-242 [PMID: 21351304 DOI: 10.1002/pds.2087]
11 **Cheng CL**, Lee CH, Chen PS, Li YH, Lin SJ, Yang YH. Validation of acute myocardial infarction cases in the national health insurance research database in taiwan. *J Epidemiol* 2014; **24**: 500-507 [PMID: 25174915 DOI: 10.2188/jea.JE20140076]
12 **Hsu TW**, Liu JS, Hung SC, Kuo KL, Chang YK, Chen YC, Hsu CC, Tarng DC. Renoprotective effect of renin-angiotensin-aldosterone system blockade in patients with predialysis advanced chronic kidney disease, hypertension, and anemia. *JAMA Intern Med* 2014; **174**: 347-354 [PMID: 24343093 DOI: 10.1001/jamainternmed.2013.12700]
13 **Banks PA**, Bollen TL, Dervenis C, Gooszen HG, Johnson CD, Sarr MG, Tsiotos GG, Vege SS; Acute Pancreatitis Classification Working Group. Classification of acute pancreatitis--2012: revision of the Atlanta classification and definitions by international consensus. *Gut* 2013; **62**: 102-111 [PMID: 23100216 DOI: 10.1136/gutjnl-2012-302779]
14 **Garg PK**. Chronic pancreatitis in India and Asia. *Curr Gastroenterol Rep* 2012; **14**: 118-124 [PMID: 22327961 DOI: 10.1007/s11894-012-0241-0]
15 **Wang LW**, Li ZS, Li SD, Jin ZD, Zou DW, Chen F. Prevalence and clinical features of chronic pancreatitis in China: a retrospective multicenter analysis over 10 years. *Pancreas* 2009; **38**: 248-254 [PMID: 19034057 DOI: 10.1097/MPA.0b013e31818f6ac1]
16 **Keim V**. Role of genetic disorders in acute recurrent pancreatitis. *World J Gastroenterol* 2008; **14**: 1011-1015 [PMID: 18286680 DOI: 10.3748/wjg.14.1011]
17 **Sekimoto M**, Takada T, Kawarada Y, Hirata K, Mayumi T, Yoshida M, Hirota M, Kimura Y, Takeda K, Isaji S, Koizumi M, Otsuki M, Matsuno S; JPN. JPN Guidelines for the management of acute pancreatitis: epidemiology, etiology, natural history, and outcome predictors in acute pancreatitis. *J Hepatobiliary Pancreat Surg* 2006; **13**: 10-24 [PMID: 16463207 DOI: 10.1007/s00534-005-1047-3]
18 **Etemad B**, Whitcomb DC. Chronic pancreatitis: diagnosis, classification, and new genetic developments. *Gastroenterology* 2001; **120**: 682-707 [PMID: 11179244 DOI: 10.1053/gast.2001.22586]
19 **Nøjgaard C**, Becker U, Matzen P, Andersen JR, Holst C, Bendtsen F. Progression from acute to chronic pancreatitis: prognostic factors, mortality, and natural course. *Pancreas* 2011; **40**: 1195-1200 [PMID: 21926938 DOI: 10.1097/MPA.0b013e318221f569]
20 **Yadav D**, Slivka A, Sherman S, Hawes RH, Anderson MA, Burton FR, Brand RE, Lewis MD, Gardner TB, Gelrud A, Disario J, Amann ST, Baillie J, Lawrence C, O'Connell M, Lowenfels AB, Banks PA, Whitcomb DC. Smoking is underrecognized as a risk factor for chronic pancreatitis. *Pancreatology* 2010; **10**: 713-719 [PMID: 21242712 DOI: 10.1159/000320708]
21 **Hartwig W**, Werner J, Ryschich E, Mayer H, Schmidt J, Gebhard MM, Herfarth C, Klar E. Cigarette smoke enhances ethanol-induced pancreatic injury. *Pancreas* 2000; **21**: 272-278 [PMID: 11039472 DOI: 10.1097/00006676-200010000-00009]
22 **Polonikov AV**, Samgina TA, Nazarenko PM, Bushueva OY, Ivanov VP. Alcohol Consumption and Cigarette Smoking are Important Modifiers of the Association Between Acute Pancreatitis and the PRSS1-PRSS2 Locus in Men. *Pancreas* 2017; **46**: 230-236 [PMID: 27846138 DOI: 10.1097/MPA.0000000000000729]
23 **Centers for Disease Control and Prevention (CDC)**. Smoking-attributable mortality, years of potential life lost, and productivity losses--United States, 2000-2004. *MMWR Morb Mortal Wkly Rep* 2008; **57**: 1226-1228 [PMID: 19008791]
24 **Wang W**, Sun XT, Weng XL, Zhou DZ, Sun C, Xia T, Hu LH, Lai XW, Ye B, Liu MY, Jiang F, Gao J, Bo LM, Liu Y, Liao Z, Li ZS. Comprehensive screening for PRSS1, SPINK1, CFTR, CTRC and CLDN2 gene mutations in Chinese paediatric patients with idiopathic chronic pancreatitis: a cohort study. *BMJ Open* 2013; **3**: e003150 [PMID: 24002981 DOI: 10.1136/bmjopen-2013-003150]
25 **Henfling PA**, Lowry LW. Nursing shortage. Catalyst for administrative/educational partnership. *J Nurs Staff Dev* 1990; **6**: 121-125 [PMID: 2362213 DOI: 10.1053/j.gastro.2013.01.069]
26 **Wittel UA**, Singh AP, Henley BJ, Andrianifahanana M, Akhter MP, Cullen DM, Batra SK. Cigarette smoke-induced differential expression of the genes involved in exocrine function of the rat pancreas. *Pancreas* 2006; **33**: 364-370 [PMID: 17079941 DOI: 10.1097/01.mpa.0000240601.80570.31]
27 **Alexandre M**, Pandol SJ, Gorelick FS, Thrower EC. The emerging role of smoking in the development of pancreatitis. *Pancreatology* 2011; **11**: 469-474 [PMID: 21986098 DOI: 10.1159/000332196]
28 **Ahmed Ali U**, Issa Y, Hagenaars JC, Bakker OJ, van Goor H, Nieuwenhuijs VB, Bollen TL, van Ramshorst B, Witteman BJ, Brink MA, Schaapherder AF, Dejong CH, Spanier BW, Heisterkamp J, van der Harst E, van Eijck CH, Besselink MG, Gooszen HG, van Santvoort HC, Boermeester MA; Dutch Pancreatitis Study Group. Risk of Recurrent Pancreatitis and Progression to Chronic Pancreatitis After a First Episode of Acute Pancreatitis. *Clin Gastroenterol Hepatol* 2016; **14**: 738-746 [PMID: 26772149 DOI: 10.1016/j.cgh.2015.12.040]
29 **Layer P**, Yamamoto H, Kalthoff L, Clain JE, Bakken LJ, DiMagno EP. The different courses of early- and late-onset idiopathic and alcoholic chronic pancreatitis. *Gastroenterology* 1994; **107**: 1481-1487 [PMID: 7926511 DOI: 10.1016/0016-5085(94)90553-3]
30 **Yamabe A**, Irisawa A, Shibukawa G, Sato A, Fujisawa M, Arakawa N, Yoshida Y, Abe Y, Igarashi R, Maki T, Yamamoto S. Early diagnosis of chronic pancreatitis: understanding the factors associated with the development of chronic pancreatitis. *Fukushima J Med Sci* 2017; **63**: 1-7 [PMID: 28450665 DOI: 10.5387/fms.2016-14]
31 **Ito T**, Ishiguro H, Ohara H, Kamisawa T, Sakagami J, Sata N, Takeyama Y, Hirota M, Miyakawa H, Igarashi H, Lee L, Fujiyama T, Hijioka M, Ueda K, Tachibana Y, Sogame Y, Yasuda H, Kato R, Kataoka K, Shiratori K, Sugiyama M, Okazaki K, Kawa S, Tando Y, Kinoshita Y, Watanabe M, Shimosegawa T. Evidence-based clinical practice guidelines for chronic pancreatitis 2015. *J Gastroenterol* 2016; **51**: 85-92 [PMID: 26725837 DOI: 10.1007/s00535-015-1149-x]
32 **Deyo RA**, Cherkin DC, Ciol MA. Adapting a clinical comorbidity index for use with ICD-9-CM administrative databases. *J Clin Epidemiol* 1992; **45**: 613-619 [PMID: 1607900 DOI: 10.1016/0895-4356(92)90133-8]
33 **Quan H**, Parsons GA, Ghali WA. Validity of information on comorbidity derived rom ICD-9-CCM administrative data. *Med Care* 2002; **40**: 675-685 [PMID: 12187181 DOI: 10.1097/00005650-200208000-00007]
34 **Shen HN**, Lu CL, Li CY. Epidemiology of first-attack acute pancreatitis in Taiwan from 2000 through 2009: a nationwide population-based study. *Pancreas* 2012; **41**: 696-702 [PMID: 22699142 DOI: 10.1097/MPA.0b013e31823db941]
35 **Shen HN**, Lu CL. Incidence, resource use, and outcome of acute

pancreatitis with/without intensive care: a nationwide population-based study in Taiwan. *Pancreas* 2011; **40**: 10-15 [PMID: 20938365 DOI: 10.1097/MPA.0b013e3181f7e750]

36 **Lai SW**, Muo CH, Liao KF, Sung FC, Chen PC. Risk of acute pancreatitis in type 2 diabetes and risk reduction on anti-diabetic drugs: a population-based cohort study in Taiwan. *Am J Gastroenterol* 2011; **106**: 1697-1704 [PMID: 21577242 DOI: 10.1038/ajg.2011.155]

37 **Lin HY**, Lai JI, Lai YC, Lin PC, Chang SC, Tang GJ. Acute renal failure in severe pancreatitis: A population-based study. *Ups J Med Sci* 2011; **116**: 155-159 [PMID: 21250932 DOI: 10.3109/03009734.2010.547636]

38 **Shen HN**, Yang CC, Chang YH, Lu CL, Li CY. Risk of Diabetes Mellitus after First-Attack Acute Pancreatitis: A National Population-Based Study. *Am J Gastroenterol* 2015; **110**: 1698-1706 [PMID: 26526084 DOI: 10.1038/ajg.2015.356]

P- Reviewer: Masamune A, Tantau A **S- Editor**: Ma RY
L- Editor: A **E- Editor**: Yin SY

World Journal of Gastroenterology

Submit a Manuscript: http://www.f6publishing.com

World J Gastroenterol 2018 November 28; 24(44): 5046-5056

DOI: 10.3748/wjg.v24.i44.5046

ISSN 1007-9327 (print) ISSN 2219-2840 (online)

ORIGINAL ARTICLE

Retrospective Study

Prognostic value of fibrinogen and D-dimer-fibrinogen ratio in resectable gastrointestinal stromal tumors

Hua-Xia Cai, Xu-Qi Li, Shu-Feng Wang

Hua-Xia Cai, Xu-Qi Li, Shu-Feng Wang, Department of General Surgery, First Affiliated Hospital of Xi'an Jiaotong University, Xi'an 710061, Shaanxi Province, China

Hua-Xia Cai, Department of General Surgery, Xi'an 141 Hospital, Yanliang 710089, Shaanxi Province, China

ORCID number: Hua-Xia Cai (0000-0002-8707-3813); Xu-Qi Li (0000-0002-2497-020X); Shu-Feng Wang (0000-0001-6730-0153).

Author contributions: Cai HX and Wang SF designed the study; Cai HX analyzed and interpreted the data and drafted the manuscript; Li XQ and Wang SF revised the controversial parts of the manuscript; all authors read and approved the final manuscript.

Institutional review board statement: This study was approved by the Medical Ethics Committee of the First Affiliated Hospital of Xi'an Jiaotong University.

Informed consent statement: All the patients or their legal guardians signed informed consent before the operation. Since this study used anonymous clinical data, patients did not need to give informed consent.

Conflict-of-interest statement: There was no conflict of interest in the present study.

Data sharing statement: No additional data are available.

Manuscript source: Unsolicited manuscript

Corresponding author to: Shu-Feng Wang, MD, PhD, Doctor, Full Professor, Surgeon, Department of General Surgery, First Affiliated Hospital of Xi'an Jiaotong University, 277 West Yanta Road, Xi'an 710061, Shaanxi province, China. dawn@mail.xjtu.edu.cn.
Telephone: +86-18991232452

Received: August 17, 2018
Peer-review started: August 17, 2018
First decision: October 14, 2018
Revised: October 27, 2018
Accepted: November 9, 2018
Article in press: November 9, 2018
Published online: November 28, 2018

Abstract

AIM

To investigate the prognostic value of preoperative fibrinogen concentration (FIB) and D-dimer-fibrinogen ratio (DFR) in gastrointestinal stromal tumors (GISTs).

METHODS

The purpose of this study was to retrospectively analyze 170 patients with GISTs who were admitted to our hospital from January 2010 to December 2015. The optimal cutoff values of related parameters were estimated by receiver operating characteristic (ROC) curve analysis. The recurrence free survival (RFS) rate was evaluated using Kaplan-Meier curves. Univariate analysis and multivariate Cox regression models were used to analyze the prognostic factors of GISTs. The relationship between the FIB, D-dimer, DFR, platelet count (PLT), and the clinicopathological features of GISTs was described by the chi-square test or nonparametric rank sum test (Mann-Whitney test).

RESULTS

In ROC analysis, the optimal cutoff values of FIB, D-dimer, DFR, and PLT were 3.24 g/L, 1.24 mg/L, 0.354, and 197.5 ($\times 10^9$/L), respectively. Univariate analysis and the Kaplan-Meier survival curve showed that FIB, D-dimer, DFR, PLT,

National Institutes of Health (NIH) risk category, tumor size, tumor location, and mitotic index were significantly relevant to the 3-year and 5-year survival rate of patients ($P < 0.05$). Cox multivariate regression analysis illustrated that FIB (*RR*: 0.108, 95%CI: 0.031-0.373), DFR (*RR*: 0.319, 95%CI: 0.131-0.777), and NIH risk category (*RR*: 0.166, 95%CI: 0.047-0.589) were independent prognostic factors of the RFS rate ($P < 0.05$). Moreover, FIB, D-dimer, DFR, and PLT were correlated with the clinical features of GISTs.

CONCLUSION

FIB, D-dimer, DFR, and PLT are all related to the prognosis of GISTs. Moreover, FIB and DFR may be independent risk factors for predicting the prognosis of resectable GISTs.

Key words: D-dimer; D-dimer-fibrinogen ratio; Prognosis; Fibrinogen; Gastrointestinal stromal tumor

Core tip: For patients with gastrointestinal stromal tumors (GISTs), postoperative recurrence and metastasis are the main factors affecting survival. Moreover, recurrence and metastasis mainly occur in moderate and high-risk patients. Therefore, it is necessary to screen these patients for adjuvant treatment at an early stage. Fibrinogen (FIB) and D-dimer were reported to be associated with the prognosis of many tumors. The purpose of this study was to investigate the value of preoperative FIB, D-dimer, the D-dimer-fibrinogen ratio (DFR), and platelets in the prognosis of GISTs. The results showed that FIB and DFR were independent risk factors for predicting the prognosis of primary resectable GIST.

Cai HX, Li XQ, Wang SF. Prognostic value of fibrinogen and D-dimer-fibrinogen ratio in resectable gastrointestinal stromal tumors. *World J Gastroenterol* 2018; 24(44): 5046-5056 Available from: URL: http://www.wjgnet.com/1007-9327/full/v24/i44/5046.htm DOI: http://dx.doi.org/10.3748/wjg.v24.i44.5046

INTRODUCTION

Gastrointestinal stromal tumors (GISTs) are the most common mesenchymal neoplasms originating from the gastrointestinal tract[1,2]. GISTs may occur anywhere in the digestive tract, including outside the gastrointestinal tract[1]. The incidence of GISTs is 60%-70% in the stomach, and 30% in the small intestine[3]. However, GISTs occurring in areas such as the colon, rectum, and esophagus are rare. The main treatment for primary localized GISTs is margin negative complete resection[1]. However, the recurrence or metastasis of the original disease after the operation are an obstacle to prolonging the survival period. It was reported that approximately 50% of the patients who undergo surgery alone will have tumor recurrence, and the median survival after recurrence is less than 2 years[4]. Unfortunately, if GISTs recur or are metastatic, the value of the operation is low. In addition, the expert consensus on GISTs in China indicates that patients in the intermediate category or high category who meet the 2008 revision risk classification standard should carry out corresponding auxiliary treatment[3]. Therefore, early screening of middle and high category patients with adjuvant therapy can significantly improve the prognosis of patients. However, the current accepted risk classification criteria for predicting the prognosis of GIST patients require pathological results to be obtained. In this case, it is important to develop some simple, noninvasive methods to accurately screen high-risk populations of GISTs and provide early adjuvant therapy to improve their prognosis.

Thrombocytopenia and coagulation abnormalities are very common in cancer patients. Research shows that cancer is a prothrombotic state, and much evidence points to a role for the fibrinogen-platelet axis in tumor biology[4]. Fibrinogen (FIB) is a glycoprotein produced mainly by liver cells, which is an important coagulation factor and contributes to the regulation of blood coagulation pathways[5]. Moreover, FIB can promote cell adhesion and inflammation in the process of coagulation. Additionally, recent evidence suggests that tumors with elevated FIB levels are more likely to develop invasion and metastasis[6,7], including esophageal, gastric, and colorectal carcinomas[8]. In the coagulation system, FIB can be transformed into fibrin by thrombin, and the end product D-dimer of fibrin is increased in cases such as colorectal cancer, lymph node metastasis, and vascular invasion[9]. In addition, it was reported that the combination of FIB and the neutrophil-lymphocyte ratio could predict tumor progression and prognosis in gastric cancer patients[8]. At the same time, D-dimer can also help predict the prognosis of metastatic gastric cancer after chemotherapy[10].

Based on the above results, we hypothesized that plasma FIB, D-dimer, and platelet count (PLT) may be associated with clinical outcomes in patients with cancer. However, as far as we know, studies assessing the prognostic value of plasma FIB, D-dimer, and PLT in patients with GISTs are rarely reported.

The aim of this study was to investigate the relationship between preoperative FIB, D-dimer, the D-dimer-FIB ratio (DFR), PLT values, and clinicopathologic characteristics and to evaluate the prognostic value of these markers in GISTs.

MATERIALS AND METHODS

Patients and clinicopathologic parameters

The research institution of this study was the First Affiliated Hospital of Xi'an Jiaotong University. One hundred and seventy patients with GISTs were treated at our department from January 1, of 2010 to December 31, 2015. Clinicopathological parameters and follow-up data were assessed for all the GIST patients (91 men and 79

women) who received initial curative surgical resection. All the patients were pathologically confirmed with GISTs. The demographic data and clinicopathologic features of each patient were collected. The average age of the patients was 61 years.

All enrolled patients must meet the following criteria: (1) the first diagnosis was primary resectable GIST; (2) complete blood test results can be obtained before treatment; (3) surgical treatment was performed, and imatinib was not administered preoperatively; and (4) there were complete postoperative follow-up data.

Patients with hematological diseases, other tumor types, the use of coagulation and anticoagulation drugs for 8 weeks, incomplete blood test results, or with myocardial infarction, cerebral infarction, and other diseases were excluded.

The preoperative assessment of GISTs was performed by abdominal or pelvic CT, magnetic resonance imaging (MRI), gastrointestinal endoscopy, or endoscopic ultrasound. This study was approved by the Medical Ethics Committee of the First Affiliated Hospital of Xi'an Jiaotong University, and all the patients signed an informed consent form before the operation.

We collected the data of all patients in the study, including patient demographics (age and gender), clinical and pathological features, comorbidities, FIB, D-dimer, PLT, operative factors (type of surgery and extent of lymph node dissection), and tumor characteristics (location, size, lymph node metastasis, mitotic number, distant metastasis, and risk category).

Data collected on preoperative plasma FIB, D-dimer, PLT, and other laboratory indexes are the closest to the results of a test of the time of surgery. It was most important that all the laboratory data were obtained from each patient before breakfast. Venous blood with no evidence of infection was collected. The DFR was calculated as D-dimer (mg/L) divided by fibrinogen concentration (g/L).

Follow-up assessments

Patients were followed once every 3 mo for 2 years, every 6 mo between 2 and 5 years, and then every year thereafter. Follow-ups were either by outpatient or inpatient review, or by contacting patients or their relatives by telephone. For the follow-up of GIST patients after surgery, chest and abdominal CT scan, abdominal (liver and adrenal) ultrasound scan, bone marrow scan and endoscopic biopsy, and positron emission computerized tomography (PET) to exclude recurrence and metastasis were utilized. According to the follow-up program, all patients were followed until the deadline of December 1, 2016 or the death of the patient. Metastatic recurrence revealed by imaging and death were considered as the end point events.

Statistical analysis

The frequency and percentage are used to represent the patient's baseline characteristics. The optimal values of FIB, D-dimer, DFR, and PLT were determined using receiver operating characteristic (ROC) curves[1]. The patients were divided into high and normal groups by the optimal values. The area under the curve was determined by ROC curve analysis, and the 95% confidence interval (CI) was determined. The correlation of tests, including binary classification variables, was performed using the Chi-square test or nonparametric rank sum test (Mann-Whitney test). Recurrence free survival (RFS) was defined as the time from the surgery to clinical or imaging evidence of recurrence for the first time. The Kaplan-Meier method was used to estimate the survival curve of RFS, and the log-rank test was used to evaluate the difference between groups. Univariate analysis was used to analyze the risk factors influencing the RFS of GISTs. A multivariate Cox proportional hazards regression model was used to identify the independent risk factors affecting RFS, with the risk ratio (RR) and the corresponding 95%CI calculated. The meaningful indicators found in univariate analysis were further evaluated by a multivariate Cox proportional hazards regression model (Forward stepwise method - conditional likelihood ratio). The Cox regression equation was as follows: $h\ (t,\ x) = h_0\ (t)\ exp\ (\beta_1 x_1 + \beta_2 x_2 + \ldots + \beta_p x_p)$, where x is covariate with time, $h\ (t,\ x)$ is a risk function that is the individual with a covariate x function of risk on the t moment, $h_0\ (t)$ is the baseline hazard function, and β_I (I = 1, 2 ,..., p) is population regression. The prognostic index (PI) model was as follows: $PI = \beta_1 x_1 + \beta_2 x_2 + \ldots + \beta_p x_p$.

All data were statistically analyzed using SPSS software (version 18.0; SPSS Inc., Chicago, IL, United States). All tests were two-sided, and *P*-values below 5% were considered statistically significant.

RESULTS

ROC analysis

The optimal cutoff values of FIB, D-dimer, DFR, and PLT were determined using ROC curves. The areas under the ROC curves for FIB, D-dimer, DFR and PLT were 0.758 (95%CI: 0.666-0. 850; $P < 0.01$), 0.739 (95%CI: 0.629-0. 850; $P < 0.01$), 0.709 (95%CI: 0.596-0. 822; $P = 0.001$), and 0.625 (95%CI: 0.517-0. 733; $P = 0.050$), respectively (Figure 1). For all GIST patients, FIB = 3.24 g/L, D-dimer = 1.24 mg/L, DFR = 0.354, and PLT = 197.5 ($\times 10^9$/L) had the highest sensitivity (87.5%, 70.8%, 66.7%, and 75%) and specificity (61.6%, 76%, 80.1%, and 51.4%), respectively (Table 1).

Baseline patient characteristics

All 170 patients in this study were confirmed with GISTs by pathology. The age of the study population ranged from 19 to 80 years, with a median age of 61 years. In all patients, there were 91 male cases, accounting for 53.5%; the male to female ratio was 1.15:1. The most common site of GISTs was the stomach (122 cases), accounting for 71.76%, followed by the small intestine

Table 1 Area under the curve

Variable	Area	SE	*P* value	95%CI
FIB (g/L)	0.758	0.047	< 0.01	0.666-0.850
D-dimer (mg/L)	0.739	0.056	< 0.01	0.629-0.850
D-dimer/FIB	0.709	0.058	0.001	0.596-0.822
PLT (10^9/L)	0.625	0.055	0.05	0.517-0.733

FIB: Fibrinogen; CI: Confidence interval; PLT: Platelet count.

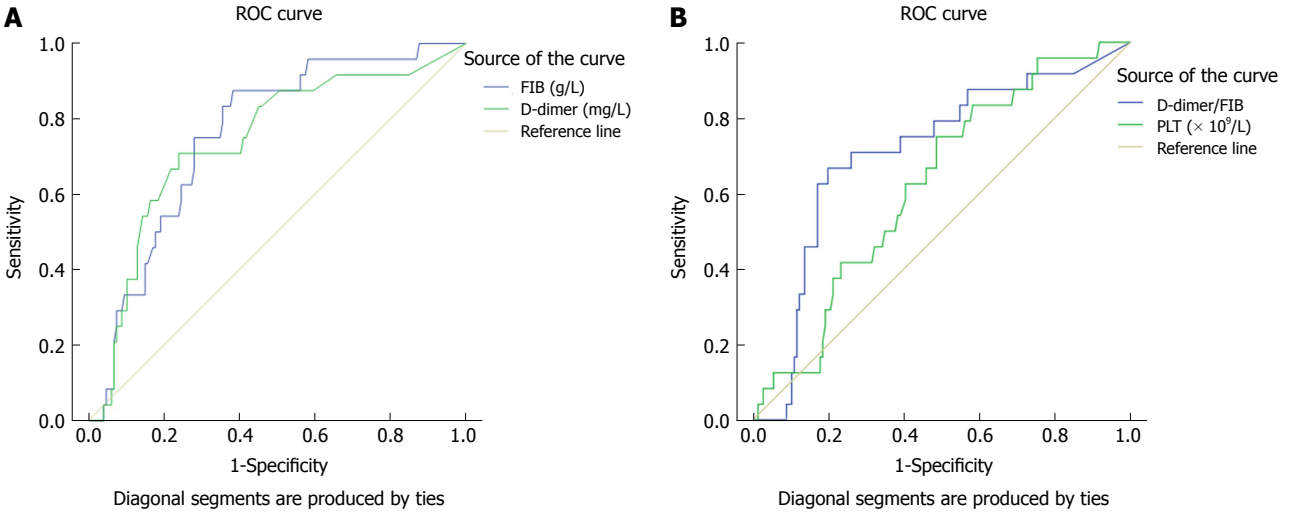

Figure 1 Receiver operating characteristic curves for predicting recurrence free survival among 170 gastrointestinal stromal tumor patients. A and B: Plasma fibrinogen (FIB), D-dimer, D-dimer to FIB ratio (D-dimer/FIB), and platelet count. ROC: Receiver operating characteristic ; RFS: Recurrence-free survival; GIST: Gastrointestinal stromal tumor.

(20%; 34/170), colon and rectum (5.88%; 10/170), pelvic cavity (1.76%; 3/170), and esophagus (0.59%; 1/170). The median diameter of tumors in this study was 5 cm, with a minimum of 0.5 cm and a maximum of 29 cm. According to the revised NIH (National Institutes of Health) risk category of 2008[10], of the total 170 patients, 18 were at very low risk (10.59%), 65 at low risk (38.24%), 37 at intermediate risk (21.76%), and 50 at high risk (29.41%). The mitotic count was more than 5/50 high power fields (HPFs) in 125 (73.53%) patients. There were 48 (55.17%, 48/87) patients receiving adjuvant imatinib following surgery in the intermediate and high risk categories. During follow-up, 24 patients showed recurrence or metastasis, 15 patients suffered from GIST related deaths, and 1 patient died in a car accident. The 3- and 5-year RFS rates in the 170 patients with GISTs were 85% and 75%, respectively.

Univariate analysis of prognostic factors

Of the 170 patients in this study, the median RFS survival time was 32 mo (1 mo to 80 mo) postoperatively. Univariate analyses of demographic and clinicopathologic factors were performed to assess the prognostic factors associated with survival. Univariate analysis showed that gender (male and female) and age (< 61 years *vs* ⩾ 61 years) were not relevant to the prognosis of patients with GISTs ($P > 0.05$). However, other demographic and clinical pathology factors were risk factors that affected the prognosis of the patients. These risk factors included FIB (⩾ 3.24 g/L *vs* < 3.24 g/L, $P < 0.01$), D-dimer (⩾ 1.24 mg/L *vs* < 1.24 mg/L, $P < 0.01$), DFR (< 0.354 *vs* ⩾ 0.354, $P < 0.01$), PLT (⩾ 197. 5 × 10^9/L *vs* < 197.5 × 10^9/L, $P = 0.014$), mitotic index (⩽ 5/50 HPFs *vs* > 5/50 HPFs, $P < 0.01$), tumor size (⩽ 5 cm *vs* > 5 cm, $P < 0.01$), tumor location (gastric *vs* extragastric, $P = 0.001$), and NIH risk category (very low and low *vs* intermediate and high, $P < 0.01$). The results of these univariate analyses are shown in Table 2.

We divided the patients into a normal group and a high group based on serum FIB level, D-dimer, DFR, and PLT, respectively, and investigated the relationship between the above parameters and the prognosis of GIST patients. We found that patients with high pre-operative FIB, D-dimer, DFR, or PLT had a shorter RFS than normal controls (Figure 2A-D). In the first 3 years, the survival time of patients who received the adjuvant imatinib was significantly longer than that of the untreated in the intermediate and high risk category group (Figure 2E).

In addition, extragastric tumors, tumors larger than 5 cm, intermediate-high NIH risk category, and mitotic image count above 5/50 HPFs were associated with a poorer prognosis (log-rank, $P < 0.01$) (Table 2).

This study also evaluated the prognostic value of FIB concentration combined with D-dimer in patients with GISTs, as well as its clinical applicability and clinical value.

Table 2 Univariate analysis of association between clinicopathologic features and prognosis in gastrointestinal stromal tumor patients

Characteristic	Number	3-yr RFS (%)	5-yr RFS (%)	95%CI	*P* value
Gender					
Male	91	80	75	61.170-72.86	0.498
Female	79	90	80	56.828-65.996	
Age (yr)					
< 61	78	85	81	58.018-66.650	0.406
⩾ 61	92	83	78	61.508-73.445	
NIH risk category					
Very low, low	83	97	95	73.805-80.329	< 0.01
Intermediate, high	87	80	65	50.488-62.245	
Tumor size (cm)					
⩽ 5	97	95	95	75.130-80.262	< 0.01
> 5	73	63	55	49.388-63.256	
Tumor location					
Gastric	122	92	85	67.968-76.637	0.001
Extragastric	48	76	55	42.703-56.229	
FIB (g/L)					
< 3.24	95	95	95	75.248-80.253	< 0.01
⩾ 3.24	75	65	50	48.878-62.958	
D-dimer (mg/L)					
< 1.24	118	95	88	70.09-88.603	< 0.01
⩾ 1.24	52	65	55	46.163-62.647	
DFR					
< 0.354	126	95	85	70.237-78.220	< 0.01
⩾ 0.354	44	70	50	43.262-61.237	
PLT ($\times 10^9$/L)					
< 197.5	81	92	85	68.060-78.540	0.014
⩾ 197.5	89	76	68	55.307-67.619	
Mitotic index					
⩽ 5/50 HPFs	125	95	90	70.431-77.808	< 0.01
> 5/50 HPFs	45	65	35	39.663-55.513	
Adjuvant imatinib[1]					
Yes	48	70	55	48.468-64.287	0.940
No	39	75	55	41.127-64.055	

[1]Intermediate and high risk gastrointestinal stromal tumor patients. GIST: Gastrointestinal stromal tumor; NIH: National Institutes of Health; FIB: Fibrinogen; RFS: Recurrence-free survival; DFR: D-dimer to FIB ratio (D-dimer/FIB); PLT: Platelet count.

We divided GIST patients into four groups based on the following criteria: low FIB and low D-dimer; low FIB and high D-dimer; high FIB and low D-dimer; and high FIB and high D-dimer. The prognosis of the high FIB and high D-dimer group was significantly worse than that of the low FIB and/or low D-dimer group (38% *vs* 95% *vs* 92% *vs* 82%, $P < 0.01$, Figure 3).

Multivariate analysis of prognostic factors

To determine the independent risk factors for GIST patients, we used the Cox proportional hazard model to assess the outcome.

Multivariate analysis was used to further analyze the risk factors affecting the prognosis of GISTs in univariate analysis. Factors in the multivariate analysis included FIB levels, D-dimer levels, DFR, PLT, tumor size, tumor location, and NIH risk category. The results showed that FIB (RR: 0.131, 95%CI: 0.039-0.443, $P = 0.001$), DFR (RR: 0.334, 95%CI: 0.139-0.802, $P = 0.014$), and NIH risk category (RR: 0.206, 95%CI: 0.059-0.711, $P = 0.012$) were independent risk factors for the prognosis of GISTs (Table 3).

The Cox regression formula for the present study was $h(t, x) = h_0(t)\, exp\,(2.035\ \text{FIB} + 1.097\ \text{DFR} + 1.582\ \text{NIH risk category})$. The PI of the present study was PI = 2.035 FIB + 1.097 DFR + 1.582 NIH risk category.

To exclude confounding the analyses by the treatment of GIST patients with the tyrosine kinas inhibitor imatinib, we recalculated the RFS of GISTs by a hierarchy of whether patients received adjuvant imatinib or not after surgery. This multivariate analysis indicated that FIB, DFR, and NIH risk category (RR: 0.108, 95%CI: 0.031-0.373, $P < 0.01$; RR: 0.319, 95%CI: 0.131-0.777, $P = 0.012$; RR: 0.166, 95%CI: 0.047-0.589, $P = 0.005$; respectively) were still independent risk factors associated with GIST prognosis, as shown in Table 4. The Cox proportional regression model was $h(t, x) = h_0(t)\, exp\,(2.223\ \text{FIB} + 1.141\ \text{DFR} + 1.795\ \text{NIH risk category})$. The PI of the present study was PI = 2.223 FIB + 1.141 DFR + 1.795 NIH risk category.

Correlation of FIB, D-dimer, DFR, and PLT levels with clinicopathologic factors in GIST patients

The clinicopathologic features of high and low FIB, D-dimer, DFR and PLT GIST patients were analyzed and are summarized in Tables 5-8, respectively. The results showed that age, sex, tumor location, tumor size, NIH risk category, and mitotic index were correlated with the

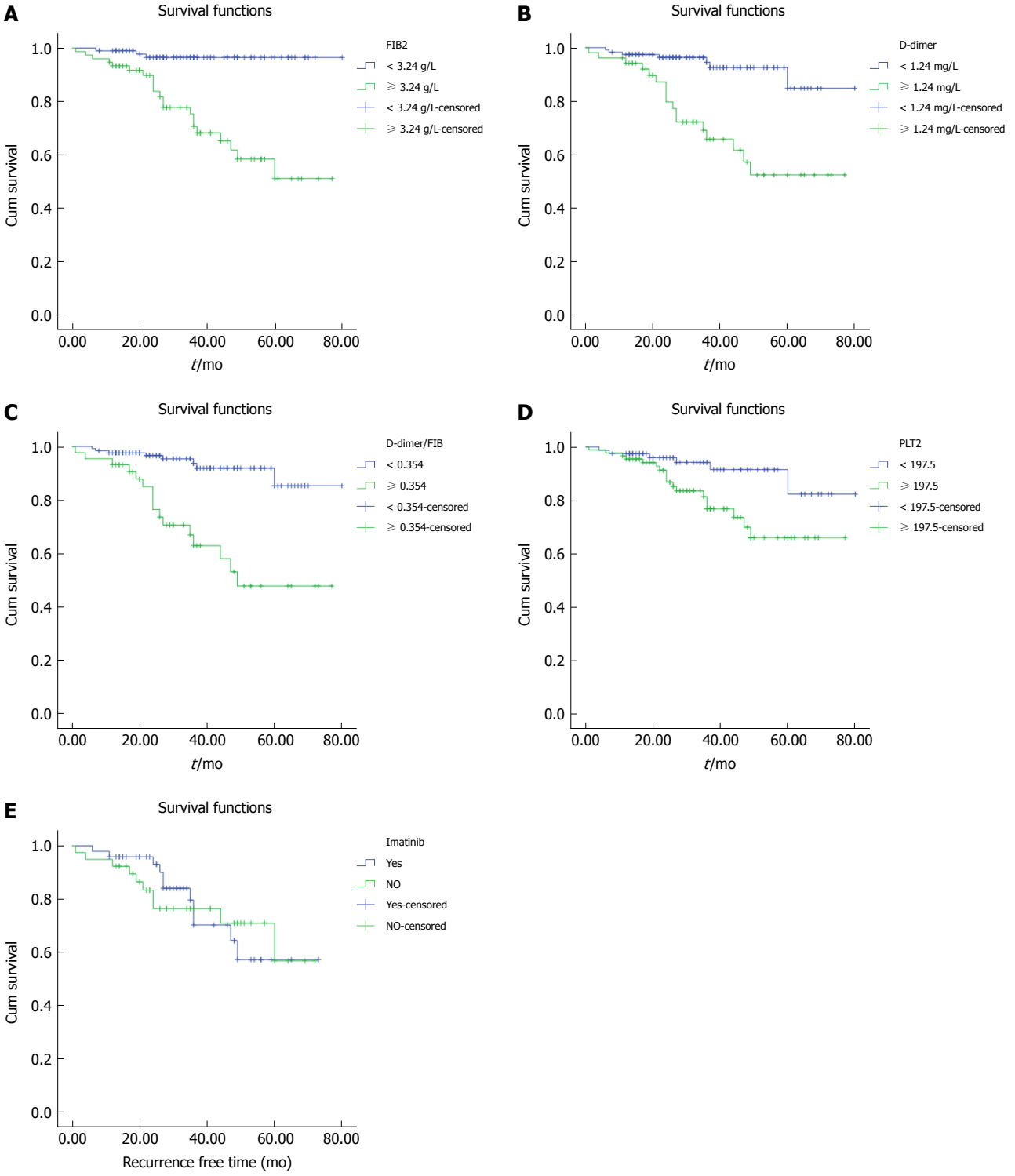

Figure 2 Kaplan-Meier survival curves of high and normal groups of different indicators in 170 resected primary gastrointestinal stromal tumor patients. (A) Fibrinogen (FIB) category; (B) D-dimer category; (C) D-dimer-fibrinogen ratio (DFR) category; (D) Platelet (PLT) category; (E) Adjuvant imatinib treatment of intermediate and high risk gastrointestinal stromal tumor patients. RFS was significantly lower for each variable in the high group than in the low group ($P < 0.05$). FIB: Fibrinogen; DFR: D-dimer-fibrinogen ratio; RFS: Recurrence-free survival; GIST: Gastrointestinal stromal tumor.

above indexes ($P < 0.05$). This finding indicated that the correlation between the above parameters and prognosis may be attributed to their correlation with tumor size, mitotic index, and NIH risk category.

DISCUSSION

It was reported that FIB could strongly predict the prognosis of various malignant tumors, such as lung, stomach, and pancreatic cancer[11]. D-dimer was related to the stage of the tumor in patients with prostate, lung, cervix, ovary, breast, or colorectal cancer[12-14]. PLT was associated with the prognosis of epithelial ovarian carcinoma and pancreatic cancer[4,15]. However, the data for FIB, D-dimer, and PLT predicting the prognosis of primary resectable GISTs are still very limited. We

Table 3 Multivariate analysis of the significant variables determined by univariate analysis

	B	SE	Wald	*P* value	RR (95%CI)
FIB	-2.035	0.622	10.692	0.001	0.131 (0.039-0.443)
Risk	-1.582	0.633	6.249	0.012	0.206 (0.059-0.711)
DFR	-1.097	0.447	6.022	0.014	0.334 (0.139-0.802)

FIB: Fibrinogen classification (FIB < 3.24 and FIB ⩾ 3.24); Risk: Risk category (very low, low and intermediate, and high risk); DFR: D-dimer to FIB classification (DFR ⩾ 0.354 and DFR < 0.354); RR: Risk ratio; CI: Confidence interval.

Table 4 Multivariate analysis of the significant variables determined by univariate analysis on the hierarchy of adjuvant imatinib

	B	SE	Wald	*P* value	RR (95%CI)
FIB	-2.223	0.632	12.385	0.000	0. 108 (0.031-0.373)
Risk	-1.795	0.645	7.736	0.005	0.166 (0.047-0.589)
DFR	-1.141	0.454	6.325	0.012	0.319 (0.131-0.777)

FIB: Fibrinogen classification (FIB < 3.24 and FIB ⩾ 3.24); Risk: Risk category (very low, low and intermediate, and high risk); DFR: D-dimer to FIB ratio classification (DFR ⩾ 0.354 and DFR < 0.354); RR: Risk ratio; CI: confidence interval.

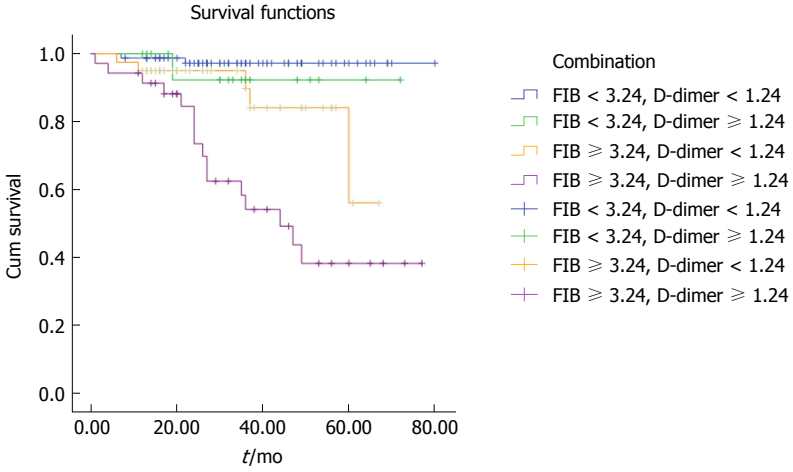

Figure 3 Recurrence-free survival of gastrointestinal stromal tumor patients, according to the combination of fibrinogen and D-dimer. The prognosis of the high fibrinogen and high D-dimer group was worse than that in the other groups. FIB: Fibrinogen; RFS: Recurrence-free survival; GIST: Gastrointestinal stromal tumor.

found only one study that examined the role of D-dimer in primary GISTs[16]. That study found that a baseline D-dimer level greater than 1000 ng/mL was inversely associated with total GIST survival rate and progression-free survival rate. Recently, another study found that high levels of FIB were associated with decreased overall survival (OS) and RFS in patients with GISTs[17]. However, as far as we know, there is little research on the value of these markers in the prognosis of patients with GISTs.

In the present study, we explored the clinical association of FIB, D-dimer, DFR, and PLT with pathological features and the prognosis of GISTs. Our purpose was to determine whether the above parameters could be associated with the prognosis of GISTs. We found that preoperative plasma FIB, D-dimer, PLT, NIH risk category, tumor location, tumor size, and mitotic index were associated with RFS in GIST patients who underwent surgical excision. To eliminate the interference of various factors on the predicted results of FIB and D-dimer, we calculated the DFR and found that DFR was also a prognostic indicator of GISTs. In addition, we combined FIB and D-dimer and divided the patients into four groups to show that the prognosis of the high D-dimer and high FIB group was significantly poorer than that of others. By inputting the statistically significant indexes that were found in the univariate analysis results into the Cox proportional hazards models, multiple factor regression analysis indicated that elevated FIB, DFR, and high NIH risk category were independent risk factors for poor prognosis of GISTs. There was also a correlation between the preoperative FIB, D-dimer, DFR, PLT and the clinicopathologic features of GISTs. If we can predict the prognosis of GISTs by using hematology markers such as FIB, D-dimer, DFR, and PLT, especially FIB and DFR, the analysis will be more convenient. We can easily monitor and predict the recurrence and metastasis of patients.

It is well known that the failure of many cancer treatments is closely related to tumor metastasis. A positive correlation between coagulation and tumor metastasis was observed many years ago[18]. Coagulation system

Table 5 Clinicopathologic characteristics of gastrointestinal stromal tumor patients grouped by preoperative fibrinogen

Characteristic	Low FIB (< 3.24 g/L)	High FIB (≥ 3.24 g/L)	*P* value
Age (yr)			< 0.01
< 61	78	0	
≥ 61	17	75	
Gender			< 0.01
Male	91	0	
Female	4	75	
Location			< 0.01
Gastric	95	27	
Nongastric	0	48	
Tumor size (cm)			< 0.01
≤ 5	95	2	
> 5	0	73	
NIH risk category			< 0.01
Very low	18	0	
Low	65	0	
Intermediate	12	25	
High	0	50	
Mitotic index			< 0.01
≤ 5/50 HPFs	95	30	
> 5/50 HPFs	0	45	

FIB: Fibrinogen; HPFs: High power fields.

Table 6 Clinicopathologic characteristics of gastrointestinal stromal tumor patients grouped by preoperative D-dimer

Characteristic	Low D-dimer (< 1.24 mg/L)	High D-dimer (≥ 1.24 mg/L)	*P* value
Age (yr)			< 0.01
< 61	78	0	
≥ 61	40	52	
Gender			< 0.01
Male	91	0	
Female	27	52	
Location			< 0.01
Gastric	118	4	
Nongastric	0	48	
Tumor size (cm)			< 0.01
≤ 5	97	0	
> 5	21	52	
NIH risk category			< 0.01
Very low	18	0	
Low	65	0	
Intermediate	35	2	
High	0	50	
Mitotic index			< 0.01
≤ 5/50 HPFs	118	7	
> 5/50 HPFs	0	45	

NIH: National Institutes of Health; HPFs: High power fields.

abnormalities are usually associated with tumor progression, and the coagulation cascade is often amplified in cancer patients. Approximately 50% of local tumor patients and most metastatic tumor patients have several coagulation factor abnormalities[9,19].

FIB is a plasma protein that plays an important role in the process of coagulation. Some studies have shown that FIB is positively related to cancer progression[20]. The elevated FIB is associated with distant tumor metastasis, suggesting that FIB plays an important role in the adhesion of tumor and vascular metastasis of the target organ. In addition, FIB plays an important role in angiogenesis and tumor cell growth, which may be associated with the promotion of growth factor fusion and cell adhesion, proliferation, and migration. Moreover, platelet fibrin malignancies play an important role in the early development of tumor cells, avoiding the host's autoimmune surveillance by providing protection[20]. Other research evidence indicates that the FIB fragment promotes tumor progression and metastasis by inhibiting tumor angiogenesis and binding and downregulating the expression of vascular endothelial cells[20]. However, the exact mechanism of the role of FIB in the progression of tumor remains unclear and requires further study.

D-dimer is not only a product of fibrin degradation that is found in blood after the coagulation cascade but

Table 7 Clinicopathologic characteristics of gastrointestinal stromal tumor patients grouped by preoperative D-dimer-fibrinogen ratio

Characteristic	Low DFR (< 0.354)	High DFR (≥ 0.354)	*P* value
Age (yr)			< 0.01
< 61	78	0	
≥ 61	48	44	
Gender			< 0.01
Male	91	0	
Female	35	44	
Location			< 0.01
Gastric	122	0	
Nongastric	4	44	
Tumor size (cm)			< 0.01
≤ 5	97	0	
> 5	29	44	
NIH risk category			< 0.01
Very low	18	0	
Low	65	0	
Intermediate	37	0	
High	6	44	
Mitotic index			< 0.01
≤ 5/50 HPFs	125	0	
> 5/50 HPFs	1	44	

HPFs: High power fields; DFR: D-dimer to fibrinogen ratio.

Table 8 Clinicopathologic characteristics of gastrointestinal stromal tumor patients grouped by preoperative platelet count

Characteristic	Low PLT (< 197.5 × 10^9/L)	High PLT (≥ 197.5 × 10^9/L)	*P* value
Age (yr)			< 0.01
< 61	78	0	
≥ 61	3	89	
Gender			< 0.01
Male	81	10	
Female	0	79	
Location			< 0.01
Gastric	81	41	
Nongastric	0	48	
Tumor size (cm)			< 0.01
≤ 5	81	16	
> 5	0	3	
NIH risk category			< 0.01
Very low	18	0	
Low	63	2	
Intermediate	0	37	
High	0	50	
Mitotic index			< 0.01
≤ 5/50 HPFs	81	44	
> 5/50 HPFs	0	45	

NIH: National Institutes of Health; HPFs: High power fields.

also a specific marker for fibrinolysis. Similarly, D-dimer is an important marker of coagulation abnormalities. Studies have indicated that coagulation disorders exist in 90% of cancer patients, such as shortened prothrombin and partial thromboplastin time, and increased factors Ⅱ, Ⅴ, Ⅷ, Ⅸ, XI, XII, FIB, and fibrin degradation products[11,13]. There are other studies determining whether the level of D-dimer significantly increased in patients with disseminated intravascular coagulation (DIC), deep vein thrombosis, pulmonary embolism, myocardial infarction, cerebral infarction, and other thromboembolic events[18].

In addition, we speculate that another cause of the increase in FIB and D-dimer may be related to the liver because the blood clotting related indicators are produced by the liver. Furthermore, it is not ruled out that the prognostic effect of FIB and DFR on GISTs may be due to the correlation between these indexes and the clinicopathologic features of GISTs.

The relationship between PLT and tumors can be understood by the fact that PLT plays a very important role in tumor vascular growth through various platelet-

derived vascular growth factors, and platelet-derived transforming growth factor β (TGF-β) can coactivate TGF-β/Smad and NF-κB pathways in cancer cells, thus promoting tumor metastasis[21].

At present, the prognostic factors of GISTs, such as mitotic count, tumor location, size, rupture, and metastasis[2,22], all depend on postoperative pathological results. Biomarkers to screen for the recurrence or progression of GISTs are still limited, but many studies support the notion that the prognosis of tumors can be judged using tumor biomarkers[13]. For example, marker CA-153 is associated with the recurrence and metastasis of breast cancer, CEA is used to monitor the treatment of colorectal cancer and gastric cancer, and CA-199 is associated with ovarian cancer.

Moreover, in most hospitals, the tests for plasma FIB, D-dimer, and PLT have been included in conventional preoperative coagulation and routine blood tests, and the values are easy to obtain. Based on this, it is easy for clinicians to use FIB, D-dimer, and PLT as prognostic markers in GIST patients. Therefore, before an operation, we could roughly predict the prognosis of GISTs by hematological indicators, to give early intervention therapy, and thus obtain a better prognosis. Especially for those patients who cannot obtain pathological results, it is more significant to use these hematological indicators to predict the prognosis of GISTs. Furthermore, combining these hematological parameters with the clinical features of GISTs can significantly improve the prognostic evaluation of GISTs.

This study has some limitations. First, it is a single center, retrospective, nonrandomized, controlled study. More prospective research is needed to verify the predictive value of these indicators. Second, its small sample size may cause some bias; therefore, a larger sample size study is required to further validate our results. Third, this study also included a number of deleted cases that did not survive for 5 years after surgery, which may lead to bias in the survival analysis. Fourth, some of the NIH risk categories of high risk GIST patients in this study failed to receive adjuvant treatment or to complete adjuvant treatment as a result of their high drug costs or adverse drug reactions. Furthermore, we only analyzed the predictive value of these indicators in primary resectable and preoperative GISTs without adjuvant medication, and the predictive value of these markers in patients receiving adjuvant imatinib and nonoperative GISTs needs further study.

However, considering the low cost and ease of operation of hematological testing, plasma FIB, D-dimer, DFR, and PLT should be considered as prognostic indicators for GIST patients, especially in developing countries. It is known that clinicians are better at screening patients requiring adjuvant therapy and formulating targeted general treatment and monitoring programs. Nevertheless, this finding also requires a large, prospective study to further confirm.

In light of these results, it is concluded that preoperative plasma FIB, D-dimer, DFR, and PLT can be used as effective hematological biomarkers for monitoring the prognosis of GIST patients that do not require special measuring devices. It was also indicated that clinicians should obtain FIB, D-dimer, DFR, and PLT values as part of routine care. In particular, the value of FIB and DFR in predicting the prognosis of GISTs should be emphasized. These values should be added to the currently accepted preoperative risk categories, such as size, primary tumor site, and genetic mutation.

ARTICLE HIGHLIGHTS

Research background

It is well known that moderate and high-risk gastrointestinal stromal tumor (GIST) patients have a high recurrence rate and need adjuvant targeted therapy to improve prognosis. Therefore, early screening of this protion of patients to give adjuvant treatment is particularly important. At present, the prediction of GISTs is obtained by postoperative pathology, and there is no effective index to predict the prognosis of GISTs before operation. The purpose of this retrospective study was to investigate the role of fibrinogen (FIB), D-dimer-fibrinogen ratio (DFR) in the prognosis of GISTs before operation.

Research motivation

The increase of blood coagulation indexes such as fibrinogen content and D-dimer before operation can predict the adverse prognosis of many kinds of cancer, but there is little discussion about the relationship between these indexes and GISTs.

Research objectives

The retrospective study analyzed the role of FIB, D-dimer, DFR, and platelet count (PLT) in the prognosis of GISTs before operation.

Research methods

This study included 170 patients with GISTs who met the criteria. The data of all the patients were collected before and after operation to make statistical analysis. All data were analyzed using the SPSS 18.0 statistical software, with a *P*-value below 0.05 considered statistically significant.

Research results

In the present study, univariate analysis showed that FIB, D-dimer, DFR, and PLT were correlated with the 3- and 5-year survival rates of GIST patients. In addition, there was a correlation between the clinical features and FIB, D-dimer, DFR, and PLT in GISTs. Moreover, multivariate analysis showed that FIB and DFR had an independent effect on the prognosis of GIST patients.

Research conclusions

This retrospective study showed that FIB, D-dimer, DFR, and PLT were the prognostic factors of GISTs, but there was an independent correlation between FIB and DFR and GIST prognosis. These factors may help screen out high-risk patients early and to administer adjuvant intervention as soon as possible.

Research perspectives

For patients with GISTs, the prognosis can be preliminarily estimated according to hematological indexes such as FIB and DFR before the operation, and adjuvant therapy can be given early to improve the prognosis of patients. Of course, the results of this study need to be further verified by a large sample size prospective study.

ACKNOWLEDGMENTS

Thank you to all those who contributed to the design and modification of this article. The authors are

responsible for obtaining written permission to use any copyrighted text and/or illustrations.

REFERENCES

1 **Goh BK**, Chok AY, Allen JC Jr, Quek R, Teo MC, Chow PK, Chung AY, Ong HS, Wong WK. Blood neutrophil-to-lymphocyte and platelet-to-lymphocyte ratios are independent prognostic factors for surgically resected gastrointestinal stromal tumors. *Surgery* 2016; **159**: 1146-1156 [PMID: 26688506 DOI: 10.1016/j.surg.2015.10.021]

2 **Joensuu H**, Eriksson M, Hall KS, Hartmann JT, Pink D, Schütte J, Ramadori G, Hohenberger P, Duyster J, Al-Batran SE, Schlemmer M, Bauer S, Wardelmann E, Sarlomo-Rikala M, Nilsson B, Sihto H, Ballman KV, Leinonen M, DeMatteo RP, Reichardt P. Risk factors for gastrointestinal stromal tumor recurrence in patients treated with adjuvant imatinib. *Cancer* 2014; **120**: 2325-2333 [PMID: 24737415 DOI: 10.1002/cncr.28669]

3 **Li J**, Ye Y, Wang J, Zhang B, Qin S, Shi Y, He Y, Liang X, Liu X, Zhou Y, Wu X, Zhang X, Wang M, Gao Z, Lin T, Cao H, Shen L, Chinese Society Of Clinical Oncology Csco Expert Committee On Gastrointestinal Stromal Tumor. Chinese consensus guidelines for diagnosis and management of gastrointestinal stromal tumor. *Chin J Cancer Res* 2017; **29**: 281-293 [PMID: 28947860 DOI: 10.21147/j.issn.1000-9604.2017.04.01]

4 **Qiu J**, Yu Y, Fu Y, Ye F, Xie X, Lu W. Preoperative plasma fibrinogen, platelet count and prognosis in epithelial ovarian cancer. *J Obstet Gynaecol Res* 2012; **38**: 651-657 [PMID: 22413879 DOI: 10.1111/j.1447-0756.2011.01780.x]

5 **Lee SE**, Lee JH, Ryu KW, Nam BH, Cho SJ, Lee JY, Kim CG, Choi IJ, Kook MC, Park SR, Kim YW. Preoperative plasma fibrinogen level is a useful predictor of adjacent organ involvement in patients with advanced gastric cancer. *J Gastric Cancer* 2012; **12**: 81-87 [PMID: 22792520 DOI: 10.5230/jgc.2012.12.2.81]

6 **Jiang Z**, Zhang J, Li Z, Liu Y, Wang D, Han G. A meta-analysis of prognostic value of KIT mutation status in gastrointestinal stromal tumors. *Onco Targets Ther* 2016; **9**: 3387-3398 [PMID: 27350754 DOI: 10.2147/OTT.S101858]

7 **Zhu JF**, Cai L, Zhang XW, Wen YS, Su XD, Rong TH, Zhang LJ. High plasma fibrinogen concentration and platelet count unfavorably impact survival in non-small cell lung cancer patients with brain metastases. *Chin J Cancer* 2014; **33**: 96-104 [PMID: 23958057 DOI: 10.5732/cjc.012.10307]

8 **Arigami T**, Uenosono Y, Matsushita D, Yanagita S, Uchikado Y, Kita Y, Mori S, Kijima Y, Okumura H, Maemura K, Ishigami S, Natsugoe S. Combined fibrinogen concentration and neutrophil-lymphocyte ratio as a prognostic marker of gastric cancer. *Oncol Lett* 2016; **11**: 1537-1544 [PMID: 26893776 DOI: 10.3892/ol.2015.4049]

9 **Kilic L**, Yildiz I, Sen FK, Erdem MG, Serilmez M, Keskin S, Ciftci R, Karabulut S, Ordu C, Duranyildiz D, Tas F. D-dimer and international normalized ratio (INR) are correlated with tumor markers and disease stage in colorectal cancer patients. *Cancer Biomark* 2015; **15**: 405-411 [PMID: 25792472 DOI: 10.3233/CBM-150477]

10 **Go SI**, Lee MJ, Lee WS, Choi HJ, Lee US, Kim RB, Kang MH, Kim HG, Lee GW, Kang JH, Lee JH, Kim SJ. D-Dimer Can Serve as a Prognostic and Predictive Biomarker for Metastatic Gastric Cancer Treated by Chemotherapy. *Medicine* (Baltimore) 2015; **94**: e951 [PMID: 26222870 DOI: 10.1097/MD.0000000000000951]

11 **Yu W**, Wang Y, Shen B. An elevated preoperative plasma fibrinogen level is associated with poor overall survival in Chinese gastric cancer patients. *Cancer Epidemiol* 2016; **42**: 39-45 [PMID: 27010728 DOI: 10.1016/j.canep.2016.03.004]

12 **Joensuu H**. Risk stratification of patients diagnosed with gastrointestinal stromal tumor. *Hum Pathol* 2008; **39**: 1411-1419 [PMID: 18774375 DOI: 10.1016/j.humpath.2008.06.025]

13 **Tekeşin K**, Bayrak S, Esatoğlu V, Özdemir E, Özel L, Melih Kara V. D-Dimer and Carcinoembryonic Antigen Levels: Useful Indicators for Predicting the Tumor Stage and Postoperative Survival. *Gastroenterol Res Pract* 2016; **2016**: 4295029 [PMID: 27651789 DOI: 10.1155/2016/4295029]

14 **Liu L**, Zhang X, Yan B, Gu Q, Zhang X, Jiao J, Sun D, Wang N, Yue X. Elevated plasma D-dimer levels correlate with long term survival of gastric cancer patients. *PLoS One* 2014; **9**: e90547 [PMID: 24618826 DOI: 10.1371/journal.pone.0090547]

15 **Wang H**, Gao J, Bai M, Liu R, Li H, Deng T, Zhou L, Han R, Ge S, Huang D, Ba Y. The pretreatment platelet and plasma fibrinogen level correlate with tumor progression and metastasis in patients with pancreatic cancer. *Platelets* 2014; **25**: 382-387 [PMID: 24001199 DOI: 10.3109/09537104.2013.827782]

16 **Afshar M**, Hamilton P, Seligmann J, Lord S, Baxter P, Marples M, Stark D, Hall PS. Can D-Dimer Measurement Reduce the Frequency of Radiological Assessment in Patients Receiving Palliative Imatinib for Gastrointestinal Stromal Tumor (GIST)? *Cancer Invest* 2015; **33**: 347-353 [PMID: 26135352 DOI: 10.3109/07357907.2015.1047504]

17 **Lu J**, Chen S, Li X, Qiu G, He S, Wang H, Zhou L, Jing Y, Che X, Fan L. Gastrointestinal stromal tumors: Fibrinogen levels are associated with prognosis of patients as blood-based biomarker. *Medicine* (Baltimore) 2018; **97**: e0568 [PMID: 29703047 DOI: 10.1097/MD.0000000000010568]

18 **Diao D**, Wang Z, Cheng Y, Zhang H, Guo Q, Song Y, Zhu K, Li K, Liu D, Dang C. D-dimer: not just an indicator of venous thrombosis but a predictor of asymptomatic hematogenous metastasis in gastric cancer patients. *PLoS One* 2014; **9**: e101125 [PMID: 24983619 DOI: 10.1371/journal.pone.0101125]

19 **Zhang W**, Dang S, Hong T, Tang J, Fan J, Bu D, Sun Y, Wang Z, Wisniewski T. A humanized single-chain antibody against beta 3 integrin inhibits pulmonary metastasis by preferentially fragmenting activated platelets in the tumor microenvironment. *Blood* 2012; **120**: 2889-2898 [PMID: 22879538 DOI: 10.1182/blood-2012-04-425207]

20 **Lee JH**, Hyun JH, Kim DY, Yoo BC, Park JW, Kim SY, Chang HJ, Kim BC, Kim TH, Oh JH, Sohn DK. The role of fibrinogen as a predictor in preoperative chemoradiation for rectal cancer. *Ann Surg Oncol* 2015; **22**: 209-215 [PMID: 25384698 DOI: 10.1245/s10434-014-3962-5]

21 **Labelle M**, Begum S, Hynes RO. Direct signaling between platelets and cancer cells induces an epithelial-mesenchymal-like transition and promotes metastasis. *Cancer Cell* 2011; **20**: 576-590 [PMID: 22094253 DOI: 10.1016/j.ccr.2011.09.009]

22 **Li J**, Zhang H, Chen Z, Su K. Clinico-pathological characteristics and prognostic factors of gastrointestinal stromal tumors among a Chinese population. *Int J Clin Exp Pathol* 2015; **8**: 15969-15976 [PMID: 26884871 DOI: 10.3892/ol.2018.9320]

P- Reviewer: Grau JM, Lee SW, Negreanu L **S- Editor**: Wang XJ
L- Editor: Wang TQ **E- Editor**: Yin SY

Published by **Baishideng Publishing Group Inc**
7901 Stoneridge Drive, Suite 501, Pleasanton, CA 94588, USA
Telephone: +1-925-223-8242
Fax: +1-925-223-8243
E-mail: bpgoffice@wjgnet.com
Help Desk: http://www.f6publishing.com/helpdesk
http://www.wjgnet.com

ISSN 1007-9327